2

LATE QUATERNARY LAHARS FROM MOUNT RUAPEHU IN THE WHANGAEHU RIVER VALLEY, NORTH ISLAND, NEW ZEALAND

A thesis presented in partial fulfilment of
the requirements for the degree of
Doctor of Philosophy in Soil Science
at Massey University

Katherine Anne Hodgson
1993


KA
949
NZGR
TANGIWAI
24 · 12 · 53

ACKNOWLEDGEMENTS

The completion of the thesis presented here realises a vision that has sustained me through the ups and downs of what has been an intense learning experience; a vision which may not have been fulfilled without the encouragement from my chief supervisor, Associate Professor V. E. Neall. For this I am truly grateful.

I would also like to acknowledge Dr A. S. Palmer for his valuable discussions and suggestions which helped to iron out the grittiest of problems. Dr R. B. Stewart tried to keep me on the straight and narrow.

The study was funded by the Vice Chancellors's Study Award, for which the author is appreciative. The Department of Conservation and Ministry of Civil Defence provided funding for the field based research central to this project.

During summer fieldwork I had the good fortune to be able to abuse the hospitality of the following households:

1989-90	Kandy Barrett and Craig Mott, Jeremy and Jenna, of Oruakukura Road.
1990-1992	Pam, Ginnie and Merv Matthews of Waipunga, Whangaehu Valley Road.
1992	Margaret, Tim, Anne and John Matthews of Mangatipona Road.

I thank you all, especially Pam, Ginnie and Merv, for putting up with all my aberrations. I shall never forget the time I spent in the Whangaehu Valley, neither the hospitality of the local people nor their amused interest in my activities. Pam and Anne are also acknowledged for their conscientious barometer reading.

I would like to thank Steve Morris, Planning and Development, Massey University for both his patience and his ingenuity which helped create the Versacad plots depicted in Chapter 7.

I would also like to acknowledge Malcolm Boag and Mike Bretherton, both Department of Soil Science, Massey University; the former for his tolerance of all the various demands I made of him during my study, and the latter for helping to sort out those niggly computer problems.

I have met so many new people, several of them through the Department of Soil Science, most of whom supplied the essential element of friendship to my new life in New Zealand. It was a particular delight to meet so many other International students. I cannot name everyone here but, for old times sake, I would like to thank Aravind (a compatriot from the very beginning), Lee and Mike - all fellow members of the alternative teaclub. I left my old home, the United Kingdom, five years ago, and my gratitude goes to friends there, and all over the globe, who kept writing, helping to keep me in touch.

Finally, my heartfelt thanks go to my family in New Zealand, and in the United Kingdom. There was no easy way to make it through the past few years; I am indebted to you for your confidence and reassurance, and for waiting (patiently?) for me to rejoin you all on the other side.

ABSTRACT

The stratigraphic record of lahars in the Whangaehu River reveals that in the past 180,000 years this route has been one of the main conduits for lahars from Mount Ruapehu, the highest active andesitic stratovolcano in the Central North Island of New Zealand. Both debris flows and hyperconcentrated flows have engulfed surfaces up to 160 km distance from the Volcano. Eight episodes of laharic activity are recognized by the distinctive lithology and similar age of their deposits. The newly defined upper Pleistocene Whangaehu Formation provides evidence for the earliest lahar event in the Valley, *c.* 180,000-140,000 years ago. There is only meagre evidence for laharic activity following this event until the Ohakean and Holocene, although two new informally named deposits - the Mangatipona pumice sand (*c.* 37,000 years B.P.) and Apitian lahars (*c.* 32,000-25,500 years B.P) - are recognized, of minor extent. The formerly defined late Quaternary Te Heuheu (*c.* 25,500-14,700 years B.P.), Tangatu (*c.* 14,700-5,370 years B.P.), Manutahi (*c.* 5,370-3,400 years B.P.), Mangaio (*c.* 4,600 years B.P.) and Onetapu (< *c.* 1,850 years B.P.) Formations are here described and interpreted.

Triggering mechanisms for lahar deposits are distinguished based on lithological criteria.

(a) Bouldery deposits in the Whangaehu Formation are interpreted to have been emplaced by a single highly competent debris flow triggered by a southerly-directed flank collapse at Mount Ruapehu. This debris flow was competent enough to transport boulders up to 2 m in diameter over 140 km from the Volcano. Bouldery deposits are also recognized in the Onetapu Formation, but are restricted to higher gradient surfaces on the Mount Ruapehu ring plain. The Onetapu Formation deposits are interpreted to have been emplaced by lahars resulting from catastrophic drainage of Crater Lake, which occupies the active crater on Mount Ruapehu.

(b) Pebbly and sandy deposits are interpreted to have been emplaced by low competence debris flows and hyperconcentrated flows. These lahar deposits are recognized in all formations described. The lithology in these deposits is

commonly pumice and they are interpreted to have been triggered by eruptions and/or high rainfall events at the Volcano.

Formations, and individual members within Formations, were dated by radiocarbon dating of organic material found below, within or above lahar deposits, or by coverbed stratigraphy. Both rhyolitic and andesitic tephras provided recognizable time planes in the late Quaternary coverbeds overlying lahar deposits. In this study quantitative analysis of quartz abundance, which is shown to vary between loesses and palaeosols, is used as an indirect means of establishing a surrogate for past climate changes which have been correlated to the deep sea oxygen isotope curve. A minimum age for the newly defined Whangaehu Formation is established by this method.

The accumulation rate for lahars in the Whangaehu River has accelerated from 1 km^3 every *c.* 23,000 years in the past *c.* 160,000 years to 1 km^3 in 589 years in the past *c.* 2,000 years. This acceleration probably results from the increased frequency of lahars in the River following the development of Crater Lake *c.* 2,000 years B.P. According to this pattern an estimated 0.17 km^3 volume of lahars could be anticipated over the next 100 years. If the 2,000 year accumulation rate were to be met over the next 100 years there would be 170 lahars of 10^6 m^3 in this time interval, or 17 lahars of 10^7 m^3 (or 1.7 lahars of 10^8 m^3). The largest reported volume for an historic lahar is 10^6 m^3 and these have occurred on average once every 30 years. The accumulation rate for historic lahars is 0.0054 km^3 in 100 years. Therefore, although the accumulation rate appears to have slowed down, further large lahars with magnitudes 10 or 100 times greater than those witnessed could be expected.

TABLE OF CONTENTS

VOLUME ONE

CHAPTER 1

LATE QUATERNARY LAHARS FROM MOUNT RUAPEHU

CHAPTER 2

THE WHANGAEHU RIVER AND ITS GEOLOGICAL SETTING

CHAPTER 3

LAHARS: DEFINITION AND TERMINOLOGY

CHAPTER 4

THE WHANGAEHU FORMATION

CHAPTER 7

THE ONETAPU FORMATION

CHAPTER 8

HISTORIC LAHARS

CHAPTER 9

THE HAZARDS AND RISKS FROM LAHARS IN THE WHANGAEHU RIVER

CHAPTER 10

CONCLUSIONS

LIST OF TABLES

CHAPTER 4

CHAPTER 6

CHAPTER 7

CHAPTER 8

CHAPTER 9

CHAPTER 10

LIST OF FIGURES

CHAPTER 1

CHAPTER 2

CHAPTER 3

CHAPTER 4

CHAPTER 5

CHAPTER 6

CHAPTER 7

CHAPTER 8

CHAPTER 9

LIST OF APPENDICES (VOLUME 2)

Tables

Section descriptions

Figures

LIST OF PLATES (VOLUME 2)

CHAPTER 1

CHAPTER 4

CHAPTER 5

CHAPTER 6

CHAPTER 7

CHAPTER 8

LIST OF MAPS (VOLUME 2)

CHAPTER 1

LATE QUATERNARY LAHARS FROM MOUNT RUAPEHU: OBJECTIVES AND STUDY AREA

1.1 INTRODUCTION

Mount Ruapehu is an active andesitic stratovolcano which lies in the Central North Island of New Zealand. Volcanic hazards from Mount Ruapehu include magmatic and phreatomagmatic eruptions, flank and sector collapses, and lahars. Lahars are recognized as presenting the greatest hazard, compounded by the presence of a lake (Crater Lake) in the active crater. To date they have resulted in the loss of 151 lives (The Tangiwai Disaster, 1953) and infrastructure damage both in proximity to the volcano and more distally in the rivers which drain the volcano.

1.2 OBJECTIVES

The objectives of this study were to map, date and reconstruct the conditions governing the numerous lahar events in the Whangaehu River, which drains the east side of Mount Ruapehu (see Figure 1.1). Prior to this study very little was known about the nature and distribution of lahars and their deposits within the middle and lower catchment of the River. The loss of life and structural damage on both the volcanic edifice and ring plain, caused directly by lahars from Mount Ruapehu in 1953, 1969 and 1975, however, served to highlight the potential risk that this particular hazard poses, and the necessity for a comprehensive study to be made of their impact throughout the catchment of the River. This study complements research carried out by Purves (1990) and Donoghue (1991) who detailed the impact of lahars in the upper Catchment of the Whangaehu River on the Mount Ruapehu ring plain.

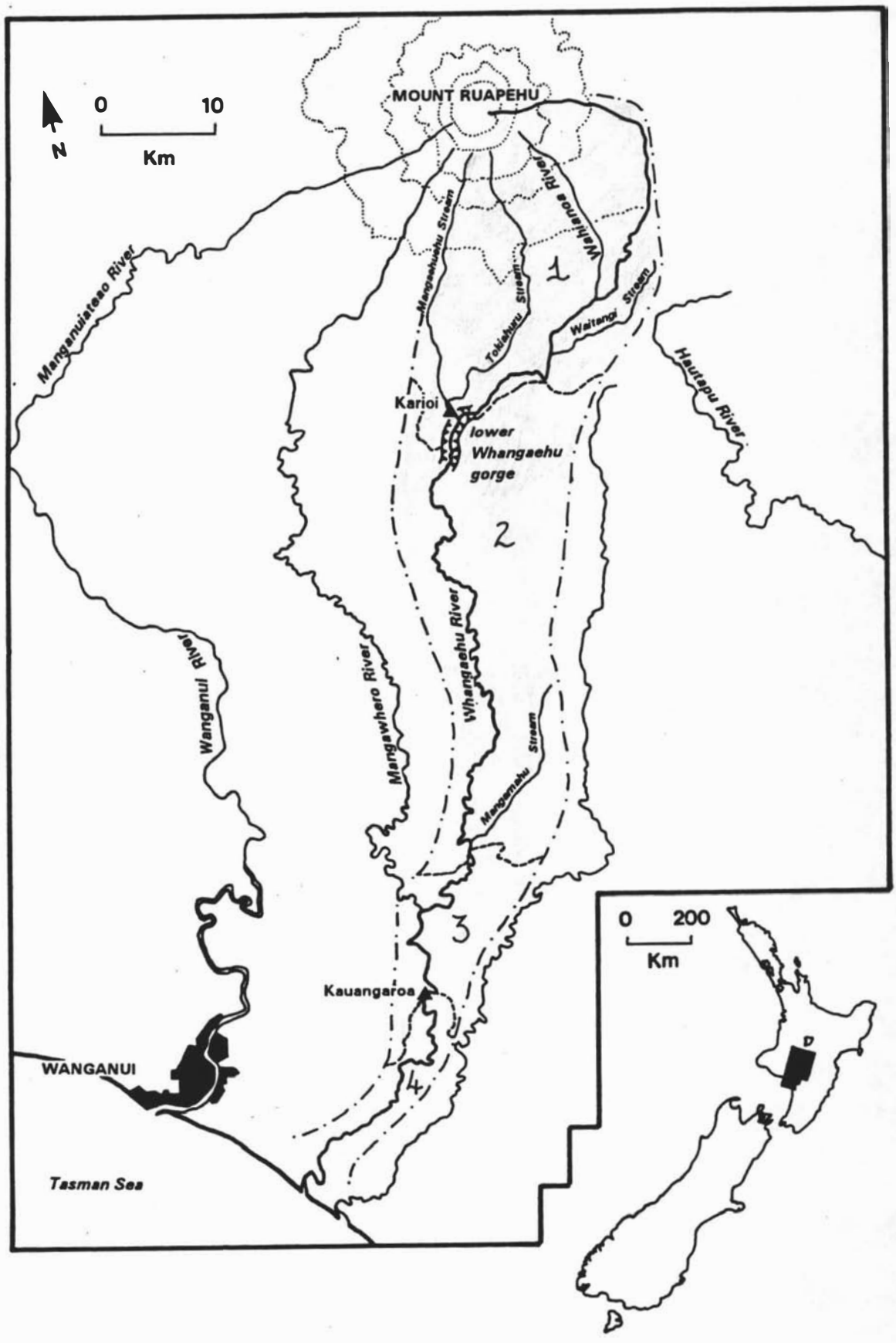

Figure 1.1 The Whangaehu River catchment; (— ·) defines the outer margins of the Catchment, and (---) boundaries between reaches within the Catchment.

1.3 METHODS

Both geological and historical evidence for laharic activity was investigated during the course of this study.

Geological investigations included detailed fieldwork examining exposures of lahar deposits throughout the field area. It was possible to date the deposits directly using tephrochronology and loess/palaeosol stratigraphy of coverbeds overlying lahar deposits, coupled with radiocarbon dating of contained wood or underlying peat. Detailed examination of the lithology and sedimentology of deposits revealed their dominant flow mechanism, and mode of emplacement. Total volumes for most lahar deposits (or suites of deposits) have been estimated, and velocity and peak discharge rates calculated for selected Holocene events.

Further evidence came in the form of written reports and eye-witness accounts of lahars which occurred in historic times. These were either printed in journals and newspapers, or related directly to the author. From these sources it has been possible to establish that there have been 19 lahars (of different magnitudes) in the Whangaehu River since the earliest reported lahar which occurred in 1861. Historical records provided information on travel times and flow heights for lahars from which it was possible to estimate velocities, discharge rates, and total volumes for early historic lahars. Lahar magnitudes have also been determined through comparison of the volume of Crater Lake water lost during lahar events. Long term automatic water level recording stations at Karioi (established 1962) and Kauangaroa (established 1971) provide absolute velocity and discharge rates for lahars which occurred in the past *c.* 30 years (Paterson, 1976; Welles and Fowles, 1980).

1.4 THE WHANGAEHU RIVER

The source of the Whangaehu River is Crater Lake, a body of acid water 0.16 km^2 in area (Houghton *et al.*, 1987), which occupies the active crater on Mount Ruapehu. The water in Crater Lake is heavily impregnated with sulphur and fine-grained volcanic

mud, which imparts an acid quality and milky appearance to the water in the Whangaehu River. Mean flow from Crater Lake is normally dependant on the rate of snow and ice melt on the summit region and varies from 0.03 $m^3 s^{-1}$ in the winter to 0.12 $m^3 s^{-1}$ in the summer (Otway *et al.*, 1988-91). The mean discharge rate for the Whangaehu River at Karioi, about 57 km from source, is 13.5 $m^3 s^{-1}$. At Kauangaroa, 169 km from source, this has increased to 39.1 $m^3 s^{-1}$. The River finally drains into the Tasman Sea 12 km southeast of Wanganui.

Major tributaries of the Whangaehu River are the Wahianoa, Mangaehuehu, and Mangawhero Rivers. These all drain the south and east flanks of the volcano and supply fresh water to the Whangaehu River, in contrast to the acidic source water from Crater Lake. The Whangaehu River catchment is bounded to the west by the Wanganui River Catchment and to the east by the Turakina and Rangitikei River Catchments (see Figure 1.1).

1.4.1 *THE WHANGAEHU RIVER CATCHMENT*

The Catchment of the Whangaehu River can be divided into four reaches, (1) the upper catchment, (2) the middle catchment, (3) the lower catchment, and (4) the coastal plain (see Figure 1.1).

The upper catchment extends from the source of the river at Crater Lake to the edge of the volcanic ring plain (see Figure 1.2, and Plate 1.1). This reach can be divided into three main geomorphological zones (1) the volcanic edifice, (2) the Whangaehu Fan and (3) the ring plain. The volcanic edifice is built from successive layers of lava, pyroclastic debris and tephra. The present edifice supports 6 small glaciers and there is evidence that in the past these were much more extensive, deeply eroding the flanks of Mount Ruapehu. From Crater Lake the River flows down the steep flanks of the volcano through the upper Whangaehu gorge.

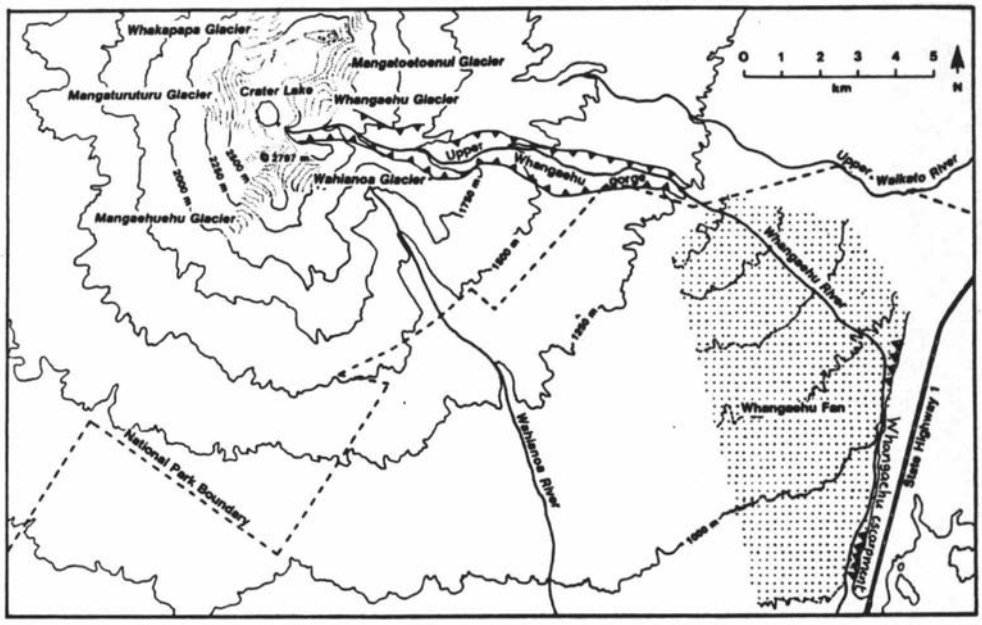

Figure 1.2 The source area of the Whangaehu River - the Southeast sector of Mount Ruapehu including Crater Lake, summit glaciers, the upper Whangaehu gorge, and the Whangaehu Fan.

At about 1,200 m, 10 km from source, the River debouches onto a debris fan, here called the Whangaehu Fan, which accumulated from deposits of recent lahars which aggraded below this point. Here the waters of the Whangaehu River diverge in a deltaic fashion, until they encounter the Whangaehu escarpment, where the waters flow southwards and merge once again on the volcanic ring plain. The Mount Ruapehu ring plain comprises principally tephra, lahar and ignimbrite deposits, with lesser fluvial and glacial sediments (Gregg, 1960; Grindley, 1960; Hackett and Houghton, 1989). The Wahianoa River and Mangaehuehu Stream join the Whangaehu River at approximately 35 and 57 km from source, respectively, on the ring plain (see Figure 1.1).

The middle catchment extends southwards from the edge of the ring plain through dissected hill country comprising uplifted Tertiary marine sandstones and siltstones, which are Pliocene in age (Fleming, 1953; Lensen, 1959; and see Figure 1.3 and Plate 1.2). The channel of the River is deeply incised and tortuous throughout this section.

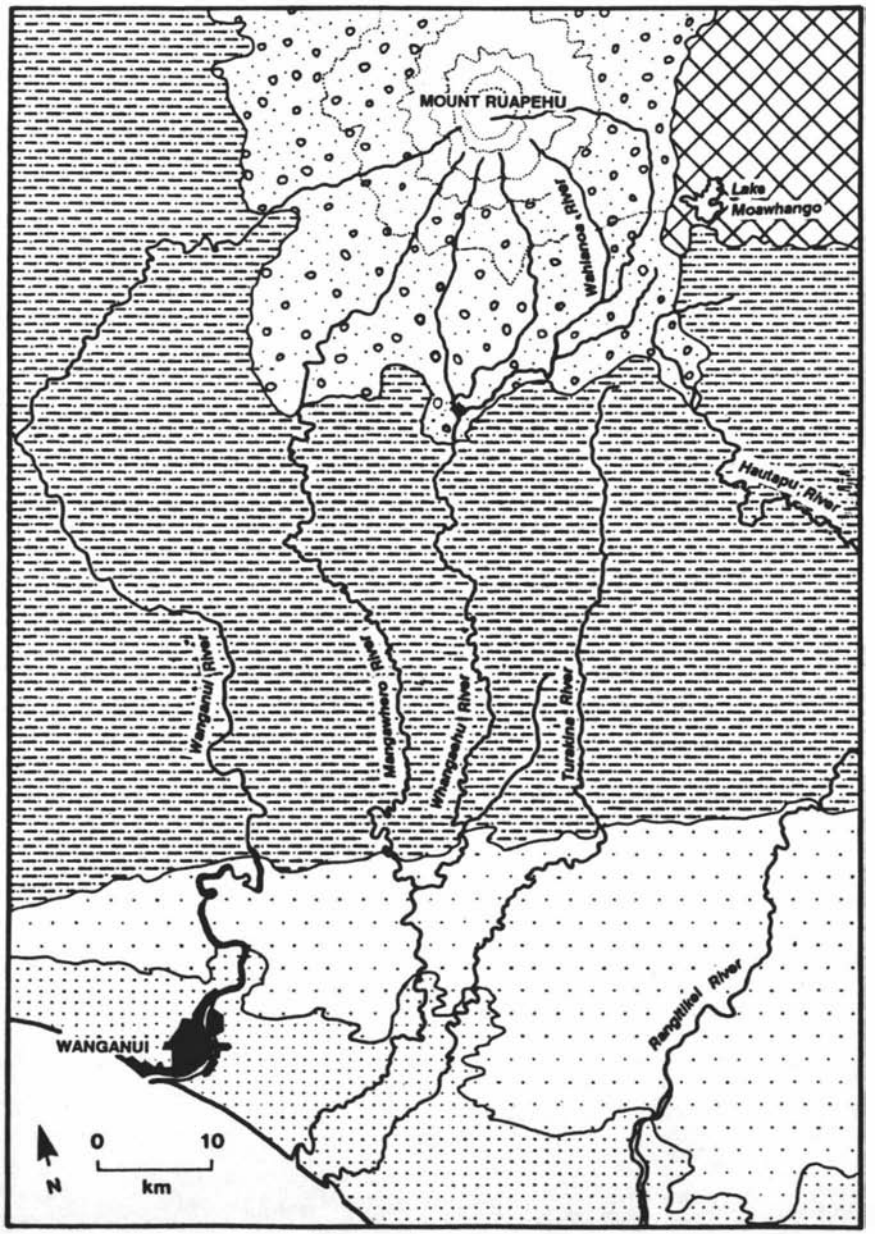

Mount Ruapehu volcanic cone

Mount Ruapehu volcanic ring plain and tephra

Sand dunes, marine benches and loess

Quaternary sandstone and siltstone

Tertiary sandstone, siltstone and limestone

Mesozoic greywacke and schist

Figure 1.3 Geology of Wanganui and Tongariro Districts, through which the Whangaehu River flows.

The boundary between Tertiary and Quaternary sediments, near Mangamahu, 137 km from source, also marks the boundary between the middle and lower catchments of the River (see Figures 1.1 and 1.3 and Plate 1.3). In the lower reach, which extends south to Kauangaroa, the River is confined within suites of late Quaternary river terraces either comprising, or capped with, volcaniclastics (Fleming, 1953). The Mangawhero River joins the Whangaehu River at 152 km from source in this reach.

The final reach of the River, here defined as the coastal reach, extends from Kauangaroa to the mouth of the River at Whangaehu Beach. This reach is characterized by a wide alluvial flood plain confined within late Quaternary river marine terraces (see Plate 1.4).

1.4.2 *SOILS, CLIMATE AND AGRICULTURE*

Soils of the upper catchment, and the upper part of the middle catchment, are typically allophanic yellow-brown loams which have developed within Holocene tephra (Pullar *et al.*, 1973) . Throughout the lower reaches of the middle catchment yellow-grey earth soils are formed in dominantly quartzofeldspathic sandstone and siltstone. Late Quaternary terraces within the middle catchment are constructed from Holocene lahar deposits. A characteristic soil type, the Kakatahi silt loam, has developed within these gravelly volcaniclastic deposits. Soils in the lower catchment are typically yellow-grey earths, recent alluvial soils, and yellow-brown sands developed into dune sands on the coastal fringe (Campbell, 1977).

The climate in much of the Whangaehu catchment is mild, with the weather pattern dominated by westerly airflow. Mean annual rainfall ranges from over 5,000 mm at Mount Ruapehu to below 900 mm at the coast. The average temperature at the summit of Mount Ruapehu is -3° C, but at Karioi, 648 m altitude, the mean air temperature is 9.6° C, ground frosts are experienced on average 9 days in each year, and snow on 9.3 days. At Wanganui, 12 km northwest of the mouth of the Whangaehu River and at an altitude of 22 m, mean air temperature is 13.4° C, ground frost is experienced on an average of 11 days in each year, and snow on 0.1 days (Welles and Fowles, 1980).

Agriculture in the region is dominantly controlled by relief, climate and soils. Winter vegetables are grown in the distinctive and amenable yellow-brown loam soils. In the middle catchment sheep and cattle grazing predominates. The lower catchment and coastal plain are characterized by extensive sheep and cattle farming, with horticultural development, primarily kiwifruit, on terraces close to the River at and below Mangamahu (Wellesand Fowles, 1980).

1.4.3 *INFRASTRUCTURE AND LANDUSE*

The infrastructure in the catchment here includes all population centres, and the roads and railways that connect them. It also includes all road and rail bridging points over the River, and bridges over tributary streams close to the River. These are all depicted in Figure 1.4.

The Whangaehu River flows through a remote region of the North Island. On the Mount Ruapehu ring plain, in the upper catchment of the River (including the Mangawhero River and Waitangi Stream) major population centres are located at Raetihi (pop. *c.* 1,100), Ohakune (pop. *c.* 1,185) and Waiouru (pop. *c.* 2,130). In the middle and lower catchment the only population centres are located at Mangamahu and Whangaehu. In proximity to the River the rural population is probably no more than 4,000 people (Wells and Fowles, 1980; Department of Statistics, Wellington, *pers. comm.*, 1993).

State Highway 49, connecting Ohakune and Waiouru, crosses the upper part of the middle catchment. 11 km east of Ohakune the Whangaehu Valley Road branches to the south and follows the east bank of the channel of the Whangaehu River for much of its length. Access to farm stations on the west bank of the river in the upper middle catchment is by Old Fields Track, which used to be the major route inland to Karioi from Wanganui, via Oruakukuru Road.

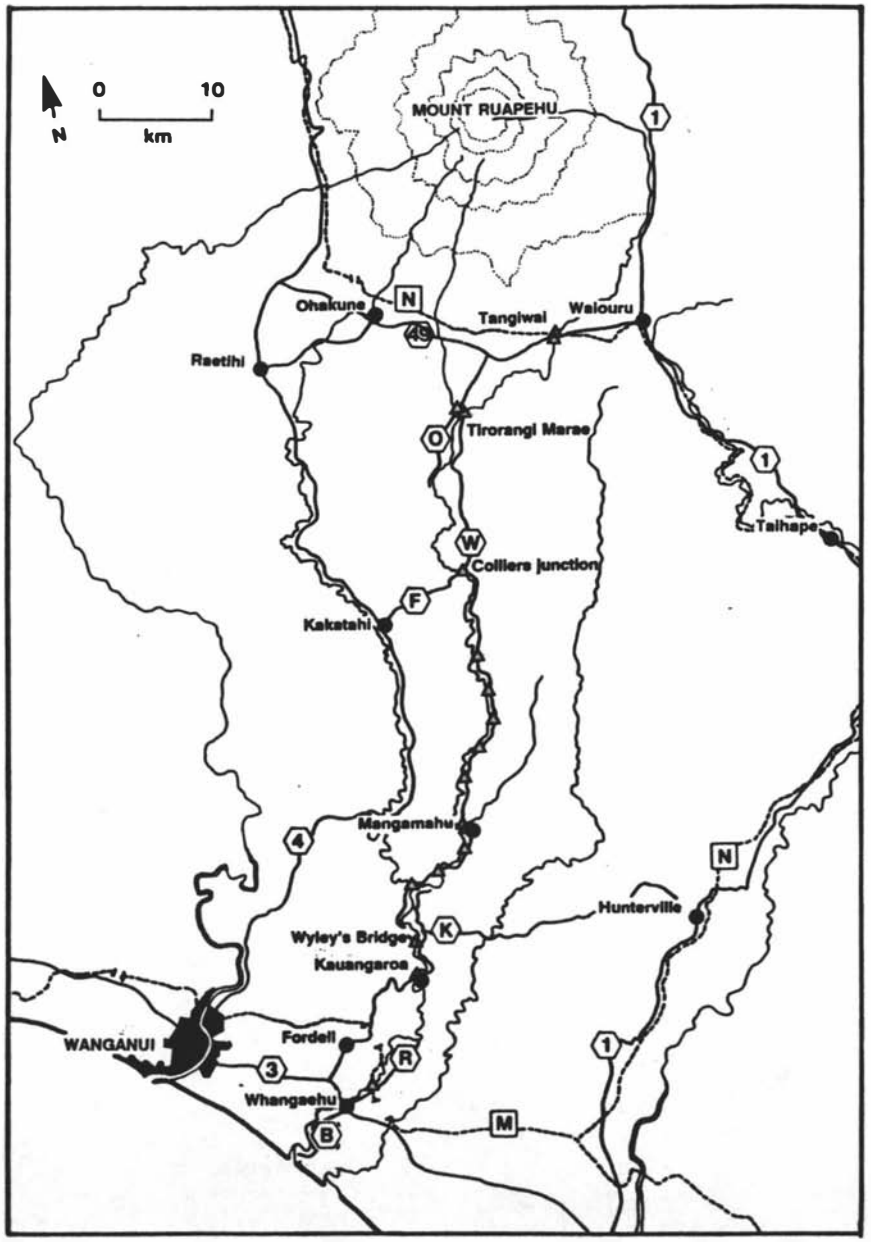

Roads

1	State Highway 1
3	State Highway 3
4	State Highway 4
49	State Highway 49
O	Old Fields Track
W	Whangaehu Valley Road
F	Fields Track
K	Kaungaroa-Mangatipona Road
R	Ruatangata Road
B	Whangaehu Beach Road

Railways

N	North Island Main Trunk Line
M	Marton-New Plymouth Railway

Bridges

Mark all road and rail bridging points over the Whangaehu River

Figure 1.4 Infrastructure in Wanganui and Tongariro Districts.

At Colliers junction, Fields Track joins the Whangaehu Valley Road allowing access to State Highway 4 between Wanganui and Raetihi. At Wyley's Bridge the Whangaehu Valley Road joins the Kauangaroa - Mangatipona Road which provides access to the Turakina Valley Road and to Okirae Road. State Highway 3, between Bulls and Wanganui follows the coastal flats near to the mouth of the Whangaehu River, and access to this main route is via Kaungaroa Road and through Fordell. Access to the lower reaches of the Whangaehu River is by Ruatangata Road and Whangaehu Beach Road which both follow the east bank of the River.

Two railways traverse the Catchment of the Whangaehu River. The North Island Main Trunk Line between Wellington and Auckland crosses from Waiouru to Ohakune, closely following the route of State Highway 49, bridging the Whangaehu River at Tangiwai (see Plate 1.5). The Marton-New Plymouth Railway exits from a tunnel cut through hill country between the Turakina and Whangaehu Valleys, traverses the alluvial coastal plain of the River, and enters another tunnel in hill country east of Fordell. The railway line bridges the Whangaehu River approximately 4 km east of Whangaehu.

Major bridging points are at Tangiwai (road and rail), Tirorangi Marae (road), Colliers junction (road), Mangamahu (road), Wyley's Bridge (road), Kauangaroa (road) and Whangaehu (road and rail). Other bridging points are over the Mangaehuehu Stream at its confluence with the Whangaehu River, at the confluence of the Mangamahu Stream with the Whangaehu River, at Manurewa (below Mangamahu), and over the Mangawhero River above its confluence with the Whangaehu River. In the middle and lower catchment bridges provide access to farm stations sited on the opposite side of the River to that served by the Whangaehu Valley Road.

The principle landuses in the Catchment are agriculture, light industry and recreation. Agricultural landuse was outlined in section 1.4.2.

Industrial landuse is largely confined to the upper catchment and comprises forestry, saw-milling, pulp-milling, and hydro-electric power generation. Forestry in the area commenced in 1927 and this supplies both a saw-mill at Tangiwai and a pulp mill at

Karioi. The Wahianoa Diversion (part of the Tongariro Power Scheme) diverts water from tributaries of the Whangaehu River in the eastern Mount Ruapehu ring plain through a system of subterranean aqueducts into Lake Moawhango. Subsequently the waters pass through the Rangipo Power Station to Lake Rotoaira, and then through the Tokaanu Power Sation to Lake Taupo. A potential scheme currently under investigation by the King Country Electricity Power Board involves damming of the Tokiahuru Stream above its confluence with the Whangaehu River. It is anticipated that water would be diverted through an upper power house, down through a tunnel approximately 20 km long to a second power house below Colliers junction.

Mount Ruapehu lies within the Tongariro National Park (see Figure 1.2). In the first two months of 1993 an estimated 120,000 people visited the Park, this estimate based on the 40,000 visitors to the Department of Conservation Visitor Centre located at the Chateau Tongariro (Staff at the Centre advised the author that approximately one third of tourists in the Park actually visit the Centre). During the winter two major skifields operate on the Mountain (Whakapapa, on the north flank, and Turoa, on the south), and one minor one (Tukino, on the east). On any single day up to 13,000 skiers may be present on the Mountain (J. Allen, Department of Conservation, Whakapapa, *pers. comm.*).

CHAPTER 2

THE WHANGAEHU RIVER AND ITS GEOLOGICAL SETTING

2.1 INTRODUCTION

The Whangaehu River drains the eastern side of Mount Ruapehu which, at an altitude of 2,797m, is the highest mountain in the North Island of New Zealand (see Figures 1.1 and 1.2). It lies at the southern end of the Tongariro Volcanic Centre (TgVC), a linear complex of four andesite volcanoes in the central North Island from north to south named Kakaramea, Pihanga, Mount Tongariro, and Mount Ruapehu (Grindley, 1960; and see Figure 2.1). The Explosion Craters at Ohakune, which are in fact basaltic andesite scoria cones, on the lower south flank of the volcano mark the southern limit of TgVC and the Taupo Volcanic Zone (Cole and Nairn, 1975). The oldest dated lava from Mount Ruapehu is 230,000 years old (Cole *et al.*, 1986). However the maximum age for the onset of volcanic activity from TgVC is unclear. The first occurrence of TgVC-sourced andesite is reported by Fleming (1953) in Nukumaruan Group sediments 1.4 - 1 million years old (Beu and Edwards, 1984) in the Wanganui Basin. In the Rangitikei River valley andesite pebbles are found in Castlecliffian Group sediments 360 - 320,000 years old (Beu and Edwards, 1984). Hence it is believed that TgVC developed during the past 1.4 million years of New Zealand's geological history, corresponding approximately to the Quaternary.

TgVc is bounded to the north by the rhyolitic Taupo Volcanic Centre and to the south by uplifted siltstones, sandstones and limestones of Tertiary and Quaternary age (see Figure 1.3). Mount Ruapehu is built on a basement of Mesozoic greywacke overlain by Tertiary sandstone and siltstone (Gregg, 1960). However Mesozoic strata do not crop out in the vicinity of the Whangaehu River, and it is Wanganui Series strata that form much of the deeply dissected landscape of the middle reaches of the River.

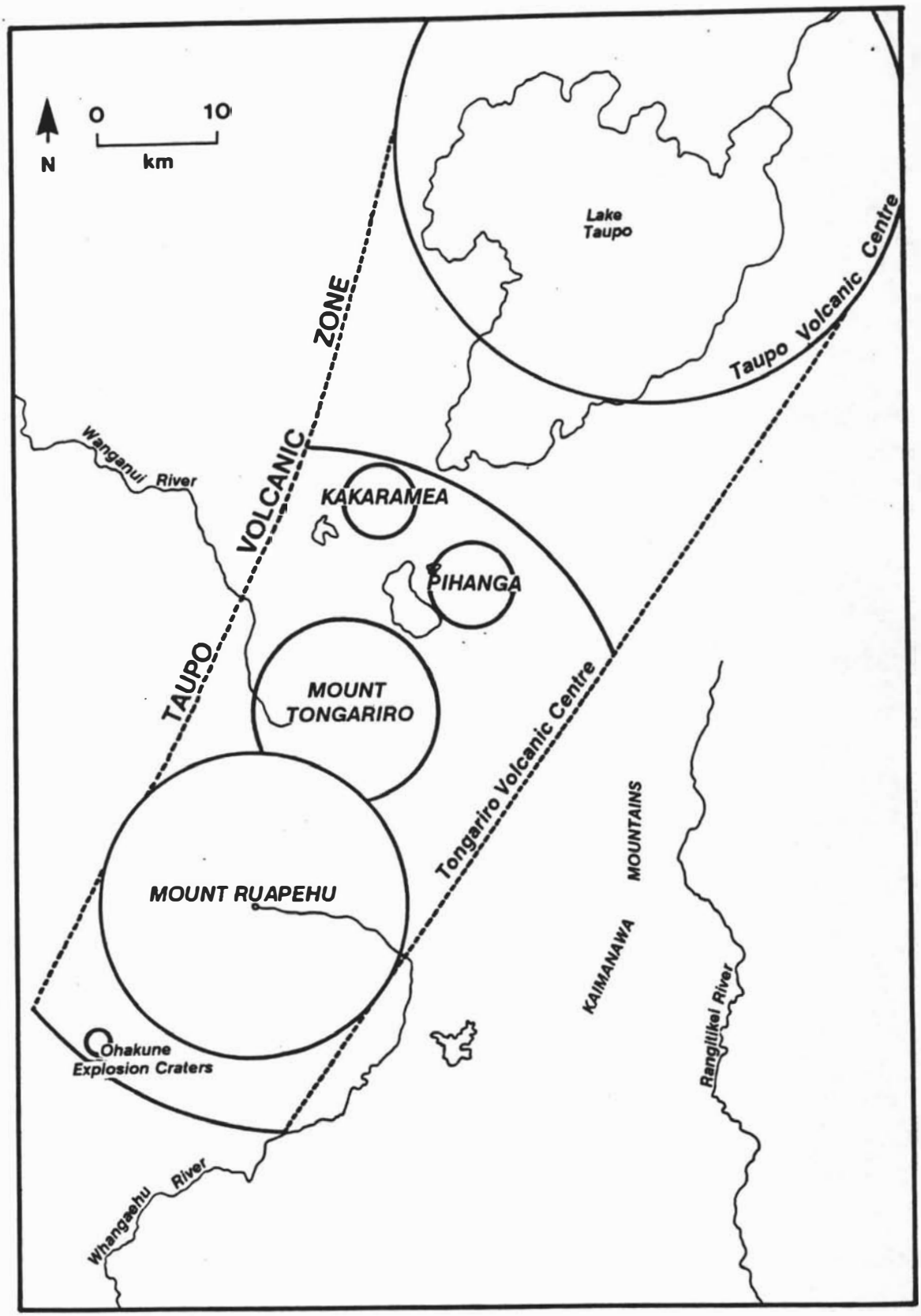

Figure 2.1 The Tongariro Volcanic Centre.

2.2 THE VOLCANIC SETTING

2.2.1 *MOUNT RUAPEHU VOLCANIC CONE STRATIGRAPHY*

Mount Ruapehu volcano is a composite cone which has had a complex history of development reflecting several cone-building episodes. Hackett (1985) defined four formations each corresponding to a cone-building episode (see Figure 2.2). In the north is the Te Herenga Formation (*c.* > 120,000 years old) comprising the deeply eroded remnants of a central and flank vent association and proximal cone-building facies. Source vents for the Te Herenga Formation are thought to lie in the north and northwest of Mount Ruapehu. Next youngest is the Wahianoa Formation (*c.* 120,000 to 60,000 years old) which comprises central and flank vent, proximal cone-building, and distal ring plain facies (Hackett and Houghton, 1989). Source vents are thought to lie in the southeast quadrant of Mount Ruapehu. Both Te Herenga and Wahianoa Formations are of andesitic composition.

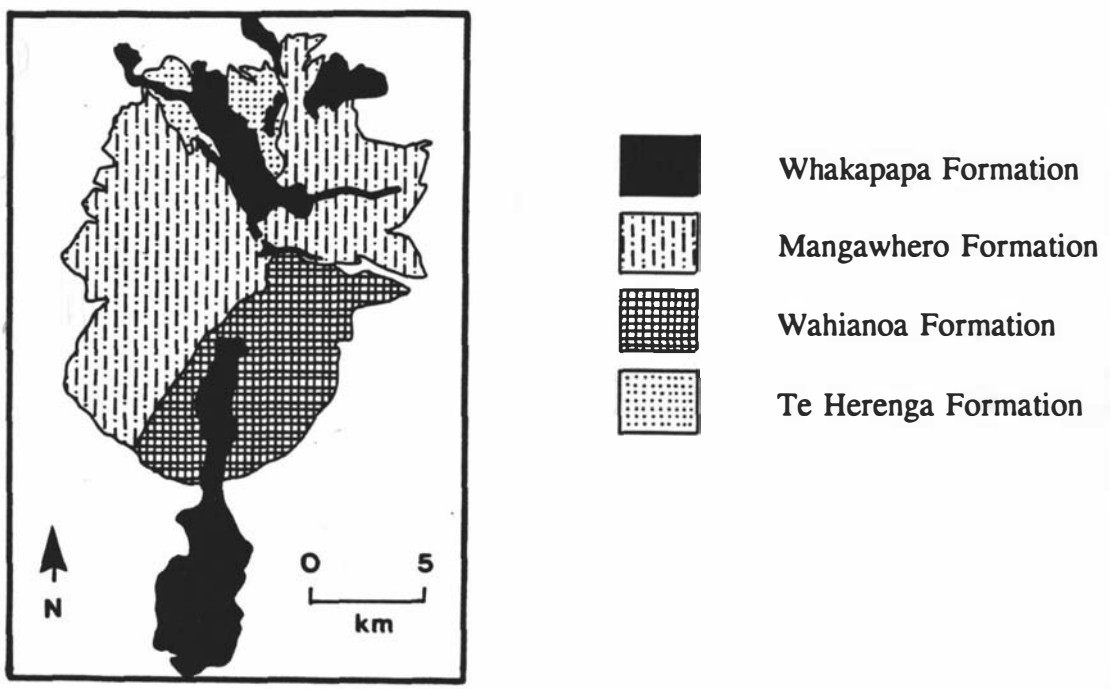

Figure 2.2 Lithostratigraphy of the Mount Ruapehu volcanic cone, adapted from Hackett and Houghton (1989).

Stratigraphically above the Wahianoa Formation is the Mangawhero Formation (*c.* 60,000 to 15,000 years old) of a basalt to dacite composition. This Formation occupies the present summit region of Mount Ruapehu. A subsequent cone-building facies which includes the present summit and flank vents is distributed widely over the volcano and mapped as Whakapapa Formation.

2.2.2 *MOUNT RUAPEHU RING PLAIN STRATIGRAPHY*

The stratigraphy of the Mount Ruapehu ring plain is dominated by deposits from lahars. These represent periods of aggradation in response to flank collapses, volcanic eruptions and Crater Lake outbursts. Aggradation in post- and inter-eruption intervals continues as a result of reworking of volcaniclastic debris by lahars during high rainfall storm events. The presence of an extensive winter snow cover, glacier ice and a crater lake on Mount Ruapehu all provide potential sources of water for initiation of lahars. The Crater Lake drains through a subglacial tunnel into the headwaters of the Whangaehu River and both the historic and geologic record provide evidence that the Whangaehu River has been a major conduit for lahars from Mount Ruapehu.

Lahars tend to follow existing river channels, hence their deposits are largely confined to the existing river courses. Large events, with discharges greater than the bankfull discharge of the river or stream occupied, then spill over and flood adjacent low-lying areas. Most of the deposits preserved on the ring plain are of this nature; the deposits of smaller events confined to the channel of the stream are liable to be incorporated into subsequent events and are unlikely to leave any geological evidence. With increasing distance from Mount Ruapehu, lahars reach the outer margin of the ring plain and become confined to deeply dissected and tortuous river valleys. Deposits from lahars are found perched on terraces above the river, on meander cutoffs and are best preserved in side valleys where tributary streams feed into the main channel.

2.2.2.1 *The Waimarino and Murimotu Lahars*

The oldest volcaniclastic deposits of the Mount Ruapehu ring plain were mapped by Grindley (1960) and Hay (1967) at the 1:250,000 scale as the Waimarino Lahars. These are overlain by coverbeds which include the Kawakawa Tephra, a widely dispersed tephra from the Taupo Volcanic Centre dated at *c.* 22,500 years B.P. (Wilson *et al.*, 1988). Much of the older ring plain material to the southeast of Mount Ruapehu, investigated by Donoghue (1991), is buried by more recent deposits. Topping (1974) asserts that many of the deposits originally mapped by Hay (1967) as Murimotu Lahars properly belong to the Waimarino Lahars. Waimarino Lahars virtually encircle Mount Ruapehu and in the north abut Mount Tongariro-sourced Rangipo Lahars (Grindley, 1960).

Overlying Waimarino Lahars to the northwest of Chateau Tongariro are conspicuous mounds which were informally referred to as the Murimotu Lahars and were first described by Grindley (1960). These mounds were in fact derived from a collapse (debris avalanche) of Te Herenga Formation deposits from the western sector of the volcanic edifice. The date of this collapse has been determined as *c.* 9,540 years B.P. from a piece of wood found within Murimotu Lahar deposits (Topping, 1974). Subsidiary laharic deposits form the lateral margins of the event as well as being found in low lying zones between the debris avalanche mounds. The debris avalanche mounds and lahar deposits are collectively referred to as the Murimotu Formation (Palmer and Neall, 1989).

2.2.2.2 *Lahar deposits on the Southeast Mount Ruapehu ring plain*

Purves (1990) and Donoghue (1991) detail the stratigraphy and chronology of volcaniclastic deposition on the southeastern sector of the Mount Ruapehu ring plain. Careful mapping and correlation of lahar deposits has allowed for a comprehensive assessment of the impact of rapid sediment influx from lahars in a proximal situation. Ring plain aggradational sequences comprise deposits from normal streamflow, hyperconcentrated flow and debris flow. Recent aeolian sand dunes mantle large areas, but do not appear to have been significant land-forming elements in the geological past.

Donoghue (1991) defines four formations, each corresponding to discrete aggradational episodes during the late Quaternary (see Figure 2.3). The oldest deposits are exposed in bluffs above the upper Whangaehu River to the north of Waiouru. These deposits are referred to as the Te Heuheu Formation and accumulated during the late Pleistocene. The timing of the onset of debris flow and hyperconcentrated flow accumulation within the Te Heuheu Formation is not clear, but may have coincided with the onset of climate deterioration during the Otiran (last) glacial. Donoghue (1991) highlights the problem in distinguishing between volcanic and glacial deposits. Glaciation was much more extensive during the Otiran than at present (M^{c}Arthur and Shepherd, 1990) and hence the supply of clastic material to the fluvial system was increased. However, Te Heuheu Formation deposits are dominantly of laharic rather than glacial origin. Glacial and fluvioglacial deposits appear to be confined to the upper reaches of the ring plain and it seems likely that much of the detrital material incorporated into the lahars was of glacial or fluvioglacial origin. Te Heuheu Formation is overlain by Rerewhakaaitu Tephra, dated at *c.* 14,700 years old (Froggatt and Lowe, 1990)[1] and this provides an upper age limit for emplacement of the lahar deposits. Deposits from the Te Heuheu Formation extend throughout the southeastern ring plain and are recognised as being the major constructional surface in the Waiouru region.

The fluvial and laharic deposits of the Tangatu Formation accumulated during a period of intense eruptive activity in the late Pleistocene and early Holocene. Upper and lower bracketing ages for the Formation are provided by the Motutere Tephra, *c.* 5,370 years old, which rests at the base of coverbeds which overlie the Formation, and the presence of Rerewhakaaitu Tephra, *c.* 14,700 years old, below. The Rerewhakaaitu Tephra overlies a widespread erosional unconformity. During the earlier part of this time large volumes of tephric material were erupted and are formally recognised as the Bullot Formation (Donoghue, 1991). These tephras were directly mobilized into lahars that descended former drainage channels. Between eruption phases storm events continued to generate lahars that remobilized the unconsolidated tephras. Tangatu Formation debris flow and hyperconcentrated flow deposits are dominantly pumiceous in nature.

---

[1]Donoghue (1991) used the date (NZ716) of 14,700 ± 200 years B.P. for the Rerewhakaaitu Tephra published by Vucetich and Pullar (1973). In this study the date of 14,700 ± 110 years B.P., a mean of 3 dates, published by Froggatt and Lowe (1990), is used.

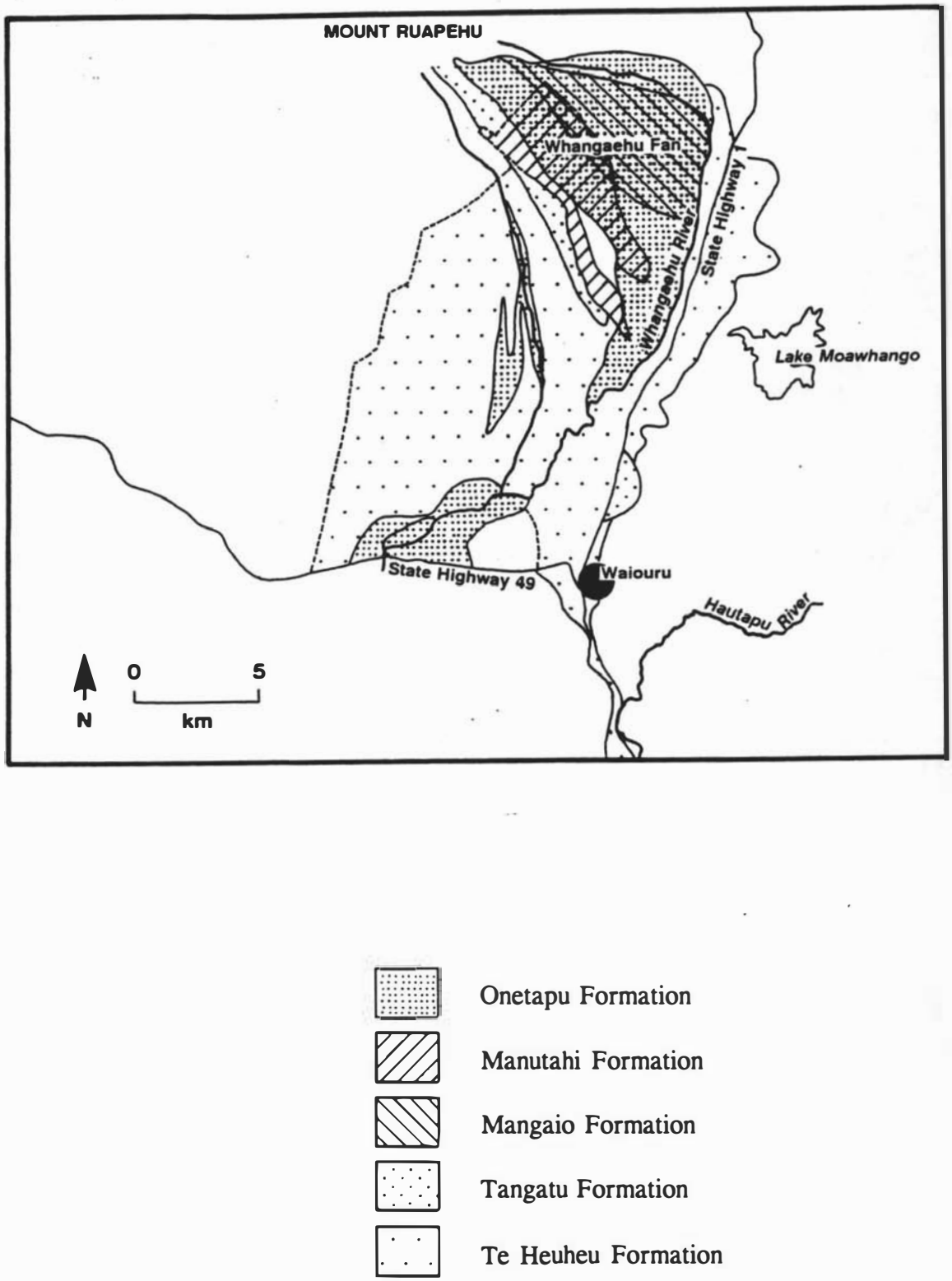

Figure 2.3 Lithostratigraphy of the Southeast Mount Ruapehu ring plain, adapted from Donoghue (1991).

The Manutahi Formation is comprised principally of sands and gravels, with common pumice pebbles, that accumulated during a period of rapidly aggrading fluvial and hyperconcentrated flows. Donoghue (1991) interprets Manutahi Formation as being

derived from floods resulting from ablation of summit glaciers during the early-mid Holocene. Overlying these deposits is the Mangaio Formation, a debris flow which resulted from collapse of a hydrothermally altered eastern sector of the volcano. The Mangaio Formation has been dated at *c.* 4,600 years B.P. (Donoghue, 1991). Mangaio Formation is lithologically quite distinct from Manutahi Formation. The boundary between the Manutahi Formation and the older Tangatu Formation is marked by the presence of the Motutere Tephra which is *c.* 5,370 years old. An upper age for Manutahi and Mangaio Formations of *c.* 3,300 years B.P. (Froggatt and Lowe,1990) is supplied by overlying Waimihia Tephra[2].

The recent prehistoric and historic lahar deposits from Mount Ruapehu are mapped as the Onetapu Formation. These deposits overlie Manutahi and Mangaio Formations and, where present, the Taupo Ignimbrite, which is dated as *c.* 1,850 years B.P. (Froggatt and Lowe, 1990). It has been proposed that Crater Lake developed at the time of onset of the Formation, based on a shift from magmatic to phreatomagmatic tephra eruptives (Donoghue, 1988) and a change in the nature of lahar deposits. The youngest deposits mapped correspond to one of the most recent lahars of historical times (Purves, 1990) when in 1975 an eruption in Crater Lake ejected 1.6×10^6 m^3 of Crater Lake water. This created lahars in many of the rivers that drain Mount Ruapehu. In the Whangaehu River the total discharge for the 24 April 1975 lahar was 1.8×10^6 m^3. Purves (1990) identifies deposits from this event dispersed widely throughout the channels on the Whangaehu Fan where they typically form boulder lags, or thin sandy veneers.

The Whangaehu Fan is a distinct geomorphological feature on the Mount Ruapehu ring plain and comprises lahar deposits of Onetapu Formation (see Figure 1.2). Older Onetapu Formation deposits preserved on the ring plain record much larger lahars. These are thicker and more extensive than historic age Onetapu Formation deposits. Purves (1990) was able to distinguish between lahar deposits on the basis of clast and matrix characteristics. He recorded twelve individual events from units that followed closely in time after the Taupo Ignimbrite eruption. Field descriptions of Onetapu Formation age lahars by Purves (1990), Donoghue (1991) and in this thesis, combined with historical evidence, now complete the record of post-Taupo Ignimbrite lahar events

---

[2]Donoghue (1991) used an approximate age of 3,400 years B.P. (Healy, 1964) for the Waimihia Tephra. In this study the date of 3,280±20 years B.P., a mean of 17 dates, published by Froggatt and Lowe (1990), is used.

throughout the entire catchment of the Whangaehu River. A total of thirty-five events were recorded in this study. A chronology for the prehistoric lahars has been established by radiocarbon dating of interbedded peats and wood found associated with their deposits. The dated record reveals intervals of instability and aggradation, resulting from eruptions or lake-breakouts, followed by periods of stability when soils and tree stumps are found between deposits. Deposits are observed to pinch out with distance from source, and only deposits from the largest lahars are preserved in distal areas.

2.2.2.3 *Holocene lahar deposits on Northwest Mount Ruapehu ring plain*

A complex record of post-Murimotu Formation lahar aggradation on the Northwest Mount Ruapehu ring plain has been elucidated by Palmer (1991). Her study shows that prior to the eruption of the Mangatawai Tephra Formation, *c.* 2,500 years B.P. (Topping, 1973), the Whakapapanui Stream was the major route for lahars. Subsequently the Whakapapaiti Stream has become a major route for lahars to the northwest of Mount Ruapehu. A divergence in lahar routes occurred between 2,500 and 2,000 years ago when lahar deposits accumulated in the Waiere Stream, which drains to the north of Pinnacle Ridge.

2.2.3 *LAHAR DEPOSITS IN THE RIVER VALLEYS THAT DRAIN MOUNT RUAPEHU*

A review of the distribution of lahar deposits in the major river valleys that drain Mount Ruapehu and the Central North Island is presented by Gregg (1960). Initially many of these deposits were interpreted to have been laid down by glaciers, and Park (1910) refers to the great Waiouru, Waimarino, and Hautapu glaciers. In 1931 Grange astutely proposed that these were emplaced by lahars from Mount Ruapehu and were attributable to "*...eruption from a crater-lake, or...the action of rain and volcanic ash during or following an eruption...*". Gregg expands on this by adding that "*As the lahars took place in the Pleistocene, melting of the more extensive glaciers by the eruption of hot material may have provided much of the water for these tremendous floods*".

Te Punga (1953) mapped a deposit of large andesitic boulders from Mount Ruapehu which he named the Hautapu Valley Agglomerate. He attributed the deposit to a single huge lahar that flowed down this valley up to 250 km from source. As a result of vertical movement along the Whangaehu fault during accumulation of the Te Heuheu Formation the Mount Ruapehu-sourced headwaters of the Hautapu River were cut off (Donoghue, 1991) *c.* 14,700 years B.P. and subsequently no younger lahars have travelled this route.

Fleming (1953) discussed the distribution of a widespread, poorly sorted valley-fill consisting of "***...scoriaceous, poorly rounded andesitic rubble, grit, breccia, and conglomerate...***" within the valley of the Whangaehu River. He called it the "***Whangaehu valley-fill***" and hypothesised that the deposits might have been lain down by "***...turbid, overloaded rivers..after periodic eruptive or mudflow activity in the volcanic regions at their headwaters...***". These deposits are now recognized to have resulted from a collapse from the southern flank of Mount Ruapehu *c.* 160,000 years ago (see Chapter 4, this study).

Lahar deposits in the Manganuiateao River have only recently been mapped, and two suites of deposits are recognized. The first form a distinct *c.* 60,000 year old valley-wide terrace and are considered to have been emplaced by a single lahar event. A further *c.* 10,000 year old lahar deposit is mapped in the Valley which may represent distal detritus from an event coeval with emplacement of the Murimotu Formation (Hodgson and Neall, 1993).

More recent deposits in the valley of the Whangaehu River are described by Campbell (1973). He examined gravelly deposits exposed in a metal pit north of Mangamahu, approximately 134 km from Mount Ruapehu, and asserted that they had accumulated in response to episodic laharic activity. Four discrete lahar deposits were identified which Campbell interpreted to have accumulated sometime following deposition of the Taupo Ignimbrite (which is found at this locality), some time after 1,850±50 and before 756±56 years B.P., between 756±56 and before 407±70 years B.P., and after 407±70 years B.P. (Campbell, 1973). These deposits correspond in age and stratigraphic position to Onetapu Formation lahar deposits described by Donoghue

(1991). The fourth lahar deposit, which Campbell believed predated the Taupo Ignimbrite, has here been correlated to an informal member of the Onetapu Formation. The clasts in the Taupo Ignimbrite deposit exposed at Managamahu are well rounded and it is believed that the pumice is reworked rather than primary.

Historically lahars have flowed down the Whakapapanui and Whakapapaiti Streams, the Mangaturuturu River (which eventually drains into the Manganuiateao River) and Whangaehu River. All these Rivers were impacted by lahars following eruptions in 1969 and 1975 (Paterson, 1976; Healy *et al.* 1978; Nairn *et al.* 1979). In 1975 small lahars also flowed down the Wahianoa, Mangatoetoenui and Mangaehuehu Streams (see Figure 2.4).

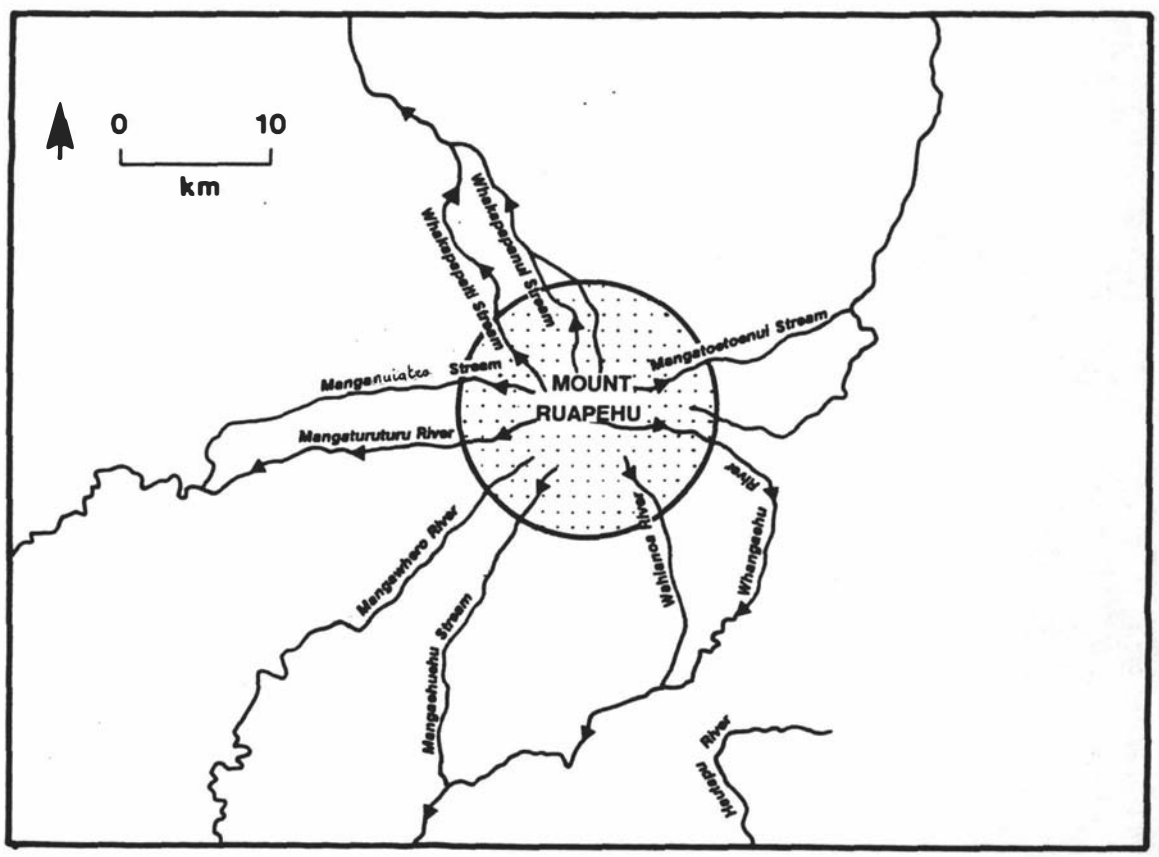

Figure 2.4 Map showing major rivers and streams that drain from Mount Ruapehu. Arrows indicate the routes taken by historic lahars.

2.3 QUATERNARY TEPHROSTRATIGRAPHY

The Quaternary history of the Central North Island has been strongly influenced by large eruptions from the rhyolitic volcanic centres in the north of the Taupo Volcanic Zone (see Figure 2.5). Both voluminous and extensive, the products of these eruptions have dominated landscape development in proximity to their source areas. The airfall equivalents of the major eruptions mantled large areas of the palaeo-landscape and now provide useful time marker planes. Fall out patterns are determined largely by prevailing southwesterly winds; hence, with distance south away from Lake Taupo products of the eruptions are sparse and generally tephras from only the largest of the eruptions are preserved.

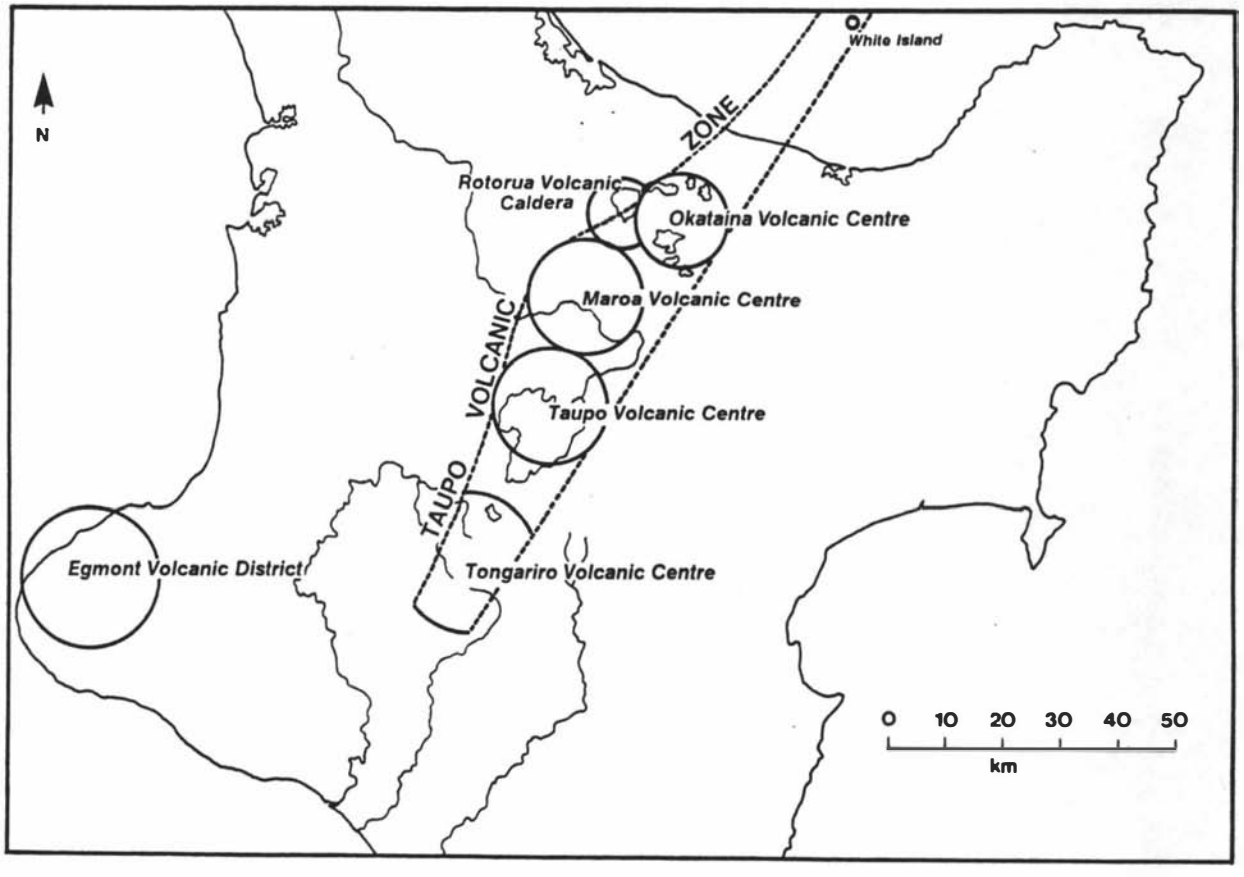

Figure 2.5 The Taupo Volcanic Zone with associated volcanic centres, and Egmont Volcanic District.

Upper Pleistocene Okataina- and Taupo Volcanic Centre-sourced tephra are found in cover bed sequences both close to the mountain and in distal coastal regions. Topping and Kohn (1973) and Donoghue (1991) detail the stratigraphy and distribution of a number of both Okataina- and TVC-sourced tephras which are found in the Tongariro region. On the Mount Ruapehu ring plain these interdigitate with Mount Tongariro- and Mount Ruapehu-sourced tephras which record the late Quaternary eruptive activity from these southern volcanoes (Topping, 1973; Donoghue, 1991).

Campbell (1977), while mapping the soils of Whangaehu Valley, recognized both reworked Kawakawa Tephra and Taupo Ignimbrite which had been washed down the Whangaehu River. Fleming (1953) describes a number of reworked rhyolite tephras which are exposed in sediments ranging from Pliocene through to Holocene age. Low-lying areas of Wanganui city are built on *c.* 2 m thick deposits of reworked Taupo Ignimbrite which have been washed down the Wanganui River.

Major Pleistocene rhyolite eruptions recorded in coverbed sequences of the Wanganui Basin (Pillans, 1988) are the Taupo Ignimbrite, 1,850±10 years B.P. (Froggatt and Lowe, 1990), the Kawakawa Tephra, 22,590±230 years B.P. (Wilson *et al.*, 1988), the Rotoehu Tephra, dated by Potassium-Argon [K-Ar] methods at 64,000±4,000 yrs B.P. (Wilson *et al.*, 1992), Upper, Middle and Lower Griffin Road Tephras, the Fordell Ash, and the Rangitawa Tephra, dated by zircon fission track [ZFTA] methods at 350,000±40,000 yrs B.P. (Kohn *et al.*, 1992).

The most persistant tephric time plane in the regional stratigraphy of the Whangaehu River is the Kawakawa Tephra, representing the outfall from a catastrophic *c.* 500 km^3 in volume (Wilson *et al.*, 1988) late Quaternary eruption from Lake Taupo.

2.4 THE QUARZTOFELDSPATHIC SETTING

The underlying geology of the landscape through which the Whangaehu River flows comprises uplifted marine sediments of Tertiary and Quaternary age (see Figure 1.3). The oldest deposits are found in proximity to Mount Ruapehu where Grindley (1960)

mapped lower Wanganui Series sediments which crop out in bluffs facing the south slopes of the volcano. Fleming (1953) presented a major comprehensive investigation of Tertiary and Quaternary sediments in the Wanganui Subdivision. Much of this has subsequently been revised, particularly in the north of the Wanganui region (Pillans, 1988 & 1990); however in the lower reaches of the Whangaehu River much of what Fleming reported remains applicable today.

2.4.1 QUATERNARY CLIMATE CHANGE

Perhaps the most complete and continuous record of Quaternary environmental change has been provided by deep sea cores. Imbrie *et al.* (1984) state that the long and relatively undisturbed record preserved in deep sea sediments provides an ideal medium for obtaining a chronology of past climatic events. Observations of oxygen isotope ratios in these sediments provide information about past ice volumes and ocean surface temperatures. Emiliani (1955) pioneered a method of analysis of these cores which involved measuring isotope variations in planktonic foraminifera. The isotope variations occur as a function of the waxing and waning of global ice sheets in response to astronomically forced climate change (Shackleton and Opdyke, 1973; Imbrie *et al.*, 1984). Since the pioneering work of Emiliani a number of deep ocean cores have been sampled and analysed from open-ocean sites throughout the world. A detailed master chronology of oxygen isotope ratios and magnetic variation has now been developed which extends through the past *c.* 900,000 years, providing a continuous record of climate change during the Pleistocene unmatched elsewhere in the geological record. The chronology proposed by Shackleton and Opdyke (1973) and adopted by Imbrie *et al.* (1984) will be applied in this thesis because of its use as a globally accepted palaeoclimatic reference tool.

2.4.2 *THE QUATERNARY OF NEW ZEALAND*

The Quaternary stratigraphy of New Zealand is represented by a wealth of marine and terrestrial sediments. Subdivision of the Quaternary System has been based on either

marine biostratigraphy or climatostratigraphy. The internationally recognised Plio/Pleistocene Boundary, which marks the beginning of the Quaternary, is now placed at 1.63 million years ago within sedimentary strata at Vrica in Italy. In New Zealand the preferred boundary in the past has been placed at the base of the Nukumaruan Stage, *c.* 2.2 million years ago (Beu and Edwards, 1984). It is marked by the influx of Pleistocene index fossils *Phialopecten triphooki*, *Chlamys patagonia delicatula*, *Globoratalia crassula* and *G. crassaformis* (Beu, 1969; Beu and Edwards, 1984). The International Plio/Pleistocene Boundary is now placed above the middle of the Nukumaruan Stage; at the Nukumaruan type section this lies just above the Pukekiwi Shell sand (Beu and Edwards, 1984). In New Zealand no index fossils mark this zone.

Pillans (1991) reviewed the Quaternary stratigraphy of New Zealand, drawing on information from the Wanganui Basin marine sequence, together with glacial, alluvial and loess deposits in both the North and South Islands. In the Wanganui Basin correlation with the oxygen isotope record is corroborated for at least the last 500,000 years by a terrestrial cover bed stratigraphy on exposed marine terraces. Palaeoenvironmental reconstruction is based on the interpretation of temporal changes in biostratigraphy, utilizing both pollen assemblages in terrestrial sediments and palaeofaunas in marine strata. The oldest Quaternary record can only be determined from marine sediments.

The marine strata exposed in the Wanganui Basin reveal cycles of sedimentation which can be interpreted to correspond to periods of eustatic sea level change. By careful interpretation of the sequence stratigraphy coupled with time control provided by dated interbedded rhyolite pumices, Beu and Edwards (1984) have been able to correlate the Wanganui Basin stratigraphy to Pacific Core V28-238 of Shackleton and Opdyke (1973).

2.4.2.1 *Defining the late Quaternary*

During the late Quaternary there have been a number of climatic fluctuations ranging from temperatures close to present through to periods of intense cold. The cold periods

(or stadials) were of sufficient severity and duration to leave a permanent record of loessal and glacial deposits in both the North and South Islands of New Zealand. A vital part of the Southern Hemisphere glacial record is found in relict moraines and outwash surfaces preserved in the South Island of New Zealand. Suggate (1990) recognises deposits from four glacials (Nemona, Waimaunga, Waimea and Otira glacials) that have occurred during the Quaternary based on evidence compiled from a number of locations throughout the South Island. In the North Island, these glacials are represented by loess sheets which are best preserved in the Wanganui-Rangitikei River region. Milne and Smalley (1979) distinguish five separate loess sheets above the Rangitawa Tephra which was erupted *c.* 350,000 years ago near the end of oxygen isotope stage 10. This time horizon equates with the boundary between Castlecliffian and Haweran Stage deposits in the Wanganui Basin, defined as the top of the Putiki Shellbed (Beu *et al.*, 1987; Pillans, 1991). The late Quaternary is here defined as representing the interval of time from the eruption of the Rangitawa Tephra, approximately 350,000 years ago, up until the present day.

A summary diagram of the New Zealand Quaternary litho- and chronostratigraphy is presented in Figure 2.6, below.

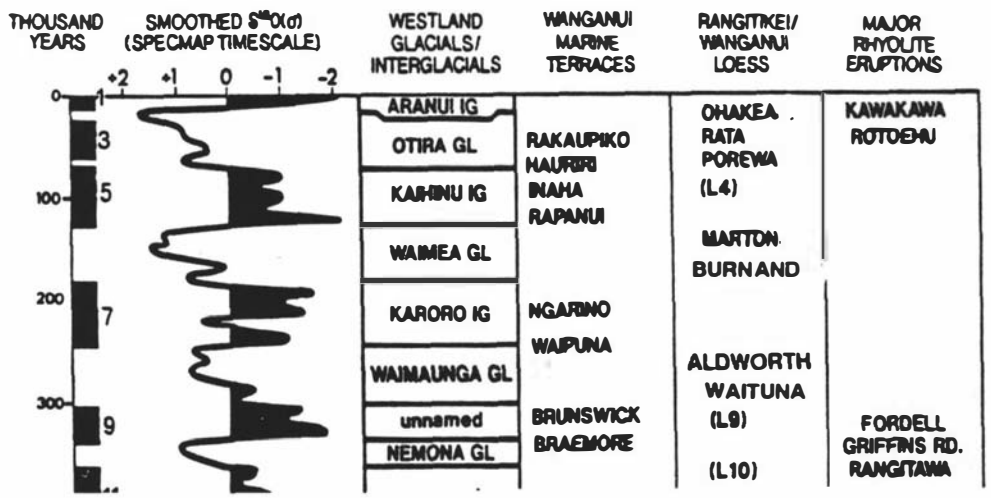

Figure 2.6 Late Quaternary litho- and chronostratigraphy, from Pillans (1991).

2.4.2.2 *Late Quaternary loess stratigraphy*

The Rangitawa Pumice, here used to define the lower limit of the late Quaternary, lies within a loess sheet, L10, which Pillans estimates to have accumulated between 370,000 and 340,000 years ago. Loess L9 is believed to have accumulated between the cutting of the Braemore Marine Terrace at *c.* 340,000 years ago (Pillans, 1988; Bussell and Pillans, 1992), and cutting of the Brunswick Marine Terrace at *c.* 310,000 years ago. Pillans (1988) recognizes two loess sheets which would have accumulated during the Waimungan glacial; the Aldworth and Waituna loess which he infers to have accumulated during oxygen isotope stage 8, between 270,000 and 240,000 years ago.

Between approximately 240,000 and 180,000 years ago, and corresponding to oxygen isotope stage 7, the Ngarino Marine Terrace was cut and, inland, dunesand was deposited on older terrace surfaces (Pillans, 1988). In the Rangitikei River Valley up to 10 m of sands were deposited (Milne and Smalley, 1979). Pillans also recognizes the presence of a well developed palaeosol, in northwestern Wanganui coverbeds, which formed at this time. This period of ameliorating climate correlates to the Terengian interglacial of Suggate (1990).

Milne and Smalley (1979) propose that during the penultimate glacial period, which Suggate called the Waimean glacial, there were two cold episodes separated by warmer intervals. During the earlier cold period, called the Burnandan stadial, accumulation of Burnand loess was interrupted by sporadic inputs of rhyolite tephra. Milne and Smalley contend that this loess accumulated between 180,000 and 170,000 years ago, sometime early in Oxygen Isotope Stage 6. Marton loess accumulated between 140,000 and 130,000 years ago during the Martonan stadial which corresponds to Oxygen Isotope Stage 6.

In the Rangitikei coverbed sequences the Oturian interglacial is represented by either a very distinct, well developed palaeosol indicative of a prolonged period of warmer climate, or by dunesands, *e.g.* Mount Stewart Dunesand, which accumulated between *c.* 125,000 and 120,000 years ago (Milne and Smalley, 1979). At this time the Rapanui Marine Bench was cut, approximately 120,000 years ago, or during oxygen isotope stage 5e (Bussell, 1992).

Absent in Rangitikei cover bed sequences are loesses which accumulated immediately following the cutting of the Rapanui marine bench during oxygen isotope stage 5e. These additional loesses have been observed in exposures in Taranaki (Alloway *et al.*, 1987), the Wanganui Basin (Pillans, 1988) and are described in this thesis. Alloway believes the two loesses in the Taranaki sequence (Huirangi and Kaimata loess) to have accumulated during oxygen isotope stages 5d and 5b. Pillans also later recognised a single loess sheet, L4, which he estimated to have accumulated between 120,000 and 100,000 years ago.

The Porewan loess, which accumulated during the Porewan stadial, is separated from the Ratan loess by a palaeosol. Within this palaeosol are Tongariro Volcanic Centre-sourced tephras which were probably erupted sometime late during the Porewan stadial (Milne and Smalley, 1979). Other workers (Alloway *et al.*, 1987, and Hodgson, this volume, see Chapter 4, section 4.4.2.2) report the presence of a rhyolite tephra, the Rotoehu Tephra, in the palaeosol on Porewa loess. An age estimate of c. 64,000 years old (K-AR, Wilson *et al.*, 1992) for the tephra suggests that the Porewan stadial may have lasted a longer period of time than the 80,000 to 70,000 years ago estimated by Milne and Smalley (1979). Clearly the Porewan stadial corresponds to oxygen isotope stage 4. Following the Porewan, and prior to emplacement of the next loess sheet, was a period of ameliorating climatic conditions, the Orouan interstadial (Milne, 1973b).

The penultimate loess sheet, the Rata loess, accumulated during the Ratan stadial between 40,000 and 32,000 years ago, during oxygen isotope stage 3. A palaeosol developed into Rata loess records a period of warmer climate prior to the Ohakean stadial. The Ratan stadial was followed by the Apitian interstadial, which marks a warmer climatic interval prior to the last stadial (Milne, 1973b).

The most recent loess sheet, the Ohakea loess, accumulated during the Ohakean stadial (Milne and Smalley, 1979), *i.e.* during the most recent climatic deterioration towards the end of the Otiran glacial (Suggate, 1990). The Ohakea loess is distinguished by the presence of Kawakawa Tephra which lies in loess approximately one third of the thickness above its contact with the underlying palaeosol. Milne and Smalley (1979) suggest that the Ohakea loess accumulated between 25,500 and 9,480 years ago. The younger age they propose for the upper boundary of the Ohakean stadial is supported by Marden and Neall (1990) who date the termination of the Ohakean stadial at *c.* 10,350 years B.P.

2.4.3 *REGIONAL LANDSCAPE DEVELOPMENT DURING THE LATE QUATERNARY*

The Quaternary of the region investigated in this study is characterised by the steady uplift of marine sediments coupled with global fluctuating sea levels. Major marine transgressions, indicating warmer interglacial conditions, are represented by sea cliff cutting and landward migration of shorelines. During stadials the sea level falls (as water is stored in global icesheets). The severe climate reduces vegetation cover resulting in landscape instability and increased erosion, more especially at higher altitudes (Pillans, 1991). The rivers respond by aggrading their beds, as they are unable to transport the increased amounts of bedload debris through the fluvial system, and broad-valleyed braided river systems develop. Milne (1973a) proposed that the river terraces mantled with fluvial gravels in the Rangitikei River each represented these cold climate episodes. Coverbeds overlying the terraces record the cool episodes in the form of loess. The loess accumulated by aeolian transportation of silts and clays from the wide aggradational floodplains of the braided rivers onto the surrounding landscape (Cowie, 1964). Palaeosols developed within the upper parts of these loess sheets represent warmer climate intervals when soil development was stronger due to the more favourable conditions for plant growth. Interbedded tephras provide the age control for dating these climatic fluctuations.

In the Whangaehu Valley this pattern of landscape development was accompanied by sporadic injections of volcaniclastics into the River's headwaters in response to volcanic activity at Mount Ruapehu. Lahar deposits in the Valley preserve the record of the mobilization of these volcaniclastics down through the River Valley. In this southerly draining Catchment, away from the prevailing regional winds, these lahar deposits provide the main evidence for volcanism at source.

CHAPTER 3

LAHARS: DEFINITION AND TERMINOLOGY

3.1 INTRODUCTION

The term "***lahar***" is an Indonesian word which is used in the local language to describe the phenomenon of hot and cold mudflows which are a frequently occurring event on Indonesian volcanoes (Van Bemmelen, 1949). Van Bemmelen used the word to describe both the flow event and its deposits, defining it as meaning "***volcanic breccias transported by water***". It had previously been used by Scrivenor (1929) who presented an account of the 1919 eruption from the crater lake on Mount Kelut, also in Indonesia, and the ensuing mudstreams, or lahars. It was also used by Escher (1922) when describing deposits in the Valley of Ten Thousand Smokes in Alaska. Recently "***lahar***" has become the commonly used term of the scientific community when referring to events of this nature. The expression "***volcanic mudflow***" is generally adopted by journalists and reporters as a more familiar term for the public although there is a certain amount of controversy over its use. The two terms lie at extremes in the debate; volcanic mudflow is argued to be too specific (Harrison and Fritz, 1982; Scott, 1988), and lahar too general and/or ambiguous (Smith, 1986), when used to describe an event whose behaviour traverses rheological boundaries, and whose deposits embrace a wide range of grain sizes and distributions. Having deliberated the arguments for and against the continued use of each term, and taking into consideration recently proposed definitions (see later in text), lahar is the preferred term used in this text.

3.1.1 *DEFINITION OF THE TERM "LAHAR"*

During the 1989 Penrose Conference on influences on terrestrial sedimentation, a discussion group involving all conference participants dealt with the controversy over the misuse and misunderstanding of the term "***lahar***". This was precipitated as a result of the feeling that, because of the interdisciplinary approach to volcaniclastic research, the

lack of standard terminology and definition between research groups was impeding communication. It was argued that the term "***lahar***" be retained and be defined as a "***general term for a rapidly flowing mixture of rock debris and water (other than normal stream flow) from a volcano. A lahar is an event; it can refer to one or more discrete processes, but does not refer to a deposit***" (Smith and Fritz, 1989).

Careful observation of the flow behaviour of lahars and detailed field descriptions of resultant deposits has allowed the recognition of similar past events in the geological record. Lahars are now recognized to be one of the major hazards from volcanoes, especially since their portent for destruction is now well established following disasters in Colombia (Nevado del Ruiz, 1985), New Zealand (Tangiwai, 1953), the United States of America (Mount St. Helens 1980, 1982) and most recently at Mt. Pinatubo in the Philippines. Neall (1976a) submitted that lahars had caused the loss of more than 22,250 lives in historical times. Since this review was written perhaps the greatest single loss of life from lahars followed the eruption of Nevado del Ruiz when over 23,000 people were killed (Pierson *et al.*, 1990). The revised figure for loss of life resulting from lahars, updated from 1976, is in the order of 50,000 people. In 1976 Neall stated that "***A review of the causal mechanisms of lahars, flow behaviour and protective measures....is therefore appropriate to the understanding of this major geological hazard***". These issues will be addressed in this chapter by way of an introduction to current understanding of lahars. Following chapters will detail the nature, distribution, sedimentology and genesis of lahars in the catchment of the Whangaehu River.

3.2 LAHARS: THEIR CAUSE, BEHAVIOUR AND EFFECTS

By definition a lahar is a volcanogenic phenomena, *i.e.* an event that is confined to volcanoes (Smith and Fritz, 1989). However, it would be erroneous to interpret this to mean that they are solely eruption-induced phenomena. Evidence shows that lahars may result from the bulking up of normal floods following heavy rainfall (typhoon-induced lahars); the breakout of lake waters, expressly crater lakes; the incorporation of pyroclastic material or debris from a collapsed portion of the volcanic edifice into

existing streams; or from the bulking up of floods caused by the melting of snow and ice by hot pyroclastic material during eruptions (Crandell, 1971; Neall, 1976a, 1976b).

The nature of lahars is determined to a large degree by the volume of available water, which provides the fluid medium, and the amount of material which is incorporated into the flow (Pierson *et al.*, 1990). Lahars which result from the sudden catastrophic release of large amounts of stored water, e.g the collapse of a barrier of a crater lake, involve high discharges of water with sufficient energy to erode and incorporate debris from the flanks of the volcano and the beds of the channels along which the lahars flow (Scott, 1988a, 1988b). Some of the most devastating lahars have occurred from volcanoes with large amounts of stored water, either in the form of lakes or permanent snow and ice (Neall, 1976a; Major and Newhall, 1989).

In tropical environments the instability of pyroclastic material which has accumulated on the flanks of volcanoes makes the slopes particularly susceptible to erosion or collapse following high rainfall events. This may occur during, or between, eruptive episodes (Ulate and Corrales, 1966; Waldron, 1966; Rodolfo, 1989; Rodolfo and Arguden 1991; Arguden and Rodolfo, 1990). It is also now recognized that eruptions can cause storm events (Rodolfo, 1989; Pierson *et al.* 1992). Although on an individual scale not necessarily as destructive as the scenarios described in the previous paragraph, typhoon-induced lahars, by virtue of their increased frequency, may deliver equal amounts of volcaniclastic debris from the flanks of the volcano to the ring plain that surrounds it.

An important contribution to the understanding of processes that allow lahars to flow and to be able to support high sediment concentrations has been drawn from observations made during the past decade. The catastrophic eruption of Mount St. Helens in 1980 and subsequent eruption- and lake breakout-induced lahars have provided invaluable field observations of both lahar behaviour and the resultant deposits. The importance of basic ground truthing research was realized following the 13 November 1985 eruption of Nevado del Ruiz in Colombia. Melting of snow and ice on the summit of the volcano by pyroclastic flows during a relatively small eruption resulted in lahars which inundated the township of Armero, killing an estimated 23,000 people.

The most common cause of lahars is volcanic activity, either directly at the time of eruption (syn-eruptive), or in post- or inter-eruptive periods through mobilization of erupted material. Therefore any discussion of laharic activity is incomplete without mention of the preceding eruptive events.

The hazard from lahars has been shown to be an historic reality. Case studies of recent lahars can be used to show that lahars may result from a number of causes. The examples utilized are drawn from published reports of lahars following volcanic eruptions in Costa Rica (Irazu Volcano, eruptions in 1963- 65), Northwest U.S.A. (Mount St. Helens, eruptions in 1980 and 1982), Colombia (Nevado del Ruiz, eruption in 1985), the Philippines (Mayon Volcano, eruption in 1984), and the 1991 eruption of Mt. Pinatubo, also in the Philippines.

3.2.1 *SPECIFIC CASE STUDIES OF LAHARS*

3.2.1.1 *Lahars following the 1963 eruptions of Irazu Volcano, Costa Rica*

From March 13, 1963 to March 19, 1965 Irazu Volcano underwent a period of violent eruptive activity. The flanks of the volcano were plastered with ash, which buried stabilizing vegetation and formed an impermeable crust. Accelerated runoff and intensified erosion during high rainfall events caused floods which assimilated large quantities of the volcaniclastic material and were transformed to lahars. Beneath the impermeable crust the ash was soft and loose; once the impermeable crust was destroyed this ash was readily eroded. Erosion style on the slopes of Irazu Volcano was dominantly sheet or rill. The most disastrous lahars occurred towards the close of the 1963 rainy season. One large lahar flowed down the Rio Reventado, which drains the south west flank of Irazu, and had an estimated discharge of 407 m^3 s^{-1}, and in places exceeded 12 m in height. During the rainy season of 1964 more than 90 lahars occurred, 40 in the Rio Reventado valley. Lahars also occurred in 1965 (Ulate and Corrales, 1966; Waldron, 1966).

3.2.1.2 *Lahars following the 1980 and 1982 eruptions of Mount St. Helens, Northwest U.S.A.*

In May 1980 large lahars followed a catastrophic eruption of Mount St. Helens. The 1980 eruption was characterised by collapse of the volcanic edifice, which in turn exposed the magma chamber with a ensuing directed blast and pyroclastic activity. Lahars resulted from (1) slumping of water-saturated debris avalanche material, (2) rapidly flowing mixes of eruption material, including water and entrapped air, and (3) melting of snow and ice. Within 10 minutes of the eruption a lahar had flowed down the South Fork Toutle River. The largest lahar occurred in the North Fork Toutle River about 5 hours after the main eruption and resulted from dewatering and slumping of a portion of the debris avalanche material. Peak discharge ranged between 6×10^3 and 8×10^3 m^3 s^{-1}, with velocity peaking between 6 and 12 m s^{-1}. Lahars also flowed down Pine Creek and Muddy Rivers which drain the east flank of Mount St. Helens. These were triggered by pyroclastic surges that incorporated snow and ice and transformed to lahars. Peak discharge for the Pine Creek Lahar was estimated to be in the order of 2.9×10^4 m^3 s^{-1}, and 2.2×10^4 m^3 s^{-1} for the Muddy River Lahar (Scott, 1988a).

The lahars created on 18 May 1980 devastated large areas in proximity to Mount St. Helens, and their impacts were felt in the Colombia River more than 100 km distant (Janda *et al.*, 1981; Pierson, 1985; Scott, 1988a).

Following the catastrophic eruption of 1980 there followed a period of quiescence and dome-building. Mount St. Helens erupted again on 19 March 1982. An eruption from the dome, nested in the new volcanic crater, initiated an avalanche of snow and debris from the encompassing crater walls. The lahars that resulted from the eruption were caused by melting of snow and ice which had accumulated in the post-1980 eruption enlarged crater, and from collapse of saturated avalanche debris. A temporary lake then formed behind the dome; this suddenly discharged releasing a flood of admixed water and pumice which flowed north into the headwaters of the North Fork Toutle River, eroding and incorporating debris from the flanks of the volcano and developing into a lahar. Peak discharge was estimated to be at least 1.38×10^4 m^3 s^{-1}. 81 km downstream from the volcano, peak discharge was measured at 450 m^3 s^{-1}. Although not as destructive as events in 1980, this eruption and subsequent lahars emphasized the hazard from lahars from this volcano (Waitt *et al.*, 1983; Pierson and Scott, 1985).

3.2.2.3 *Eruption and post-eruption lahars from Mayon Volcano, the Philippines*

Mayon Volcano, which lies approximately 13° North of the Equator in the Philippines, is one of the worlds most active volcanoes. Lahars from Mayon are triggered exclusively by rainfall, either at the time of an eruption when lahars may be hot, or during post-eruptive periods when lahars are cold. The lahars are very erosive and carve out channels along their flow routes. An eruption in 1984, which lasted from 10 September to 6 October, produced at least 12 "***hot***" lahars (Arguden and Rodolfo, 1990; Rodolfo and Arguden, 1991). The eruption was accompanied by heavy rains, probably stimulated by eruption updrafts. Large quantities of pyroclastic material and ash were emitted during the eruption and these were promptly assimilated into lahars by the readily available water. These lahars destroyed coconut groves, housing, and roads. Attempts to contain or divert lahars foundered because artificial channels became choked with lahar debris, and the lahars then cut new routes.

During the interval from 1984 to 1989 following this eruption a further 138 "***cold***" lahars were reported. These were caused by intense rainfall during tropical storms which mobilized loose material on the flanks of the volcano. By carefully matching precipitation records to the occurrence of lahars Rodolfo and Arguden (1991) hypothesised that there was a critical threshold for rainfall intensity and duration above which lahars were triggered. Rodolfo *et al.* (1989) report the occurrence of one of these rainfall-or typhoon-triggered lahars which occurred during Typhoon Saling on 17 and 18 October 1985. Total rainfall was gauged to be 127.8 mm over the two days, although on the volcano this was likely to be much higher. The resulting lahars blocked up existing lahar channels and cut new ones. Lahars which flowed down the new channel destroyed ten houses. Hence the problem of frequently occurring lahars is exacerbated by an inability to control their behaviour.

Recent eruptive activity, which commenced on February 2, 1993, was characterised by emplacement of lava flows, small pyroclastic flows and ash ejection. During the latter half of February small channel-confined high rainfall-triggered lahars occurred on the southeast flank of the Volcano. The initial February 2 eruption killed 75 people, and over 45,000 people fled their homes during the early stages of the eruption (PHI VOLCS, 1993a and 1993b).

3.2.2.4 *Catastrophic lahars following the 1985 eruption of Nevado del Ruiz, Colombia*

On 13 November 1985 the world's attention was drawn to the horror and chaos suffered by the people of Colombia following destructive lahars which inundated the town of Armero with a death toll exceeding 23,000. The eruption of the volcano Nevado del Ruiz was relatively small. However, widely distributed snow on the summit area provided a plentiful supply of water (when melted by hot pyroclastic flows) for lahar generation. These lahars flowed down the Chinchina, Guali and Lagunillas drainage systems. 23,080 people were killed, 4,420 injured, 5,092 homes were demolished and 2,100 km^2 of land ruined. The town of Armero, where the devastation was extensive, is situated 74 km from Nevado del Ruiz at the mouth of the Rio Lagunillas Canyon (Lowe *et al.*, 1986; Pierson *et al.*, 1990).

The eruption proceeded in two parts. Firstly, at 15:05 on the afternoon of 19 November a strong phreatic explosion from Crater Arenas was followed by a short eruption. Earthquakes and tremors followed these events until 21:08 that evening when eruptive activity resumed. This second period of activity was characterised by the ejection of explosion breccias, pyroclastic surges and pyroclastic flows, that came to rest on the snow-covered flanks of the volcano.

Early in the day earthquake tremors had triggered a landslide in the Rio Azufrado River which transformed to a lahar. However, the most devastating lahars resulted from the dynamic interaction of the pyroclastic flows with snow and ice on the summit. Pierson *et al.* (1990) estimate that approximately 2×10^7 m^3 of water was released into the headwaters of all the streams draining the volcano. The source of this water was the melting of entrained snow and ice that had been incorporated into the pyroclastic surges and flows by erosion. Floods of admixed meltwater and eruption material transformed to lahars as they assimilated quantities of loose debris in the canyons down which they flowed. The ability of these flows to erode underlying material was evident in the aftermath of the events as canyon floors and walls were observed to be stripped of vegetation and scoured by the passage of the lahars. The largest lahar flowed down the Rio Azufrado, which meets the Rio Lagunillas above Armero township. The peak discharge for this lahar was 4.8×10^4 m^3 s^{-1}. Peak discharges for lahars in the Guali and Molinas/Nereidas river channels were in the order of 2×10^4 m^3 s^{-1} (Pierson *et al.* 1990). The lahar which flowed down the Rio Lagunillas was smaller and travelled

more slowly than the one in the Rio Azufrado. The latter arrived at the confluence of the two rivers and field observations indicate that the Azufrado lahar flowed back up into the channel of the Rio Lagunillas. Hence at Armero, which lies downstream of this confluence, a number of distinct lahar pulses were experienced resulting from multiple pulses during the Azufrado event, culminating in a single pulse from the Lagunillas event.

Pierson *et al.* (1990) stressed the important lessons that have been learned from this relatively small eruption of Nevado del Ruiz and the subsequent disaster at Armero. These were that (1) catastrophic lahars can result from minor eruptions, (2) the surface area, as opposed to total volume, of available snow and ice is a critical factor in determining lahar magnitude and hazard, (3) dynamic mixing of hot eruptive products with snow and ice by vigorous pyroclastic surges and flows is more effective at triggering lahars than low energy flows, (4) lahars may greatly increase their volumes by eroding into and incorporating bank and bed materials, and (5) local relief may serve to enhance the lateral extent of lahars.

3.2.2.5 *Recent lahars following the eruption of Mt. Pinatubo in the Philippines*

In 1991 the international headlines were dominated by the reports of catastrophic eruptions from volcanoes in Japan and the Philippines. Pierson *et al.* (1992) detail the eruption sequence of Mt. Pinatubo and the impact of the numerous lahars that followed. The 15 June eruption was accredited to be one of the largest this century. The eruptive episode began on 2 April and during a climactic eruption between 12 and 16 June 1991 approximately 7-11 km^3 of material was ejected (Pierson *et al.*, 1992). To date an estimated 600 people have perished as a result of this eruption, and 70,000 remain in emergency evacuation areas (PHIVOLCS, 1992b). The environmental impact was devastating. Most of the basins that drained the volcano were choked with pyroclastic debris, and the hillsides were mantled with pumice. Fine-grained ash formed an impermeable crust, as happened at Irazu in Costa Rica, and the vegetation was either destroyed or buried. Runoff following eruption-triggered storm events flooded through the congested basins, rapidly eroding into the poorly consolidated pyroclastic material and forming destructive lahars. Lahar initiation concurred with the onset of eruptive activity on 12 June and between that date and 10 September at least 140 lahars occurred in the region. These lahars were hot; the floods eroded into pyroclastic deposits which

were still several hundred degrees Celsius. More than a year later reports of hot lahars in the area indicate that the pyroclastic deposits have retained much heat. Lake-breakout lahars also occurred in response to the temporary damming of eroded channels by slumping of pyroclastic material in the channel walls. During the 1992 rainy season post-eruption typhoon-induced lahars were directly responsible for 6 deaths and destruction of 1,712 dwelling houses (PHI VOLCS, 1992a).

The impact of these lahars in the low-lying land has been devastating. In addition to the productive land lost during the eruption, sandy lahar deposits have buried nearly 150 km^2 of low lying agricultural land.

3.3 THE RHEOLOGICAL AND SEDIMENTOLOGICAL CHARACTERISTICS OF LAHARS AND THEIR DEPOSITS

The rheological behaviour of lahars fall into the category of non-Newtonian fluids. Pierson and Costa (1987) propose a three/fold classification of non-Newtonian fluid types based on mean flow velocity and sediment concentration. Velocity is interpreted to be inversely related to yield strength, which in turn reflects the sediment concentration and grain size distribution. Matrix strength (cohesion) is determined largely by the proportion of fine material (silt and clay) in the slurry mix. In matrix-rich lahars cohesive, or viscous, forces dominate sediment support, whereas dynamic, or inertial support mechanisms, such as grain dispersion, control sediment support and transport processes in matrix poor lahars. A near continuum of sediment concentrations and grain size combinations exists between Newtonian fluid flow of normal stream flow through to grainflow, in which little or no water is present, and water is unlikely to be acting as the fluid medium. Lahars fall roughly into the zone where sediment concentration has increased sufficiently for non-Newtonian, or plastic, fluid behaviour to overwhelm turbulent Newtonian processes. With increasing sediment concentration and the consequent increase in yield strength, viscous forces begin to dominate and fluid behaviour is typically laminar. Slurry mixes with a high sediment to water ratio are referred to as debris flows. Sediment concentrations at the transition zone between Newtonian and non-Newtonian fluids are low and a combination of processes may

operate. With reduced sediment concentration fluid behaviour bears characteristics which lie between debris flow and normal stream flow. These flow types are referred to as hyperconcentrated flows.

3.3.2 *DEBRIS FLOWS*

3.3.2.1 *Debris flow rheology*

According to Costa (1988) debris flow sediment concentrations lie between 70 and 90 % by weight, or 47 and 77 % by volume, and saturated bulk density ranges from 1.80 to 2.30 Mg/m^3. The high sediment concentration of debris flows imparts a high yield strength and their rheological behaviour is viscoplastic. The generally accepted model, the Coulomb-viscous model, for debris flows combines concepts of plastic behaviour, specified by the Coulomb equation (Costa, 1988):

$$\tau = c + \sigma \tan \alpha \tag{3.1}$$

where τ = shear stress
c = cohesion
σ = normal stress
α = angle of internal friction

and Newtonian flow, explained by the Newtonian equation:

$$\tau = \mu \frac{dv}{dy} \tag{3.2}$$

where μ = dynamic viscosity
v = velocity
y = depth

Newtonian fluids are unable to resist shear stress, and have a linear relationship between applied shear stress and rate of strain (see Figure 3.1). For pure water, which is a Newtonian fluid, yield strength is essentially zero. However, a small finite yield strength may exist in floods with large sediment loads (Costa, 1988).

Cohesion and internal friction constitute yield strength in the Coulomb model, which has the form (Costa, 1988):

$$\tau = c + \sigma \tan \alpha + \mu \frac{dv}{dy} \qquad (3.3)$$

and internal friction becomesmore important.

If the expression of shear resistance resulting from cohesion and internal friction is replaced by yield strength, κ, this conceptual representation of debris flow rheological behaviour may be expressed as the Bingham plastic model (Johnson, 1970; Enos, 1977):

$$\tau = \kappa + \mu_b \varepsilon_s \; for \; \varepsilon \geq \kappa \qquad (3.4)$$

where κ = threshold strength

μ_b = Bingham plastic viscosity

ε_s = shear strain, analogous to the expression $\frac{dv}{dy}$ in Equations 3.2 and 3.3.

The expression $\mu_b \varepsilon_s$ is a Newtonian viscosity term with a critical shear stress threshold ($\varepsilon_s = 0$) above which rheological behaviour is Newtonian, and below which debris will not flow (see Figure 3.2).

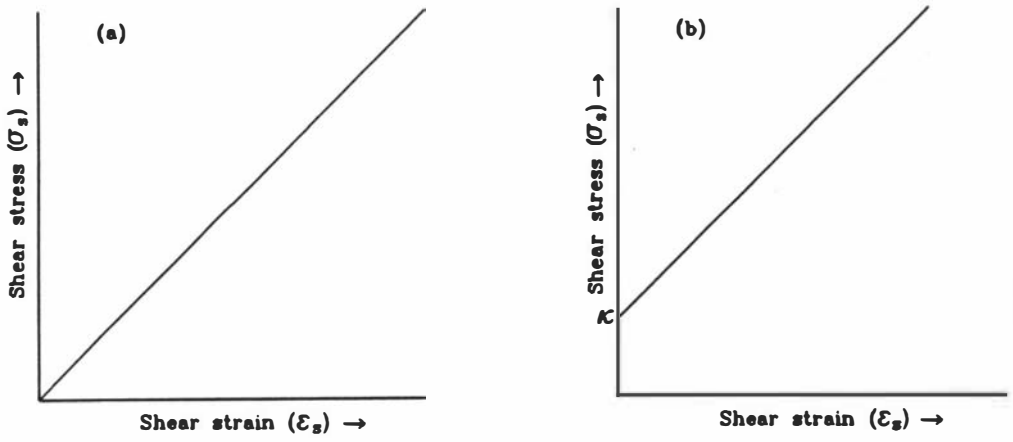

Figure 3.1 Flow curves for (a) Newtonian fluids,and (b) Bingham plastics, adapted from Enos (1977). The x-axis represents shear strain (ε_s), and the y-axis shear stress (σ_s). The intercept κ in (b) marks the threshold yield strength.

The predominant flow type within debris flows is laminar, and they tend to flow as a solid plug of material with intense shear zones at the channel boundary (Enos, 1977, Costa, 1988). Characteristically a steep frontal lobe develops at the snout of debris flows (Sharp and Nobles, 1953; Johnson, 1970; Pierson, 1986), as clasts within the flow are moved forward to this frontal embankment, being pushed along by the material following behind.

The competence of debris flows is rated as a measure of the largest clasts that the flow is able to suspend completely above the bed (Pierson, 1981; Nemec and Steel, 1984). Nemec and Steel investigated the possible relationship between flow competence and depositional thickness of debris flow deposits. The effectiveness of thickness dependent support mechanisms, such as grain to grain interactions, increase with unit thickness. Cohesion is a thickness-independent rheological parameter. Hence debris flows with some element of cohesion (typically a higher content of silt- and clay-sized particles) will possess a measure of base level competence. With increasing depth, thickness-dependant dynamic support mechanisms play an increasing role and the competence of the debris flow increases (Nemec and Steel, 1984). Variations in clast concentration will have some influence on this relationship. In plotting maximum clast size against bed thickness for debris flows, the regression line for cohesionless debris flows with

little or no silt and clay in their matrices intersects the axes at the origin. In debris flows with some measure of cohesion (therefore a base level of competence) the regression line intersects the Y-axis, which represents the yield strength of the material, at some point above zero (see Figure 3.3).

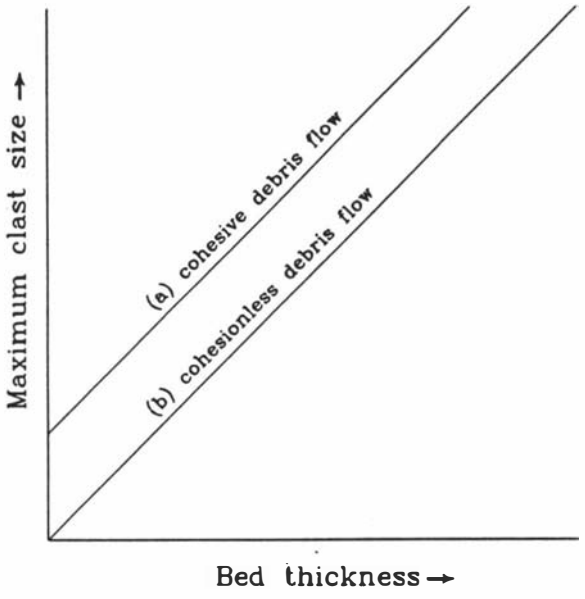

Figure 3.2 Correlation of maximum clast size and bed thickness in (a) cohesive, and (b) cohesionless debris flows, adapted from examples presented in Nemec and Steel (1984).

3.3.2.2 *Debris flow sedimentology*

Costa (1988) asserts that debris entrainment in debris flows is irreversible and hence deposition is *en masse*. Therefore the deposits resulting from emplacement by debris flowswill reflect the dominant rheological parameters operating to support and transport material within the flow immediately prior to deposition. The sedimentological characteristics of debris flows vary between deposits and within deposit . Internal grading of clasts within a debris flow and its resultant deposits has been used to interpret which mechanisms dominate. The major types of grading observed in debris flows are, (1) no grading, (2) inverse grading, and (3) normal grading. Debris flows

do not necessarily display exclusively any one of these, and combinations of the three types may be observed in a single unit.

Ungraded and inversely graded beds imply a greater interaction between clasts and increasing role of dispersive pressure, buoyancy, and grain-to-grain interactions (Hampton, 1979; Naylor, 1980; Pierson, 1981; Nemec and Steel, 1984; Shultz, 1984). Scott (1988a) interprets inverse grading in debris flow deposits from Mount St. Helens as the product of a boundary effect, *i.e.* principally as a result of the preferential movement of large clasts away from flow boundaries as a result of clast-to-clast interactions. In the same paper Scott also discusses a process of "kinetic sieving", proposed by Middleton (1970), whereby small grains are "sieved" through the spaces between larger grains. Scott considers that this may be responsible for inverse grading in clast-supported units.

Normal grading is usually interpreted to reflect a turbulent flow regime with the more fluid nature of these flows reflecting a lower sediment to water ratio. Nemec and Steel (1984) and Shultz (1984) consider that normal grading results from preferential deposition of coarser and denser material from these weaker flows, following deposition. However, if debris entrainment is irreversible, as asserted by Costa (1988), and deposition *en masse*, it may be that larger clasts in these weaker flows are transported at the base of the flow as a traction bedload or graded suspension, a process debated by Walton and Palmer (1988).

As mentioned in the previous section, maximum clast size is related to competence, or yield strength, hence, irrespective of flow type, a deposit that supports large clasts will have resulted from a more competent debris flow than one with only small clasts, provided all clast sizes are available for entrainment.

3.3.3 *HYPERCONCENTRATED FLOWS*

3.3.3.1 *Hyperconcentrated flow rheology*

Hyperconcentrated flow sediment concentrations lie between 40 to 70 % by weight, or 20 to 47 % by volume and their saturated bulk density ranges from 1.33 to 1.80 Mg/m^3 (Costa, 1988). Their rheological behaviour is non-Newtonian. In hyperconcentrated flows buoyancy, dispersive stress and turbulence have been implicated as the primary support mechanisms. However, Beverage and Culbertson (1964) rejected the role of turbulence in suspending high concentrations of sediment, this based on observations of hyperconcentrated flows in which turbulence had been dampened by the high sediment concentrations. In quoting Bagnold (1955) they hypothesised that the mechanism permitting the support of such high sediment concentrations in the absence of turbulence was possibly some form of dispersive pressure. Although small scale turbulence in the form of eddies or surface waves was not observed, it would seem likely that some form of large scale turbulence could develop due to the influences of channel roughness and sinuosity. No models of hyperconcentrated flow behaviour have yet been proposed. Hyperconcentrated flows, therefore, occupy the intermediate position between debris flow and normal streamflow behaviour. Consequently, in rheological behaviour and sedimentary features, hyperconcentrated flows exhibit characteristics of both.

3.3.3.1 *Hyperconcentrated flow origins and sedimentology*

The origin of hyperconcentrated flows has been a popular topic for discussion in the past decade. Prior to the eruption of Mount St. Helens in 1980 hyperconcentrated flow went largely unrecognized as being distinct from dilute debris flow or highly concentrated stream flow. Pierson and Scott (1985) detailed the development of hyperconcentrated flow (which they referred to as hyperconcentrated streamflow, or lahar runout flow) as a consequence of the dilution of debris flows resulting from the 1982 eruption of Mount St. Helens. This dilution was hypothesized to occur as the debris flow incorporated stream flow and saturated streambed material which it overran

as it flowed down the channel of the North Fork Toutle River. The transformation from debris flow to hyperconcentrated flow was not observed, but deposits in the region 27 to 43 km from the crater recorded the transition. The poorly sorted, matrix-supported gravelly unstratified deposits of the debris flow phase had been replaced, from the bottom up, with sandier, faintly stratified, clast-supported hyperconcentrated flow deposits. The contact between the two facies was generally gradational. Pierson and Scott proposed that the progressive settling out of larger clasts from the debris flow phase may also bring about this transition. Pierson and Scott report that transformation of a lahar from debris flow to hyperconcentrated flow in the North Fork Toutle River began at a sediment concentration of about 78 % by weight (57 % by volume). Smith (1986, 1987) outlines the sedimentological characteristics that he used to distinguish deposits of hyperconcentrated flow. These he described as typically clast-supported, usually normally-graded and unstratified, although some evidence of stratification may be observed. Deposits are dominated by clasts in the sand and gravel range. Occasional outsize clasts held in suspension by the continuous phase are commonly observed. Smith (1986) characterises rheological conditions within hyperconcentrated flow as partly turbulent with high sediment concentrations dampening out small eddies. He implicates turbulence, grain dispersive pressure and buoyancy as sediment support mechanisms for this type of flow. He interprets the contrast between massive and stratified beds as distinguishing between rapid deposition of clasts in the former, and deposition of clasts in low-amplitude, long wave-length dunes in the latter.

Smith and Lowe (1991) argue that hyperconcentrated flow does not necessarily have to result from dilution of a debris flow stage of a lahar. For example some may begin as hyperconcentrated flows or may result from the bulking up of normal stream flow and flood flow. Other terms that have been used for this flow behaviour are hyperconcentrated streamflow (Beverage and Culbertson, 1964; Pierson and Costa, 1987) and hyperconcentrated flood flow (Smith, 1986). Hyperconcentrated flow is used in this thesis as the preferred term. It is non-genetic, avoiding misinterpretation of both flow type and resultant deposits implied by the other terms.

To date, hyperconcentrated flow remains a largely unexplored phenomenon. Its rheological behaviour is interpreted to represent the gradation between stream flow and debris flow. Hence, at lower sediment concentrations the turbulent behaviour of Newtonian fluids would be the principal means of sediment support and transport. With increasing sediment concentration,dilatancy and grain dispersion are more important as turbulence becomes dampened. These factors are represented in the range of deposits that have been interpreted to represent hyperconcentrated flow. Generally clast supported, they range from being gravel- to sand-dominated. The coarser grained gravelly deposits are likely to be massive, whereas faint, weakly developed stratification may be observed in finer grained sandy deposits (Smith, 1986). Deposits from hyperconcentrated flow are characteristically less well sorted than deposits of streamflow, but better sorted than debris flow deposits (Costa, 1988).

CHAPTER 4

THE WHANGAEHU FORMATION

4.1 INTRODUCTION

The Whangaehu Formation comprises upper Pleistocene gravel- and sand-dominated diamictites which extend from the southern sector of the Mount Ruapehu ring plain over 160 km to the coastal plain near the mouth of the Whangaehu River. These deposits record the influx of large quantities of andesitic debris from the Tongariro Volcanic Centre in response to catastrophic volcanic activity. The Whangaehu Formation is well exposed in cliffs which confine the Whangaehu River in the lower Whangaehu gorge, and in isolated outcrops throughout the middle and lower and coastal reach of the River catchment. In the middle reaches of the River the Whangaehu Formation forms a terrace which constitutes a major geomorphological feature in this region (see Map 2, Appendix). Whangaehu Formation deposits have buried the underlying dissected terrain creating a valley-wide plain with a gently seawards-dipping surface. Below the lower Whangaehu gorge outcrop is intermittent. Andesitic boulders mantle the valley sides in the middle and lower catchment of the River providing evidence for the emplacement of the Whangaehu Formation prior to its redistribution by subsequent fluvial and slope processes.

Lithologies within the Whangaehu Formation are dominantly Mount Ruapehu-sourced andesite, although rip-up clasts of underlying Tertiary sandstone and siltstone are observed. Deposits are commonly lithified. Occasional volcanic bombs are found in upper beds of the Whangaehu Formation in the middle catchment, and lower beds in the coastal reach of the catchment are marked by the presence of dacitic pumice clasts. Near to the base of the Formation in its most distal exposures, a thin andesitic lapilli bed is found in siltstone between the two thickest and lowermost beds.

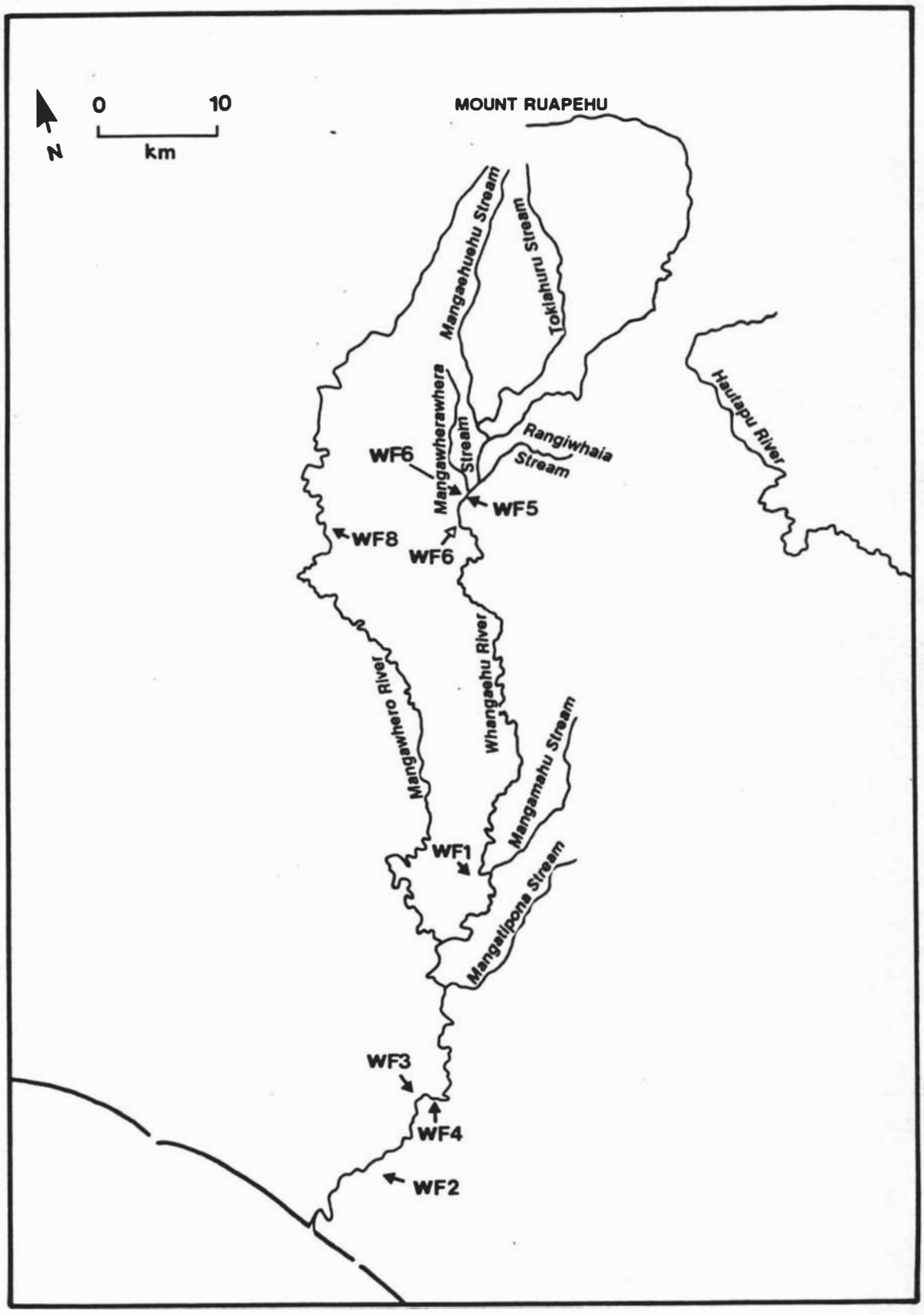

Figure 4.1 Map showing locality of the Whangaehu Formation type locality, reference sections, and observation sites.

4.2 TYPE LOCALITY AND DEFINITION OF THE WHANGAEHU FORMATION

The Whangaehu Formation is an adapted formation name for upper Pleistocene-aged Mount Ruapehu-sourced andesitic gravel- and sand-dominated diamictites. The type locality for the Whangaehu Formation is located approximately 1.5 km west of Mangamahu (WF1, Figure 4.1 and Plate 4.1, Map 4 and section description in the Appendix). The thick sequence of andesitic gravels exposed at this site were first described by Fleming (1953) who called them the "***Whangaehu valley-fill***". He further discussed the distribution of a widespread, poorly sorted valley-fill consisting of "***scoriaceous, poorly-rounded andesitic rubble, grit, breccia, and conglomerate***" within the valley of the Whangaehu River[1]. In this thesis it is interpreted that this valley-fill deposit, described originally in the lower reaches of the Whangaehu River, correlates with diamictites described by this author in the middle and lower reaches of the River and defined as the Whangaehu Formation. Fleming (1953) proposed that the Whangaehu valley-fill accumulated at the time the Rapanui terraces formed, indicating that it was > 120,000 years old (Pillans, 1988).

At the type locality the Whangaehu Formation infills a channel approximately 300 m wide cut into Nukumaruan sandstone and siltstone. The base of the Formation is at 250 m above sea level. The basal unit in the Formation is 18 m of clast-supported, very poorly sorted andesitic boulders, cobbles and pebbles, with a few sandstone and siltstone rip up clasts. It is ungraded, and the clasts are commonly subrounded to rounded. Within this unit there are discontinuous zones of stratified andesitic sands and granules. The contact with the underlying Quaternary sandstone and siltstone shows evidence of severe erosion. The contact between this basal unit and the next overlying unit is not clearly exposed. The overlying unit is 3 m of poorly sorted, clast-supported, stratified, andesitic gravel and sands. It is ungraded, and the clasts are subangular to subrounded. A distinct contact separates this from the uppermost unit observed, which is 3 m of thick clast-supported, very poorly sorted, weakly stratified andesitic gravel and sand. This unit is normally graded, and the clasts are commonly subangular to

[1]Fleming (1953) also describes similar deposits in the Mangawhero River Valley, which may be correlatives of the Whangaehu Formation.

subrounded. All three units are strongly lithified. No younger deposits overlie the Formation at this locality, and the top of the exposure is at 300 m above sea level.

In proximity to Mount Ruapehu a near continuous overview of marginal lithofacies of the Formation is exposed in the cliffs of the lower Whangaehu gorge, and these can be seen from Old Fields Track (S21/195834 and S21/183819, see Plate 4.2). The most distal exposure of the Formation (WF2, Figure 4.1 and Plate 4.3; S23/965295) shows the relationship between the younger infilling Whangaehu Formation and older Pleistocene marine-cut terraces.

4.3 DESCRIPTION OF SEDIMENTS

Sedimentological details were obtained from sections logged during fieldwork combining criteria used by sedimentologists and pedologists. The features of the resultant deposits of particular importance to any successful analysis of rheological conditions responsible for emplacement of the diamictites described were:

1. bed thickness
2. supporting mechanism (clast or matrix)
3. estimate of the degree of sorting
4. modal clast size
5. the size of the largest clast[2]
6. evidence of bedforms
7. clast shape

and 8. nature of the matrix.

Section descriptions were supported by field sketches drawn at each exposure which depict the sometimes complex physical relationship between different deposits. Most of the section descriptions are composite.

[2]*The largest clasts were measured within a 5 m zone on either side of the vertical profile described.*

4.3.1 *LITHOFACIES DESCRIPTION*

Thirteen different diamictite lithofacies types are identified in the Whangaehu Formation. These are outlined in Tables 4.1 - 4.3.

A primary distinction was made between (1) gravel-dominated and (2) sand-dominated diamictites. Gravel-dominated diamictites were further divided into bouldery and pebbly deposits. Therefore three main lithofacies groups were identified (1) bouldery diamictites (Group 1 and 2 subfacies), (2) pebbly diamictites (Group 3 and 4 subfacies), and (3) sandy diamictites (Group 5 diamictites).

4.3.1.1 *Bouldery diamictites*

Deposits within this lithofacies form the greatest stratigraphic thickness of deposits described in the Whangaehu Formation. Boulder-sized clasts within these groups of deposits are dark grey, hard andesite and are commonly subrounded to rounded. The matrix is coarse-grained and comprises subangular to subrounded grey, red and yellow granules and pebbles. Clasts within this matrix are commonly soft and altered. Two main groups are identified, (1) clast-supported (Group 1) and (2) matrix-supported (Group 2) diamictites. The characteristics of these groups of deposits are outlined in Table 4.1.

Group 1 diamictites are dominantly proximal, whereas matrix-supported diamictites generally form thinner beds in proximal and distal situations. In thick individual beds of bouldery diamactites both clast- and matrix-supported facies may be present, and complex sequences containing lenses of both were observed. Description of these exposures was difficult because contacts between lithofacies were not always distinct. Where lithological boundaries were distinct, deposits were treated as single entities and each described according to the dominant fabric and grading characteristics observed. In deposits where zone boundaries were indistinct the whole thickness was described as a single thick individual bed.

Table 4.1 Bouldery lithofacies within Whangaehu Formation diamictites

Lithofacies identifier	Lithofacies description	Total number of beds	Total thickness of beds (m)	Bed thickness range (m)	Maximum clast size (m)	Modal clast size (Wentworth)
1a	*clast-supported bouldery gravel, normally graded*	3	60.0	0.4 - 30	1.5	boulder
1b	*clast-supported bouldery gravel, ungraded*	8	116.5	0.3 - 30	1.5	boulder
1c	*clast-supported bouldery gravel, inversely graded*	3	13.0	0.3 - 0.5	2.0	boulder
2a	*matrix-supported bouldery gravel, normally graded*	4	14.0	2.0 - 4.5	2.2	cobble
2b	*matrix-supported bouldery gravel, ungraded*	7	36.5	3.0 - 10.0	1.5	cobble
2c	*matrix-supported bouldery gravel, inversely graded*	2	20.0	5.0 - 15.0	1.0	boulder

Three main grading types were observed in bouldery diamictites, (1) normally graded, (2) ungraded, and (3) inversely graded beds, corresponding to subfacies 1a-c for clast-supported and 2a-c for matrix-supported diamictites (see Table 4.1).

4.3.1.2 *Pebbly diamictites*

Lithofacies groups identified within this subgroup are similar to those defined for bouldery diamictites, *i.e.* (3) matrix-supported (Group 3 subfacies) and (4) clast-supported (Group 4 subfacies). Clasts within Group 3 subfacies are commonly grey, red and yellow andesite. Weathered paler clasts probably represent pumice lapilli and blocks. Clasts are subangular to rounded in shape. The matrix component of the deposits is finer-grained than in Group 1 and 2 diamictites, and comprises muddy, very fine to very coarse sand. Clasts within Group 4 subfacies are dominantly subangular to rounded grey andesite. Clasts are commonly vesicular, especially in distal

exposures. The deposits contain a low percentage (< 5 %, visual estimate) of fine sand matrix. Group 3 and 4 subfacies form the upper part of the Whangaehu Formation where it is exposed in the lower Whangaehu gorge. Clasts and matrix within these beds may be soft, and this alteration is interpreted to have been caused by subsequent weathering.

Table 4.2 Pebbly lithofacies within Whangaehu Formation diamictites

Lithofacies identifier	Lithofacies description	Total number of beds	Total thickness of beds (m)	Bed thickness range (m)	Maximum clast size (m)	Modal clast size (Wentworth)
3a	*matrix-supported pebbly gravel, normally graded*	4	10.08	0.58 - 6.5	0.3	pebble
3b	*matrix-supported pebbly gravel, ungraded*	10	19.46	0.26 - 4.5	0.25	pebble
3c	*matrix-supported pebbly gravel, normally graded*	1	2.00	2.00	0.15	pebble
4a	*clast-supported pebbly gravel, massive*	11	18.85	0.70 - 3.0	0.2	pebble
4b	*clast-supported pebbly gravel, stratified*	10	26.25	0.75 - 7.0	1.0	pebble

Within the Group 3 subfacies a distinction was made between deposits with normally graded, ungraded or inversely graded beds (subfacies 3a-c). In Group 4 subfacies, however, deposits were distinguished by their internal bedding characteristics, *i.e.* whether they were (1) massively bedded (subfacies 4a), or (2) stratified (subfacies 4b). The characteristics of these subfacies are outlined in Table 4.2.

4.3.1.3 *Sandy diamictites*

All sandy diamictite beds described are clast-supported. Clasts within these Group 5 subfacies are commonly hard grey vesicular andesite and are angular to subangular.

Two types of deposit are distinguished within this subfacies, (1) massively bedded (subfacies 5a), or (2) stratified (subfacies 5b) sandy diamictites (see Table 4.3).

Table 4.3 Sandy lithofacies within Whangaehu Formation diamictites

Lithofacies identifier	Lithofacies description	Total number of beds	Total thickness of beds (m)	Bed thickness range (m)	Maximum clast size (m)	Modal clast size (Wentworth)
5a	*clast-supported, sands, massive*	12	13.6	0.7 - 2.8	0.07	very coarse sand
5b	*clast-supported sands, stratified*	6	14.2	0.4 - 5.5	0.05	very coarse sand

4.3.2 *LITHOFACIES INTERPRETATION*

Subfacies 1a-c, 2a-c, and 3a-c display most of the features decribed by Nemec and Steel (1984) as being diagnostic for gravelly conglomerates (in this case diamictites) that have been emplaced by debris flows. These include:

1. sheet-like beds, with limited or insignificant basal erosion[3]
2. ungraded to graded beds
3. absence of stratification
4. deposits are very poorly sorted, and range from clast-supported to matrix-suppported
5. thicker beds tend to contain coarser clasts.

Beds in subfacies 1a-c and 2a-c, however, which tended to be the lowermost beds in exposure, had erosional contacts (see Plate 4.2). Rip up clasts of the underlying Tertiary sandstone and siltstone, commonly boulder-sized, were commonly observed in these beds (see Plate 4.4). Otherwise deposits were stacked one of top of another with little or no erosion at their contacts.

---

[3]*Scott (1988a, 1988b) however presents evidence for lahars from Mount St. Helens which were highly erosive, and this is implicit in the term "bulking", which he used to describe the process by which lahars entrain material from the beds and banks of the river channels within which they flow.*

Beds in subfacies 4a-b and 5a-b display the characteristics of deposits emplaced by hyperconcentrated flows as described by Pierson and Scott (1985) and Smith (1986, 1987). These include:

1. sheet-like beds with non-erosional contacts
2. ungraded to graded beds
3. beds may be massive, or horizontally stratified
4. deposits are poorly sorted and clast-supported
5. deposits may contain outsize clasts

Therefore diamictites in the Whangaehu Formation are interpreted to have been emplaced by debris flows and hyperconcentrated flows, sourced from Mount Ruapehu. The variety in sedimentological characteristics observed within the Formation indicates that a wide range of flow types were responsible for the transport of the dominantly volcaniclastic debris through the catchment of the Whangaehu River. These will be discussed in the following section, and are summarised in Table 4.4.

4.3.2.1 *Subfacies 1a-c*

Bouldery subfacies in the Whangaehu Formation are generally found in basal and proximal exposures. Where they are exposed overlying Tertiary sandstone and siltstone, the basal contacts are strongly erosional and rip up clasts of the underlying lithologies are commonly observed in these beds. A very competent and highly erosive transporting agent must have been responsible for such a high concentration of coarse grained clasts and the degree of erosion observed in subfacies 1a-c.

The clast-support in Group 1 subfacies implies deposition from a clast-rich debris flow. Dispersive pressure, which is commonly cited as the mechanism which disperses clasts throughout debris flow, is likely to have resulted from collisions between these clasts (inertial dispersive pressure). In the absence of a cohesive matrix, the high competence of the debris flow must have been derived from a high flow velocity. The combination of inertial dispersive pressure and high velocity would create the highly

erosive flow, capable of the erosion observed at the base of Group 1 subfacies.

Non-cohesive flows are thought to be turbulent, which in turn implies more fluid flow. Normal grading in debris flows is generally accepted to represent settling of coarser clasts out of these flow types. Alternatively clasts may be transported at the base of the flow as a traction load. Low cohesion in matrix-poor debris flows would provide little resistance to preferential settling, and in these highly competent flows this is proposed as the dominant mechanism leading to development of normal grading in subfacies 1a. Ungraded and inversely graded subfacies 1b and 1c are interpreted to represent the deposits from flows where clast dispersion and support was maintained on deposition. This may reflect localized variations in matrix concentrations where increasing cohesion lead to preservation of the original flow grading characteristics. Another factor may have been a higher clast concentration not permitting preferential settling of heavier clasts. This would also act to preserve the original pre-deposition sedimentology of the flow, which may have been normally graded, ungraded, or inversely graded.

All beds in Group 1 subfacies are interpreted to have been emplaced by highly competent, fast flowing, and turbulent clast-rich debris flows. Inertial dispersive pressure, turbulence, and high velocity are implicated as the main support and transport mechanisms.

4.3.2.2 *Subfacies 2a-c*

Debris flows responsible for emplacement of thick beds of subfacies 2a-c must also have been very competent. However the lack of distinct erosional basal contacts indicates that the flow type was less erosive. Matrix-support of clasts within the flows (inferred from matrix-support of clasts in the deposits) would increase cohesion and act to promote the development of ungraded and inversely graded beds through viscous dispersive pressure (where clasts are not in collision) and buoyant support of these dispersed clasts. Increased cohesion would preserve these grading characteristics by preventing fall out of heavier clasts.

Lithofacies identifier (WF)	Sedimentological characteristics	Rheology characteristics	Mode of emplacement
1a	BOULDER-DOMINATED; CLAST-SUPPORTED; NORMALLY GRADED	HIGHLY COMPETENT, CLAST-RICH DEBRIS FLOW; NON-COHESIVE; LOW VISCOSITY; TURBULENT; INERTIAL DISPERSIVE PRESSURE, TURBULENCE AND HIGH VELOCITY DOMINANT SUPPORT MECHANISMS	REDUCTION OF VELOCITY BELOW CRITICAL YIELD STRENGTH, PREFERENTIAL FALL OUT OF HEAVIER AND DENSER CLASTS ON DEPOSITION
1b	BOULDER-DOMINATED; CLAST-SUPPORTED; UNGRADED	AS ABOVE	REDUCTION OF VELOCITY BELOW CRITICAL YIELD STRENGTH, DEPOSITION EN MASSE, SEDIMENT "FREEZES"
1c	BOULDER-DOMINATED; CLAST-SUPPORTED; INVERSELY GRADED	AS ABOVE	AS ABOVE
2a	BOULDER-DOMINATED; MATRIX-SUPPORTED; NORMALLY GRADED	AS ABOVE	REDUCTION OF VELOCITY BELOW CRITICAL YIELD STRENGTH, PREFERENTIAL FALL OUT OF HEAVIER AND DENSER CLASTS ON DEPOSITION
2b	BOULDER-DOMINATED; MATRIX-SUPPORTED; UNGRADED	HIGHLY COMPETENT, MATRIX-RICH DEBRIS FLOW; COHESIVE; HIGH VISCOSITY; LAMINAR; VISCOUS DISPERSIVE PRESSURE AND BUOYANCY DOMINANT SUPPORT MECHANISMS	REDUCTION OF VELOCITY BELOW CRITICAL YIELD STRENGTH, DEPOSITION EN MASSE, SEDIMENT "FREEZES"
2c	BOULDER-DOMINATED; MATRIX-SUPPORTED; INVERSELY GRADED	AS ABOVE	AS ABOVE
3a	PEBBLE-DOMINATED; MATRIX-SUPPORTED; NORMALLY GRADED	LOW COMPETENCE, MATRIX-RICH DEBRIS FLOW; NON-COHESIVE; LOW VISCOSITY; TURBULENT; INERTIAL DISPERSIVE PRESSURE AND TURBULENCE DOMINANT SUPPORT MECHANISMS	REDUCTION OF VELOCITY BELOW CRITICAL YIELD STRENGTH, PREFERENTIAL FALL OUT OF HEAVIER AND DENSER CLASTS ON DEPOSITION
3b	PEBBLE-DOMINATED; MATRIX-SUPORTED; UNGRADED	LOW COMPETENCE, LOW ENERGY, MATRIX-RICH DEBRIS FLOW; COHESIVE; HIGH VISCOSITY; LAMINAR; VISCOUS DISPERSIVE PRESSURE AND BOUYANCY DOMINANT SUPPORT MECHANISMS	REDUCTION OF VELOCITY BELOW CRITICAL YIELD STRENGTH, DEPOSITION EN MASSE, SEDIMENT "FREEZES"
3c	PEBBLE-DOMINAED; MATRIX-SUPPORTED; INVERSELY GRADED	AS ABOVE	AS ABOVE
4a	PEBBLE-DOMINATED; CLAST-SUPPORTED; MASSIVELY BEDDED	LOW COMPETENCE; CLAST-RICH HYPERCONCENTRATED FLOW; NON-COHESIVE; LOW VISCOSITY; INERTIAL DISPERSIVE PRESSURE AND TURBULENCE DOMINANT SUPPORT MECHANISMS	AS ABOVE
4b	PEBBLE-DOMINATED; CLAST-SUPPORTED; STRATIFIED	AS ABOVE, ALTHOUGH TURBULENCE DOMINATES	RAPID DEPOSITION AS LOW-AMPLITUDE, LONG-WAVELENGTH DUNES
5a	SAND-DOMINATED; CLAST-SUPPORTED; MASSIVELY BEDDED	LOWER COMPETENCE THAN ABOVE, CLAST-RICH HYPERCONCENTRATED FLOW; NON-COHESIVE, INERTIAL DISPERSIVE PRESSURE AND TURBULENCE DOMINANT SUPPORT MECHANISMS	REDUCTION OF VELOCITY BELOW CRITICAL YIELD STRENGTH, DEPOSITION EN MASSE, SEDIMENT "FREEZES"
5b	SAND-DOMINATED; CLAST-SUPPORTED; STRATIFIED	AS ABOVE, ALTHOUGH TURBULENCE DOMINATES	RAPID DEPOSITION AS LOW-AMPLITUDE, LONG-WAVELENGTH DUNES

Table 4.4 Lithofacies identified within Whangaehu Formation diamictites, interpreted rheological characteristics and interpreted mode of emplacement.

4.3.3.3 *Subfacies 3a-c*

The finer grain size in subfacies group 3 diamictites indicate that debris flows responsible for their emplacement must have been less competent than those which emplaced subfacies groups 1 and 2. Matrix-strength (cohesion) is likely to be a more important support mechanism in these matrix-supported deposits. Over 50 % of beds described in Group 3 subfacies are ungraded or inversely graded, which implies that dispersion and buoyancy promoted the dispersal of clasts throughout the flow, and their support was maintained by matrix strength.

4.3.4.4 *Subfacies 4a-b and 5a-b*

These four subfacies, whose characteristics are defined in Table 4.2 and 4.3, are all interpreted to have been emplaced by hyperconcentrated flow. Clast size variations between pebbly and sandy diamictites reflect higher and lower competence flows respectively. Outsize clasts were observed more commonly in massively bedded deposits which supports this contention.

Flow behaviour in hyperconcentrated flows may appear to be (1) smooth and laminar (Beverage and Culbertson, 1964; Scott, 1988a) or (2) pulse-like and turbulent (Pierson and Scott, 1985; Scott, 1988a). These observed variations between laminar and turbulent flow regimes probably reflect a decrease from higher sediment concentration in laminar flows to lower sediment concentration in the turbulent flows. A consequent move away from dispersive pressure to turbulence as the main support mechanism is probable under these conditions.

Massive beds in subfacies 4a and 5a indicate that some mechanism was operating to disperse and then maintain support of clasts throughout the flow thickness. In the absence of a cohesive matrix, dispersive pressure is the most likely candidate for this effect. Subfacies 4a and 5a are interpreted to have been emplaced by higher sediment concentration flows.

The stratification within deposits defined by subfacies 4b and 5b comprises stacked sequences of inversely graded beds. It is unlikely that these represent deposition *en masse*, and are more likely to have resulted from rapid accumulation of thin pulses of a hyperconcentrated flow regime, spaced so closely in time as to be indistinguishable as individual events. Inverse grading within these individual thin beds implies that dispersive pressure and buoyancy were operating to support and transport clasts within the flows. The beds are generally thin, and thus clast size is correspondingly fine, this indicating that the flows which emplaced them were low competence and probably (by inference) lower in sediment concentration, and fluid. Assuming a continuing supply of sediment and water (necessary for lahar propagation) these would continue to accumulate. Considering that the beds are inferred to have been deposited very closely in time (*i.e.* immediately following one another) it seems appropriate to assume that these deposits are representatives of the pulsing hyperconcentrated flows described by Pierson and Scott (1985), from which sediment would be deposited as low amplitude, long wavelength dunes, a process proposed by Smith (1986).

4.3.3 *LITHOFACIES ARCHITECTURE*

Palmer *et al.* (1991) define a three dimensional lithofacies architectural model for unconfined and confined volcanic debris avalanches. This model recognizes distinct assemblages of lithofacies which vary as a function of the size of the event and the physiography of the ring plain in its flow path. The model distinguishes between three major assemblages, (1) axial-A, (2) axial-B, and (3) marginal lithofacies. Axial-A assemblages comprise self-supporting megaclasts, whereas those in axial-B are matrix-supported. Both, however, are interpreted to represent deposition from an initial debris avalanche phase. Marginal lithofacies assemblages comprise matrix-supported clasts and are interpreted to have been deposited by debris flow resulting from transformation of the debris avalanche at its lateral and distal margins.

Deposits in the Whangaehu Formation can be divided into 4 architectural assemblages, (1) marginal-A, (2) marginal-B, (3) distal, and (4) veneer lithofacies (see Figure 4.2). The following section will describe these, and discuss the implications of the resulting pattern of Whangaehu Formation diamictites.

Marginal-A lithofacies comprise dominantly Group 1 and 2 bouldery diamictites which are interpreted to have been emplaced by a very competent and powerfully erosive agent of transport. The similarity in lithology between beds in this assemblage of deposits, combined with their physiographical association, *i.e.* all are proximal in location and lie at the base of any described sequence of Whangaehu Formation beds, indicates that marginal-A lithofacies were probably emplaced by a single large debris flow (see Plates 4.2 and 4.5). The origin of such a large debris flow is most likely to have been a collapse of part of the southern sector of Mount Ruapehu.

The nature of these events (commonly referred to as volcanic debris avalanches) and their characteristic deposits have been described by a number of authors from both recently observed events (Bezymianny Volcano, Kamchatka, Gorshkov, 1959; Shiveluch Volcano, Kamchatka, Gorshkov and Dubik, 1970; Mount St. Helens, northwest U.S.A, Voight *et al.*, 1981) and ancient events preserved in the geological record (Mount Egmont, New Zealand, Neall, 1979; Mount Shasta, northern California, U.S.A, Crandell *et al.*, 1984, Crandell, 1988; Socompa Volcano, northern Chile, Francis *et al.*, 1985; Mount Ruapehu, New Zealand, Palmer and Neall, 1989). Volcanic debris avalanches result from massive slope failure of a portion of a volcanic cone (Siebert, 1984). Diagnostic features of debris avalanche deposits are (1) their distinctive hummocky surface expression, comprising discrete, typically fractured and shattered megablocks of homogeneous debris, and (2) local matrix-supported fragmental rock clasts or megaclasts. The preservation of both blocks and clasts has been interpreted to indicate that debris avalanche material is transported downslope by laminar plug flow (Voight *et al.* 1981; Siebert, 1984).

The surface expression of marginal-A lithofacies is buried beneath subsequent lahars, but the upper contact, where it is exposed, is planar. Neither debris-avalanche megablocks nor megaclasts were observed in exposures of the Whangaehu Formation (signifying that application of the nomenclature "axial-A lithofacies", as defined by Palmer *et al.* (1991) is inappropriate). This means that (1) marginal-A lithofacies were not emplaced by a debris avalanche mechanism, (2) debris avalanche lithofacies are buried beneath younger volcaniclastic deposits closer to the volcano, or (3) as Crandell (1988) suggests that debris avalanches originating in saturated rock, or that became saturated during flow, may transform directly into lahars.

The increased mobility of these flows would act to break up megablocks and megaclasts creating deposits with internally homogenous (*i.e.* well mixed) lithology, and planar surface expression. If the collapse event which emplaced marginal-A lithofacies of the Whangaehu Formation transformed directly to a lahar, then this would explain the absence of diagnostic debris avalanche facies. This third explanation is preferred to explanations (1) and (2). Highly competent and fluid rheological behaviour has here been interpreted for debris flows that emplaced marginal-A lithofacies (Group 1 and 2 subfacies; see this chapter, section 4.3.2.1 and 4.3.2.2) which would not support deposition from laminar plug flow typical of debris avalanches. However explanation (2) cannot be entirely discounted.

Between 50 and 100 km downstream from the most proximal exposure of Whangaehu Formation three lithofacies trends are observed: (1) a change from dominantly Group 1 to Group 2 and 3 subfacies, (2) a reduction in thickness of the individual beds, and (3) a corresponding reduction from boulder to cobble modal clast size. Beds within this zone are referred to as marginal-B lithofacies. This assemblage of deposits is interpreted to have been deposited by the initial debris flow, with the distinguishing features described in points 1-3 in this paragraph indicating an overall reduction in competence.

The total volume of all marginal-A and -B deposits in the Whangaehu Formation is estimated to be 6.3×10^8 m^3.

In proximal exposures of the Formation marginal lithofacies are mantled by Group 3, 4 and 5 subfacies. These are interpreted as representing smaller lahars that occurred following the initial large collapse and are collectively referred to as veneer lithofacies.

In distal exposures of the Whangaehu Formation in the lower catchment of the River, deposits are dominated by Group 3, 4 and 5 subfacies (see Plates 4.3 and 4.6). These are interpreted to be distal correlatives of both marginal and veneer lithofacies described in the middle catchment of the River. These deposits are collectively referred to as distal lithofacies. This architectural group may have originated through transformation of marginal debris flow facies, or as downstream extensions of veneer lithofacies.

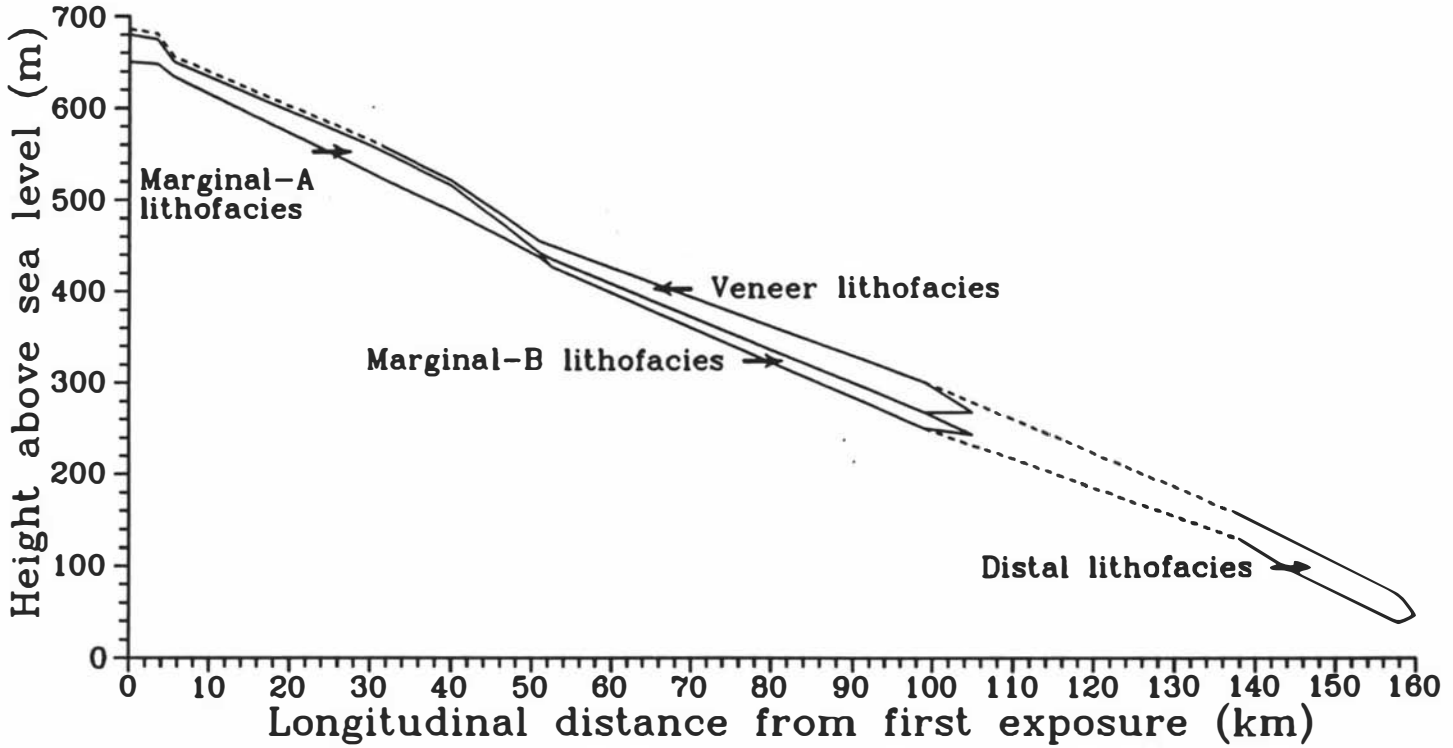

Figure 4.2 Lithofacies assemblages within Whangaehu Formation. Lower and upper contacts of each assemblage are based on barometric heights measured in this study.

The total volume of all Whangaehu Formation deposits mapped in the Whangaehu Valley is estimated to be in the order of 7×10^8 m^3. However the total volume of material emplaced by lahars in this Valley is likely to have been much greater. By projecting the areal extent of the Formation across the width of the Valley from the existing remaining deposits, a total volume of *c.* 1.2×10^9 m^3 for the lahars has been calculated.

4.3.4 *WAS EMPLACEMENT OF WHANGAEHU FORMATION LAHARS ASSOCIATED WITH ERUPTIVE ACTIVITY?*

Debris avalanches at Bezymianny Volcano, Shiveluch Volcano and Mount St. Helens, were all accompanied by catastrophic eruptive activity. The 1980 eruption of Mount St. Helens was characterised by collapse of the volcanic edifice (the initial debris avalanche), which in turn exposed the magma chamber with ensuing directed blast and pyroclastic surges. This activity was followed by lahars. The largest lahar resulted from dewatering and slumping of a portion of the debris avalanche material. Other lahars resulted from rapidly flowing mixtures of eruption material, including water and entrapped air, the bulking up of floods caused by melting snow and ice, and from pyroclastic surges that incorporated snow and ice and transformed to lahars (Scott, 1988a).

No pumiceous material was observed in marginal lithofacies of the Whangaehu Formation, implying that the initial collapse was not associated with an eruption. In proximity to the volcano, however, veneer lithofacies commonly contain pale yellow, weathered pumice lapilli and blocks, and occasional volcanic bombs. In addition to this, clasts within these deposits are commonly scoriaceous, in contrast to the dense, non-scoriaceous lithology of clasts in the bouldery marginal deposits. The base of the distal lithofacies, where they overlie fluvial gravels mantling an older terrace surface, is marked locally (WF2, Figure 4.1, and section description) by two *c.* 0.80 m thick pumice block bearing sandy units. These are overlain by a very thick coarse-grained pebbly hyperconcentrated flow, which comprises the lowermost bed of a sequence of at least two thick hyperconcentrated flows. The clasts within this hyperconcentrated

flow, and other distal deposits are dominantly scoriaceous. Lithified silts which have accumulated between this and the overlying hyperconcentrated flow contain a thin andesitic tephra about 0.72 m above the contact with the lowermost hyperconcentrated flow. This tephra is recognized on field characteristics at other localities in the coastal reaches of the study area. At another locality (WF3, Figure 4.1, Plate 4.6 and section description) the basal distal lithofacies contain common to abundant dacitic pumice lapilli and blocks. Deposits of distal lithofacies cannot be correlated to marginal or veneer lithofacies further upstream. However the lithological similarity between veneer and distal lithofacies , *e.g.* the presence of pumice and scoriaceous clasts in both of these but not marginal lithofacies, implies that distal lithofacies are probably downstream correlatives of the veneer lithofacies.

It has been established that the marginal lithofacies were emplaced by a large debris flow, probably initially in the form of a debris avalanche. The transformation of this debris avalanche to a debris flow may have occurred as a result of slumping of water-saturated debris, as was hypothesised by Crandell (1988) and observed at Mount St. Helens (Scott, 1988a). From the evidence outlined above it seems likely that the initial sector collapse exposed the magma chamber at the volcano triggering pyroclastic surges or flows, which subsequently transformed to lahars in the channel of the proto-Whangaehu River. These flowed over the top of the main debris flow deposit and downstream through the catchment over 160 km to the coastal plain where occasional boulders (up to 2 m in maximum diameter) are observed resting on terraces, and in the present channel of the River (WF4, Figure 4.1; S22/045377). These must have been brought downstream by Whangaehu Formation lahars and attest to their competence even at distances of over 170 km from source. The presence of the thin fine-grained marker bed may represent the airfall equivalent of a Plinian eruption at this time, at Mount Ruapehu.

The overall facies model for development of the Mount Ruapehu edifice (Hackett, 1985; Hackett and Houghton, 1989) may relate to the scenario proposed here for emplacement of Whangaehu Formation lahars. According to Hackett and Houghton's model (see Chapter 2, section 2.2.1), before about *c.* > 120,000 years ago volcanism was centred around a vent (or vents) in the (present) northern sector of Mount Ruapehu leading to accumulation of the Te Herenga Formation. Between about 120,000 and 60,000 years ago extrusive volcanism became centred in the south of the volcano. A large southward sector collapse of the volcano, here represented by the marginal deposits of the Whangaehu Formation, probably shifted the focus of further extrusive activity to the south of the volcano. This resulted in a lateral shift of the active vent zone from the north (Te Herenga Formation) to the south (Wahianoa Formation) before 120,000 years ago.

4.4 AGE OF THE WHANGAEHU FORMATION

No direct dating techniques were available for determining the approximate time interval during which the Whangaehu Formation lahar deposits were emplaced. As mentioned in section 4.2 the Whangaehu Formation is interpreted to be greater than *c.* 120,000 years old. In the coastal reach of the catchment a valley was cut into the 210,000 year-old Ngarino marine terrace (Pillans, 1988 & 1990) and subsequently partially filled by Whangaehu Formation deposits. This relationship is observed at WF2 (see Figure 4.1 and Plate 4.3) where the contact between older marine and fluvial sediments comprising the Ngarino terrace and the younger abutting laharic deposits is exposed. Pillans (1988 & 1990) presents a chronology for marine benches in the Wanganui region, and his work established that the Ngarino marine terrace had been cut by 180,000 years ago, and this date provides a maximum age for the Whangaehu Formation. Coverbed stratigraphy of sediments overlying the Whangaehu Formation at this site indicates that the deposits are at least 80,000 years old, based on interpretation of a core augered on the surface of the Whangaehu Formation terrace. 4 m of sediments were extracted from this core, and when these were examined three pale loess deposits separated by darker coloured palaeosols were identified. This sequence overlies sands through which it proved too difficult to auger further. By simple count back methods the loess deposits were correlated to Ohakean, Ratan, and Porewan loess, and the sands to Mount Stewart Dunesand. This placed the age of the bottom of the core at approximately the end of the Last Interglacial, and provided a minimum age for the underlying sediments of about 80,000 years.

In proximity to Mount Ruapehu two relatively undisturbed coverbed sequences, which directly overlie the Whangaehu Formation, provide a record of subsequent major rhyolite and andesite eruptives and climatic fluctuations during the late Quaternary. From detailed descriptions and laboratory analysis of these coverbeds it has been possible to determine a more accurate upper bracketing age for emplacement of the Whangaehu Formation lahar deposits. These two sites will be described in greater detail and the methods and implications of laboratory analysis now discussed.

4.4.1 *COVERBED STRATIGRAPHY: QUANTITATIVE XRD AS AN INDIRECT DATING TECHNIQUE*

In New Zealand, quartz in soils derived principally from andesitic ash has been shown to be of aeolian origin (Mokma *et al.* 1972; Stewart *et al.* 1977, 1986a, 1986b). Alloway (1989) and Alloway *et al.* (1992) present a methodology for quantitatively assessing the total amount and accumulation rate of quartz in a tephric-dominated coverbed sequence in north Taranaki. Alloway *et al.* (1992) conclude that the variations in quartz accumulation rate provide a reliable record of post-125,000 year climate change. Increase in total quartz content and accumulation rate is interpreted to reflect increased intensity and expansion of global wind systems, coupled with increased aridity during glacial periods, leading to transport of greater amounts of quartz globally (Stewart, 1986). By comparing the amount of quartz present in terrestrial and marine sediments sampled in New Zealand, Stewart (1986) concludes that terrestrial based cover bed sequences present a more representative record of the influx of aeolian quartz as controlled by climatic forcing, rather than marine sequences which were affected by increased accumulation from extensive aggradational river flood plains.

Quartz has been shown to be an important indicator mineral in both marine and terrestrial sediments for climate change (Bowles, 1975; Stewart *et al.*, 1986a; Alloway, 1989; Alloway *et al.*, 1992). Stewart *et al.* (1986a) also note that "...*within a region the aerosolic quartz content has a potential use for estimating relative ages of accumulating material*". The coverbed stratigraphy of tephric and loessal deposits which have accumulated over the Whangaehu Formation provides a means of determining a palaeoclimatic record based on the influx of quartz during times of extreme cold (stadials), against a background of the steady accession of andesitic tephra. Dated rhyolitic tephras found both macroscopically and microscopically within these coverbeds also provide some time control stretching back to approximately 64,000 years ago for interpretation of the upper part of the sequence.

Methods for assessing quantitatively the amount of quartz present in sediments fall into two groups. The chemical pretreatment method described by Trostel and Wynne (1940) is accurate but time consuming. Phillippe and White (1950), Johnson and Beavers (1959) and Till and Spears

(1969) describe an X-ray diffraction method which is more rapid but less accurate than the chemical pretreatment method. This method was adapted by Alloway (1989) to characterize total quartz percentages in andesitic provenance coverbeds. The methodology outlined by Alloway *et al.*, 1992 was used here although, in order to reduce sample preparation time whole soil samples, rather than pretreated samples, were analysed.

4.4.2 *DETERMINING TOTAL QUARTZ IN TEPHRIC COVERBED SEQUENCES: METHODOLOGY*

Two sites were selected for detailed stratigraphic studies. The first site, WF5 (see Figure 4.1, Plate 4.7, and section description), is located about 1 km west of the Whangaehu Valley Road on the east side of the Whangaehu River. Here a complete and undisturbed coverbed sequence stretching back to before the Last Interglacial is preserved. Kawakawa Tephra provides an easily identifiable time plane at *c.* 22,590 years B.P., recognizeable in the section (see Plate 4.8). Two previously undescribed andesitic tephras, Mangawherawhera and Kaitieke tephra, are found in buried soils which have formed in loess sheets below Kawakawa Tephra. These are found at a number of localities throughout the middle catchment of the Whangaehu River and provide useful stratigraphic markers.

The second site, WF6 (see Figure 4.3, and section description), is located on the west side of the Whangaehu River. Here the upper part of the coverbed sequence is incomplete, but correlation between the two sites is possible due to the presence of newly described Mangawherawhera and Kaitieke tephras at both sites.

At both localities coverbeds directly overlie Whangaehu Formation veneer lithofacies, which overlie marginal-A lithofacies. The coverbeds were sampled at approximately 0.10 m intervals, with accommodation made for variations in the nature of the tephra and sediment based on field observation and description. Samples were analysed in order to determine two independant variables, (1) the total amount of quartz in each sample, and (2) identification of microscopic tephras which had not been observed in

the field and which might serve as useful time planes to aid the interpretation of quantitative quartz analyses.

4.4.2.1 *Stratigraphy of sample sites*

Site WF5

The coverbeds at WF5 are exposed in a disused metal pit perched on the edge of high bluffs cut into the Whangaehu Formation and underlying Tertiary sandstone and siltstone, alongside the entrenched upper Whangaehu gorge. A complete and undisturbed coverbed sequence is preserved here, and is detailed in Figure 4.4 (see Page 77). The lowermost beds are interpreted to have begun accumulating immediately following emplacement of the veneer lithofacies of the Whangaehu Formation. The coverbed stratigraphy starts with a thin gleyed loess bed, L5a. An andesite lapilli bed, the Rangiwhaia tephra, lies at the base of the next loess bed, L5b. A strongly coloured palaeosol, P5, is developed into this loess bed. Two loess units, L4 and L3, separated by a weakly developed palaeosol, P4, lie between P5 and the Mangawherawhera tephra. A thin palaeosol, P3a, has developed on L3 immediately below Mangawherawhera tephra. This tephra is divided into two separate periods of accumulation. Primary tephra is believed to be represented by a thin (0.08 m) lower lapilli-rich bed. This is overlain by a thicker (0.25 m) lapilli-rich tephric palaeosol, P3b, which may represent aeolian reworking. A loess bed, L2, accumulated between underlying Mangawherawhera and overlying Kaitieke tephras. A palaeosol, P2, has developed into loess and andesitic ash overlying Kaitieke tephra. A thick bed of loess, L1a & b, which contains Kawakawa Tephra approximately 0.3 m above its base overlies P2. This bed is overlain by andesite ash which has accumulated subsequent to emplacement of L1, and is represented by a palaeosol, P1.

Site WF6

Coverbeds at WF6 are exposed alongside a track, which has been cut through beds of veneer and marginal-A lithofacies of the Whangaehu Formation. Figure 4.5 (see page 78) details the stratigraphy at this locality. The lowermost coverbed is a thick sheet of loess, L5a. A tephric palaeosol, P5a, which contains an andesitic lapilli-bed, the Rangiwhaia tephra, has formed in this loess, and is itself overlain by thin loess sheet L5b. A very well-developed palaeosol, P5b, has developed into the loess. Two loess beds, L4 and L3a, which are separated by a thin weakly developed palaeosol, P4, have accumulated over this palaeosol. Accumulation of loess in the uppermost bed was interrupted by an andesite tephra, the Rangiahu tephra, which is not recorded in cover-beds at WF5. A palaeosol, P3, developed into the upper loess (L3b) is overlain by Mangawherawhera tephra. The cover-bed sequence is compressed in the upper part of this section and Mangawherawhera and Kaitieke tephra are separated by only a thin loess bed, L2. The Kaitieke tephra marks the upper boundary of the cover-bed sequence at WF6.

4.4.2.2 *Tephrostratigraphy of coverbeds at Sites WF5 and WF6*

Macroscopically identified rhyolitic tephras were Taupo Ignimbrite and Kawakawa Tephra. It seemed likely that other rhyolitic tephras would be present in the coverbeds, as these have been described in sequences much further to the west and south away from source (Pillans, 1988). Therefore samples obtained from both coverbed sequences were chemically cleaned, and the percentage of glass shards present in grain mounts of the very fine sand size range were determined.

Subsamples were cleaned using 0.2 M ammonium oxalate-oxalic acid according to the method described by Blakemore *et al.* (1987) to remove short range order clays and organic material. Some of the older heavily iron-stained samples required further pretreatment using citrate dithionite according to the method described by Mitchell *et al.* (1971) and Blakemore *et al.* (1987) to remove ferric oxide. The mineral grains obtained following these treatments were sieved into very fine sand, fine sand and medium sand size fractions. Preliminary mineralogical analysis indicated that grain

counting of the very fine sand fraction gave better defined glass peaks so therefore this was used as the standard size fraction for glass counting. Grains from whole samples were mounted in resin, and counts of 400 grains were made (Wallace *et al.*, 1985), and the percentage of rhyolitic glass determined from these.

Three glass peaks were observed in coverbeds sampled from WF5 (see Figure 4.4 and Plate 4.7), the uppermost corresponding to Kawakawa Tephra (22,590±230 years B.P). The lower two glass peaks were originally correlated with the Mangaone Tephra and Rotoehu Tephra. Microprobe analysis carried out by Dr B. Pillans (Victoria University of Wellington) identified the upper glass peak as Omataroa Tephra, which is an Okataina Volcanic Centre-sourced tephra dated at 28,220±630 years B.P. (Howorth, 1975; Froggatt and Lowe, 1990). The lower glass peak was identified as the Rotoehu Tephra, also an Okataina-sourced tephra with a recently determined age of 64,000±230 years B.P. (Wilson *et al.*, 1992). Omataroa Tephra is located in L2 underlying Kaitieke tephra. Rotoehu Tephra lies in the lapilli-rich palaeosol overlying the andesite Mangawherawhera tephra.

At WF6 Kawakawa Tephra was not preserved, and no other rhyolite tephras were observed macroscopically. Only 0.12 m of loess separated Kaitieke from Mangawherawhera tephra, and a distinct glass peak in this horizon probably represents a mixed population of Omataroa and Rotoehu Tephra (see Figure 4.5).

Four newly described and informally named andesite tephras, Rangiwhaia, Rangiahu, Mangawherawhera and Kaitieke tephras are identified at WF5 and WF6. The two latterly mentioned and younger tephras can be confidently correlated between sites, and are ubiquitous throughout sections in the upper and middle catchment of the Whangaehu River.

Rangiwhaia tephra is found in coverbeds at WF5 where it is a speckled dominantly coarse ash and fine lapilli, and is deeply weathered. This may reflect local depositional conditions, since the underlying loess, L5a, is strongly gleyed. It is probable that L5a and Rangiwhaia tephra were deposited in a wet enironment, *e.g.* a swamp. The tephra is named after the Rangiwhaia Stream which joins the Whangaehu River approximately 1.5 km above WF5 (S21/205832). The Rotoehu Tephra, *c.* 64,000 years old, provides a minimum age for Rangiahu and Rangiwhaia tephras.

Rangiahu tephra is found in coverbeds at WF6, and is named after the Rangiahu Stream which enters the Whangaehu River just upstream of WF6 (S21/178808). It is similar in physical appearance to Mangawherawhera tephra, but contains multi-coloured, as opposed to mono-coloured lapilli.

Mangawherawhera tephra is grey in colour, and is enriched in lapilli size particles and is friable. It is named after the Mangawherawhera Stream, a tributary of the Whangaehu River. In a road cutting beside Old Fields Track approximately 1 km downstream of their confluence, Mangawherawhera tephra is well exposed in coverbeds mantling the Whangaehu Formation (WF7, see Figure 4.1, Plate 4.9 & 4.10, and section description). This exposure lies almost directly opposite to WF5, but on the west side of the River. Mangawherawhera tephra underlies the Rotoehu Tephra and is therefore older than 63,770 years B.P.

Kaitieke tephra is a distinctive grey-coloured lithified ash (WF5, WF6 and WF7, see Figure 4.1, Plate 4.9 & 4.10, and section descriptions). It is named after the Kaitieke Stream which enters the Whangaehu River just below WF6 (S21/177803), where Kaitieke tephra is the uppermost bed described. Kaitieke tephra was erupted post-Omataroa and pre-Kawakawa Tephra eruptions and thus is aged between 28,850 and 22,360 years B.P.

4.4.2.3 *Quantitative quartz analysis of cover-bed sequences*

The method employed to assess total quartz content in cover-bed sediments closely follows that proposed by Alloway (1989) and Alloway *et al.* (1992). In this study Linde-A (Al_2O_3) is used as the internal standard. All the samples collected from both coverbed sequences were analysed. Samples were oven dried but not chemically pretreated. The ammonium oxalate-oxalic acid pretreatment used by Alloway (1989) is time consuming, and in an endeavour to cut down on analysis time whole soil samples were analysed.

Preparation of a standard curve

A standard curve was prepared from standard mixes of ground quartz, Linde-A, and a $MgO/CaCO_3$ matrix with a bulk mass absorption corresponding to the mean chemical composition determined for selected loess and palaeosol samples drawn from cover-beds at Site WF5 (X-ray fluorescence data courtesy of Mr K. Palmer, Victoria University of Wellington). Quartz was ground in a mill grinder and the $< 20\ \mu$ fraction obtained by settling according to Stokes Law. Standard mixes ranging from 0 % to 25 % total quartz content were prepared. Each standard comprised a known amount of quartz combined with $MgO/CaCO_3$ matrix to make up one gram, and a constant amount (0.25 g) of Linde-A as the internal standard. The standard mixes were shaken overnight in an end over end shaker. Samples were shaken end over end for a further hour, with a ball-bearing included in the mix, prior to analysis. Thorough mixing of the individual components of the mix is essential if this method of analysis is to be successful.

Samples were scanned using a Phillips 1840 X-ray diffractometer under the following parameters:

CoK-Fe-filtered radiation
Slit, 0.2; T.C. 5;
Range, 5×10^3
Chart speed, 0.005
Step size, 0.01

The most accurate measure of quartz in the standards and unknown samples is afforded by setting the diffractometer to a slow speed and small step size, although this does increase analysis time. The 24.25 theta quartz and 29.88 theta Linde-A reflections were scanned, and the area under each peak calculated. Five replicates of each standard were scanned, and the standard curve drawn by plotting the known percentage of quartz in each sample against the ratio between peak quartz intensity and peak Linde-A intensity (see Figure 4.3). The coefficient of variation of all standards scanned was between 4.87 % (25 % quartz) and 32.89 % (0 % quartz).

Quartz %	Qtz/L.A.	Mean	SD	CV
0 %	0.04	0.06	0.02	32.29
	0.07			
	0.03			
	0.07			
	0.06			
5 %	0.36	0.34	0.04	10.81
	0.30			
	0.38			
	0.37			
	0.31			
10 %	0.63	0.66	0.08	11.88
	0.61			
	0.69			
	0.77			
	0.57			
15 %	0.81	0.95	0.14	14.58
	0.81			
	0.97			
	1.08			
	1.09			
20 %	1.08	1.19	0.12	9.76
	1.36			
	1.21			
	1.09			
	1.22			
25 %	1.35	1.41	0.07	4.87
	1.50			
	1.41			
	1.35			
	1.47			

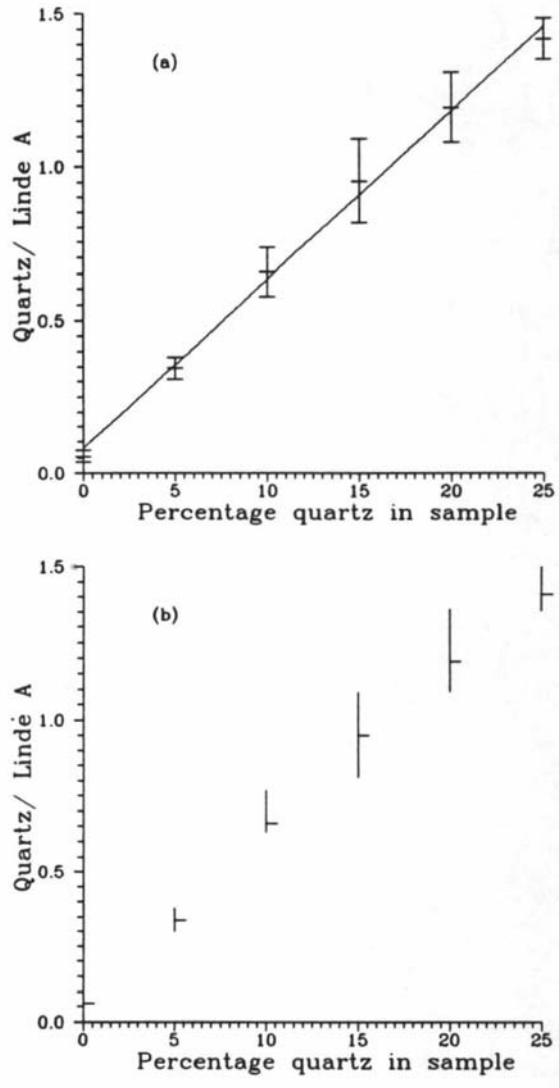

Figure 4.3 Results of XRD analysis, and standard curve, for quartz standard replicates. Five replicates of each mix were analysed, and the results are tabled above. Mean and standard deviation for each set of replicates is plotted in graph (a); the standard curve is drawn from all data points. Graph (b) plots high-low and mean values for each set of replicates.

A linear relationship was found between the percentage of quartz and the Quartz/Linde-A peak intensity ratio which satisfied the regression equation:

$$\frac{quartz}{Linde\text{-}A} = 0.0551543\, percentage\, quartz + 0.0792381 \qquad (4.1)$$

Analysis of unknown samples

Samples obtained from the coverbed sequences at WF5 and WF6 were oven dried at 500°C to remove excess water and were hand ground in a mortar and pestle to a talc-like consistency. Samples were then prepared in a similar fashion as the standards, combining one gram of sample with 0.25 grams of Linde-A, and shaken end over end overnight and for one hour with a ball-bearing prior to analysis. Samples were scanned under exactly the same conditions as the standards, although only three replicates were analyzed. The percentage of quartz in each sample was calculated using the regression equation derived from the standard curve:

$$percentage\, quartz = \frac{intensity \frac{quartz}{Linde\text{-}A} - 0.0792381}{0.0551543} \qquad (4.2)$$

The results of this analysis are detailed in Figures 4.4 and 4.5 and Tables A2-A6 (see Appendix). The coefficients of variation for all samples was found to range between 0.41 to 74.69 %. High coefficients of variation compared to those calculated by Alloway (1989) suggest that in order to obtain more accurate results acid-oxalate pretreatment of samples, and the extraction and analysis of only the < 20 μ fraction is preferable.

4.4.2.4 *Variations in total quartz content at WF5 and WF6.*

At WF5 total quartz content is observed to vary systematically with depth (see Figure 4.4). In the lower part of the cover-bed sequence total quartz percent is high, in the order of 20 %. However tephric inputs from Rangiwhaia tephra drown the signal at approximately 5.45 to 5.35 m below ground surface. Between 5.00 and 4.50 m below ground surface total quartz percent falls to below 5 %, and then steadily climbs through

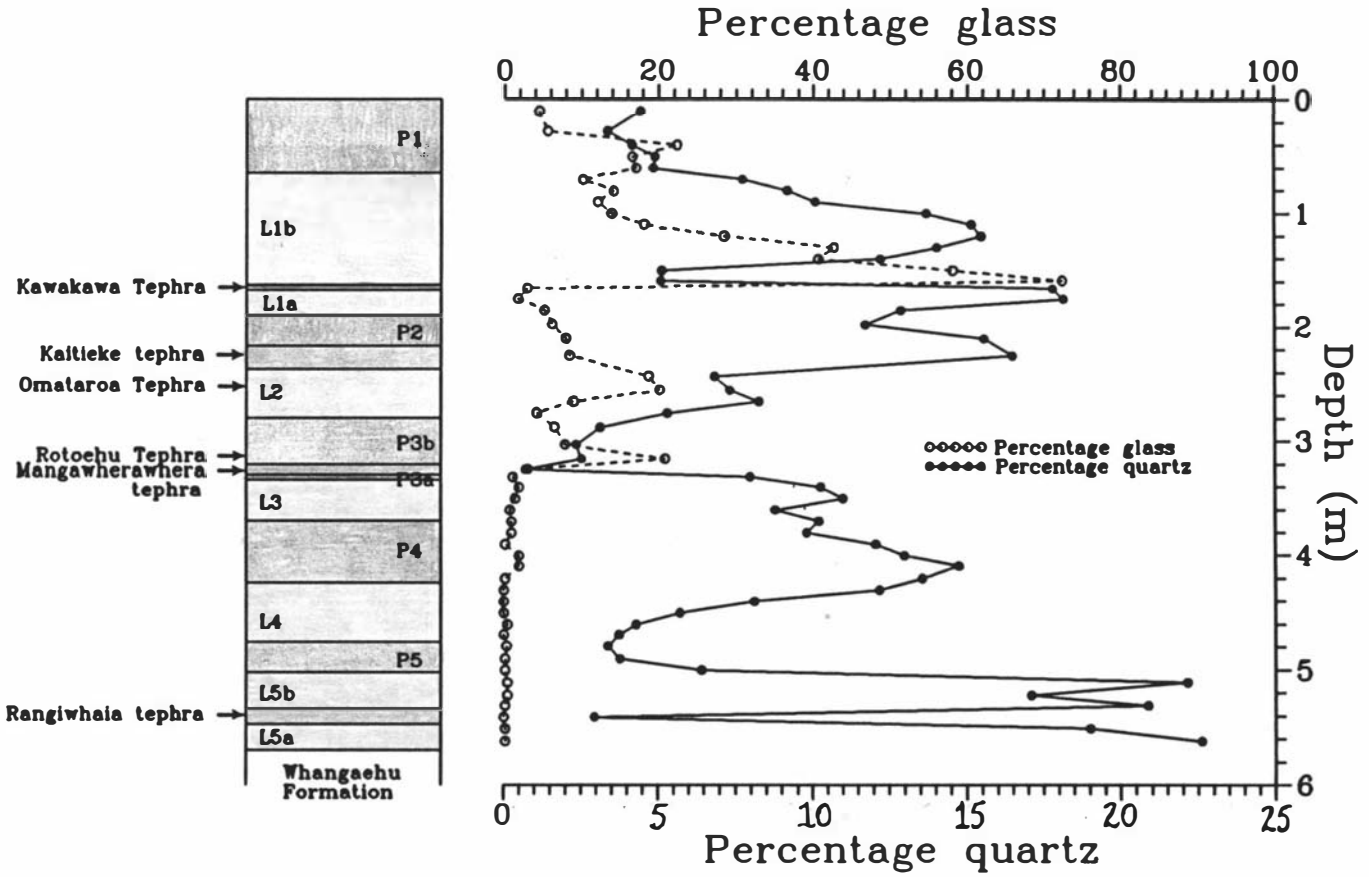

Figure 4.4 Stratigraphy and percentage of rhyolite glass and quartz in coverbeds at WF5; (P) marks palaeosols, (L) marks loesses, ( ) marks andesite and ( ) rhyolite tephras.

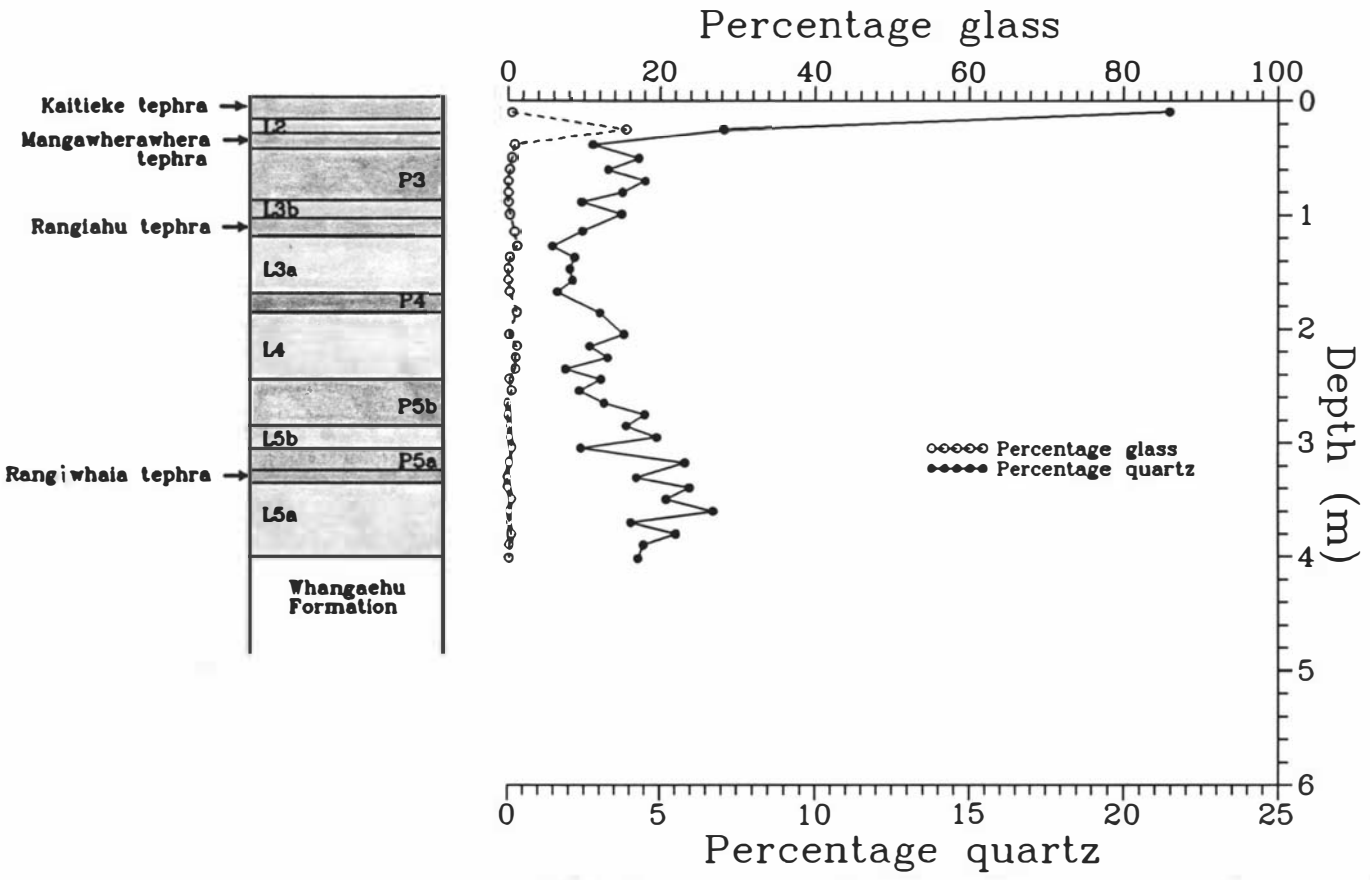

Figure 4.5 Stratigraphy and percentage of rhyolite glass and quartz in coverbeds at WF6; (P) marks palaeosols, (L) marks loesses, ( ) marks andesite and ( ) rhyolite tephras.

the next 1 m to the order of 10 %. Eruption of Mangawherawhera tephra dampens the signal between 3.28 and 3.20 m below ground level, and total quartz percent remains low through the palaeosol which mantles this tephra. However values for total quartz percent increased through the next 1.5 m, peaking at the Kaitieke tephra, which is unexpected and indicates that either (1) this tephra is enriched with quartz, or (2) the tephra accumulated in a quartz rich coverbed. The low content of quartz throughout the coverbeds at this locality does not support the second explanation, and the first explanation seems more likely. A microscopic investigation of the mineralogical nature of the quartz in this horizon would help elucidate its nature and origin. A short reversal in the trend for increasing quartz percent corresponds with a palaeosol which overlies Kaitieke tephra. The Kawakawa Tephra lies in loess above this horizon and total quartz percent falls to 5 % in the zone where the glass counts are highest. Total quartz percent then rises rapidly in sediment overlying the Kawakawa Tephra before falling gradually to a level of about 5 % in the most recent sediments.

At WF6 total quartz content is generally low, rarely rising above 6 % (see Figure 4.5). The most noticeable peak is in the uppermost sample, Kaitieke tephra, which has a total quartz percent of 21.47 % (C.V. 22.89 %). The very low total quartz content in sediments here made it difficult to identify the trends observed at WF5. However overall the total quartz content decreased gradually upwards through the sequence of coverbeds. The low quartz content of these coverbeds may be a consequence of the location of this exposure to the west of the Whangaehu River and near to the summit of a spur where quartz accumulation rates were probably low.

4.4.2.5 *Palaeoclimatic inferences from variations in total quartz content of coverbed overlying the Whangaehu Formation*

By combining the field observations with the mineralogical analyses of samples obtained from the coverbeds at WF5 and WF6, a record of late Quaternary climate change for the region can be established.

The best record is preserved at WF5. Here an early peak in total quartz percent coincident with L5 corresponds to accumulation of Marton loess, which accumulated between about 140,000 and 130,000 years ago (oxygen isotope stage 6). A very low total quartz percentage is recorded in the Rangiwhaia tephra. The total quartz percent

is low through P5, which is interpreted to represent a well-developed soil that formed during the Oturian or Last Interglacial (oxygen isotope stage 5e). Total quartz percent increased through L4, which is here correlated to Huiranga loess observed in north Taranaki (Alloway *et al.*, 1987) and estimated to have accumulated during oxygen isotope stages 5d (*c.* 107,000), and to L4 in the Wanganui Basin (Pillans, 1988). Pillans estimated that this loess sheet accumulated between 120,000 and 100,000 years ago. This correlation is based on the similarity in time frame covering the period of accumulation for both loess beds, combined with the greater proximity of L4 (Pillans, 1988) to the field area in this study. Total quartz percent decreased in P4, but increased in L3, which is interpreted to correspond to accumulation of Porewan loess (oxygen isotope stage 4).

Milne and Smalley (1979) proposed that Porewan loess accumulated between 80,000 and 70,000 years ago; however Alloway *et al.* (1987) and Hodgson (this volume) present evidence for the presence of Rotoehu Tephra in the palaeosol developed into Porewan loess (P3b, this volume) immediately above Mangawherawhera tephra, and *c.* 0.25 m below the contact with overlying Ratan loess. The Rotoehu Tephra has recently been assigned a new age of 64,000±230 years B.P. (Wilson *et al.*, 1992). This may indicate that either (1) the Porewan stadial lasted longer than previously thought, *i.e.* between *c.* 80,000 and 63,770 years ago, or (2) deposition of loess was followed by a period of accumulation of andesitic (and rhyolitic) medial material, much as is happening under present Holocene time, prior to the onset of the Ratan stadial. Support for the latter hypothesis can be found in the presence of a thick sequence of andesitic tephra, referred to in this thesis as the Mangawherawhera tephra. It is identified in coverbeds in the Whangaehu and Mangawhero catchments, and is here considered to be the near-source correlative of the Tongariro Volcanic Centre-sourced tephra found in coverbeds in the Rangitikei catchment by Milne (1973_a). The amount of quartz in the underlying loessial sediment appeared to be dropping off prior to emplacemnt of Mangawherawhera tephra and this is interpreted as representing the closing stages of the Porewan stadial.

Total quartz percent in the Mangawherawhera tephra is the lowest throughout the whole coverbed sequence. A small peak is recorded in the overlying loess bed, L2, and this

is interpreted as corresponding to Ratan loess (oxygen isotope stage 3). This had been considered to have accumulated between 40,000 and 32,000 years ago (Milne and Smalley, 1979), but the presence of Omataroa tephra, at approximately one half of the thickness of L2, at this locality, gives a new perspective on the age of Ratan loess. A new age established for Omataroa Tephra of 28,220±630 years B.P. suggests that the Ratan stadial lasted for longer than Milne and Smalley (1979) originally proposed, *i.e.* an upper age limit of at least 27,590 years B.P. The Kaitieke tephra marks the closing stages of the Ratan stadial. The overlying palaeosol, P2, in which total quartz percent decreases, indicates an interval of ameliorating climate during the Apitian interstadial. A late peak in total quartz percent, coincident with L1, corresponds to accumulation of Ohakean loess (oxygen isotope stage 2), and this is corroborated by the presence of Kawakawa Tephra in L1. Total quartz percent decreases in P1, the uppermost coverbed in the sequence, which marks the Holocene, and lapilli-sized clasts of Taupo Ignimbrite are found scattered throughout the upper 0.40 m of this bed.

The record at WF6 is not as complete as at WF5, so will not be described here in the same detail. A weak trend is observed between P beds and low total quartz percent and L beds with higher quartz percent; however total quartz percent is so low in most samples that it was difficult to avoid being subjective in these interpretations. The best defined peak in quartz content lies at the base of these cover-beds, in L5a and L5b. This is interpreted to correspond to accumulation of Marton loess, which also marks the base of the cover-bed sequence at WF5.

High total quartz content values measured within Marton, Porewan (including L4) and Ohakean loess sheets suggests that the palaeoclimate was most severe during these times. Total quartz content within the Ratan stadial is much lower, and this is interpreted to reflect a less severe climate, supporting a similar contention proposed by Alloway *et al.* (1992).

By interpreting the palaeoclimatic record of the coverbed stratigraphy at WF5 and WF6, it is possible to then provide a minimum age estimate of the underlying Whangaehu Formation. This evidence indicates the Formation was deposited immediately prior to or during the accumulation of Marton loess *c.* 140,000 years ago, *i.e.* during oxygen

isotope stage 6. Near to the coast Whangaehu Formation deposits are confined within the Ngarino marine cut terrace which is proposed to have been cut by 180,000 years ago, and gives a maximum age for deposition of the Formation. Thus it is here interpreted that the Whangaehu Formation was emplaced in the period between 180,000 and 140,000 years ago.

4.5 *DEPOSITS OF THE WHANGAEHU FORMATION IN THE MANGAWHERO AND HAUTAPU RIVER CATCHMENTS*

Te Punga (1953) attributed boulders found in the Hautapu Valley Agglomerate to deposition from a single huge lahar which flowed down the valley of the Hautapu River from Mount Ruapehu. In the middle reaches of the Mangawhero River, beside State Highway 4 approximately 15 km south of Raetihi, a steeply graded road cutting has exposed thick sequences of gravelly lahar deposits (WF8, see Figure 4.1). Coverbed stratigraphy at this locality is similar to that at WF5 and WF6 in the Whangaehu River Valley (see Plate 4.11), and correlation is facilitated by the presence of Mangawheraw hera tephra in the upper sequence of coverbeds at all three localities. The valley sides in the upper and middle reaches of all three catchments are mantled with andesitic boulders and this author believes these were probably emplaced by the Whangaehu Formation marginal lithofacies debris flow, and consequently that deposits recognized in the Whangaehu, Hautapu and Mangawhero River Valleys are correlatives of this catastrophic event.

CHAPTER 5

POST-WHANGAEHU FORMATION LATE PLEISTOCENE LAHARS

5.1 INTRODUCTION

The Whangaehu Formation, described in the previous chapter, represents an episode of intense volcanic activity from Mount Ruapehu, injecting vast quantities of volcaniclastic material into the headwaters of the proto-Whangaehu River. This material was mobilized as lahars throughout the catchment of the River. Following this interval of activity the next youngest volcaniclastic deposits are dated at *c.* 37,000 and 29,000 years ago, recording laharic aggradation in the middle and lower catchment of the River during the Ratan stadial and Apitian interstadial, respectively. These deposits, however, are not widely distributed and probably record only small scale laharic activity. There is evidence for major laharic activity on the southeast Mount Ruapehu ring plain between *c.* > 22,590 and 14,700 years B.P., the deposits of which are referred to as Te Heuheu Formation (Donoghue, 1991). In this study deposits correlated to this Formation are restricted to the edge of the Mount Ruapehu ring plain in the upper Catchment of the Whangaehu River.

This chapter will describe the distribution and nature of late Pleistocene-aged deposits in the middle and lower reaches of the Whangaehu River, and offer an explanation for the low volume of laharic sediment in the Valley during the time interval of approximately 140,000 to 14,700 years B.P.

5.2 THE MANGATIPONA PUMICE SAND

Approximately 1 km upstream of Wyley's Bridge, at the confluence of the Whangaehu River with the Mangatipona Stream (MA1, see Figure 5.1, Plate 5.1 and section description), a 1 m thick pumice-rich gravelly diamicton is exposed underlying a sequence of late Quaternary coverbeds.

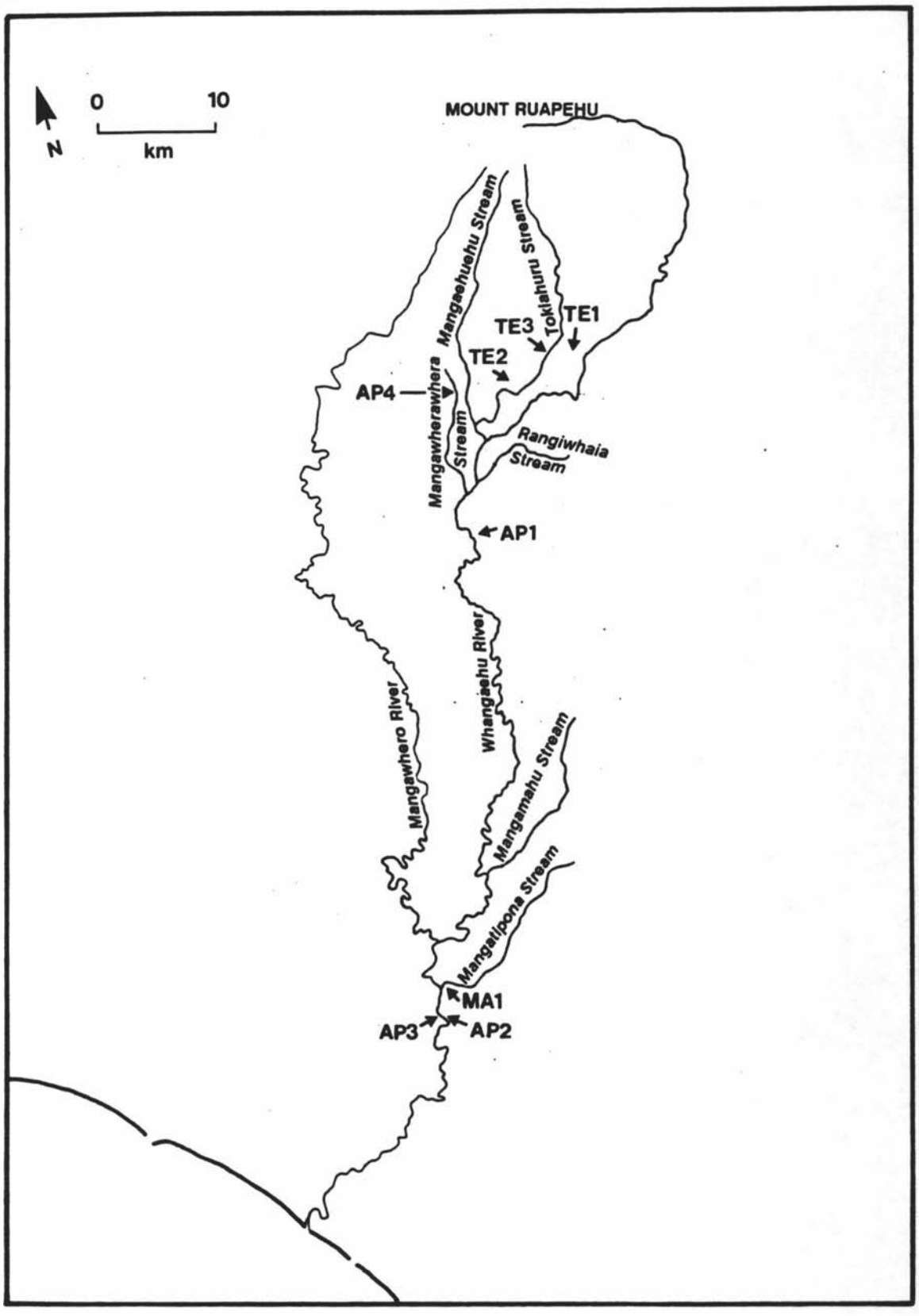

Figure 5.1 Map showing locality of Mangatipona pumice sand, Apitian lahars, and Te Heuheu Formation reference sections and observation sites.

These coverbeds include, in sequence, an immediately overlying 1 m of quartzofeldspathic sands, overlain by 0.75 m of andesitic fluvial gravels. This is overlain by 4.5 m of alternating silty sand and loessial beds. The deposit comprises clast-supported granule- and sand-sized pale grey pumice and is here interpreted to have been emplaced by a hyperconcentrated flow. This previously undescribed deposit is here informally named the Mangatipona pumice sand. Common flecks and pieces of charcoal are contained within this deposit, and a date (Wk-2681) of 37,030±730 years B.P. was obtained from a piece of this charcoal. No corresponding pumice deposit has been described closer to the probable source, Mount Ruap ehu, although the age of the deposit described here is beyond the lower age limit of deposits studied by Donoghue (1991). The monolithic nature of this deposit implies a common source for the contained pumice clasts. This was probably a pyroclastic flow from Mount Ruapehu. Further support for this explanation is the presence of the charcoal within the deposit, possibly resulting from the charring of wood incorporated into a hot pyroclastic flow. Further research mapping the distribution of older Pleistocene volcaniclastics on Mounts Ruapehu and Tongariro ring plains being conducted by S.J. Cronin, Massey University, might elucidate the origin of the Mangatipona pumice sand.

5.3 APITIAN LAHARS

In the middle of the Whangaehu River Catchment a sequence of two sandy pumiceous diamictons are exposed overlying cliffs comprised of older Whangaehu Formation (AP1, see Figure 5.1, Map 3 and section description). The upper sandy deposits are overlain by Ohakean loess, identified by the presence of Kawakawa Tephra in overlying loessal coverbeds. This loess sheet also contains Ngamatea lapilli -1 and -2, andesitic tephra marker beds defined by Donoghue (1991) and dated at approximately 10-11,000 years B.P.

Laharic deposits which are overlain by Ohakean loess are also found in the reach of the Whangaehu River extending from Wyley's Bridge to Kauangaroa. These deposits are clast-supported pumiceous pebbly sands and are interpreted to have been emplaced by hyperconcentrated flow. About 4 km downstream of Wyley's Bridge and in the hillside

beside Kauangaroa Road, two sandy pumiceous diamictons are exposed in coverbeds overlying a terrace on the east bank of the Whangaehu River (AP2, see Figure 5.1, Map 6 and section description). This terrace surface is mantled by fluvial gravels. However the contact between the gravels and lahar deposits is not observed. The contact between the lahar deposits and overlying coverbeds is clear; the latter includes the Ohakean loess, with Kawakawa Tephra present.

The contact with underlying fluvial gravels is not commonly observed. In a metal pit approximately 4 km downstream from Wyley's Bridge, on the west bank of the River and opposite the previously described exposure, gravels are overlain by *c.* 1.7 m of silty sand and a further 3 m of silt (AP3, see Figure 5.1; S22/047414). A single sandy diamicton, 1 m thick, overlies these coverbeds, and is correlated to deposits described above. About 3 m of loess overlies this deposit although the absence of Kawakawa Tephra did not allow a positive correlation of this as Ohakean loess.

A sequence of six sandy diamictons exposed in a track cutting beside Ohutu Road in the catchment of the Mangaehuehu Stream are also considered to be correlatives of the previously mentioned deposits (AP4, see Figure 5.1, Plate 5.2, Map 1 and section description). An erosion break marks the contact between the uppermost lahar deposit and the overlying coverbeds. These coverbeds include Ohakean loess, identified by the presence of Kawakawa Tephra.

The gravels underlying the lahar deposits described in the lower catchment are here considered to be Ratan in age; the lahar deposits overlie these gravels, and no loessial sediment is recognised between the two suites of deposits. The Ratan gravels were emplaced during the Ratan stadial *c.* 40,000 to 32,000 years ago (Milne and Smalley, 1979), and here provide a maximum age of 32,000 years old for the overlying lahars deposits. The Ohakean loess began accumulating about 25,500 years ago, and this date provides a minimum age for the lahar deposits, which here are considered to have accumulated entirely within the Apitian interstadial, a period of ameliorating climate following the Ratan stadial and prior to the Ohakean stadial (Milne, 1973b). The lahar deposits recognised in this study are here informally named the Apitian lahars.

The pumiceous nature of Apitian lahar deposits imply that these lahars were triggered by eruptions at Mount Ruapehu, with erupted material mobilized as lahars during high rainfall events. The volume of Apitian lahar deposits is estimated to be 1.8×10^6 m^3.

5.4 TE HEUHEU FORMATION

The Te Heuheu Formation was first described by Donoghue (1991). Te Heuheu deposits, which largely comprise Mount Ruapehu-sourced gravelly diamictons, form the major constructional surfaces of the southeastern Mount Ruapehu ring plain. On the southeast ring plain the base of the Formation is not observed and Donoghue (1991) did not define a lower age limit. The Rerewhakaaitu Tephra, dated at *c.* 14,700 years B.P. (Froggatt and Lowe,1990), provides the minimum age for this Formation. This upper age limit is also marked by an erosional unconformity. Donoghue (1991) considers that these deposits accumulated during the Otiran glacial.

In this study, Te Heuheu deposits are rarely observed, and are only identified in proximity to Mount Ruapehu. Here gravelly diamictites mantle marginal lithofacies of the Whangaehu Formation on the southern ring plain, and are only observed on the west bank of the River (see Maps 1 & 2). In the west of the study area the Te Heuheu Formation is observed on surfaces confined within uplifted Tertiary sandstones and siltstones. A low Tertiary outcrop (*c.* 85 m high) divides the drainage between the Tokiahuru Stream and the Whangaehu River below State Highway 49, near to the junction with the Whangaehu Valley Road. Within both catchments Te Heuheu Formation deposits are only mapped on surfaces upstream of this hill. They are exposed in road cuttings beside State Highway 49 in the vicinity of Karioi (TE1, see Figure 5.1; T21/314897) and at the junction of this Highway with the Whangaehu Valley Road (TE2, see Figure 5.1, and section description). They also crop out in railway cuttings beside the North Island Main Trunk Line where it bridges the Tokiahuru Stream (TE3, see Figure 5.1 and section description). The deposits are pebbly and matrix-supported and are here considered to have been emplaced largely by debris flow. At all localities diamictite beds were mantled by *c.* 1 m of loess containing Ngamatea lapilli -1 and -2, and *c.* 1m of Holocene ash. No rhyolite tephras were observed in coverbeds exposures; however microscopic analysis of samples taken at 0.05 m intervals from coverbeds overlying the Formation exposed beside the Whangaehu Valley Road revealed a distinct glass peak immediately overlying the uppermost lahar deposit (see Figure 5.2).

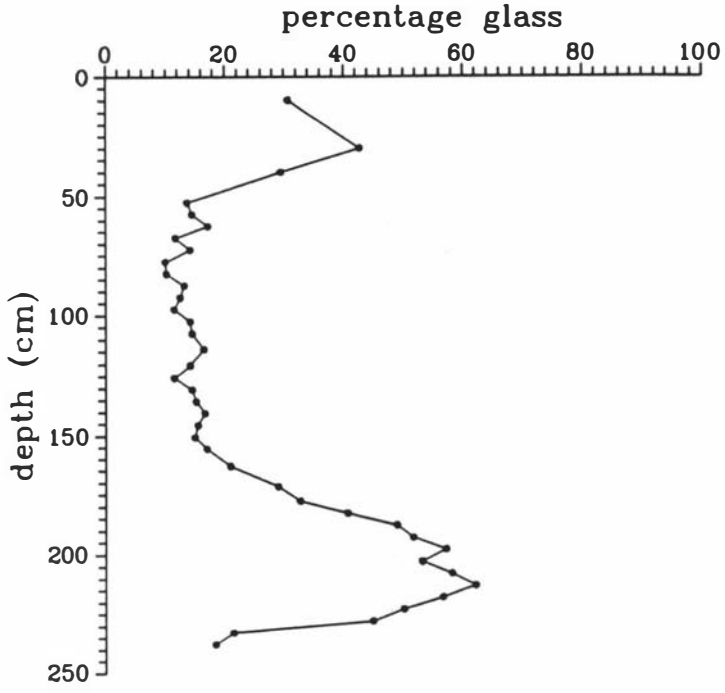

Figure 5.2 Percentage of rhyolite glass in coverbeds overlying Te Heuheu Formation at TE1; note the distinct peak beginning at *c.* 2.3 m below ground surface. The upper peak represents the Taupo Ignimbrite.

This was tentatively identified as Kawakawa tephra, and has since been confirmed by microprobe analysis (analysis performed by Dr B. Pillans, Victoria University, Wellington) indicating that here Te Heuheu deposits are older than *c.* 22,590 years B.P. The Kawakawa Tephra was not found through microscopic analysis of coverbeds at TE3 and the deposits exposed here are considered to be younger than *c.* 22,590 years B.P. Therefore on this southern sector of the Mount Ruapehu ring plain Te Heuheu Formation deposits were accumulating prior to and following emplacement of the Kawakawa Tephra. At TE1 and TE3, deposits are underlain by coverbeds containing deeply weathered andesitic lapilli which may represent any two of the late Pleistocene tephras described in coverbeds mantling the Whangaehu Formation, the youngest of which (Kaitieke Tephra) is *c.* 28,850 years old. Correlation between the tephras by mineralogical fingerprinting would provide a maximum age for the Te Heuheu Formation. In this study Te Heuheu Formation lahars are considered to have accumulated entirely within the last (Ohakean) stadial.

On the southeast Mount Ruapehu ring plain Te Heuheu Formation comprises thick sequences of bouldery diamictons. Donoghue hypothesizes that the lahars which emplaced these deposits resulted from large scale sector collapses from Mount Ruapehu. Thick bouldery deposits are also described in the Whangaehu Formation which is considered to have been emplaced by a southerly directed sector collapse from the Volcano. A similar origin for bouldery Te Heuheu deposits seems likely. However lahars must also have been triggered by eruptions from Mount Ruapehu, which were occurring during emplacement of Te Heuheu Formation. Donoghue (1991) describes the Bullot Formation, which comprises sub-Plinian airfall tephra deposits which began accumulating *c.* 22,500 years B.P. and are distributed widely over the southeast Mount Ruapehu ring plain. Bullot Formation eruptions older than *c.* 14,700 years B.P. probably provided source material for Te Heuheu Formation lahars, which were initiated by the interaction between erupted material and the more extensive valley glaciers on the summit of the Volcano at this time (the Ohakean stadial). Te Heuheu deposits recognized in the Whangaehu and Tokiahuru Valleys, which are pebbly rather than bouldery, are here considered to have been emplaced by eruption-triggered lahars and not sector collapses. The presence of a strongly weathered, steeply bedded, grey andesite lapilli bed at the top of the Te Heuheu Formation at TE1 and TE2 provides evidence for their having been eruptions at Mount Ruapehu while these Te Heuheu Formation lahar deposits were emplaced.

A modern day analogue to the eruption-triggered Te Heuheu Formation lahars would be the 1985 eruption at Nevado del Ruiz where very large lahars were triggered by the dynamic interaction of pyroclastic flows with snow and ice on the summit of the Volcano. The Bullot Formation eruptions at Mount Ruapehu were not large (*c.* 5×10^8 m^3, Donoghue, 1991), the critical factor for lahar initiation being the greater surface area of available snow and ice on the Volcano during the last Stadial.

The total volume of Te Heuheu Formation lahar deposits is *c.* 6×10^9 m^3, of which deposits mapped in this study constitutes less than 0.05 %.

5.5 VOLCANICLASTIC AGGRADATION BETWEEN 140,000 AND 25,500 YEARS AGO

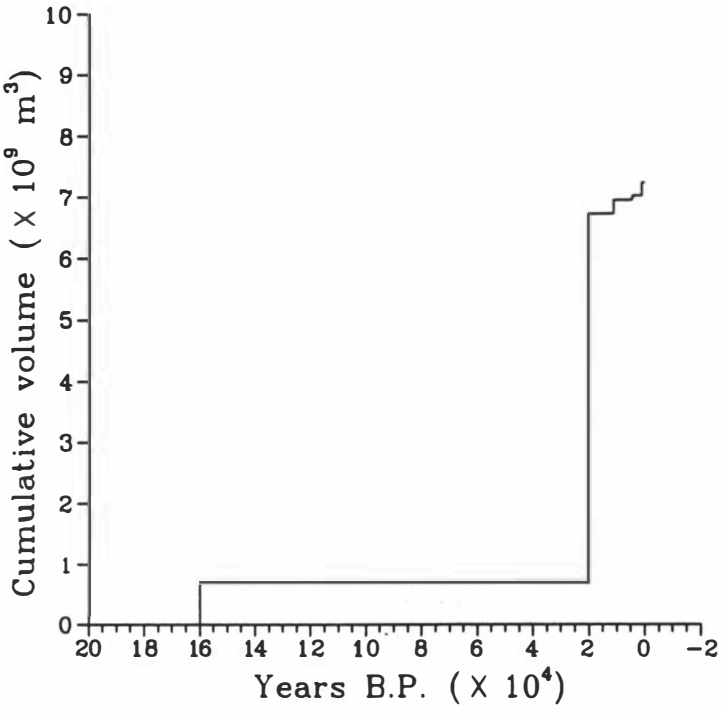

Figure 5.3 Cumulative volume of lahar deposits (within their formations) recognized in this study, from emplacement of the Whangaehu Formation, *c.* 160,000 ago to the present day. The total cumulative volume of lahar deposits is plotted against the mean age of each formation.

Figure 5.3, above, plots the accumulation of laharic deposits in the catchment of the Whangaehu River up until the present day. An interesting issue is raised here. Why is there such a low volume of volcaniclastic material mapped between the Whangaehu Formation, which had accumulated by *c.* 140,000 years ago, and emplacement of Te Heuheu Formation, which probably commenced about 25,500 years ago? The pattern of deposition implies that either (1) not many lahars actually flowed down the River during this time interval, or (2) lahars did flow through the valley, but their deposits are not preserved. This latter explanation seems unlikely considering that in the middle and lower catchment of the Whangaehu River, where late Pleistocene river terraces are

mapped, lahar deposits are only occasionally found on their surfaces. Also, Te Heuheu deposits are widely distributed in the Hautapu catchment (Donoghue, 1991). This provides strong evidence that drainage from the east flank of Mount Ruapehu was directed southeast into the upper Hautapu River, during emplacement of the Te Heuheu Formation. The majority of Te Heuheu Formation lahars flowed down this route, although the presence of Te Heuheu deposits in the area of this study indicates that a few lahars also flowed down the proto-Whangaehu River. Uplifting of the Whangaehu escarpment by late Quaternary faulting may have commenced *c.* 14,700 years ago, creating a barrier to southeast drainage into the Hautapu River and henceforth waters from the the east flank of Mount Ruapehu drained south via the Whangaehu River in its present configuration. Mount Ruapehu-sourced lahars younger than *c.* 14,700 years B.P. subsequently followed this route.

Therefore it seems most likely that not many lahars actually flowed down the Whangaehu River between emplacement of the Whangaehu Formation and the Te Heuheu Formation. The majority of Te Heuheu lahars flowed southeast down the Hautapu River rather than south down the Whangaehu River. Pre-Te Heuheu lahars may also have flowed down this Valley, although the only evidence for older laharic aggradation in the catchment is the Hautapu Agglomerate (Te Punga, 1953), which is here considered to be a correlative of the Whangaehu Formation. A further explanation for the absence of laharic deposits between 140,000 and 25,500 years ago is that Mount Ruapehu was quiescent at this time. Waimarino Lahars, mapped on the western ring plain of Mount Ruapehu, are now considered to have accumulated prior to 60,000 years ago (Hodgson and Neall, 1993), and the age of these deposits would not support this explanation. Therefore, although post-Whangaehu Formation upper Pleistocene lahars did flow down rivers draining the western flank of Mount Ruapehu, no evidence was found in this study to show that these lahars flowed down the Whangaehu River.

CHAPTER 6

THE TANGATU FORMATION

6.1 INTRODUCTION

The Tangatu Formation comprises late Pleistocene and early Holocene gravel- and sand-dominated diamictons. This Formation was first described by Donoghue (1991) who defined it as Mount Ruapehu-sourced diamictons and weakly bedded sands which accumulated on the Mount Ruapehu ring plain between about 14,700 and 5,370 years B.P. These lower and upper bracketing ages are supplied by rhyolite tephra marker beds, the Rerewhakaaitu and Motutere Tephras which respectively underlie and overlie the Formation (Donoghue, 1991). In the upper catchment the Formation overlies late Pleistocene Te Heuheu Formation. In this study Tangatu Formation is recognized throughout the middle and lower catchment of the Whangaehu River where it forms a distinct aggradational terrace which is confined within late Pleistocene aged river terraces (see Maps 2-6). It is exposed only intermittantly in the coastal reach of the catchment.

Lithology within the Tangatu Formation is almost exclusively Mount Ruapehu-sourced andesitic and dacitic sands and gravels. Deposits are moderately to weakly lithified and clasts within the deposits are commonly pumiceous.

6.2 PREVIOUS DESCRIPTIONS

At and below Mangamahu the Whangaehu River is entrenched below terraces comprising thick volcaniclastic beds. These were first described by Fleming (1953) who considered that they had been emplaced by Mount Ruapehu-sourced lahars. In this study two terrace sequences are identified and mapped as older Tangatu and younger Onetapu Formation (which will be described in Chapter 7). Campbell (1977) mapped a distinct soil type, the Kakatahi loam, which has developed in the gravelly andesitic alluvium which Tangatu and Onetapu Formation terraces are constructed from.

6.3 AGE

The lower and upper bracketing ages for the Tangatu Formation are from the rhyolitic Rerewhakaaitu (14,700±110 years B.P., Froggatt and Lowe, 1990) and Motutere Tephras (5,370±90 years B.P., Froggatt, 1981), respectively (Donoghue, 1991). These, however, are not observed in coverbeds examined in the study area of this thesis. Therefore alternative means of dating the deposits in the middle and lower catchment of the River were needed.

Tangatu Formation is observed in gravels and coverbeds which form part of the Ohakean terrace but not in Ratan coverbeds which mantle the Ratan terrace. This is interpreted to indicate that Tangatu Formation began accumulating prior to the degrading of the Ohakean terrace during the Holocene and probably at some time during the last Stadial, which commenced about 25,500 years B.P. (Milne and Smalley, 1979). This provides a maximum age of 25,500 years B.P. for the Formation. However, Kawakawa Tephra (22,590±230 years B.P., Wilson *et al.*, 1988), which is pervasive as either airborne tephra or reworked lapilli throughout the catchment, was not observed in Tangatu Formation, hence Formation deposits recognized in this study are younger than *c.* 22,820 years B.P.

At the edge of the Mount Ruapehu ring plain at the margin between the upper and middle catchment of the Whangaehu River, emplacement of Tangatu Formation has impeded drainage of the Mangawherawhera Stream. This Stream flows south in a channel, which marks the margin between the Whangaehu Formation constructional terrace to the east and dissected hill country to the west to its confluence with the Whangaehu River 8 km downstream from Karioi (S21/198831). A sample of wood from a tree stump engulfed by silts as a result of this impeded drainage (TG1, see Figure 6.1, Plate 6.1 and section description) was dated (Wk-1773) at 7,800±70 years B.P., which indicates that Tangatu Formation continued to accumulate in this region until at least 7,730 years B.P.

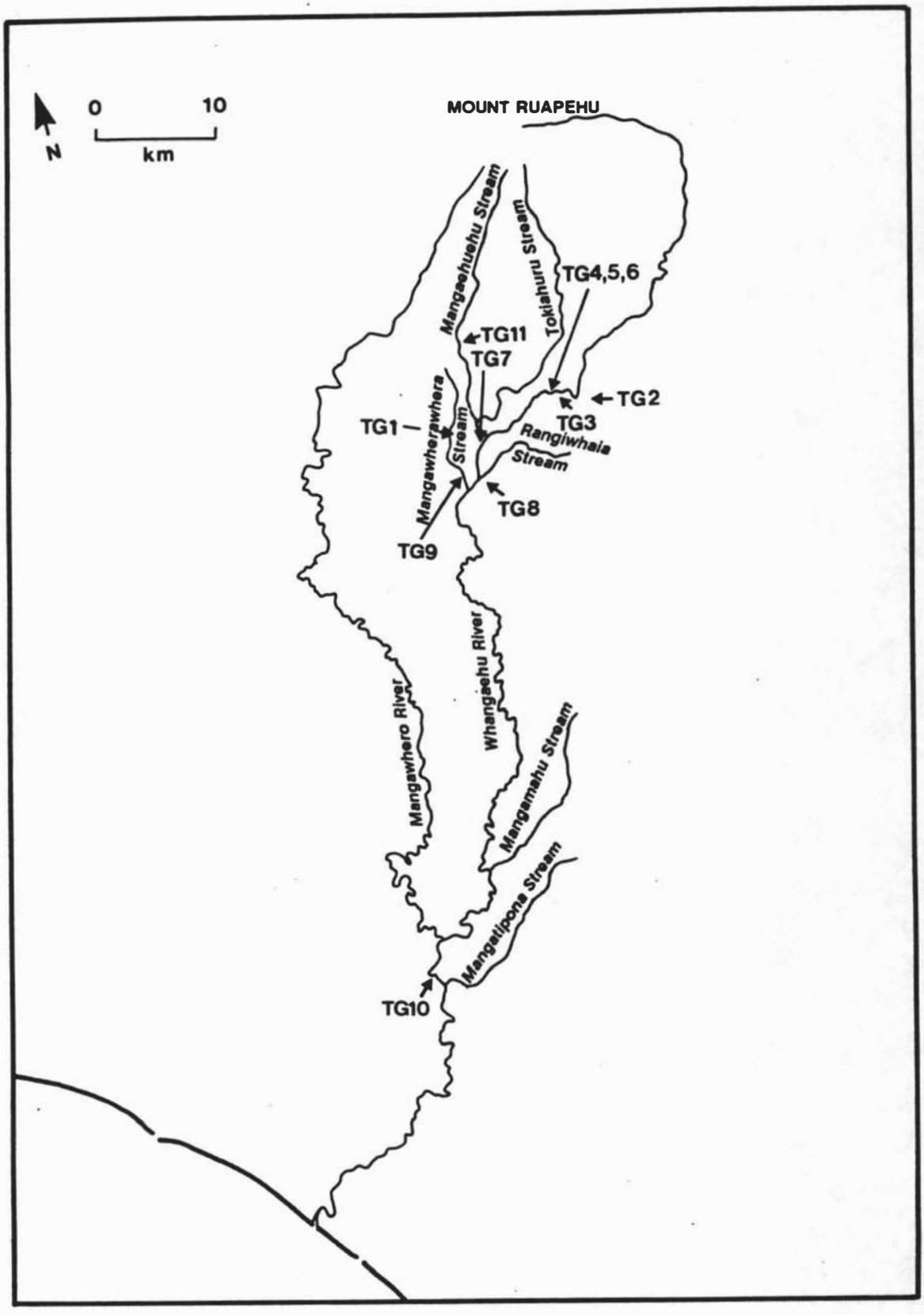

Figure 6.1 Map showing locality of the Tangatu Formation reference sections, and observation sites.

6.4 DISTRIBUTION

Exposures of the Tangatu Formation in the Rangipo Desert, as described by Donoghue (1991), are largely confined to low lying terrain between the Whangaehu escarpment in the east, and a distinct topographic high comprising Te Heuheu Formation in the west. Deposits of Tangatu Formation are believed to underlie the Whangaehu Fan which is constructed from younger Onetapu Formation diamictons. Tangatu Formation is also found in the Waitangi Stream catchment, and therefore must have been able to breach the Whangaehu escarpment north of Waiouru.

Below Tangiwai, on the margins of the ring plain, Tangatu Formation is first exposed below the confluence of the Waitangi Stream with the Whangaehu River (TG2, see Figure 6.1; T21/316889). Here the Formation forms low aggradational terraces on both sides of the river. Only the upper few beds of Tangatu Formation are exposed in these terraces, and are mantled by *c.* 1.5 m of allophanic yellow-brown loam, in turn capped by Taupo Ignimbrite. Microscope analysis of samples taken at 0.05 m intervals in coverbeds at TG2 indicated that no other rhyolite tephras were present in these allophanic yellow-brown coverbeds.

The best exposures of Tangatu Formation are at TG3 (see Figure 6.1, Plate 6.2 and section description), TG4 (see Figure 6.1, Plate 6.3 and section description) and TG5 (see Figure 6.1; S21/277884). At TG3 up to 50 m of diamictons is revealed in a sequence of channel cutting and infilling. At TG4 the upper beds in a sequence of 8 beds, representing nearly 25 m of aggradation, contain pumice blocks tentatively correlated to the Pourahu member of the Bullot Formation. This was emplaced by a Mount Ruapehu-sourced pyroclastic flow between *c.* 11,000 and 10,000 years B.P. (Donoghue, 1991).

At TG6 (see Figure 6.1 and section description), the Formation laps onto an older, higher surface constructed from Whangaehu Formation. Here thin sandy Tangatu Formation diamictons interdigitate with Ngamatea lapilli-1 and -2, formal members of the Bullot Formation, which are also dated at *c.* 11,000 - 10,000 years B.P. (Donoghue, 1991).

Tangatu Formation is also well exposed at the junction of Old Fields Track and Oruakukuru Road, a bridging point of the Mangaehuehu Stream about 200 m above its confluence with the Whangaehu River (TG7, see Figure 6.1; S21/218868).

Downstream of the Mangaehuehu confluence, Formation deposits are confined within the cliffs of the lower Whangaehu gorge. However, about 7 km downstream of this locality they are exposed in road cuttings beside the Whangaehu Valley Road on the eastern side of Rangiwhaia Stream (TG8, see Figure 6.1 and Plate 6.4; S21/211835) which joins the Whangaehu River at this point. This exposure is *c.* 30 m above the present level of the River. Formation deposits lap onto the Whangaehu Formation terrace on the western side of the River, and are exposed in road cuttings beside Old Fields Track where it bridges the Mangawherawhera Stream (TG9, see Figure 6.1; S21/195845), and in road cuttings up to 0.5 km further south of this locality.

Between the confluence of the Mangaehuehu Stream and Mangamahu, 80 km downstream, the Tangatu Formation is restricted to the deeply entrenched valley of the Whangaehu River, and exposure of Formation deposits is intermittent. Downstream of the lower Whangaehu gorge low level terraces are mantled with Tangatu Formation sandy diamictons. This relationship is only exposed in a few localities, and the distribution of Tangatu Formation was determined by augering through coverbeds on these terraces. Three distinct terrace associations were determined by this exercise, (1) terraces with coverbeds comprising *c.* 1 m of allophanic yellow brown loam soil overlying poorly sorted andesitic sands, (2) terraces with coverbeds comprising fluvially reworked Taupo Ignimbrite (a sample of which was analysed by Dr B. Pillans, Victoria University of Wellington, to confirm this identification) and andesitic sands, and (3) terraces with coverbeds comprising very poorly sorted andesitic gravels with a thin, dark brown topsoil. Allophanic yellow-brown coverbeds on terrace association (1) correspond to those overlying Tangatu Formation where it is exposed above the lower Whangaehu gorge, and the underlying sands are interpreted to represent Tangatu Formation sandy diamictons. Terrace association (2) corresponds to a period of aggradation of fluvially reworked Taupo Ignimbrite, which entered the River in the upper catchment. Terrace association (3) represents deposits from younger Onetapu Formation.

Above the confluence of the Whangaehu and Mangawhero Rivers (S22/066471) two discrete suites of terraces comprising andesitic sands and gravels are observed (see Plate 1.2). The upper terrace comprises Tangatu Formation diamictons, containing characteristic pumiceous clasts, which are commonly stained yellow brown. These deposits are mantled by *c.* 1 m yellow-brown loam yellow-grey earth intergrade, silty alluvium and Formation volcaniclastics. Below the confluence of the Rivers Onetapu Formation is absent and Tangatu Formation forms a valley wide plain abutting older late Pleistocene terraces. Tangatu Formation is exposed in undercut banks of the Whangaehu River above Wyley's Bridge (TG10, see Figure 6.1 and Plate 6.5; S22/056448); below this locality deposits are largely confined to low lying point bars (see Plate 1.4).

Tangatu Formation is not confined to the Whangaehu River. On State Highway 49, between Waiouru and Ohakune, where it bridges the Mangaehuehu Stream (TG11, see Figure 6.1; S20/220929) two thin sandy andesitic diamictons interdigitate with Ngamatea lapilli-1 and -2 and these deposits are correlated to the Tangatu Formation. The Mangaehuehu Stream flows along an entrenched channel cut into Whangaehu Formation marginal-A deposits, and Tangatu Formation deposits are observed draping the steep sides of this channel. Tangatu Formation is also found in the catchment of the Tokiahuru Stream above its confluence with the Mangaehuehu Stream. Above State Highway 49, which bridges the Tokiahuru Stream (S21/264894), Tangatu Formation forms low terraces on the banks of the Stream. Below the bridging point the Stream is confined between two older, high surfaces comprising uplifted Tertiary sandstone and siltstone and Tangatu deposits are not observed. They reappear locally where the Whangaehu Valley Road bridges the Tokiahuru Stream (S21/236882), and in undercut banks of the Stream downstream to its confluence with the Mangaehuehu Stream. Tangatu deposits in the Tokiahuru Stream are typically sandy, weakly lithified, and pumiceous in nature.

6.5 LITHOFACIES DESCRIPTION

Seven different lithofacies types are identified in the Tangatu Formation. These are outlined in Tables 1 and 2. Supplementary information has been drawn from Donoghue (1991) for the Tangatu Formation upstream of Tang iwai. As in the previously described Whangaehu Formation (see Chapter 4) a primary distinction was made between gravel-dominated and sand-dominated diamictons. Coarse-grained bouldery subfacies as described in the Whangaehu Formation are not observed in Tangatu Formation, although boulder-sized clasts are observed in a few deposits.

6.5.1 *GRAVELLY DIAMICTONS*

Two main groups of gravelly deposits are observed: (1) matrix-supported (Group 1) and (2) clast-supported (Group 2) deposits.

Deposits in Group 1 are not commonly observed and individual beds are thin (< 1 m). They contain common black, grey and red lithic clasts. The matrix in all deposits is dominantly silty sand. Three subfacies are observed, (1) normally graded (subfacies 1a), (2) ungraded (subfacies 1b), and (3) inversely graded (subfacies 1c). The sedimentological characteristics of these subfacies are outlined in Table 6.1.

Group 2 diamictons (see Table 6:1) are distinguished on the basis of their observed bedding characteristics, *i.e.* whether they are (1) massive (subfacies 2a) or (2) stratified (subfacies 2b). Both subfacies contain common to abundant pale grey vesicular pumice clasts and few to common black, grey, and red scoriaceous and non-scoriaceous clasts.

Deposits in subfacies 2b form the greatest thickness of beds described in Tangatu Formation and are characterised by sequences of centimetre thick inversely graded beds. Contacts between beds are indistinct and usually marked by very thin muddy laminae. The beds are laterally continuous over at least 2 m. An upward reduction in the bed thickness and dominant grain size is observed in most deposits described, although the pumiceous nature of contained clasts led to inverse grading in some beds, reflecting

density variations. Density grading is also observed in deposits in subfacies 2a. Horizontal stratification is characteristic of subfacies 2b; however inclined beds are also observed. Another feature typical of subfacies 2b is the presence of centimetre thick, laterally discontinuous beds of fine sand and silt which lie between coarser-grained beds. Occasional outsize clasts are observed in both massive (up to 0.3 m) and stratified (up to 1.5 m) subfacies.

Table 6.1 Gravelly diamicton lithofacies in the Tangatu Formation

Lithofacies identifier	Lithofacies description	Total number of beds	Total thickness of beds (m)	Bed thickness range (m)	Maximum clast size (m)	Modal clast size (Wentworth)
1a	*matrix-supported pebbly gravel, normally graded*	4	2.90	0.34 - 1.00	0.50	pebble
1b	*matrix-supported pebbly gravel, ungraded*	3	0.69	0.16 - 0.75	0.50	pebble
1c	*matrix-supported pebbly gravel, inversely graded*	5	1.54	0.15 - 0.50	0.32	pebble
2a	*clast-supported pebbly gravel, massive*	18	13.52	0.48 - 4.00	0.30	pebble
2b	*clast-supported pebbly gravel, stratified*	12	59.22	0.35 - 20.0	1.50	pebble

6.5.2 *SANDY DIAMICTONS*

Subfacies identified in sand-dominated diamictons are detailed in Table 6.2. They are clast-supported, and may be (1) massive (subfacies 3a) or (2) stratified (subfacies 3b). Common to abundant vesicular pale grey hard vesicular pumice clasts are observed in both subfacies. Few to common hard scoriaceous and non-scoriaceous black, grey, red and white lithic clasts are also present.

Deposits in subfacies 3b are the most commonly occurring beds described in this Formation. Stratification is characterised by sequences of centimetre thick inversely graded beds and millimetre thick laminae. Outsize clasts are observed in both massive (clasts up to 0.3 m) and stratified (clasts up to 0.15 m) beds.

Table 6.2 Sandy diamicton lithofacies in Tangatu Formation

Lithofacies identifier	Lithofacies description	Total number of beds	Total thickness of beds (m)	Bed thickness range (m)	Maximum clast size (m)	Modal clast size (Wentworth)
3a	*clast-supported sands, massive*	8	5.74	0.08 - 2.50	0.30	very coarse sand
3b	*clast-supported sands, stratified*	41	43.08	0.08 - 5.00	0.15	very coarse sand

6.5.3 *LITHOFACIES INTERPRETATION*

The criteria used to distinguish between diamictons of volcanogenic origin were discussed in Chapter 4, and are outlined in Table 6.3. Through identification of sedimentological features typical of different flow types, Tangatu Formation subfacies groups are interpreted to have been emplaced by either (1) debris flow (Group 1 subfacies) or hyperconcentrated flow (Group 2 and 3 subfacies).

Table 6.3 Sedimentological characteristics of debris flow and hyperconcentrated flow deposits (from Chapter 4, section 4.3.2)

Deposit characteristics	Debris flow	Hyperconcentrated flow
Bed geometry	*sheetlike beds, with limited or insignificant erosion*	*sheetlike beds with distinct erosional and non-erosional contacts*
Grading	*ungraded to graded beds*	*ungraded to graded beds*
Internal stratification	*no stratification*	*beds may be massive, or horizontally stratified*
Clast-support mechanism	*clast-supported to matrix-supported*	*clast-supported*
Sorting	*deposits are very poorly sorted*	*deposits are poorly sorted*
Clast size	*presence of a wide range in clast sizes; thicker beds tend to contain coarser clasts*	*clasts commonly pebbly or sandy; deposits may contain outsize clasts*

Subfacies in Tangatu Formation (TG) are comparable to those identified within the Whangaehu Formation (WF). Table 6.4 delineates groups within both Formations which have similar lithofacies expression. Similarities are found between (1) Group 1 (TG) and Group 3 (WF), (2) Group 2 (TG) and Group 4 (WF), and (3) Group 3 (TG) and Group 5 (WF) subfacies and it is considered that similar processes were operating during emplacement of these deposits. These processes were described in Chapter 4, and are also outlined in Table 6.4.

6.5.3.1 *Subfacies 1a-c*

Deposits in Group 1 subfacies were emplaced by debris flow (see Tables 6.3 and 6.4). The differences in grading characteristics observed in Group 1 subfacies probably reflect variations in the viscosity of the matrix. The more fluid flows, identified as normally graded beds of subfacies 1a, probably resulted from flows, or zones within flows, with slightly less mud in their matrices. This would result in a less viscous (less cohesive) debris flow allowing the preferential fall out of denser clasts on deposition.

The matrices in Tangatu Formation diamictons are typically fine sand or silty sand, and a small increase in their mud content would increase cohesive strength. Ungraded and inversely graded beds, identified by subfacies 1b and 1c respectively, are interpreted to represent cohesive debris flows. Viscous dispersive pressure is implicated in dispersing clasts throughout the flow thickness, and this dispersed pattern is maintained at deposition by virtue of this cohesive matrix. The vesicular and scoriaceous nature of clasts within the Tangatu Formation would promote these grading characteristics through the development of buoyant support of these lower density clasts. In pumice rich deposits vesicular pumice clasts are commonly found at or near the top of the deposits, and are interpreted to have migrated here during flow, and were rafted downstream on the surface of the debris flow.

Lithofacies identifier (WF)	Sedimentological characteristics	Rheology characteristics	Mode of emplacement	Correlated lithofacies (TG)
1a	BOULDER-DOMINATED; CLAST-SUPPORTED; NORMALLY GRADED	HIGHLY COMPETENT, CLAST-RICH DEBRIS FLOW; NON-COHESIVE; LOW VISCOSITY; TURBULENT; INERTIAL DISPERSIVE PRESSURE, TURBULENCE AND HIGH VELOCITY DOMINANT SUPPORT MECHANISMS	REDUCTION OF VELOCITY BELOW CRITICAL YIELD STRENGTH, PREFERENTIAL FALL OUT OF HEAVIER AND DENSER CLASTS ON DEPOSITION	NO
1b	BOULDER-DOMINATED; CLAST-SUPPORTED; UNGRADED	AS ABOVE	REDUCTION OF VELOCITY BELOW CRITICAL YIELD STRENGTH, DEPOSITION EN MASSE, SEDIMENT "FREEZES"	NO
1c	BOULDER-DOMINATED; CLAST-SUPPORTED; INVERSELY GRADED	AS ABOVE	AS ABOVE	NO
2a	BOULDER-DOMINATED; MATRIX-SUPPORTED; NORMALLY GRADED	AS ABOVE	REDUCTION OF VELOCITY BELOW CRITICAL YIELD STRENGTH, PREFERENTIAL FALL OUT OF HEAVIER AND DENSER CLASTS ON DEPOSITION	NO
2b	BOULDER-DOMINATED; MATRIX-SUPPORTED; UNGRADED	HIGHLY COMPETENT, MATRIX-RICH DEBRIS FLOW; COHESIVE; HIGH VISCOSITY; LAMINAR; VISCOUS DISPERSIVE PRESSURE AND BUOYANCY DOMINANT SUPPORT MECHANISMS	REDUCTION OF VELOCITY BELOW CRITICAL YIELD STRENGTH, DEPOSITION EN MASSE, SEDIMENT "FREEZES"	NO
2c	BOULDER-DOMINATED; MATRIX-SUPPORTED; INVERSELY GRADED	AS ABOVE	AS ABOVE	NO
3a	PEBBLE-DOMINATED; MATRIX-SUPPORTED; NORMALLY GRADED	LOW COMPETENCE, MATRIX-RICH DEBRIS FLOW; NON-COHESIVE; LOW VISCOSITY; TURBULENT; INERTIAL DISPERSIVE PRESSURE AND TURBULENCE DOMINANT SUPPORT MECHANISMS	REDUCTION OF VELOCITY BELOW CRITICAL YIELD STRENGTH, PREFERENTIAL FALL OUT OF HEAVIER AND DENSER CLASTS ON DEPOSITION	1a
3b	PEBBLE-DOMINATED; MATRIX-SUPORTED; UNGRADED	LOW COMPETENCE, LOW ENERGY, MATRIX-RICH DEBRIS FLOW; COHESIVE; HIGH VISCOSITY; LAMINAR; VISCOUS DISPERSIVE PRESSURE AND BUOYANCY DOMINANT SUPPORT MECHANISMS	REDUCTION OF VELOCITY BELOW CRITICAL YIELD STRENGTH, DEPOSITION EN MASSE, SEDIMENT "FREEZES"	1b
3c	PEBBLE-DOMINATED; MATRIX-SUPPORTED; INVERSELY GRADED	AS ABOVE	AS ABOVE	1c
4a	PEBBLE-DOMINATED; CLAST-SUPPORTED; MASSIVELY BEDDED	LOW COMPETENCE; CLAST-RICH HYPERCONCENTRATED FLOW; NON-COHESIVE; LOW VISCOSITY; INERTIAL DISPERSIVE PRESSURE AND TURBULENCE DOMINANT SUPPORT MECHANISMS	AS ABOVE	2a
4b	PEBBLE-DOMINATED; CLAST-SUPPORTED; STRATIFIED	AS ABOVE, ALTHOUGH TURBULENCE DOMINATES	RAPID DEPOSITION AS LOW-AMPLITUDE, LONG-WAVELENGTH DUNES	2b
5a	SAND-DOMINATED; CLAST-SUPPORTED; MASSIVELY BEDDED	LOWER COMPETENCE THAN ABOVE, CLAST-RICH HYPERCONCENTRATED FLOW; NON-COHESIVE, INERTIAL DISPERSIVE PRESSURE AND TURBULENCE DOMINANT SUPPORT MECHANISMS	REDUCTION OF VELOCITY BELOW CRITICAL YIELD STRENGTH, DEPOSITION EN MASSE, SEDIMENT "FREEZES"	3a
5b	SAND-DOMINATED; CLAST-SUPPORTED; STRATIFIED	AS ABOVE, ALTHOUGH TURBULENCE DOMINATES	RAPID DEPOSITION AS LOW-AMPLITUDE, LONG-WAVELENGTH DUNES	3b

Table 6.4 Lithofacies identified within Whangaehu Formation (WF) diamictites, and correlated lithofacies within Tangatu Formation (TG) diamictons, interpreted rheological characteristics and interpreted mode of emplacement.

6.5.3.2 *Subfacies 2a-b*

Subfacies 2a and 2b were emplaced by hyperconcentrated flow (see Tables 6.3 and 6.4). The clast-rich nature of deposits in subfacies 2a, which resemble subfacies 4a in the Whangaehu Formation, implies that inertial dispersive pressure is likely to have been the dominant support and transport mechanism. A more turbulent regime would be likely to follow a reduction in the clast concentration, as a result of either depostion of clasts or incorporation of water or saturated sediments. This is considered responsible for the stratification characteristic of subfacies 2b. As mentioned in the discussion of similar deposits in the Whangaehu Formation (subfacies 4b, see Chapter 4, section 4.3.4.4), stratification is probably indicative of turbulent, pulsing flow. Each individual bed or laminae within deposits of subfacies 2b is inversely graded, which implies that inertial dispersive pressure played an important role in clast support within each pulse. As in subfacies 2a vesicular pumice clasts are commonly found concentrated at the top of each strata, implying that buoyant support mechanisms were also operating.

The presence of the thin fine sand and silt beds observed between beds in subfacies 2b was intriguing. There are three possible explanations for their development (1) that they represented thin soils which developed between beds, implying that deposition of groups of beds were separated by intervals of time sufficiently long for these to develop (at least ten years), or (2) that they represent rip-up clasts of soil which were rafted along within the flow, or (3) they represent zones within the flow where escaping pore fluid, charged with entrained fine sand and silts, was ejected immediately following emplacement, and subsequently overlain by the next pulse of flow. The bedding characteristics of subfacies 2b are considered to represent rapid accumulation of thin pulses of a hyperconcentrated flow regime, spaced closely in time, which would not support explanation (1). In the present the sediment preserved in these layers is structureless and shows none of the allophanic characteristics of the soils which form the overlying coverbeds. The process of sediment and water escape described in explanation (3) is usually associated with liquefaction of saturated sediments. In the porous gravelly hyperconcentrated deposits this process would probably only occur immediately following deposition, *i.e.* while the deposits are still saturated. However, sediment and water escape is a highly energetic process, which usually deforms

previously existing bedding structures (as witnessed in Onetapu Formation hyperconcentrated flow deposits, refer forward to Chapter 7, section 7.6) and both the preservation of the silty deposits, and the undisturbed nature of the underlying and overlying beds does not provide support this explanation. So, although in this study the third explanation is preferred, the origin of these silty layers remains a mystery.

6.5.3.3 *Subfacies 3a and 3b*

Subfacies 3a and 3b resemble subfacies 5a and 5b (WF), respectively. They also resemble Group 2 subfacies described in the previous section, although the modal grain size is less. Similar processes are implicated in their emplacement, *e.g.* hyperconcentrated flow with inertial dispersive pressure and turbulence as the principal support mechanisms. The smaller modal grain size may reflect (1) that coarser grains were not available for transport, or (2) that these flows were less competent.

6.5.4 VOLUME AND EXTENT OF TANGATU FORMATION

The total areal extent of the Formation below Tangiwai is 19.38 km^2. The mean number of units in exposure was 4.7 m, with a mean unit thickness of 1.3 m. The total volume of Tangatu Formation deposits in this study is estimated to be 1.22×10^8 m^3. Donoghue (1991) estimates that the total volume of Tangatu Formation deposits on the Mount Ruapehu ring plain is in the order of 9.4×10^7 m^3. Hence the combined total volume for the Formation is 2.16×10^8 m^3.

6.6 WAS EMPLACEMENT OF THE TANGATU FORMATION ASSOCIATED WITH ERUPTIVE ACTIVITY?

Lahar deposits of the Tangatu Formation are found interbedded with Bullot Formation (Donoghue, 1991) tephra deposits, which mark a period of intense volcanic activity at Mount Ruapehu during the last stadial. The Tangatu Formation is interpreted to have accumulated from lahars which occurred contemporaneously with eruptions or in immediate post-eruptive intervals. The large volume of laharic material mobilized and deposited throughout the catchment of the Whangaehu River indicates that large volumes of pumiceous material must have been erupted at this time. Donoghue recognises tephra from up to 60 eruptions in the Bullot Formation, each with an estimated volume erupted of 5×10^8 m^3. Further material would be derived from glacial and fluvioglacial sources as valley glaciers on Mount Ruapehu ablated during the transition from glacial to post-glacial conditions.

Donoghue (1991) proposes a causal link between eruption of Bullot tephras and lahar initiation, as evidenced by the stratigraphic association of these deposits. Additional support for this hypothesis can be found in the middle catchment of the Whangaehu River. At TG6 Ngamatea lapilli-1 and -2 of the Bullot Formation interdigitate with thin pumice-rich hyperconcentrated flow deposits. Eruption of each lapilli unit appears to have been closely followed by a lahar. Preservation of Ngamatea lapilli members is unlikely within channel situations, but at TG6, where the lahars have washed up onto an older surface this relationship is preserved. At TG11, where Tangatu Formation lahar deposits are found in the banks of the Mangaehuehu Stream, a similar stratigraphic relationship is exposed. Furthermore pumice blocks, which probably originate from the Pourahu member (Donoghue, 1991), a pyroclastic flow deposit recognized within the Bullot Formation, are found dispersed as secondary clasts throughout the upper beds in Tangatu Formation lahar deposits in the upper catchment of the River. On the southeast Mount Ruapehu ring plain the Pourahu member interfingers with gravelly Tangatu diamictons (containing common pumice lapilli blocks), which this author interprets as showing the transformation of the pyroclastic flow to a lahar, possibly through interaction with the existing drainage, or the incorporation of meltwater from the valley glaciers on the Volcano.

6.6.1 *MODERN DAY ANALOGUES OF TANGATU FORMATION LAHARS*

In Chapter 3, case studies of the principal causes, behaviour and effects of major recent global lahar events were presented. From a number of lines of evidence the closest analogue of the environment of deposition of the Tangatu Formation is that of the Mount Pinatubo eruption in the Philippines, although it is appreciated that, overall, events in the Whangaehu catchment were on a smaller scale. This evidence is principally that (1) Tangatu Formation lahars occurred during a period of intense eruptive activity at Mount Ruapehu, (2) there were relatively short intervals of time between emplacement of individual deposits, and these intervals are marked only by thin weakly developed soils, and (3) the deposits accumulated rapidly as expressed by the sedimentology of the deposits, which comprise thick aggradational sequences with channel filling and overwhelming of existing deposits. Eruptives ejected during emplacement of Bullot Formation were, however, of airfall tephra (with one exceptional pyroclastic flow, the Pourahu member, Donoghue, 1991) as opposed to the voluminous pyroclastic flows which characterized the Pinatubo eruption. During the 1991 Mount Pinatubo eruption 7-11 km^3 of material was erupted, and ensuing lahars buried nearly 150 km^2 of low lying land. The total volume of 5×10^8 m^3 for each of the 60 eruptions recognised in the Bullot Formation (Donoghue, 1991) is only 3 % of the minimum volume erupted at Mount Pinatubo. It can be calculated that an estimated 3×10^{10} m^3 of material was erupted in the *c.* 12,500 years that the Bullot Formation was accumulating, much of which was mobilized by Te Heuheu and Tangatu Formation lahars.

The time interval *c.* 22,500 to 10,000 years B.P. encompasses two defined periods of lahar aggradation on the southeast Mount Ruapehu ring plain, (1) the Te Heuheu Formation (*c.* 25,500 to 14,700 years B,P.) and (2) the Tangatu Formation (*c.* 14,700 to 5,370 years B.P.). Prior to uplift of the Whangaehu Escarpment *c.* 14,700 years ago lahars resulting from mobilization of older Bullot Formation tephras flowed down the Hautapu Valley (with a few flowing into the upper Whangaehu Valley); after *c.* 14,700 lahars triggered by younger Bullot Formation-aged eruptions flowed down the Whangaehu Valley.

Laharic activity in the Philippines was sometimes triggered by eruption induced rainstorms, but predominantly by passing monsoons creating periods of intense heavy rainfall. A greater potential store of water would have been available for initiation of lahars in the form of ablating snow and ice on Mount Ruapehu at the close of the Ohakean stadial (M^{c}Arthur and Shepherd, 1990). In this instance the analogy is closer to the 1985 eruption of Nevado del Ruiz in Colombia in which lahars were generated by melting of snow and ice which subsequently inundated 2,100 km^2 of land. There is no evidence to suggest any major collapse of the Mount Ruapehu volcanic edifice prior to emplacement of Tangatu Formation: hence an analogy with the 1980 Mount St. Helens eruption and resultant lahars is inappropriate.

6.7 LAHARS FOLLOWING EMPLACEMENT OF THE TANGATU FORMATION

Mount Ruapehu appears to have undergone a period of relative quiescence following emplacement of Tangatu Formation. This interval was marked by active channel erosion through Formation deposits, and the formation of an allophanic yellow-brown loam soil on their upper surface. Donoghue (1991) describes aggradational sequences of inter-eruptive fluvial sand and gravel deposits, mapped as the Manutahi Formation, which accumulated between emplacement of the rhyolitic Motutere and Waimihia Tephras. These tephras are dated at 5,370$\pm$90 (Froggatt, 1981) and 3,280$\pm$20 years B.P. respectively. Hence the lower and upper age constraints on the Manutahi Formation are respectively 5,460 and 3,260 years B.P. (Donoghue, 1991). The total volume of Manutahi Formation deposits on the Ruapehu ring plain is *c.* 5×10^7 m^3.

Accumulation of Manutahi Formation was interrupted about 4,600 years B.P. by emplacement of the Mangaio Formation. A date (NZ7532) of 4,850$\pm$90 years B.P. on underlying peat provides a lower age limit of 4,940 years B.P. (Donoghue, 1991), and the Waimihia Tephra an upper age limit of 3,260 years ago on this Formation. A further date (NZ7729) of 4,600$\pm$100 years B.P. on wood within the Formation (Donoghue, 1991) corroborates these age ranges (Donoghue, 1991). Deposits in this Formation are distinguished by their loamy textured matrix and hydrothermally

altered clasts. They probably represent the collapse of a hydrothermally altered sector of the volcano (Donoghue, 1991). Donoghue estimates that the volume of Mangaio Formation is about 3.4×10^7 m^3.

In the middle catchment of the River the Motutere and Waimihia Tephras are not found in coverbeds and the Taupo Ignimbrite is here substituted as the upper marker bed. The interval of time following the Tangatu Formation and prior to the *c.* 1,850 years B.P. eruption of the Taupo Ignimbrite is marked by fluvial degradation of the Whangaehu River through and below Tangatu Formation deposits. However, steady accretion of fine-grained volcanic ash on more stable surfaces accompanied this period of erosion (Topping, 1973; Donoghue, 1991). The surface of the Tangatu Formation has been mantled by over 1 m of ash (Topping, 1973; Pullar *et al.*, 1973; Donoghue, 1991), now weathered to an allophanic yellow-brown loam soil. This weathering has extended down into the upper beds of the Tangatu Formation. In general at high levels above the Whangaehu River this coverbed sequence is uninterrupted, but in near channel sequences interbedded pods and lenses of clastic debris are found (see Map 2). These can be divided into the lithologically distinct Mangaio Formation, and the less readily distinguishable Manutahi Formation. The intermittent and restricted distribution of these deposits implies that events responsible for their emplacement were small, and largely confined to the channel of the River.

6.7.1 *THE MANUTAHI FORMATION*

In this study the Manutahi Formation is restricted to the edge of the Mount Ruapehu ring plain and is only observed at 3 localities. Here it comprises thin well-bedded pumiceous and lithic sands of fluvial origin. Confident correlation of the Manutahi Formation is only possible where the deposits overlie the Mangaio Formation. Otherwise they cannot be differentiated from upper beds in the Tangatu Formation.

6.7.2 *THE MANGAIO FORMATION*

In the upper and middle catchment of the Whangaehu River the Mangaio Formation is recognized at 5 localities. It is typically clast rich, with a distinctive grey mottled muddy matrix which supports common to abundant rounded andesite pebbles. A fluvial rather than laharic origin is most likely for these deposits, suggesting fluvial resorting of the Mangaio Formation lahar deposit further upstream. Based on the distribution of the Formation a volume of 2×10^4 m^3 for the deposits has been estimated, this only *c.* 0.0005 % of the volume remaining on the ring plain, and does not add significantly to the approximately 3.4×10^7 m^3 volume estimated by Donoghue (1991).

CHAPTER 7

THE ONETAPU FORMATION

7.1 INTRODUCTION

The youngest lahar deposits described in this study were originally mapped at 1:250,000 scale as "Recent Lahars of Whangaehu River" by Grindley (1960). Donoghue (1991) redefined these deposits and grouped them into the Onetapu Formation, from the original name for the Rangipo Desert. The Onetapu Formation is now defined to include all Mount Ruapehu-sourced diamictons that overlie the Mangaio Formation or Manutahi Formation. Formation deposits also overlie the *c.* 1,850 years B.P. Taupo Ignimbrite. In the middle and lower reaches of the Whangaehu River Manutahi and Mangaio Formations are generally absent, and in this study the more extensive and readily identifiable Taupo Ignimbrite is adopted to define the lower boundary of the Onetapu Formation. Onetapu Formation also includes deposits from historic lahars.

Lithology within Onetapu Formation varies from lithic-rich coarse-grained bouldery diamictons to pumice-rich sandy diamictons. A few pebble-sized rip-up clasts of underlying Tertiary sandstone and siltstone are observed. In the upper catchment Mount Ruapehu-sourced Tufa Trig Formation tephras (of phreatomagmatic origin, Donoghue, 1991) interdigitate with diamicton beds in the Onetapu Formation (Purves, 1990). These tephras are absent in the middle catchment, although reworked lapilli, possibly corresponding to Tufa Trig tephras, are found between lahar deposits. Sandy deposits in the middle catchment are marked by the presence of pumice lapilli. These are probably not derived from Tufa Trig tephras, which are predominantly fine-grained, and are more likely to represent the continued mobilization of Bullot Formation tephras. Onetapu Formation deposits are weakly lithified to unlithified. The weakly lithified deposits are commonly marked by a strongly mottled matrix, with iron nodules and pans contributing to their lithified nature.

7.2 THE DISTRIBUTION OF THE ONETAPU FORMATION

Purves (1990), Donoghue (1991) and Palmer *et al.* (1993) detail the distribution of the Onetapu Formation on the Southeast Mount Ruapehu ring plain. Here debris flow and hyperconcentrated flow deposits form the most recent constructional surface, the most distinctive feature of which is the Whangaehu Fan (see Figure 1.2). This fan has aggraded as a result of the accumulation of laharic debris and is incised by fluvial and lahar channels (Purves, 1990; Donoghue, 1991). Onetapu Formation deposits form the lateral constructional levees of these channels, and the stratigraphy of Onetapu deposits in this area is revealed in the banks of the levees. Further downstream the Whangaehu River flows off the ring plain and into an incised valley. Here Onetapu deposits are exposed in overbank situations, where lahars have spilled out onto low lying river terraces, or have washed back up into tributary streams (see Maps 2-6). Episodes of laharic aggradation appear to have been followed by rapid incision and removal of in-channel debris as the river began degrading to base level. Short term periods of quiescence between lahar events are marked by soil development into underlying lahar deposits. In some places vegetation has become well established, only to be engulfed by the next large lahar. This is best exemplified near Mangamahu where buried tree stumps in growth position have been exhumed by quarrying operations (see Plate 7.1).

7.2.1 *ONETAPU FORMATION AT THE TYPE LOCALITY*

Donoghue (1991) defines the type locality for the Onetapu Formation at Tangiwai Swamp, 300 m north of Tangiwai railway bridge. Here there is a lateral exposure of about 80 m in a drainage ditch where interbedded peats provide radiocarbon dates for a number of the younger Onetapu Formation members. At this locality Donoghue (1991) was able to recognize 7 individual units (see Figure 7.1), each representing a discrete lahar event, overlying Taupo Ignimbrite. In this study seventeen individual units are recognized throughout the catchment in this time frame, *i.e.* between *c.* 1,850 years B.P. and the present day, and a revision of the informal members defined by Donoghue (1991) is proposed.

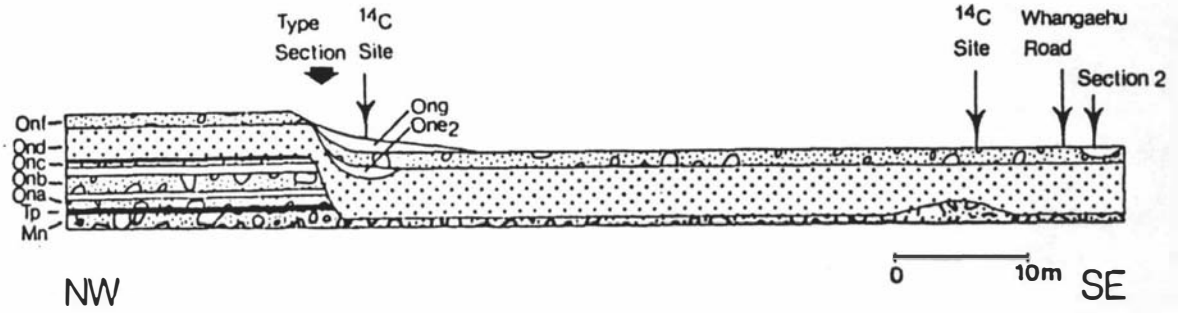

Figure 7.1 The type locality for Onetapu Formation lahars, from Donoghue (1991).

7.3 ONETAPU FORMATION LITHOLOGY

The Onetapu Formation comprises a variety of lithological types. In this following section these will be described in greater detail, with explanations presented for the variations. Thirteen different lithofacies are identified in the Onetapu Formation, and these are outlined in Tables 7.1 - 7.3. As in previously described Whangaehu Formation and Tangatu Formation a primary distinction was made between gravel-dominated and sand-dominated diamictons. Bouldery deposits were observed in the Onetapu Formation, therefore three main lithological types were observed and these were (1) bouldery, (2) pebbly or (3) sandy diamictons.

7.3.1 *BOULDERY DIAMICTONS*

Deposits in this lithological group were not commonly observed and throughout the catchment only 11 beds are described. Group 1 subfacies comprise clast-supported bouldery deposits described by Purves (1990) on the Mount Ruapehu ring plain. He

defines three main subfacies reflecting observed grading characteristics. These are (1) normally graded (Dcn), (2) ungraded (Dcu) and (3) inversely graded (Dcr) diamictons. Table 7.1 outlines the characteristics of these subfacies based on details taken from Purves' (1990) section descriptions. Each subfacies is assigned a simple letter and number identifier compatible to those used for other Onetapu Formation subfacies. Clasts within Group 1 subfacies are typically grey non-scoriaceous andesite. The matrix component of the deposits varies from fine pebbles and sand to muddy-sand.

Table 7.1 Bouldery lithofacies within Onetapu Formation, including subfacies Dcn, Dcu, and Dcr of Purves (1990)

Lithofacies identifier	Lithofacies description	Total number of beds	Total thickness of beds (m)	Bed thickness range (m)	Maximum clast size (m)	Modal clast size (Wentworth)
Dcn (1a)	*clast-supported bouldery gravel, normally graded*	1	0.2	0.1 - 0.3	0.15	pebble
Dcu (1b)	*clast-supported bouldery gravel, ungraded*	3	1.0	0.1 - 0.6	0.7	cobble
Dcr (1c)	*clast-supported bouldery gravel, inversely graded*	2	0.87	0.2 - 0.37	0.2	cobble
2a	*matrix-supported bouldery gravel, normally graded*	2	5.4	2.4 - 3	0.6	cobble
2b	*matrix-supported bouldery gravel, ungraded*	1	1.5	1.5	1.2	boulder
2c	*matrix-supported bouldery gravel, inversely graded*	1	1.5	1.5	0.9	cobble

In this study, downstream of Tangiwai, four bouldery deposits were described. All were matrix-supported and distinguished according to observed grading characteristics. These are detailed in Table 7.1 and include (1) normally graded (subfacies 2a), (2) ungraded (subfacies 2b), and (3) inversely graded (subfacies 2c) beds. Clasts within subfacies 2a are commonly subrounded to rounded grey non-scoriaceous andesite. Both beds within this group are marked by a distinctive muddy matrix, and are weakly lithified. Clasts within subfacies 2b and 2c are commonly grey and black and few red lithic andesite, and the matrix is sandy.

7.3.2 *PEBBLY DIAMICTONS*

Four major and one minor subfacies were identified in Group 3 pebbly diamictons (see Table 7.2). All were observed to be matrix-supported, and subfacies are distinguished on the basis of visual grading characteristics. The four major subfacies recognized are (1) normally graded (subfacies 3a), ungraded (subfacies 3b), inversely graded (3c) and inversely graded to normally graded (subfacies 3d). Grading within subfacies 3d begins with a basal inversely graded zone, which passes upwards through an ungraded middle portion, which may occupy up to 50 % of the total bed thickness, into an upper normally graded zone. One minor subfacies was observed, which described a single bed which was normally graded to inversely graded (subfacies 3e). This was characterised by a thick matrix-supported, very poorly sorted base with pebbles and cobbles, which graded upwards into a granule-rich clast-supported middle portion. This then graded upwards into a matrix-supported pebbly upper. Subfacies described by Purves (1990) for Rangipo Desert Onetapu lahar deposits which are similar to subfacies 3a to 3c defined in this study and which were predominantly matrix-supported and ungraded (subfacies 3b), are included in Table 7.2.

Table 7.2 Pebbly lithofacies within Onetapu Formation

Lithofacies identifier	Lithofacies description	Total number of beds	Total thickness of beds (m)	Bed thickness range (m)	Maximum clast size (m)	Modal clast size (Wentworth)
3a	*matrix-supported pebbly gravel, normally graded*	19	18.3	0.2 - 2	0.5	pebble
3b	*matrix-supported pebbly gravel, ungraded*	42	30.5	0.12 - 3	0.30	pebble
3c	*matrix-supported pebbly gravel, inversely graded*	21	13.5	0.1 - 2	0.25	pebble
3d	*matrix-supported pebbly gravel, inversely to normally graded*	13	8	0.11 - 1.5	0.5	pebble
3e	*matrix-supported pebbly gravel, normally to inversely graded*	1	1	1	0.65	pebble

Clasts within Group 3 subfacies are subangular to subrounded grey, black and and a few red lithic andesite. Occasional white lithic clasts are also observed which are commonly soft and hydrothermally altered. The deposits are unlithified to weakly lithified.

7.3.3 *SANDY DIAMICTONS*

Deposits within sandy diamictons are all clast-supported, and may be either (1) massively bedded (subfacies 4a) or (2) stratified (subfacies 4b). The characteristics of these subfacies are detailed in Table 7.3.

Deposits in subfacies 4a included [i] normally graded and [ii] ungraded beds. Outsize clasts (up to 0.6 m) were occasionally observed in normally graded beds.

Internal stratification, which was diagnostic of subfacies 4b, was characterized by inversely graded beds or laminae. The most commonly observed grading characteristics within this subfacies were [i] normally graded or [ii] ungraded beds. Normally graded beds were characterised by an upward reduction in grain size and bed/laminae thickness. No marked variation in modal clast size or bed thickness was observed in ungraded deposits.

Inverse grading (4b[iii]) was described in one deposit. The modal grain size in this deposit was coarser than other sandy diamictons, and the upper portion of the deposit was pebbly. Internal bedding graded vertically upwards from basal sand- and granule-dominated centimetre thick beds upwards into thicker granule-and pebble-dominated beds.

Table 7.3 Sandy lithofacies within Onetapu Formation. The distinguishing grading characteristics in the lithofacies descriptions refer to the overall unit rather than individual beds or laminae.

Lithofacies identifier	Lithofacies description	Total number of beds	Total thickness of beds (m)	Bed thickness range (m)	Maximum clast size (m)	Modal clast size (Wentworth)
4a[i]	*clast-supported sand, massive, normally graded*	5	1.9	0.06 - 0.85	0.2	very coarse sand
4a[ii]	*clast-supported sand, massive, ungraded*	18	11.2	0.05 - 1.5	0.08	very coarse sand - granule
4b[i]	*clast-supported sand, stratified, normally graded*	11	18.5	0.2 - 3.5	0.5	very coarse sand
4b[ii]	*clast-supported sands, stratified ungraded*	48	29.25	0.08 - 2	0.15	very coarse sand
4b[iii]	*clast-supported sands, stratified, inversely graded*	1	1.3	1.3	0.3	granule
4b[iv]	*clast-supported sands, stratified, inversely graded to normally graded*	2	2.9	0.4 - 2.5	0.6	granule

Inverse to normal grading (4b[iv]) was described in two beds. The central portion of the first deposit, which was 2.5 m thick, was marked by the presence of common outsize clasts (up to 0.6 m). The thickness of internal bedding and modal clast size increase from the base of this unit up into the central portion, then decrease to the top of the unit. A similar pattern was observed in the second deposit, which was much thinner (0.4 m thick), although outsize clasts were not observed. Outsize clasts (up to 0.6 m) were commonly observed in subfacies 4b.

Clasts within deposits of Group 4 subfacies were either dominantly pale grey vesicular pumice or grey scoriaceous lithics. Few to common black, grey and red hard scoriaceous lithic clasts were also observed. The deposits were generally sandy and fines poor, although a small amount of grey muddy matrix was observed in a few deposits.

7.3.4 *LITHOFACIES INTERPRETATION*

This study, in combination with the field descriptions of Purves (1990), has identified 11 different gravel-dominated diamicton subfacies. Gravel-domimated diamictons observed in the Onetapu Formation show most of the features associated with deposition by debris flow as detailed in Table 6.3. Deposits in sandy subfacies show features associated with deposition by hyperconcentrated flow.

Subfacies in the Onetapu Formation (ON) are comparable to both Whangaehu (WF) and Tangatu (TG) Formations, and similar subfacies are presented in Table 7.4. Bouldery subfacies, previously only observed in Whangaehu Formation, are present in the Onetapu Formation, although they occupy only a minor proportion of beds described. Clast-supported pebbly subfacies, observed in both older Formations, are not found in Onetapu Formation. The similarities between subfacies in the three Formations described is here interpreted to reflect that similar processe were operating during emplacement of these deposits.

7.3.4.1 *Subfacies 1a-c (Dcn, Dcu and Dcr of Purves, 1990)*

Clast-support in these subfacies is interpreted to indicate that the debris flows responsible for their emplacement were clast-rich, and the bouldery lithology implies they were also highly competent. The absence of Group 1 subfacies downstream of Tangiwai implies that debris flows, in this lower gradient region, were incapable of transporting such a high concentration of coarse-grained clasts. A reduction in flow velocity is implicated as the cause for this reduction of competence. Inertial pressure, turbulance, and high velocity are implicated as the main support and transport mechanisms in the debris flows represented by Group 1 subfacies.

Lithofacies identifier (WF)	Sedimentological characteristics	Rheology characteristics	Mode of emplacement	Correlated lithofacies (TG)	Correlated lithofacies (ON)
1a	BOULDER-DOMINATED; CLAST-SUPPORTED; NORMALLY GRADED	HIGH COMPETENCE, CLAST-RICH DEBRIS FLOW; NON-COHESIVE; LOW VISCOSITY; TURBULENT; INERTIAL DISPERSIVE PRESSURE, TURBULENCE AND HIGH VELOCITY DOMINANT SUPPORT MECHANISMS	REDUCTION OF VELOCITY BELOW CRITICAL YIELD STRENGTH, PREFERENTIAL FALL OUT OF HEAVIER AND DENSER CLASTS ON DEPOSITION	NO	1a
1b	BOULDER-DOMINATED; CLAST-SUPPORTED; UNGRADED	AS ABOVE	REDUCTION OF VELOCITY BELOW CRITICAL YIELD STRENGTH, DEPOSITION EN MASSE, SEDIMENT "FREEZES"	NO	1b
1c	BOULDER-DOMINATED; CLAST-SUPPORTED; INVERSELY GRADED	AS ABOVE	AS ABOVE	NO	1c
2a	BOULDER-DOMINATED; MATRIX-SUPPORTED; NORMALLY GRADED	AS ABOVE	REDUCTION OF VELOCITY BELOW CRITICAL YIELD STRENGTH, PREFERENTIAL FALL OUT OF HEAVIER AND DENSER CLASTS ON DEPOSITION	NO	2a
2b	BOULDER-DOMINATED; MATRIX-SUPPORTED; UNGRADED	HIGHLY COMPETENCE, MATRIX-RICH DEBRIS FLOW; COHESIVE; HIGH VISCOSITY; LAMINAR; VISCOUS DISPERSIVE PRESSURE AND BUOYANCY DOMINANT SUPPORT MECHANISMS	REDUCTION OF VELOCITY BELOW CRITICAL YIELD STRENGTH, DEPOSITION EN MASSE, SEDIMENT "FREEZES"	NO	2b
2c	BOULDER-DOMINATED; MATRIX-SUPPORTED; INVERSLEY GRADED	AS ABOVE	AS ABOVE	NO	2c
3a	PEBBLE-DOMINATED; MATRIX-SUPPORTED; NORMALLY GRADED	LOW COMPETENCE, MATRIX-RICH DEBRIS FLOW; NON-COHESIVE; LOW VISCOSITY; TURBULENT; INERTIAL DISPERSIVE PRESSURE AND TURBULENCE DOMINANT SUPPORT MECHANISMS	REDUCTION OF VELOCITY BELOW CRITICAL YIELD STRENGTH, PREFERENTIAL FALL OUT OF HEAVIER AND DENSER CLASTS ON DEPOSITION	1a	3a 3d 3e
3b	PEBBLE-DOMINATED; MATRIX-SUPORTED; UNGRADED	LOW COMPETENCE, LOW ENERGY, MATRIX-RICH DEBRIS FLOW; COHESIVE; HIGH VISCOSITY; LAMINAR; VISCOUS DISPERSIVE PRESSURE AND BUOYANCY DOMINANT SUPPORT MECHANISMS	REDUCTION OF VELOCITY BELOW CRITICAL YIELD STRENGTH, DEPOSITION EN MASSE, SEDIMENT "FREEZES"	1b	3b
3c	PEBBLE-DOMINAED; MATRIX-SUPPORTED; INVERSELY GRADED	AS ABOVE	AS ABOVE	1c	3c
4a	PEBBLE-DOMINATED; CLAST-SUPPORTED; MASSIVELY BEDDED	LOW COMPETENCE; CLAST-RICH HYPERCONCENTRATED FLOW; NON-COHESIVE; LOW VISCOSITY; INERTIAL DISPERSIVE PRESSURE AND TURBULENCE DOMINANT SUPPORT MECHANISMS	AS ABOVE	2a	NO
4b	PEBBLE-DOMINATED; CLAST-SUPPORTED; STRATIFIED	AS ABOVE, ALTHOUGH TURBULENCE DOMINATES	RAPID DEPOSITION AS LOW-AMPLITUDE, LONG-WAVELENGTH DUNES	2b	NO
5a	SAND-DOMINATED; CLAST-SUPPORTED; MASSIVELY BEDDED	LOWER COMPETENCE THAN ABOVE, CLAST-RICH HYPERCONCENTRATED FLOW; NON-COHESIVE, INERTIAL DISPERSIVE PRESSURE AND TURBULENCE DOMINANT SUPPORT MECHANISMS	REDUCTION OF VELOCITY BELOW CRITICAL YIELD STRENGTH, DEPOSITION EN MASSE, SEDIMENT FREEZES	3a	4a
5b	SAND-DOMINATED; CLAST-SUPPORTED; STRATIFIED	AS ABOVE, ALTHOUGH TURBULENCE DOMINATES	RAPID DEPOSITION AS LOW-AMPLITUDE, LONG-WAVELENGTH DUNES	3b	4b

Table 7.4 Lithofacies identified within Onetapu Formation (ON) diamictons, and correlated lithofacies within Whangaehu Formation (WF) diamictites and Tangatu Formation (TG) diamictons, interpreted rheological characteristics and interpreted mode of emplacement.

7.3.4.2 *Subfacies 2a-c*

Group 2 subfacies are not commonly observed. As in previously interpreted Group 1 subfacies these deposits must have been emplaced by highly competent debris flows. These subfacies were only observed below Tangiwai, and in these lower velocity regions greater supporting strength of the flows is likely to have been imparted by cohesive properties supplied by the matrix which supports the clasts. Subfacies 2a is unusual; as mentioned in Section 7.3.1.1 the two deposits described which comprise this subfacies have distinctive muddy matrices. According to the accepted models of debris flow behaviour, this fine-grained component ought to lend greater cohesion to the flow, which would be reflected in the maintenance of ungraded or inversely graded bedding characteristics (which are observed in subfacies 2b and 2c, deposits which do not have muddy matrices). One explanation for the normal grading in subfacies 2a is the debris flow simply did not have enough strength to disperse the boulder-sized clasts throughout the flow thickness, and that these were transported along as a traction load at the base of the flow.

7.3.4.3 *Subfacies 3a-e*

Deposits in Group 3 subfacies are commonly observed in all three Formations. The lower modal grain size in these deposits indicates a reduced competence for debris flows responsible for their emplacement in comparison to Group 1 and 2 subfacies. Deposits in subfacies 3a are interpreted to have been emplaced by non-cohesive debris flow, with inertial dispersive pressure and turbulence as the principal support and transport mechanisms. Deposits in subfacies 3b and 3c however are interpreted to have been emplaced by more viscous debris flow, with viscous dispersive pressure and buoyancy, imparted by matrix-strength (cohesion), implicated as the main support and transport mechanisms.

Two explanations are presented to account for deposits in subfacies 3d. Firstly, the inversely graded basal portion of deposits in this subfacies are similar to boundary features described by Scott (1988). He interpreted these as representing an active shear zone at the flow boundary (with the walls of the channel within which the debris flowed) with coarse clasts moving away from this zone as a result of clast interactions. Hence large clasts would be moved away from these boundary zones and into the main portion of the debris flow. The central ungraded zone, the thickness of which varies between deposits, probably represents a transition from the lower zone of intense clast interactions into a cohesive zone in the central "plug" part of the debris flow. Normal grading in the upper part of the flow probably represents settling out of clasts on deposition, implying that the debris flow was more fluid in this upper zone. The proportion of bed thickness occupied by each grading type varies across individual exposures (both laterally and longitudinally) and this is interpreted to reflect the migration of rheological boundaries throughout the depth of the flow as it travelled away from source.

The second explanation for the grading in subfacies 3d is that the boundary between the finer-grained inversely-graded base and the ungraded centre represents a zone of transition in flow regime from debris flow to hyperconcentrated flow. This would occur as the debris flow incorporated water and saturated sediment from the channel of the river, reducing the sediment concentration and hence flow yield strength and competence (from the base of the flow upwards). This phenomenon was reported for debris flows from Mount St. Helens (Pierson and Scott, 1985; Scott, 1988a).

The absence of features associated with hyperconcentrated flow, *i.e.* clast-support and stratification, in the basal portion of these deposits lends support to the first explanation. High angularity of clasts in this zone implies that clast-to-clast interactions were occurring, causing fracturing of clasts, which would also support this being a zone of intense shear, and of inertial dispersive pressure.

Only one bed of subfacies 3e is observed. The variation from a coarse-grained matrix-supported pebbly base to clast-supported middle and then back upwards into a matrix-supported upper is interpreted to reflect a vertical gradation from debris flow to hyperconcentrated flow and back to debris flow. It is here considered that the deposition of the basal debris flow was immediately followed by deposition of a more fluid flow, which was showing signs of transformation to hyperconcentrated flow. These unusual grading characteristics are interpreted to represent deposition from a fluid, non-cohesive debris flow which may have been behaving in a pulse like fashion, normally associated with dilute hyperconcentrated flow.

7.3.4.4 *Subfacies 4a-b*

As mentioned previously Group 4 subfacies were emplaced by hyperconcentrated flow. Deposits in subfacies 4a (ON) resemble those in subfacies 5a (WF) and subfacies 3a (TG) and a similar interpretation of the principal support, transport, and deposition mechanisms as detailed in Table 7.4 is implicated for the more recent deposits.

Subfacies 4a is therefore interpreted to represent deposits from low competence clast-rich hyperconcentrated flow, with inertial dispersive pressure implicated as the principal clast support and transport mechanisms.

Lower clast-sediment-concentration flows, with pulse-like behaviour, are interpreted to be responsible for the stratification characteristic of subfacies 4a. Inverse grading within each bed implies that some combination of inertial dispersive pressure and buoyancy was acting to support clasts in each pulse.

Considering that deposits in Group 4 subfacies are interpreted to have originated as lower sediment concentration, more fluid hyperconcentrated flow (in comparison to debris flow) normal grading would be the expected grading type. However, in both subfacies 4a and 4b a variety of grading types was observed, which were outlined in section 4.3.1.3 and are detailed in Table 7.3.

Normal grading is observed in Group 4 subfacies but it is of interest that the most commonly occurring lithology in both 4a and 4b is ungraded beds. For deposits in subfacies 4a[i] this adds further support to the proposal that inertial dispersive pressure must play a role in maintaining clast support in hyperconcentrated flow. The clast-rich (but fine-grained) nature of the sediment (and by inference the hyperconcentrated flow) may have prevented settling out of clasts in a manner similar to that proposed for much coarser-grained subfacies 1a - 1c in the Whangaehu Formation, described in Chapter 4, section 4.3.2.1.

Grading characteristics in subfacies 4b are more likely to represent variations in flow competence in each successive pulse of flow. Normally graded beds would indicate a reduction in competence vertically in the flow, and, by inference, through time as subsequently thinner beds are deposited from each pulse as the flow wanes. The absence of a rising stage, which would be marked by an inversely graded basal portion suggests that these deposits were laid down by flows which had achieved their maximum carrying load, or that coarser clasts became decreasingly available for transport. The significance of ungraded beds is that there was no reduction of flow competence, or availability of a wide range in clast sizes for transport. Clasts within the one inversely graded bed observed (subfacies 4b[iii]) were dominantly lithic and scoriaceous: therefore buoyant support of low density clasts may be responsible for this phenomenon. Alternatively this grading may occur as coarser clasts become available for transport, perhaps as the hyperconcentrated flow erodes into and incorporates underlying clastic sediments. The consequent rise in sediment concentration would be accompanied by a corresponding rise in flow competence promoting the support of coarser clast sizes. As the flow begins to wane (through reduction in velocity) this competence would be reduced, resulting in the fall out of these clasts and this is forwarded as the explanation for the inversely to normally graded beds observed in subfacies 4b[iv].

7.4 ONETAPU FORMATION INFORMAL MEMBERS: CORRELATION AND STRATIGRAPHY

The stratigraphy of members within the Onetapu Formation members has been compiled through (1) correlation of deposits with distinctive sedimentological characteristics, (2) hand-over-hand mapping of deposits which are not distinct, and (3) direct and indirect dating of individual deposits and groups of deposits. By employing these methods a comprehensive assessment of the impact of recent lahars in the Whangaehu River has been determined. Figure 7.2 locates all sections referred to in the following section and their descriptions are included in the Appendices to this thesis.

Seventeen informal members have been identified in the upper and middle reaches of the Whangaehu River (see Table 7.5, and see stratigraphic columns in the Appendix). However not all of these deposits are widespread, and in some cases a unit may crop out at only a few locations. This may reflect that either (1) the deposit resulted from a smaller lahar or (2) following deposition much of the lahar debris was immediately removed through subsequent fluvial or lahar erosion. On the other hand a few of the deposits are found exposed at many locations and these are recognized from their distinctive combined sedimentological features (*e.g.* clast type and nature of the matrix) and stratigraphic position in relation to other members. By virtue of their wider distribution these deposits are mappable and will be examined in greater detail.

Tables 7.6 and 7.7 detail the general sedimentological characteristics which have been used to distinguish between individual members of the Onetapu Formation. In the following sections this information is supplemented with radiocarbon dates which provide bracketing ages for events.

7.4.1 *MEMBER Ona*

Member **Ona** (see Figure 7.3) lies stratigraphically immediately above the Taupo Ignimbrite, and this relationship is exposed in six of the localities where Ona is described (see Plate 7.2). In exposures downstream of Tangiwai member Ona is characterized by its distinctive grey matrix which is strongly mottled yellow and orange. Clasts within Ona commonly have reddish staining (see Table 7.6, page 137).

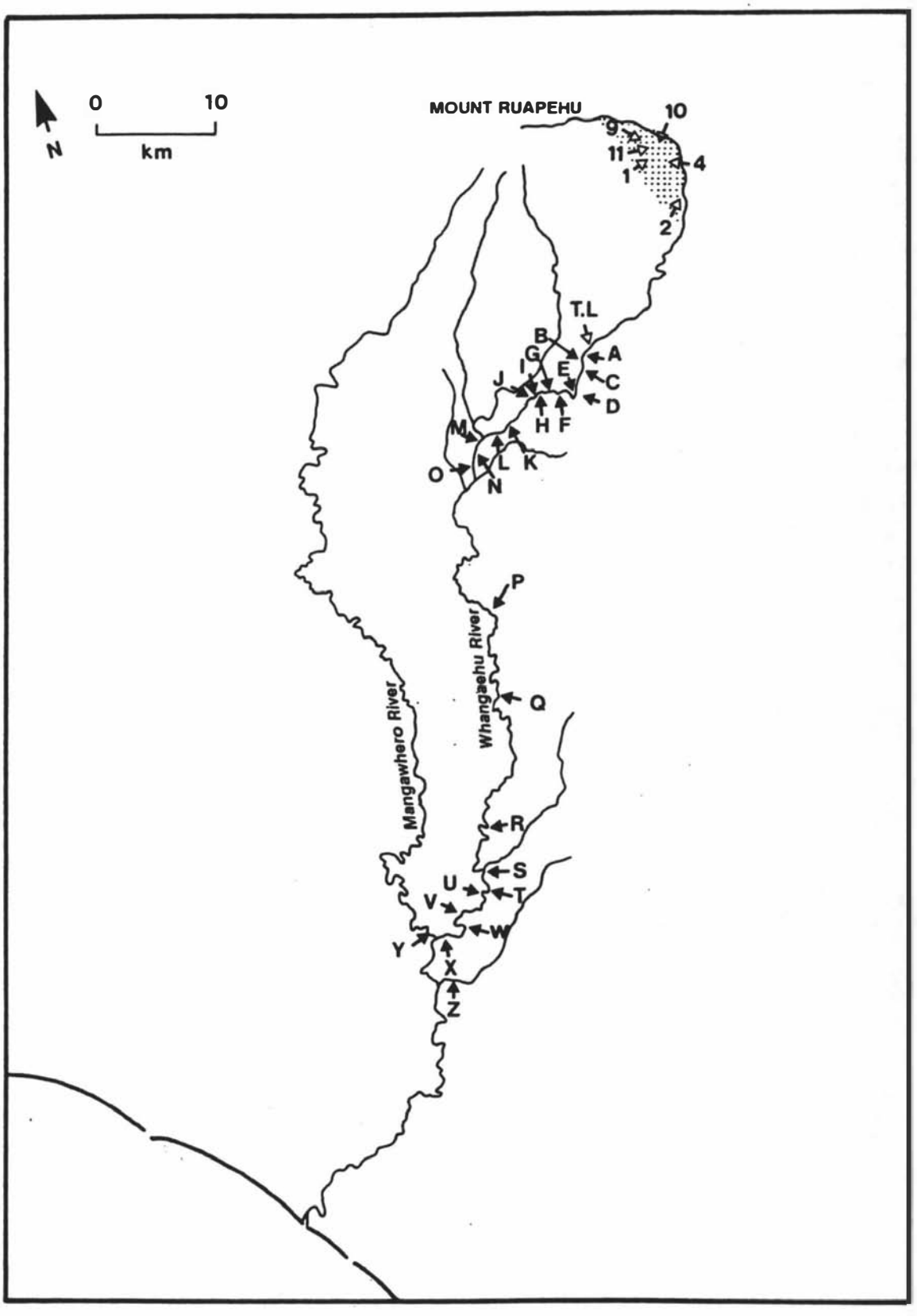

Figure 7.2 Map showing locality of the Onetapu Formation Type Locality (Donoghue, 1991), and reference sections. Sections identified on the Whangaehu Fan are from Purves (1990).

Donoghue (1991) first described Ona at the type locality for Onetapu Formation (see Figure 7.1 and Table 7.5). She describes it as a purplish grey muddy matrix-supported diamicton. Here it immediately overlies Taupo Ignimbrite lying at the base of a sequence of seven members of the Onetapu Formation. Correlation to the Rangipo Desert was based on Purves' (1990) field descriptions.

Deposits of Ona are generally thin (< 0.53 m, with one exceptional bed 1.5 m thick) and it is considered that Ona was emplaced by a thin, but cohesive debris flow. The total volume of member Ona deposits are in the order of 3.0×10^6 m^3 (see Table 7.8, page 144), including an estimate for the volume of deposits in the Rangipo Desert determined by Purves (1990). The lower age bracket for time of emplacement of Ona is provided by the Taupo Ignimbrite (1,850±10 years B.P., Froggatt and Lowe, 1990); the upper bracketing age of (Wk-2098) 890±40 B.P. (this study) is provided by a radiocarbon date on wood sampled below One (described later in this section) at Section I. Therefore Ona was emplaced within the period 1860 to 850 years B.P. (see Table 7.8). Where Ona overlies Taupo Ignimbrite the palaeosol developed into the underlying ignimbrite is a weakly developed A horizon which is thin, non sticky, non plastic, and has a fine nut and crumb structure (10YR 8/8-7/6, yellow) with few to common fine rootlets. Where Ona is absent, and the Ignimbrite is overlain by younger Onetapu Formation lahar deposits this palaeosol is a moderately developed A horizon which is gritty, non sticky, non plastic and has a fine nut and crumb structure (10YR 6/8 3/4, brownish yellow to dark yellowish brown), with common fine rootlets. From this evidence it is considered that Ona was emplaced closely following the Taupo Ignimbrite event, and probably about 1,800 years B.P.

7.4.2 *MEMBERS Onb AND Onc*

Onb and **Onc** (see Figure 7.3) are newly described informal members of the Onetapu Formation. They are not correlated to any previously defined Onetapu Formation members. In exposure they have similar sedimentological characteristics as Ona (see Table 7.6), but stratigraphically overlie it. The total combined volume of both deposits is estimated to be *c.* 1.8×10 m^3. From lithofacies observed at these localities member Onb is interpreted to have been emplaced by hyperconcentrated flow, and Onc by debris flow and hyperconcentrated flow (see Table 7.6).

Legend (see reverse) to accompany Figure 7.3, overleaf.

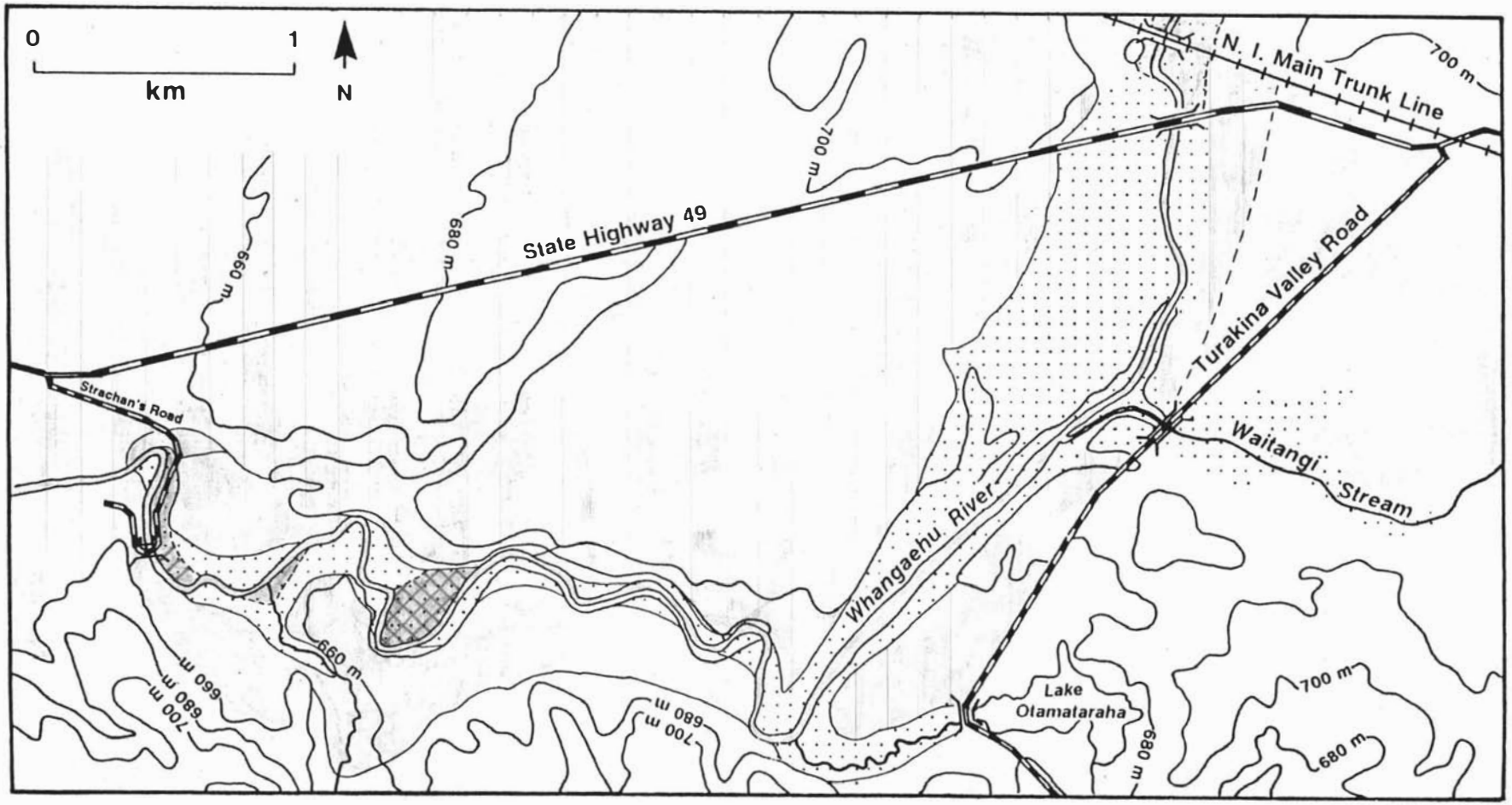

Figure 7.3 Distribution of Onetapu Formation members Ona ( ), Onb ( ) and Onc ( ) on the southern edge of the Mount Ruapehu ring plain, and distribution of older late Quaternary Formations (see page 120, above, for legend).

At Section G2 (see Figure 7.1), Onb immediately overlies Ona, the contact not being marked by any erosion break or evidence of soil forming processes. This suggests that Onb was emplaced shortly after Ona, probably about 1,750 years B.P. (see Table 7.8). Onc overlies Onb at this section, and the contact between the two deposits is marked by a thin palaeosol. At Section I (see Figure 7.1) Onc is separated from Ona by 0.11 m of reworked Taupo Ignimbrite and a thin, weakly developed, yellow (10YR 7/6) silty soil (see Plate 7.2). This soil is unlikely to represent more than 50 years of stability, so the interval of time between emplacement of Onb and Onc is considered to have been not more than 100 years at the most and is likely to have been emplaced no later than about 1,650 years B.P.

7.4.3 *MEMBER Ond*

Ond (see Figure 7.4) is a newly described informal member. It is not correlated to any previously defined Onetapu Formation members. In exposure it is represented by clast-supported sand: it does not have the muddy matrix which distinguishes the three older members described previously (see Table 7.6). For this reason Ond is distinct from other closely associated underlying and overlying Onetapu Formation deposits. Only three deposits of Ond were described and these all indicate that Ond was emplaced by turbulent hyperconcentrated flow. The estimated total volume of deposits in member Ond is 2.7×10^4 m^3. At Section I (see Plate 7.2), Ond lies as a thin 0.1 m wedge within 0.4 m thick gritty, non sticky, non plastic, moderately developed (10YR 5/6, yellowish brown) sandy loam which has a fine nut and crumb structure with abundant fine rootlets. This soil may represent a period of landscape stability of at least 500 years, *i.e.* between 1,650 (estimated age for Onc) and 1,150 years B.P. Ond is near to the top of the soil, but below fossil tree stumps, a root from which has been radiocarbon dated (Wk-2098) providing a minimum bracketing age for this, and all underlying deposits, of 890±50 years B.P. (see Table 7.5). Therefore Ond was emplaced within the range 1,650 to 840 years B.P. It is here considered that Ond was probably emplaced about 1,200 years B.P (see Table 7.8).

Table 7.5 Stratigraphic column of Onetapu Formation lahar deposits. Those units which are shaded have been correlated in this study throughout the Whangaehu River Catchment.

Date in years B.P. (calendar years)	I. B. Campbell (1973)	A. M. Purves (1990)	S. L. Donoghue (1991)	K. A. Hodgson (this study)
		(1975)		Ono
				Onn
(1750-1950)				Onm
		D 12	Ong	
		D 11	Onf	
390 ± 55				
			One2	Onl
		D 10	One1	Onk
500 ± 70				
450 ± 55	C1	D 9	Ond	Onj
407 ± 70				
		D 8		
		D 7		Oni
	C2	D 6		Onh
570 ± 45				
660 ± 50				
756 ± 56				
	C3	D 5	Onc	Ong1,2,3
		D 4		
	C4	D 3	Onb	Onf
		D 2		One
890 ± 40				
				Ond
				Onc
				Onb
		D 1	Ona	Ona
1,850 ± 10				

7.4.4 *MEMBER One*

One (see Figure 7.4) is a newly described member of the Onetapu Formation, and here is tentatively correlated to lahar deposit D2 of Purves (1990), (see Table 7.5). In exposure it is a grey muddy matrix-supported gravel (see Table 7.6 and Plate 7.2). The matrix is similar to that of the older members Ona, Onb and Onc, but it has a lower mud content. It is distinctive because it marks the lowermost occurrence of an assemblage of coarse-grained clastic lahar deposits (members Onf and Onh) which are described later. The coarse-grained clasts within One are commonly rounded. Deposits of One are described at two localities and from these descriptions it is interpreted to have been emplaced by debris flow. The estimated total volume for deposits of One is 1.8×10^6 m^3.

A lower age estimate is provided by a radiocarbon date (Wk-2098) of 890±50 years B.P. from a fossil tree stump immediately underlying One at Section I. Here the lahar which emplaced One appears to have overwhelmed small trees which were growing in a stable environment, determined by the presence of a well developed palaeosol. An upper age bracket of 756±56 years B.P. is provided from a radiocarbon date (NZ1584) on wood in sediments overlying One. Therefore One was most likely emplaced between 940 and 700 years ago. During this interval four Onetapu Formation lahar deposits were emplaced, amongst which One is the oldest and is therefore likely to be closer to the lower age bracket. Further, if it was responsible for burying the trees at Section I from which the radiocarbon date was obtained, then an estimated age of 900 years B.P. for emplacement seems most probable (see Table 7.8).

7.4.5 *MEMBER Onf*

Member **Onf** (see Figure 7.4) is correlated to lahar deposit D3 of Purves (1990), member Onb of Donoghue (1991), and to an unnamed lahar deposit described by Campbell (1973), (see Table 7.5). Onf is described at 30 different localities. The lithology of Onf is characterized by a muddy matrix-supported gravel (see Table 7.6 and Plates 7.2 and 7.3). The matrix is typically grey in colour with orange red mottling. Clasts have red staining penetrating up to 10 mm into their exterior surfaces, here interpreted to be a result of redox reactions subequent to deposition.

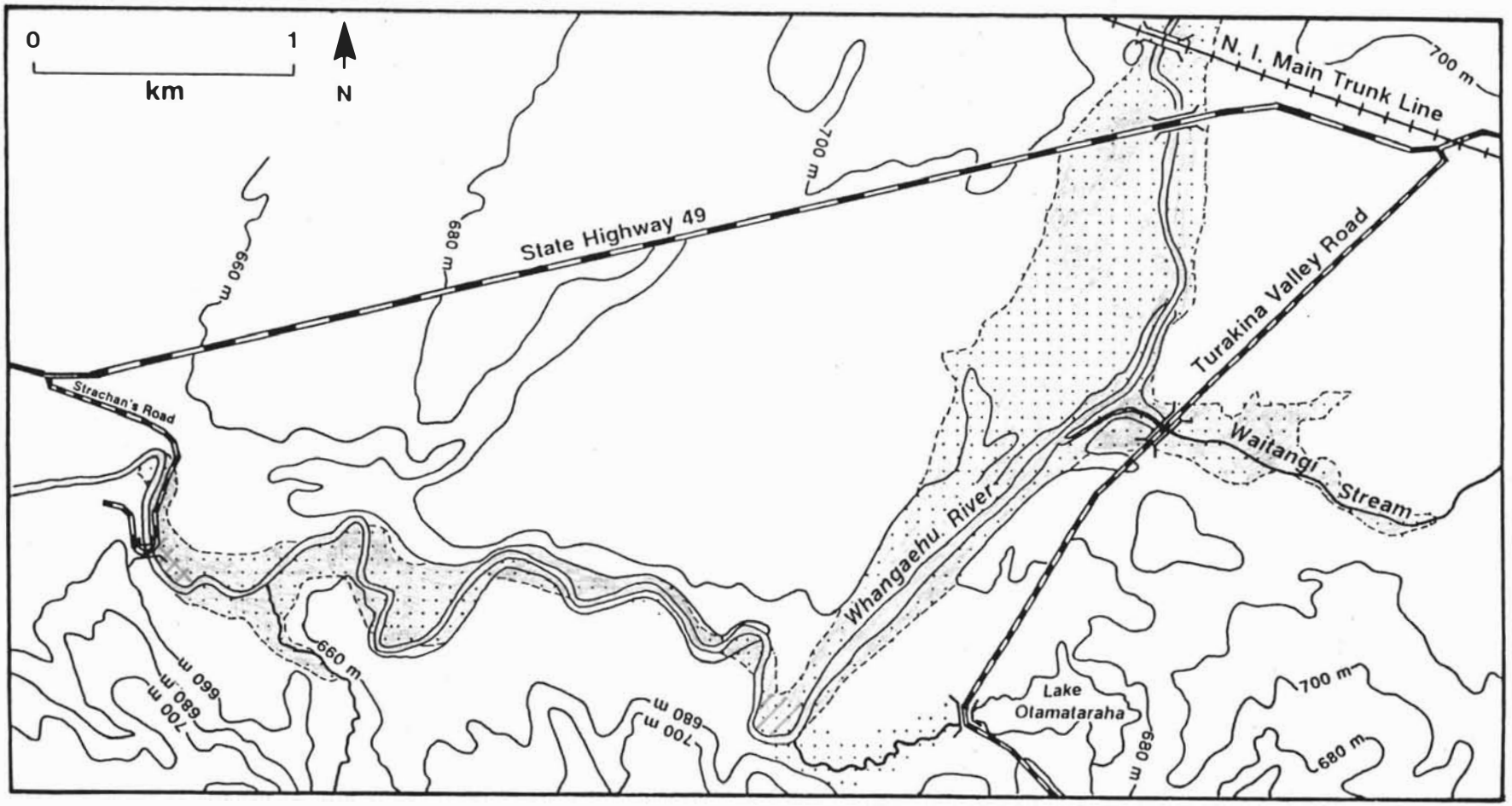

Figure 7.4 Distribution of Onetapu Formation members Ond ( ), One ( ) and Onf ( ) on the southern edge of the Mount Ruapehu ring plain.

The reason why clasts in this particular deposit should have undergone this reaction, and not in other deposits, is not known. The coarse-grained clasts in Onf are also commonly rounded. Onf deposits (see Table 7.6) suggest that they were probably emplaced by debris flow processes. Deposits of Onf are generally thicker, and more clast-rich, than other Onetapu debris flow deposits, and probably represent the products of one of the largest Onetapu lahars. The total volume for deposits is in the order of 3.2×10^6 m^3 (see Table 7.8).

Bracketing ages for emplacement of Onf are the same as for One. At the two localities where both One and Onf are described (Section E1 and I), One is immediately overlain by Onf indicating the two deposits were probably emplaced closely in time. An estimated age of 850 years B.P. is here proposed for Onf.

7.4.6 *MEMBER Ong*

Member **Ong** (see Figure 7.4) comprises up to three individual deposits (Ong1, Ong2 and Ong3) which are often indistinguishable from one another. All three may be exposed, *e.g.* at Section J1 and L1 (see Plate 7.3), or a combination of two, *e.g.* at L2, or only one, *e.g.* at Section E2 and H3 (see Figure 7.2 for all section localities). When all three deposits are exposed the middle unit, Ong2, is usually thin. When only two Ong members are exposed they are thought to represent members Ong1 and Ong3. If only one deposit is observed confident correlation to any individual Ong member is not possible. Ong is correlated to lahar deposit D5 of Purves (1990), Onetapu Formation member Onc of Donoghue (1991) and an unnamed lahar deposit (C3) described in the lower reaches of the River near to Mangamahu by Campbell (1973), (see Table 7.5). This latter site was visited by the auther but no positive identification of the lahar deposit could be made. At the time of Campbell's description, this site was being actively quarried and it is possible that deposits from Ong may have been entirely extracted. Correlation is based on the field decription supplied by Campbell (1973) and the stratigraphic position of this deposit in relation to underlying member Onf and overlying Onh. Ong is characterized by clast-supported sands and granules, with occasional gravel (see Table 7.6). Overall its colour appears brown. Deposits contain common pumice lapilli, and lithic clasts are commonly scoriaceous.

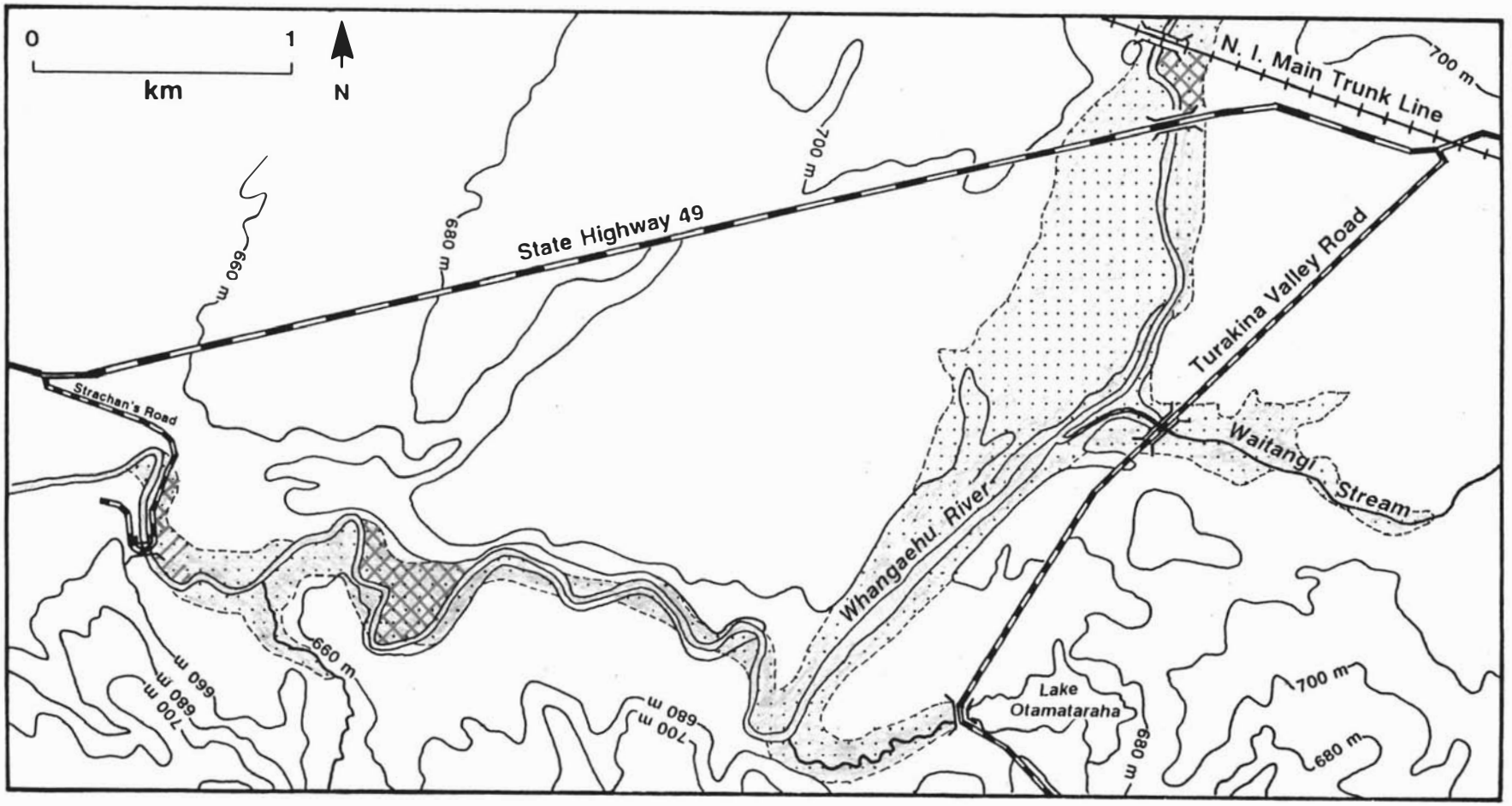

Figure 7.5 Distribution of Onetapu Formation members Ong1 ( ), Ong2 ( ) and Ong3 ( ) on the southern edge of the Mount Ruapehu ring plain.

A total of 48 localities of this deposit are described, and these indicate that Ong was emplaced by both debris flow and hyperconcentrated flow. However a low strength, turbulent hyperconcentrated flow is implicated as the principal flow type. The total volume of deposits is estimated to be 3.5×10^6 m^3.

Lower and upper bracketing ages for emplacement of Ong deposits are the same as for One and Onf (see Table 7.8). At Mangamahu (S1) fossil stumps from trees which had grown into Ong are found (see Plate 7.1). A sample from the root of one of these stumps was dated (NZ1584) and gave an age of 756±56 years B.P. (Campbell, 1973; see Table 7.9). Therefore Ong was deposited between 930 and 700 years ago. Campbell (1973) states that the date determined for the root is possibly near the average age of the tree. Hence Ong may be over 50 years older than this radiocarbon date. Based on this evidence it is considered that Ong at Mangamahu was probably emplaced about 800 years ago. The deposit described by Fleming at Mangamahu is probably the oldest member, Ong1. In the upper reaches of the River at Sections J1 and L1, sedimentological evidence points to member Onh being emplaced almost immediately after the youngest member of Ong (refer forward to section 7.6.1 this chapter, and footnote 2). At Section L1 all three members of Ong are present, hence the uppermost unit is Ong3. An estimated age of 600 years B.P. is proposed for Onh, and it seems logical to assign a similar age to Ong3. Thus the three members of Ong were emplaced in the time range between 930 and 700 years B.P.; Ong1 probably about 800 years B.P., Ong2 about 700 years B.P. and Ong3 about 600 years B.P. (see Table 7.8). A 0.03 m peat deposit at section L1 (see Plate 7.3), between Ong1 and Ong2, would have taken in the order of 50 to 100 years to accumulate (assuming a pre-compression depth of *c.* 0.1 m) this supporting the contention that Ong2 was emplaced up to 100 years after Ong1.

7.4.7 *MEMBER Onh*

Onh (see Figure 7.6) is correlated to lahar deposit D6 of Purves (1990) in the Rangipo Desert, and to an unnamed lahar deposit at Mangamahu described by Campbell (1973), (see Table 7.5). It is not preserved at the type locality for Onetapu Formation. Deposits of Onh are fine sandy matrix-supported gravel. Common black and grey and a few red clasts are observed within a brown sandy matrix (see Table 7.6 and Plate 7.4 and Plates 7.3, 7.7 and 7.13).

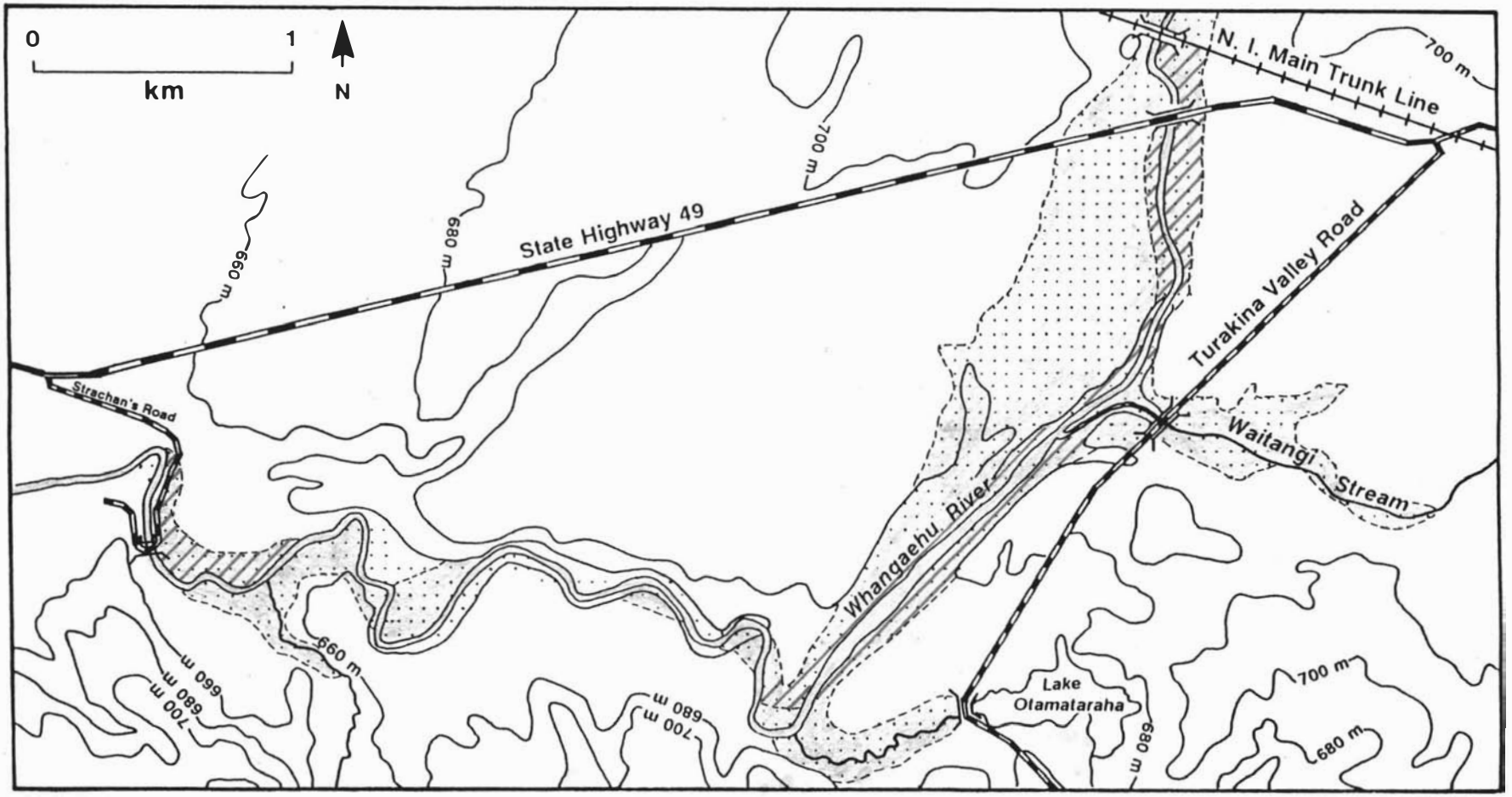

Figure 7.6 Distribution of Onetapu Formation members Onh ( ) and Oni ( ) on the southern edge of the Mount Ruapehu ring plain.

Deposits of Onh are described at 40 different localities and from these descriptions it is interpreted that Onh was emplaced principally by cohesive debris flow. In more distal localities deposits of Onh show characteristics typical of hyperconcentrated flow. Deposits from Onh are the most extensive in the catchment and this member is consistently recognized at most outcrops. The total volume for deposits in Onh is 1.8 $\times$ 10^7 m^3. Considering the wide distribution of Onh its absence at the type locality is unexpected. It can only be supposed that here the lahar was confined to the channel, or directed to the east bank of the River in this vicinity.

At Mangamahu a maximum age for emplacement of this member is provided, where Onh has engulfed trees (see Plate 7.1), wood from which has been dated (NZ1584) at 756$\pm$56 years B.P. A date (Wk-1488) of 650$\pm$50 years B.P. on peat overlying Tufa Tephra Tf5 (Donoghue, 1991) and correlated to a tephra (T.4) underlying Onh on the Mount Ruapehu ring plain (Purves, 1990) provides further support for the lower age constraint on this member. The youngest maximum bracketing age is supplied from radiocarbon dating of a piece of wood found in silt immediately underlying Onh at Section Y. This piece of wood is dated (Wk-2680) at 570$\pm$45 years B.P. At Mangamahu an upper age limit is supplied by wood found in a palaeosol which has developed into Onh. A radiocarbon date on this wood gave an age (NZ1363) of 407$\pm$70 years B.P. (Campbell, 1973). Therefore Onh was emplaced some time between 615 and 337 years B.P. Onh is here considered to have been deposited about 600 years B.P.

7.4.8 *MEMBER Oni*

Member **Oni** (see Figure 7.6) is not a distinctive unit and is defined here based on its stratigraphic position above member Onh and below Onj. Oni is tentatively correlated to lahar deposit D7 of Purves (1990), (see Table 7.5). It is represented by both matrix-supported pebbles and clast-supported sands comprising common black and grey and a few red lithic clasts and common pale grey pumice (see Table 7.7) with a silty sand matrix. Based on interpretation of the seven described exposures of Oni it is inferred to have been emplaced by debris flow and hyperconcentrated flow, principally by low strength turbulent hyperconcentrated flow. The total volume of deposits in Oni is estimated to be 3.5 $\times$ 10^6 m^3. This member lies stratigraphically within the same time frame as Onh, *i.e.* deposited between 615 and 337 years B.P.

Table 7.6 General sedimentological characteristics of Onetapu Formation informal members, including lithofacies description and inferred flow regime

Member name	General description	Number of observations	Assigned lithofacies	Interpreted flow regime
Ong3	*clast-supported sands and granules; common grey and black scoria lithic clasts; common grey pumice lapilli; overall colour 2.5YR 4/4, reddish brown*	10	4a 4b[P]	HYPERCONCENTRATED FLOW
Ong2	*clast-supported sands; abundant grey and black and few red scoria lithic clasts; few to common grey pumice lapilli; overall colour 2.5YR 4/3 - 10YR 4/3, reddish brown to dark brown*	5	4a 4b[P]	HYPERCONCENTRATED FLOW
Ong1	*clast-supported sands and granules; common grey and few black and red scoria lithic clasts; common grey pumice lapilli; overall colour 2.5YR 4/3 - 10YR 4/3, reddish brown to dark brown*	10	3b 4a 4b[P]	DEBRIS FLOW HYPERCONCENTATED FLOW
(Ong1-3)		(Total = 48)	3b 4a 4b[P]	DEBRIS FLOW HYPERCONCENTRATED FLOW
Onf	*muddy matrix-supported gravel; common grey and few black and red lithic clasts; matrix colour 10YR 5/1 - 4/1, grey to dark grey; mottles and stains on clasts 7.5YR 5/8 - 5YR 4/6, strong brown to yellowish red*	30	2a 3a[P] 3b 3c	DEBRIS FLOW
One	*muddy matrix-supported gravel; abundant grey and common black and few red and white lithic clasts; matrix colour 10YR 4/2 -3/2, dark to very dark greyish brown*	2	3b 3d	DEBRIS FLOW
Ond	*clast-supported sands and granules*	3	4b	HYPERCONCENTRATED FLOW
Onc	*muddy matrix-supported gravel; abundant grey and common black lithic clasts; matrix colour 10YR 7/6, yellow; clasts stained 5YR 4/6, yellowish red;*	2	3c 4a	DEBRIS FLOW HYPERCONCENTRATED FLOW
Onb	*clast-supported gravel; common grey and black and few red lithic clasts; matrix colour 10YR 3/2 - 5/1, strong grey to grey, with mottles 10YR 6/8 - 7/6, brownish yellow to yellow*	2	4a 4b	HYPERCONCENTRATED FLOW
Ona	*muddy matrix-supported gravel; common grey and few red and white lithic clasts; matrix colour 10YR 5/1, grey, with mottles 10YR 5/4, yellowish brown; clasts stained 5YR 4/6 yellowish red*	14	1b 3a 3b[P] 3c 3d	DEBRIS FLOW

[P] marks principal lithofacies type.

At sections H3, J1 and J2 Oni is separated from Onh by a 0.1 m thick gritty non sticky non plastic, weakly developed (10YR 3/4-4/3) sandy silt loam which with common fine rootlets. This palaeosol may have taken at least 50 years to form, so Oni is inferred to have been emplaced about 550 years ago (see Table 7.8).

7.4.9 *MEMBER Onj*

Member **Onj** (see Figure 7.7) is a distinctive deposit. It is correlated with lahar deposit D9 of Purves (1990) in the Rangipo Desert, with member Ond of Donoghue (1991) at the type locality for Onetapu Formation, and with the uppermost unnamed lahar deposit described at Mangamahu by Campbell (1973), (see Table 7.5). Deposits of member Onj are characterized as muddy matrix-supported gravels, although two of the more distal deposits are clast-supported sand (see Table 7.7). Clasts are dominantly dark grey and glassy. The matrix is a distinctive grey colour with olive mottles. In this study it is described at 19 different localities. From interpretation of the sedimentology of deposits it is inferred that Onj was emplaced principally by cohesive debris flow. In more distal localities however, hyperconcentrated flow subfacies predominate. The total volume of member Onj has been estimated for deposits both within the Rangipo Desert and downstream of Tangiwai. The combined total volume is in the order of 8.4×10^6 m^3 (Table 8.8).

The time constraints for emplacement of this lahar deposit are well established. Radiocarbon dates have been obtained from the base, (NZ1363) 407 $\pm$ 70 years B.P., (Campbell, 1973), and within the deposit, (NZ7465) 450$\pm$55 years B.P. (Donoghue, 1991) and on charcoal in sand dunes overlying it, (Wk-1487) 500$\pm$70 years B.P. (Purves, 1990). If the overlying charcoal was not retransported by aeolian processes and is thus *in situ*, then member Onj was deposited between 430 and 477 years B.P., probably about 450 years B.P.

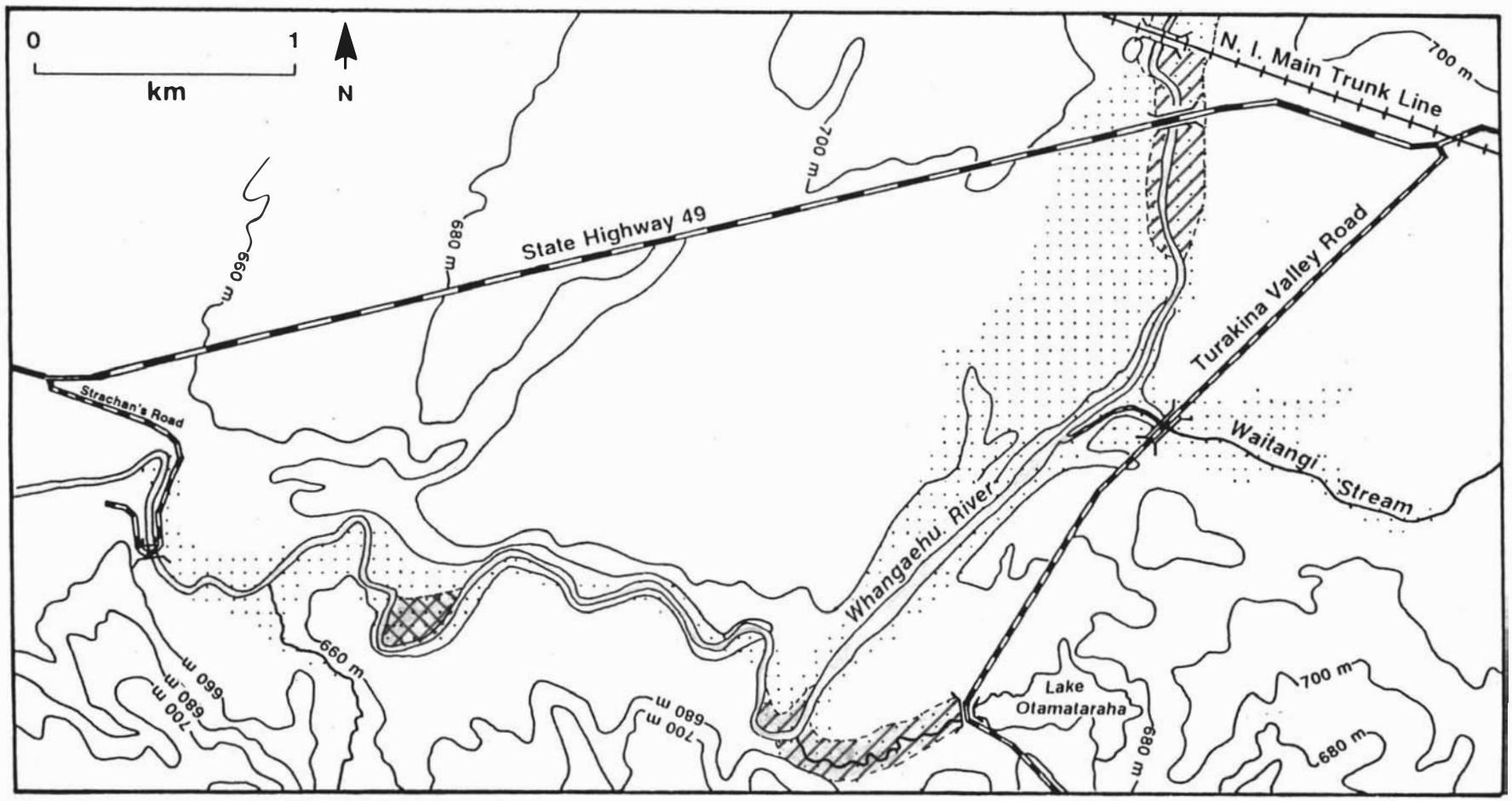

Figure 7.7 Distribution of Onetapu Formation members Onj ( ), Onk ( ) and Onl ( ) on the southern edge of the Mount Ruapehu ring plain.

7.4.10 *MEMBER Onk*

Onk (see Figure 7.7) is tentatively correlated to lahar deposit D10 of Purves (1990) and One2 of Donoghue (1991). Onk is not widely distributed but its stratigraphic position immediately overlying the major member Onj makes Onk more readily identifiable. Nine localities are described for Onk, where the sedimentology varies from sandy matrix-supported gravel to clast-supported sand. Clast types are commonly grey and black and a few red and white lithics, with common grey pumice lapilli (see Table 7.7). The overall colour of the deposit is brown. Deposits of Onk are interpreted to have been emplaced by debris flow and hyperconcentrated flow, chiefly by low strength turbulent hyperconcentrated flow. The total volume for deposits of Onk is estimated to be about 3.6×10^5 m^3.

A maximum age for Onk is provided by a radiocarbon date on wood found within underlying member Onj which gave an age of 450±55 years B.P. (Donoghue, 1991). At the Type Locality Donoghue dated peat overlying One2 (correlated to Onk) and a younger deposit One1, which gave an age (NZ7388) of 390±55 years B.P. This provides a minimum age for member Onk. Therefore Onk was deposited between 505 and 335 years B.P. At Sections L2, N and O, member Onk is separated from Onj by a 0.1 m thick very gritty, non sticky, non plastic, non greasy, sandy loam (10YR 2/2, very dark brown) with abundant fine rootlets. This is likely to have taken at least 50 years to develop. Further downstream Onk is separated from Onj by up to 1.5 m of silt. Onk is thus here considered to have been emplaced at least 50 years after Onj and probably about 400 years B.P. (see Table 7.8).

7.4.11 *MEMBER Onl*

Deposits of member **Onl** are described at only two localities, Sections G2 and G4. Onl is either a sandy matrix-supported gravel or a clast-supported gravel, with common black, red and grey lithic clasts and an overall dark grey colour. It is interpreted to have been emplaced by debris flow and hyperconcentrated flow (see Table 7.7). The total volume for deposits in Onl is about 6.6×10^4 m^3. Age constraints for deposition of Onl are the same as Onk, *i.e.* 505 - 335 years B.P., and Donoghue estimated that this deposit was *c.* 400 years old based on a radiocabon date (NZ7388) of 390$\pm$55 years B.P. on overlying peat.

7.4.12 *MEMBERS Onm, Onn AND Ono*

Deposits of the three youngest members of Onetapu Formation described in this study, **Onm**, **Onn** and **Ono**, are largely confined to Karioi quarry (locality G, see Plate 7.4). Onn and Ono are correlated to two unnamed Onetapu members described by Donoghue (1991) at the type locality.

These three youngest members are correlated to the three large historic lahars which occurred in 1861, 1953 and 1975. Correlation of the three members to historic lahars is based on the bracketing ages provided by radiocarbon dating and the evidence supplied from pine cones.

Member **Onm** is described as clast-supported sands with common black, grey and few red and white lithic clasts and an overall very dark greyish brown colour. It is interpreted to have been emplaced by hyperconcentrated flow (see Table 7.7). The total volume of deposits of Onm is estimated to be 1.6×10^5 m^3. At Section G6 Onm contains twigs and fined-grained organic material. A date (Wk-2097) determined on a piece of wood sampled here gave an age of Modern, *i.e.* between calendar years 1750 and 1950 A.D. Onm probably represents deposits from the lahar which occurred in 1861.

Member **Onn** is clast-supported gravel with common grey, black and a few red lithic clasts and common grey pumice lapilli (see Table 7.7). The overall colour of this unit is dark greyish brown. It is interpreted to have been emplaced by hyperconcentrated flow. The total volume of deposits of Onn is estimated to be 7.2×10^4 m^3. The age constraint determined for Onm, 1750 A.D., provides a maximum bracketing age for Onn, which is assumed to represent the 1953 event. About 2 km upstream from Karioi Quarry a 1.5 m thick debris flow deposit was found which contained a piece of fabric, some metal sheeting and a piece of wire. This deposit was stratigraphically isolated, although it was wedged against older Onetapu Formation deposits. It is here believed to have been emplaced by the 1953 lahar; the anthropogenic debris being derived from the carriages which were involved in the Tangiwai Disaster.

Member **Ono** is a fine sandy matrix-supported gravel, with common grey, a few black and a few soft altered white and pink lithic clasts. The matrix colour is dark grey. Ono is interpreted to have been emplaced by debris flow. The total volume of deposits in Ono is estimated to be 1.1×10^5 m^3. At Section G4 a pine cone was found in this deposit. Plantings in the Karioi State Forest began in the years 1927 - 1929. Principal exotic species planted included *Pinus nigra* and *Pinus ponderosa*. The first plantings were of *Pinus nigra* in 1928 (Donoghue, 1991). No pine species existed on the east flank of Mount Ruapehu prior to this time. Thus, lahar deposits containing pine cones, as does Ono, must have occurred post-1927 A.D. Ono, which is the uppermost and youngest deposit described in this study, is considered to have been emplaced by the most recent large lahar which occurred in 1975. The presence of a pine cone in this deposit supports this premise. Donoghue (1991) identifies three lahar deposits resting over a palaeosol containing pine cones and she considered that these represented lahars which occurred in 1953, 1969 and 1975.

Table 7.7 General sedimentological characteristics of Onetapu Formation including lithofacies description and inferred flow regime

Member name	General description	Number of beds	Assigned lithofacies	Interpreted flow regime
Ono	*fine sandy matrix-supported gravel; common pale grey and few black lithic clasts; few soft altered white and pink clasts; matrix colour 10YR 4/1, dark grey*	1	3b	DEBRIS FLOW
Onn	*clast-supported sands; common grey and black lithic clasts; common hard grey vesicular pumice lapilli; overall colour 10YR 4/2 - 4/3, dark greyish brown*	3	4a 4b^{P}	HYPERCONCENTRATED FLOW
Onm	*clast-supported sands; common red, black and grey lithic clasts; overall colour 10YR 3/2, very dark greyish brown*	3	4a 4b	HYPERCONCENTRATED FLOW
Onl	*sandy matrix-supported gravel to clast-supported sand; common grey, black and few red lithic clasts; occasional grey pumice lapilli; overall colour 10YR 5/3 -3/2, dark grey*	3	3d 4a 4b	DEBRIS FLOW HYPERCONCENTRATED FLOW
Onk	*sandy matrix-supported gravel to clast-supported sand; common grey and black and few red and white lithic clasts; common hard grey pumice lapilli; overall colour 10YR 4/4, dark yellowish brown*	9	3a 3c 3d 4b^{P}	DEBRIS FLOW HYPERCONCENTRATED FLOW
Onj	*muddy matrix supported gravel; abundant dark grey glassy lithic clasts; matrix colour 10YR 5/1, grey, with mottles 10YR 6/6 - 6/8, brownish yellow*	19	1b 3a 3b^{P} 3d 4a 4b	DEBRIS FLOW HYPERCONCENTRATED FLOW
Oni	*clast-supported sand; common black and grey and few red lithic clasts; common pale grey pumice lapilli; overall colour 10YR 5/2, greyish brown*	7	3a 3b 4b^{P}	DEBRIS FLOW HYPERCONCENTRATED FLOW
Onh	*fine sandy matrix-supported gravel; common black and grey and few red lithic clasts; matrix colour 10YR 4/3, brown to dark brown*	40	2c 3a 3b^{P} 3c^{P} 3d 4a 4b	DEBRIS FLOW HYPERCONCENTRATED FLOW

^{P} marks principal lithofacies type

Table 7.8 Extent, mean depth, volume and estimated age of Onetapu Formation informal members

Member name	Extent (m^2)	Mean depth (m)	Volume (m^3)	Age range years B.P. (calendar years)	Estimated age years B.P. (calendar years)
Ono	3×10^3	0.8	$^P9 \times 10^4$ $^H2.4 \times 10^3$ ^{T}**9.24×10^4**	(< 1928)	**(1975)**
Onn	3×10^3	0.24	**7.2×10^2**	(< 1750)	**(1953)**
Onm	3×10^3	0.53	**1.6×10^3**	(1750 - 1950)	**(1861)**
Onl	3×10^3	0.22	**6.6×10^2**	505 - 335	**400**
Onk	7.5×10^3	0.48	**3.6×10^3**	505 - 335	**400**
Onj	6.55×10^6	0.61	$^P4.4 \times 10^6$ $^H4.0 \times 10^6$ ^{T}**8.4×10^6**	477 - 395	**450**
Oni	3.6×10^6	0.4	$^P3.4 \times 10^6$ $^H1.4 \times 10^5$ ^{T}**4.8×10^6**	615 - 337	**550**
Onh	6.41×10^6	0.87	$^P1.2 \times 10^7$ $^H5.6 \times 10^6$ ^{T}**1.8×10^7**	615 - 337	**600**
Ong	3.24×10^6	1.08	**3.5×10^6**	930 - 700	**800 - 600**
Onf	2.87×10^6	0.83	$^P0.8 \times 10^6$ $^H2.4 \times 10^6$ ^{T}**3.2×10^6**	930 - 700	**850**
One	1.5×10^3	1.05	$^P1.8 \times 10^6$ $^H1.6 \times 10^3$ ^{T}**1.8×10^6**	930 - 700	**900**
Ond	9×10^3	0.3	**2.7×10^3**	1860 - 850	**1200**
Onc	4.5×10^3	0.4	**1.8×10^3**	1860 - 850	**1650**
Onb	3×10^3	0.2	**6×10^2**	1860 - 850	**1750**
Ona	5.9×10^5	0.27	$^P2.8 \times 10^6$ $^H1.6 \times 10^5$ ^{T}**3.0×10^6**	1860 - 850	**1800**

[P] Total volume estimated for deposits on the Rangipo Desert by Purves (1990).

[H] Total volume estimated for deposits below Tangiwai by Hodgson (this study).

[T] Total combined volume for deposits.

7.5 EVIDENCE FOR FLOW TRANSFORMATION IN ONETAPU FORMATION DEBRIS FLOW DEPOSITS

A diverse range of lithofacies types are described in the Onetapu Formation. These vary both between and within members and reflect changes in flow type between different lahars and within each as it progressed downstream. This next section will investigate variations in lithofacies types within individual members, and examine the evidence for flow transformation. Figure 7.2 depicts the overall stratigraphy for Onetapu Formation in the Whangaehu Valley downstream of Tangiwai, including selected vertical profiles from Purves (1990) for the Mount Ruapehu ring plain, and Donoghue (1991) at the type locality. From this overall stratigraphy, by virtue of their correlation and wide distribution throughout the catchment members Ona, Onf, Onh, and Onj were selected for further investigation.

7.5.1 *LITHOLOGICAL VARIATIONS WITHIN ONETAPU LAHAR DEPOSITS*

Table 7.9 details the lithofacies type at a variety (but not all) of exposures of the four members selected for further investigation. These indicate, in members Onh and Onj, a downstream change from highly competent debris flow to less competent hyperconcentrated flow. The two older members, Ona and Onf, showed no systematic change of this nature. Figures 7.8 and 7.9 plot maximum and modal clast size against distance downstream for each lahar deposit and these plots show a progressive reduction in both maximum and modal clast size with distance downstream. These trends would be expected as the lahars travelled from high velocity/high energy zones in proximity to the steep slopes of the volcano, to lower energy zones in more distal localities. Local variations in these trends, which are especially noticeable in Onf, reflect the contrast between deposition in in-channel or overbank situations, *i.e.* thick deposits with coarser clasts tend to occupy depositional environments interpreted to represent the main axis of lahar flow, and thinner deposits with consequent smaller clasts in overbank situations. These would correspond to the "lahar channel facies" and "lahar floodplain facies" described by Scott (1988a), for lahar deposits in the Toutle-Cowlitz River following the 1982 eruption of Mount St. Helens.

Table 7.9 Downstream variations in lithology for Onetapu Formation debris flow deposits.

Site	Distance downstream (km)	One	Onf	Onh	Onj
1	11.4	1b	-	-	-
2	20	3b	3b	3b	3b
4	16	-	-	3b	3b
5	10	-	-	-	3b
9	11.5	3b	-	3b	1b
10	12.1	-	-	3c	3c
11	12	-	-	-	1b
TL	38	3a	3a	-	3a
A	40.2	3b	3b	3a	-
C1	41	-	3b	3b	-
C2	41.2	-	3c	3a	-
D	40.6	-	-	3b	3a
E1	42	-	3a	2b	-
E2	42.2	-	3b	3b	3b
E3	42.4	-	-	3b	3b
F	43.2	-	-	3a	3a
G1	44	3b	3a	3d	-
G2	44	3d	3a	3d	3d
G3	44	-	-	3a	3d
G4	44	-	-	4b	-
G6	44	-	3c	3b	-
G7	44	-	2a	-	-
G8	44	-	3a	3c	-
G9	44	-	3a	3c	-
H1	46	-	3b	3b	-
H2	46.1	-	3d	3c	-
H3	46.4	-	3a	3c	-
I	47.1	3c	3d	-	-
J1	47.6	3c	3b	3d	-
J2	48	3c	3a	3d	-
L1	54.8	3c	2a	3b	-
L2	54.9	3b	3b	3c	3b
M1	56	3c	3c	3b	-
M2	57.1	3c	3c	3b	-
N	58	-	-	3c	3b
O	58.6	-	3d	3c	-
P	84	3b	3a	3c	-
Q	104	-	-	3b	4b
R	118	-	-	-	3b
S1	133	-	3a	3b	3b
T	137	-	-	3b	3b
U	137.1	-	-	3b	3b
V	142	3a	3d	-	-
W	148	-	-	4b	4b
X	150	-	-	4b	4b
Y	152	-	-	4b	4b
Z	160	-	-	4b	4b

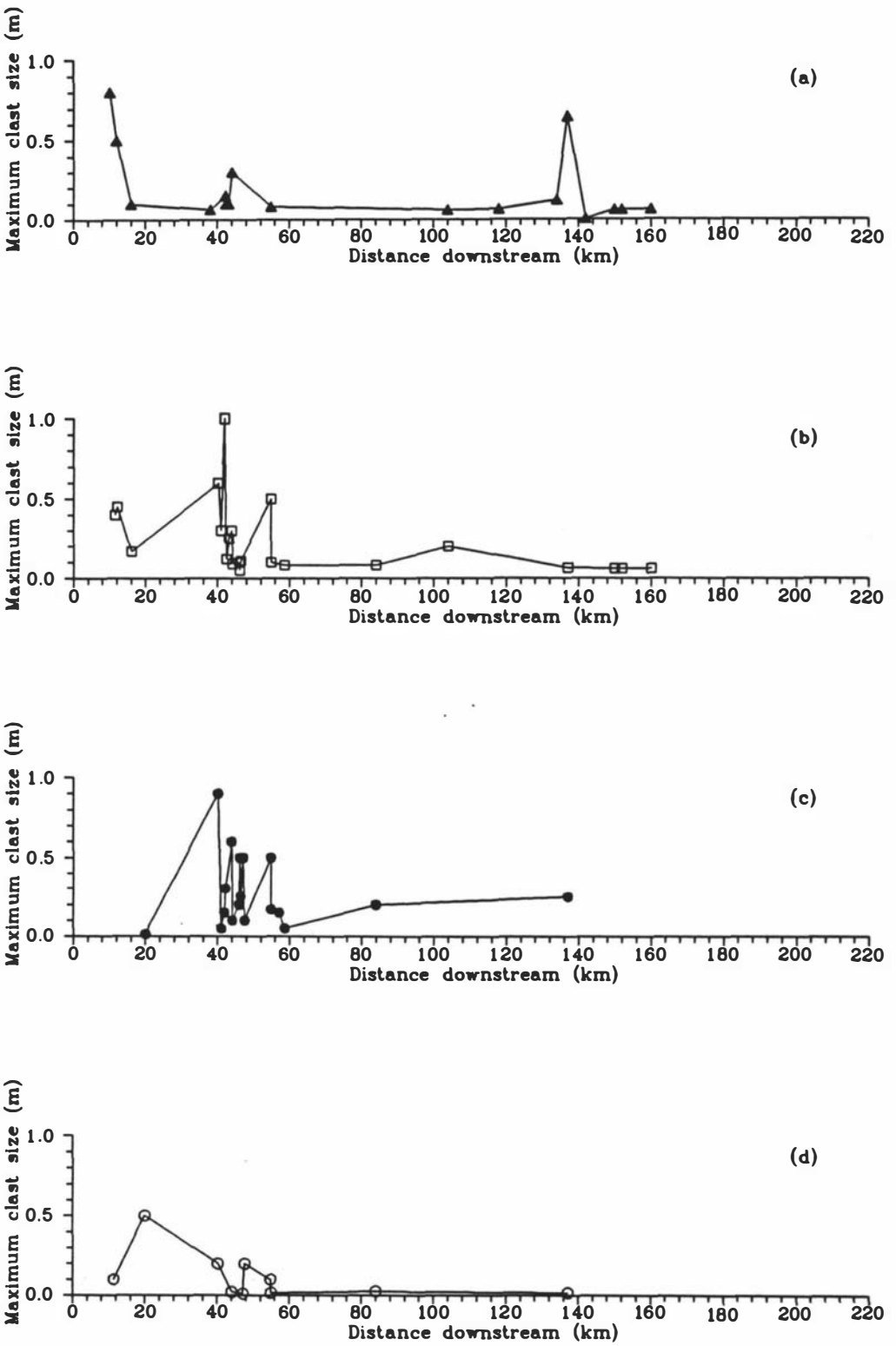

Figure 7.8 Downstream variations in maximum clast size for Onetapu Formation members (a) Onj, (b) Onh, (c) Onf and (d) Ona.

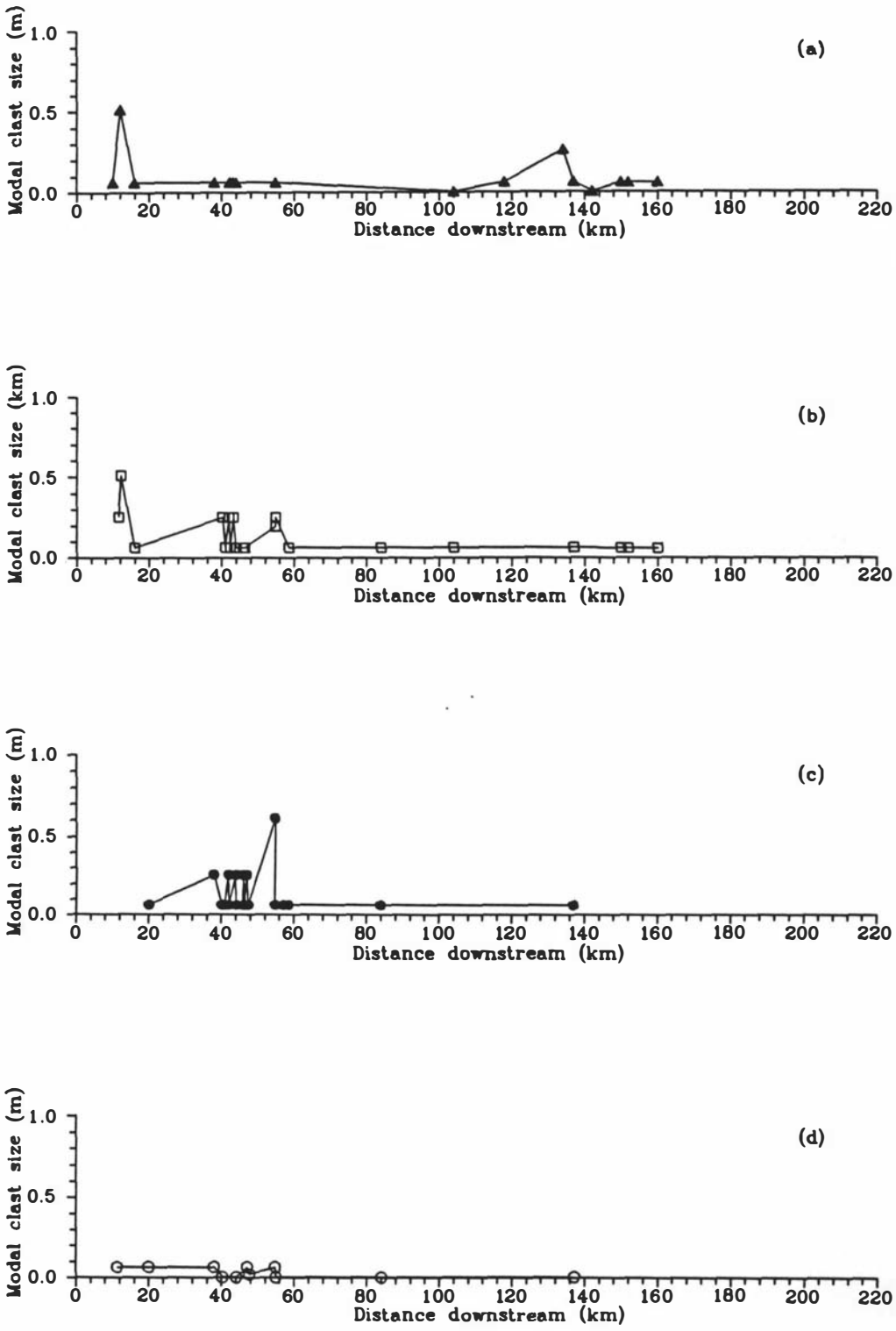

Figure 7.9 Downstream variations in modal clast size for Onetapu Formation members (a) Onj, (b) Onh, (c) Onf and (d) Ona.

In-channel deposits are not commonly observed in Onetapu Formation, probably due to their low survival potential as the river eroded through these deposits while regrading back to base level.

Deposits of members Onh and Onj are found up to 20 km further downstream of the final exposures of Ona and Onf. This may reflect the fact that (1) deposits from the older lahars did extend this far but their deposits are not preserved, or (2) the younger lahars, Onh and Onj, ran out further than the older ones. If this latter explanation is accepted then two explanations for these greater runout distances can be proposed: (1) clasts within Ona and Onf are dominantly lithic and non-scoriaceous, but Onh and Onj contain a greater proportion of scoriaceous clasts (especially noticeable in distal deposits) and therefore support of these lower density clasts is more likely to be maintained over longer distances; alternatively (2) subfacies in Onh and Onj in the extended distal 20 km zone indicate that hyperconcentrated flow was operating in both lahars. This indicates that both younger lahars underwent flow transformation from debris flows at about 140 km from source, and continued to flow downstream as hyperconcentrated flows. The lithology of Onj at Section Q indicates that the lahar had transformed from debris flow to hyperconcentrated flow by 104 km from source, and then transformed back to debris flow 33 km further downstream at Section T. The two older lahars, however, underwent no transformation and their final exposures at 137 km from source mark approximately the longitudinal flow limit of Ona and Onf lahars. Onj and Onh lahars continued to flow downstream for a further 20 km (as hyperconcentrated flows) at which point sedimentological evidence indicates that they were transforming to streamflow. The deposits which remain from both latter stages of lahar flow of Onh and Onj resemble "lahar runout facies" and "lahar-related streamflow facies" described by Scott (1988a).

7.5.2 *PARTICLE SIZE ANALYSIS OF ONETAPU FORMATION LAHAR DEPOSITS*

The most studied aspect of lahar sedimentology is particle size analysis, and this has proved to be a useful tool for showing systematic changes in sedimentology of individual deposits. In the following section the phenomenon of flow transformation, as depicted in the previous section on lithology, will be investigated. The analysis was conducted on members Onf, Onh and Onj, which were emplaced principally by debris flows, and on members in Ong which are interpreted to have behaved as hyperconcentrated flows throughout their flow history.

The original purpose of this particle size analysis had been to quantify the sedimentological characteristics of debris flow and hyperconcentrated flow. Members Onf, Ong and Onh were mostly sampled in the middle reach of the catchment, above locality P. Member Onj was not widely distributed in this middle reach and was sampled downstream of this locality.

7.5.2.1 *Methodology*

Samples of lahar deposits were collected and initially analyzed in the field. This allowed larger representative samples to be collected for the coarser grained deposits. Sample weight for debris flow deposits were between 30 and 76 kg, and for hyperconcentrated flow between 5 and 30 kg. Samples were air dried and then hand sieved to separate boulders, cobbles, fine- medium- coarse- and very-coarse pebbles. A subsample of grains smaller than pebble size was collected and taken back to the laboratory for further analysis. Preliminary wet sieving of this finer-grained subsample was conducted to obtain the silt and clay fraction which was retained for pipette analysis. The grain size distribution of the sand phase was obtained by mechanical sieving with a ring tap sieve shaker. Mean grain size, standard deviation and skewness were calculated using a grain size analysis computer software application, PC-Gran, and descriptive grain size distribution parameters as defined by Folk and Ward (1957) are presented in this thesis.

7.5.2.2 *Results*

The results of this analysis are presented in Table 7.10 and Figures 7.10-16. By comparing the calculated sorting values with the lithofacies of the deposit sampled (see Table 7.9) the lower sorting threshold for debris flow is about 2 Φ, which corresponds to the threshold between very poorly sorted and poorly sorted deposits. This overlaps with the upper sorting threshold for hyperconcentrated flow, which is 2.7 Φ, although in general the sorting values lie below 2 Φ.

Table 7.10 Results of grain size analysis of selected Onetapu Formation lahar deposits

Onetapu member	Site	Lithofacies identifier	Mean (Φ)	Sorting (Φ)	Skewness	Kurtosis	% Z & Cl
Onj	Q	4b	1	2.7	-0.35	1.16	10
	R	3b	0.9	2.6	-0.13	0.98	13.6
	S2	3b	0.25	2	0.13	1.22	6.4
	X	4b	1.9	1.8	0.14	0.85	15.7
Onh	E1	2b	-4.3	3	0.68	1.75	3.5
	G8	3c	-1.1	3.3	-0.1	0.9	4.4
	H2	3c	-1.4	3.1	0.38	0.74	7.1
	Q	3b	-0.2	2.3	0.43	0.38	8.2
Ong	E2	4b	0.76	1.8	-0.02	1.06	6
	H2	4b	1.1	1.8	-0.1	1.2	6.5
	L1	4b	0.5	2	0.14	0.08	10
	L1	4b	1.1	1.9	-1.3	1.3	7
	P	4b	-0.4	2.2	0.14	0.54	3
Onf	E2	3b	-3.9	2.9	0.5	1.12	2
	G6	3c	-2	3.8	0.1	0.68	7
	H2	3d	-3.4	3	0.75	1.4	5
	L1	2a	-5.3	2.3	0.7	2.3	3
	P	3a	-3.2	3.3	0.58	1.53	5

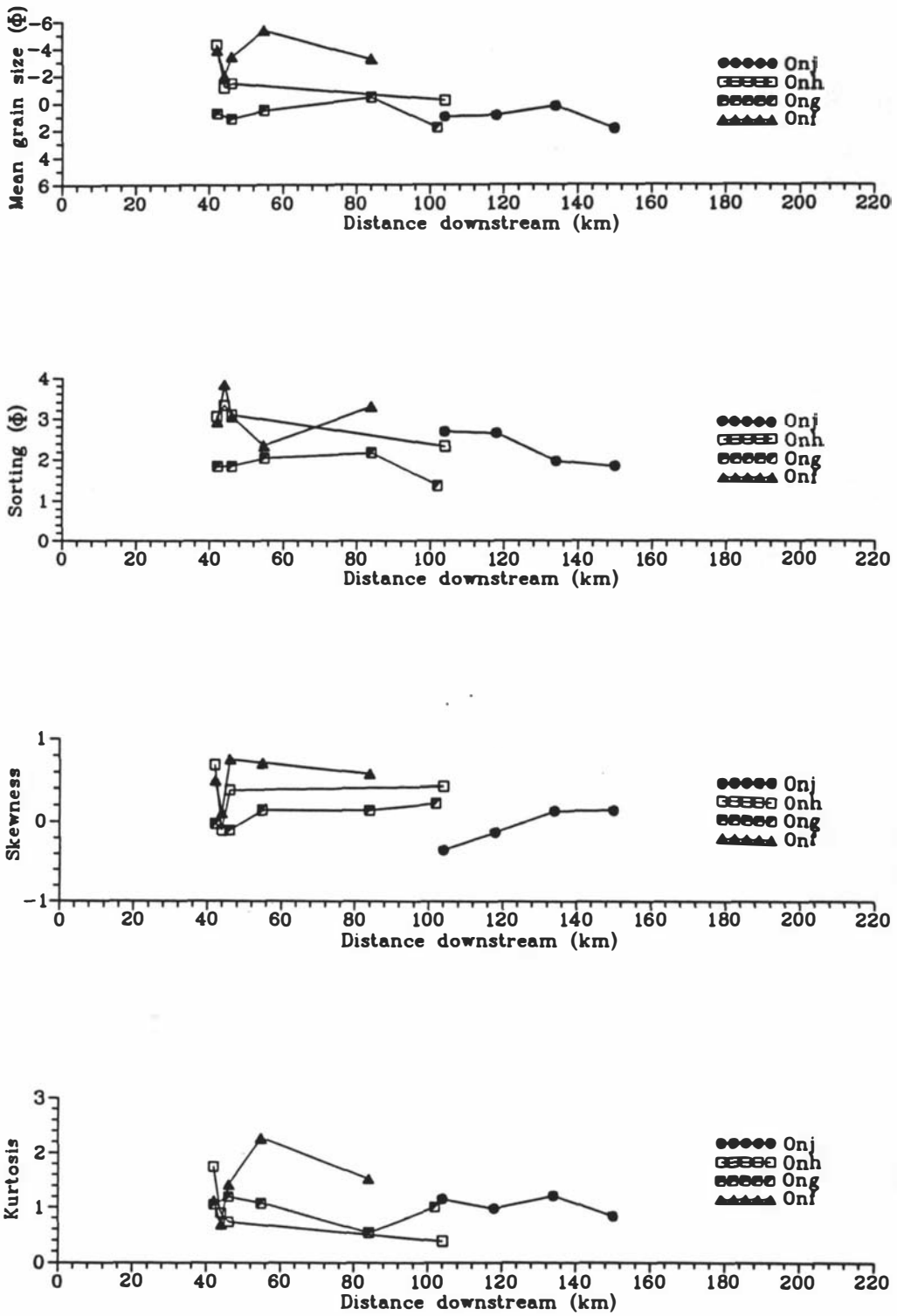

Figure 7.10 Downstream variations in sedimentological characteristics for Onetapu Formation members Onj, Onh, Ong and Onf.

Sorting values for deposits sampled from Onf ranged from 2.3 Φ to 3.8 Φ, which correspond to lithological evidence indicating that it was emplaced exclusively by debris flow processes (see Tables 7.6 and 7.9). The lowest sorting threshold value (2.3 Φ) applies to analysis of Onf at L1, where the deposit is bouldery, with a mean grain size of -5.3 Φ, and here is interpreted to have been emplaced by highly competent debris flow. The grain size distribution is highly peaked around this mean, but is strongly positively skewed, reflecting that, although the deposit contains abundant coarse-grained clasts, it still contains a large proportion of finer-grained sediment.

Although deposits in this member have a distinct muddy appearance the percentage of silt and clay they contain is < 10 % (see Table 7.10). No marked downstream trends in grain size distribution were observed.

Grain size distribution in samples taken from member Onh, the lithology of which was observed to grade from debris flow downstream to hyperconcentrated flow, show both a reduction in mean grain size and standard deviation with distance. Although a sample of hyperconcentrated flow lithology was not taken (in this member) the most downstream deposit sampled had a sorting value of 2.3 Φ, which is below the upper sorting threshold of 2.7 Φ for hyperconcentrated flow deposits (this study).

Analysis of deposits in member Onj indicate a reduction in mean grain size and standard deviation with distance downstream. At Section Q (100 km downstream), where Onj is interpreted to have been emplaced by hyperconcentrated flow, the sorting value is 2.7 Φ, although mean clast size is only 1 Φ. Outsize clasts were observed in this deposit, and the presence of these in the sample analysed is the explanation for the high sorting value. At Section T, (137 km) the sorting value is 2 Φ, below the threshold for hyperconcentrated flow. At this locality the lithology still resembles a debris flow deposit, however at Section X, 150 km downstream, the lithology shows features associated with hyperconcentrated flow, and this confirmed by a sorting value of 1.8 Φ.

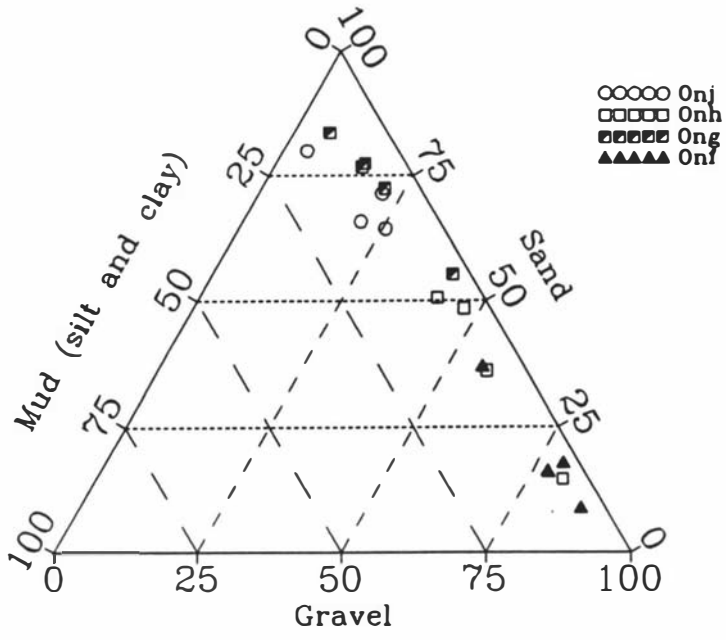

Figure 7.11 Ternary diagram showing ratio between gravel, sand, and mud for samples of selected Onetapu Formation lahar deposits

The ternary diagram in Figure 7.11 plots the percentage of gravel, sand and mud for each sample analysed. The percentage of mud is low in each sample. However all samples of Onf plot in the lower right sector, revealing the very coarse nature of this deposit. The ratio of gravel to sand increases in Onh and Onj, this increase corresponding to the downstream sedimentological trends outlined in this and the previous section.

7.5.2.3 *Discussion*

One of the most thorough examinations of the grain size distribution of deposits from lahars is presented by Scott (1988a) based on analysis of samples collected following emplacement of lahar deposits which resulted from the the 18 May 1980 eruption of Mount St. Helens. Scott describes a sequential downstream variation in grain size parameters which characterised a facies change from debris flow to hyperconcentrated flow with distance from source.

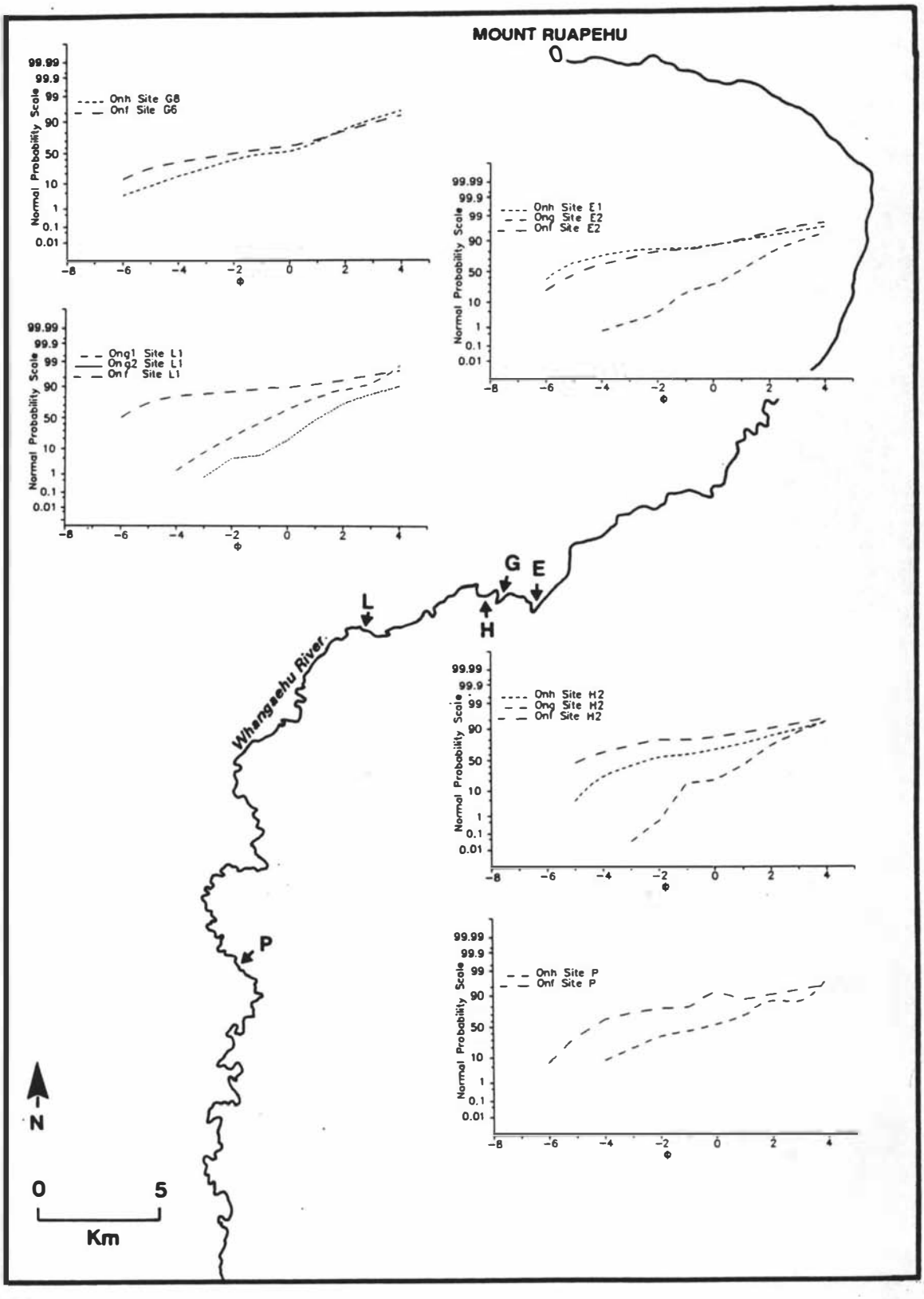

Figure 7.12 Probability curves for cumulative percentage of particle size ranges from Onetapu Formation members Onj, Onh, Ong and Onf.

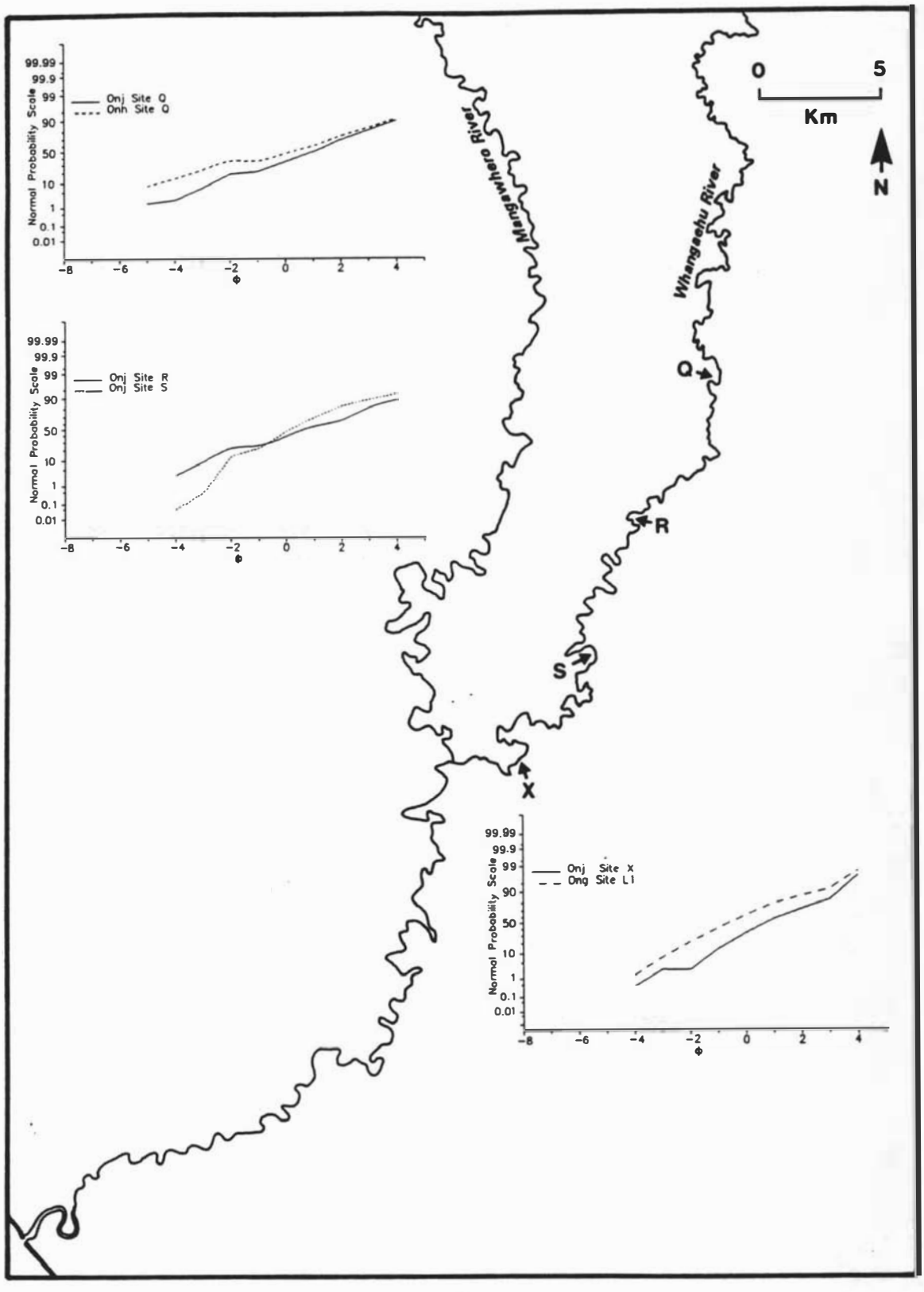

Figure 7.13 Probability curves for cumulative percentage of particle size ranges from Onetapu Formation members Onj, Onh, Ong and Onf.

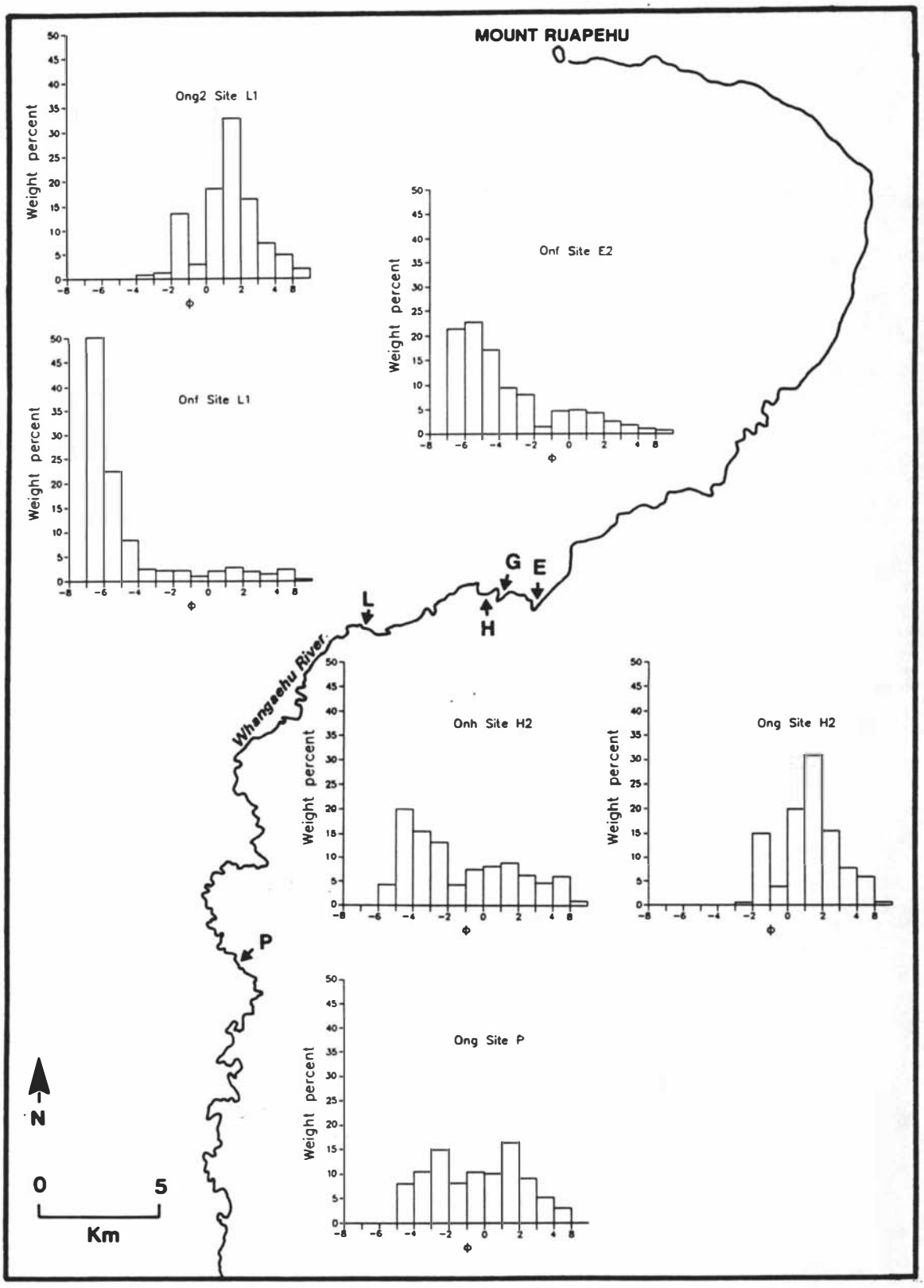

Figure 7.14 Histograms of weight percentages for particle size ranges from samples of Onetapu Formation members Onj, Onh, Ong and Onf.

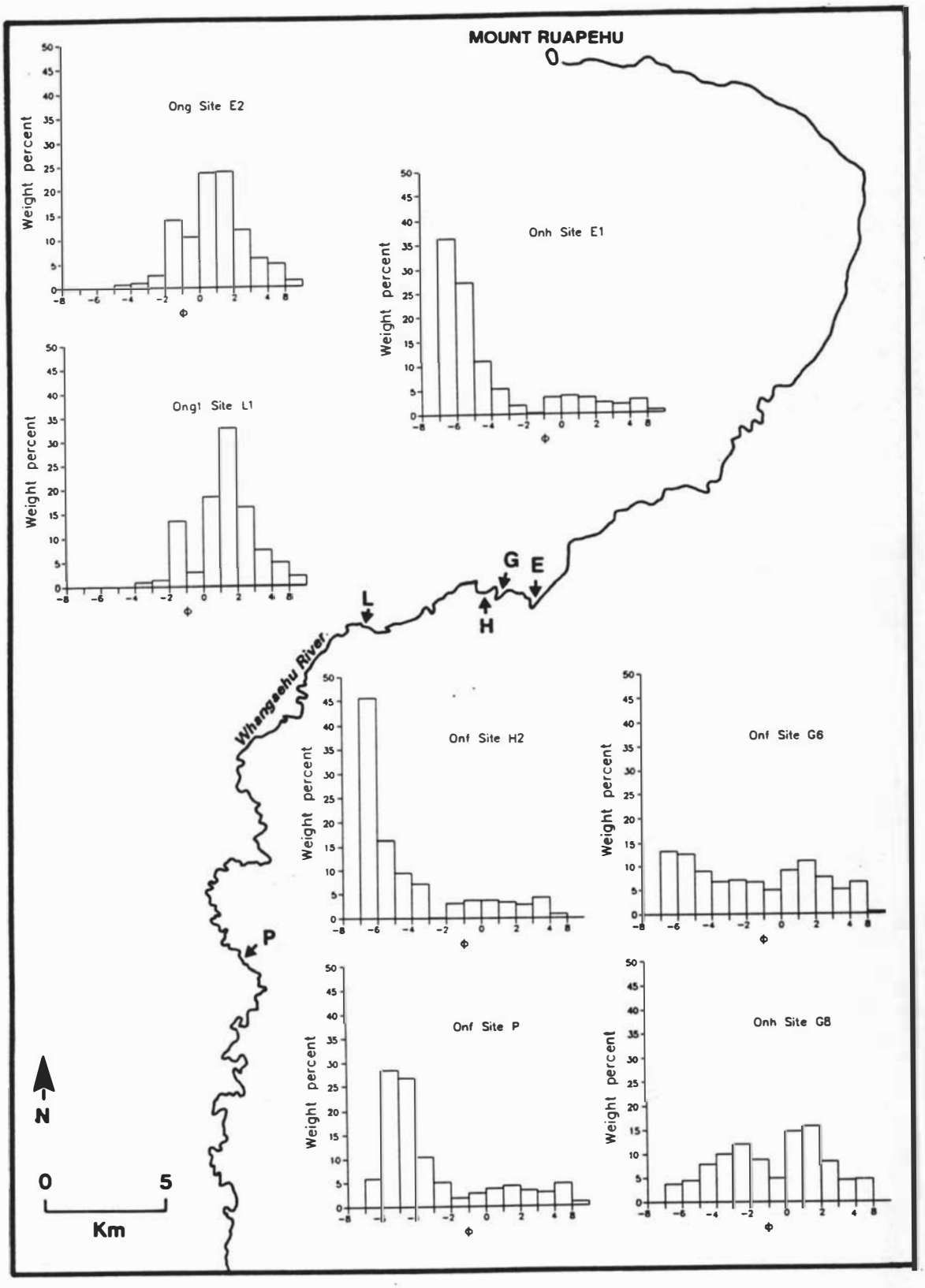

Figure 7.15 Histograms of weight percentage of particle size ranges for samples of Onetapu Formation members Onj, Onh, Ong and Onf.

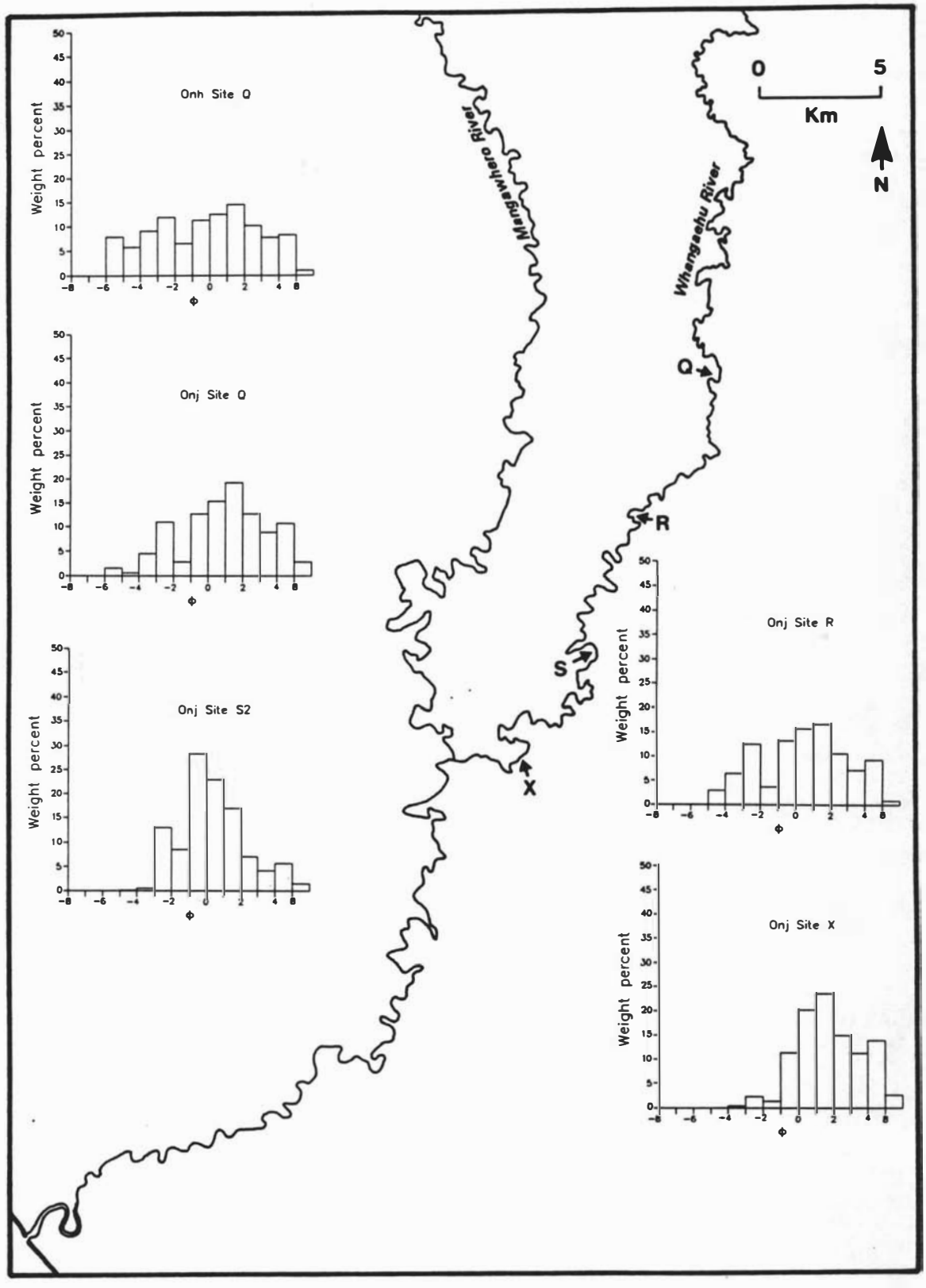

Figure 7.16 Histograms of weight percentage of particle size ranges for samples of Onetapu Formation members Onj, Onh, Ong and Onf.

This supports the evidence presented by Pierson and Scott (1985) who report the transition from debris flow to hyperconcentrated flow in a lahar following the 19 March 1982 eruption of Mount St. Helens.

Based on the evidence presented by Scott (1988a) the general downstream trend in grain size characteristics for deposits from the North Fork lahar and the South Fork lahar is an improvement in sorting values and a reduction in mean grain size. He proposes a hypothetical lower sorting threshold of 2 Φ, marking the transition from very poorly sorted to poorly sorted sediment, corresponding to transformation from debris flow to hyperconcentrated flow. This was determined from observations of lahar flow characteristics during the lahar event, and lithofacies analysis of the resultant deposits.

An investigation of deposits from selected Onetapu lahars reveals a similar pattern of events in two members, Onh and Onj. No transformation was observed in member Ona or Onf. Two possible explanations for this are proposed. Firstly, the matrix component in both these members is distinctly muddy in appearance and this is implicated in maintaining cohesion, and preventing flow transformation, within the debris flow right up until deposition. However, member Onj also has a muddy matrix and underwent transformation, which would not support this proposal. Besides, member Onf is interpreted to have been emplaced largely by non-cohesive debris flow. Further to this argument, the percentage of silt and clay in members Onf, Ong and Onh are similar and fall within the range 2 - 10 %, but are lower than the 6.4 - 15.7 % for Onj (see Table 7.10). Secondly, deposition from the more fluid Onf lahar, as interpreted from the dominance of normally graded beds in its deposits, may have occured more rapidly, bypassing any intermediate transition phaze (*i.e.* transformation from debris flow to hyperconcentrated flow). However, there are contradictions to this second explanation, as member Ona, which did not transform, was emplaced largely by cohesive debris flow, although the thinness of deposits in Ona may have prevented the recognition of normally graded beds. The second explanation is preferred, but this remains an area where further stringent sedimentological and lithological analysis of deposits may provide a more rigo rous solution.

Additionally, with regard to determining critical sorting thresholds for different lithological groups, it is apparent, from the analysis of Onetapu Formation lahar deposits, that the transition from debris flow to hyperconcentrated flow is accompanied by an improvement in sorting and a reduction in mean clast size. However the threshold between the two types, in terms of critical sorting values, is not so strictly defined as that determined by Scott (1988) for Mount St. Helens lahars.

7.6 POST-DEPOSITIONAL DEFORMATION OF ONETAPU FORMATION LAHAR DEPOSITS

Observations of water-escape structures in sandy diamictons of the Onetapu Formation resulting from post-depositional deformation reveal the potential for liquefaction and fluidization of saturated lahar deposits. Features observed are dish and pillar structures, water escape dykes, fluidization channels, and intrusion features which, in one instance, resulted in a sand volcano (see Plates 7.5-11). Lowe and LoPiccolo (1974) and Lowe (1975) present overviews describing the occurrence and probable cause of the deformation features listed. These papers, complemented by Youd (1973) who specifically addresses the cause rather than the result of sediment deformation, form the basis for the discussion that follows.

Plates 7.5-11 depict the development of water escape structures, determined from evidence of processes revealed in deposits examined at different localities in the upper and middle catchment of the Whangaehu River. Plate 7.5 depicts an undeformed bed. The coarse sandy nature of the deposit and the horizontal stratification are both characteristic features of hyperconcentrated flow deposits (see Table 7.4). Plate 7.6 depicts the onset of deformation in a similar deposit (this is a different deposit at a different locality, although both are hyperconcentrated flow deposits observed in the Manutahi Formation on the Rangipo Desert during an unofficial field trip). Water escaping through the sediment has entrained particles which are forced up into the overlying beds via fluidization channels. In this example water and sediment escape may be occurring at a weak point, indicated by the "pinching in" of the overlying coarser-grained bed. Fluidization appears to have been arrested early in the process and

the sand pillar (indicated by an arrow) appears to have been "frozen" at some stage early in its development. In Plate 7.7 the continued movement of water and entrained sediment along well-defined "escape routes" (indicated by arrows) has interrupted and upturned the beds across which the pillars have cut, resulting in grossly exaggerated dish and pillar structures. The fine grained layer mantling the deposit represents the entrained sediment which has been ejected out onto the surface of the deposit (and subsequently buried by the overlying debris flow).

In Plate 7.8-10 the scenario depicting development of water and sediment escape structures is revealed in sedimentological features exposed in a single deposit at one locality. This deposit is correlated to the deposit depicted in Plate 7.7. In Plate 7.8 early signs of the onset of deformation are the presence of dish and pillar structures. Dishes occur as more compacted unfluidized sediment settles down through the upward flowing mixture of fluidized water and sediment (Lowe and LoPiccolo, 1974; Lowe, 1975). Less permeable horizons act as partial barriers to vertical flow, forcing this to become horizontal until vertical escape is possible. Fine sediment grains are filtered out and concentrated in pore spaces, where water movement is likely to be much slower. These fine-grained horizons mark the basal margins of dishes. Small scale pillars develop at their margins. Accelerated water escape leads to the formation of pipes or chimneys (indicated by arrows in Plate 7.9). These are unrelated to dish structures (other than by genetic association) and probably occur within zones of high permeability (Lowe, 1975). In this deposit these have truncated and disrupted the pre-existing dish and pillar structures. The accelerated escape is not a gentle process and, at the contact between deposits depicted in Plate 7.10, water and sediment have erupted into overlying beds resulting in a sand volcano. This has destroyed the pre-existing sedimentary features which, in this case, included dish and pillar structures.

7.6.1 *PROBABLE CAUSES OF DEFORMATION*

Seepage forces, resulting from upward percolating pore water, are implicated in causing liquefaction of saturated sediment (Youd, 1973). In Onetapu deposits water escape features are confined to the upper portion of hyperconcentrated flows, indicating that deformation occurred as a result of seepage from lower into upper zones of the deposit, increasing pore water pressures to a critical level above which liquefaction and fluidization occurred. Artesian pressure and seismic compaction have been suggested as causing this upward seepage (Youd, 1973). In Onetapu hyperconcentrated flow deposits overburden either from the weight of the actual deposit, or inundation by subsequent lahars, is considered responsible for the deformation features observed. Hyperconcentrated flow deposits are porous and poor retainers of water, and it is likely that the overburdening of those deposits which exhibit evidence of deformation occurred while they were still saturated, *i.e.* closely following deposition. Fine-grained sediment preserved between the underlying, deformed hyperconcentrated flow and overlying debris flow in Plates 7.7 and 7.8 probably resulted from the forced ejection of water and entrained sediment through and out onto the surface of the flow, this occurring as a result of overburdening by the deposit itself. In Plate 7.10 water and sediment escape features extend into the overlying debris flow deposit (Onh), implying that the upper unit was emplaced shortly after the underlying deposit (Ong3)[1] and may have compounded the fluidization process, accelerating water escape, and promoting the development of larger scale deformation structures, *e.g.* the sand volcano identified in Plate 7.10.

Deformation structures are also observed in Whangaehu Formation sandy diamictites (see Plate 7.11) and Donoghue (1991) recognized dish and pillar structures in Tangatu Formation sandy diamictons on the southeast Mount Ruapehu ring plain.

[1] *That these two lahars were emplaced closely in time is used as evidence for determining the upper age constraint on Onetapu member Ong3 (see this chapter, section 7.4.6)*

7.7 CALCULATED VELOCITIES AND DISCHARGES FOR PREHISTORIC LAHARS

A lahar travels downstream under the force of gravity. When it encounters an obstacle, *e.g.* a hill or a meander bend it will ride up onto or around this obstacle. The height to which it rises depends on the velocity at which the lahar is travelling. By examining the cross-sectional distribution of resultant deposits at places where they have met an obstruction of this type it is possible to calculate the velocity of the lahar. Surveys were conducted across the Whangaehu River channel at selected locations in the catchment to enable construction of cross-sections for selected Onetapu Formation deposits. From this information, estimates of mean velocity and discharge rate have been calculated for the original lahars. Sites were selected on the basis of the likelihood of having preserved deposits demonstrating a height difference at a marked change in channel orientation, *i.e.* on a meander bend. Also sites were chosen where at least two prehistoric events could be correlated to both sides of the river. Two different methods of calculating velocity were attempted and the results compared to estimated velocities for historical lahars. Discharge rates were determined by multiplying the cross-sectional area of each deposit by the velocity at which it was travelling.

7.7.1 *CALCULATING VELOCITY FROM SUPERELEVATION*

The two methods used to calculate the lahar velocities were based on models used for rockslides (Crandell and Fahnestock, 1965) and for debris flows (Takahashi, 1982; Pierson and Scott, 1985). The method proposed by Crandell is based on a simple transference of the kinetic energy of the flow to potential energy of the deposit when it came to rest. The velocity of the flow is defined as a function of the amount of energy required to overcome and gain elevation against the force of gravity and is expressed by the formula:

$$v=\sqrt{2g\Delta h} \qquad (7.1)$$

where v = velocity

g = acceleration due to gravity

Δh = the difference in height of the deposit on opposite sides of the channel

Pierson and Scott (1985) adopted the method for calculating velocity proposed by Nakamura in 1926, and discussed by both Johnson (1970), and Apmann (1973). This method is based on the fundamental characteristic displayed by fluids in a bend in an open channel whereby the surface of the fluid rises on the outside bank of the meander, and lowers on the inside bank (Apmann, 1973). The centrifugal forces which operate to deform the flow surface are determined by the radius of curvature of the meander bend. According to this hypothesis velocity is expressed as:

$$v = \frac{\sqrt{g \Delta h r_c}}{b} \qquad (7.2)$$

where r_c = the radius of curvature of the channel

b = the width of the channel

Lahar deposits left mantling the channel banks would reflect the superelevation of the flow, and both Crandell and Fahnestock (1965) and Pierson and Scott (1985) were able to calculate velocities for rockfalls and lahars respectively. Both recommend that the values estimated be treated as minimum velocities for the flow because energy is likely to be lost in overcoming frictional forces at the flow boundaries. Pierson (1985) calculated the travel time for lahars following the 19 March 1982 eruption of Mount St. Helens according to Equation 7.2 and found that the calculated travel times were within 15% of recorded travel times. Vallance (1986) applied both methods to *c.* 5,200 year old Trout Lake Mudflow at Mount Adams, Washington State, U.S.A. The velocities he calculated using Equation 7.1 and 7.2 were very similar (22 m s^{-1} and 23 m s^{-1}, respectively).

7.7.2 *SITE LOCALITIES AND DESCRIPTION*

Topographical and geological cross-sections were surveyed at four localities (see Figures 7.18-21) to determine rheological parameters for a range of Onetapu Formation lahar deposits. The locations of Sites E, H, L and S are shown in Figure 7.17 (and see stratigraphic columns in the Appendix). The cross-sectional area for lahar deposits at each site was determined by plotting surveyed topographic and stratigraphic data onto a constructed cross-channel profile using Versacad, a surveying software package.

Minimum, intermediate and maximum cross-sectional areas of the lahar deposits were calculated using Versacad. The former value is a measure of the distribution of the deposits that remain. The intermediate value is a measure of the volume of the deposits that remain, plus a measure of the cross-channel area from the top to the bottom of the deposit[2]. The maximum value is an extension of this distribution to include both the deposits and the area of the river channel up to the lahar deposit profile across the river. These values would not take into account degradation of the channel since the lahar event, so would overestimate the cross-sectional area. However because the lahar deposits surveyed are all less than 1,800 years old, such an over-estimate is considered slight (for older Pleistocene lahars it is likely that there would be much greater estimate errors).

In Figures 7.18-21 the lower sketch depicts the true, unexaggerated cross-section, including the survey data on which the drawings are based. In the upper sketch the vertical scale has been exaggerated by 500 % which depicts more clearly the stratigraphy at each locality.

[2]*A planar surface to the flow is assumed in this cross-sectional distribution. In reality debris flows generally have convex flow surfaces. However, as they flow around bends their surfaces become concave (T.C. Pierson, pers comm., 1992).*

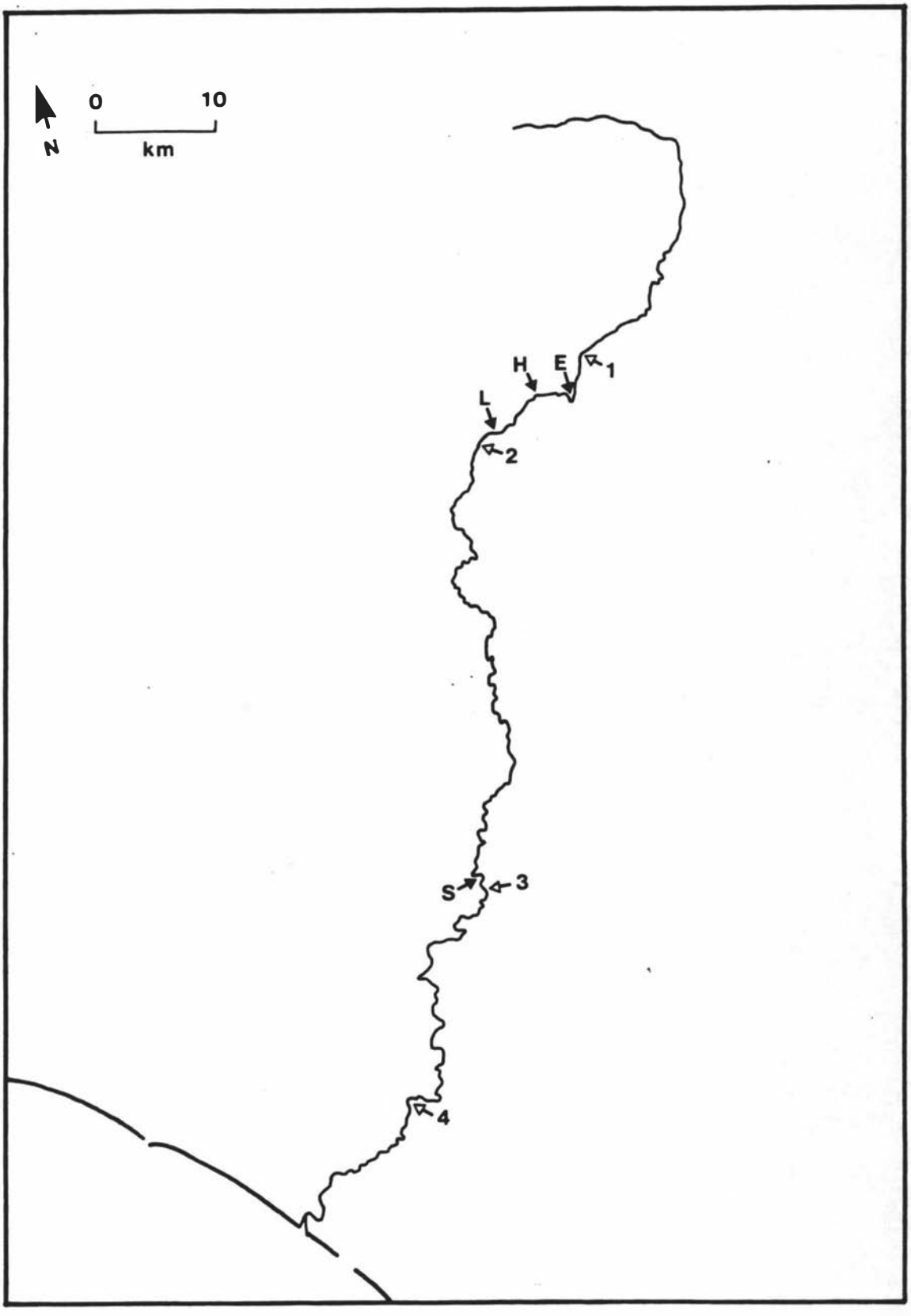

Figure 7.17 Localities where velocities for prehistoric Onetapu lahars were calculated (Sites E, H, L and S), and where velocities were gauged or estimated for historic 1953 and 1975 lahars (Sites 1 - 4)

7.7.2.1 *Site E*

At Site E (see Figure 7.18, and see Plate 7.12), situated approximately 42 km from Crater Lake, Onetapu lahars One, Onf, Ong, Onh, Oni, Onj and Onk are exposed in a now disused metal pit. The deposits occupy two channels, one approximating to the present channel of the Whangaehu River, and another further west, which has been cut into Taupo Ignimbrite. At this locality the River swings sharply west under steep bluffs of Tertiary siltsone and limestone. Here Onetapu members Ong, Onh and Onj have washed up onto the opposite bank to the metal pit and mantle a low lying terrace comprising Taupo Ignimbrite.

7.7.2.2 *Site H*

Site H (see Figure 7.19) is situated approximately 4 km downstream from Site E, and 46 km from Crater Lake. Here three Onetapu lahar deposits, Onf, Ong and Onh, are exposed in a track cutting on the east bank of the River, where the lahar flowed up into a tributary stream and spilled out onto an older Tangatu Formation terrace. On the west bank these deposits mantle a low-lying terrace. The distribution of Onetapu lahars on this terrace was extrapolated from an exposure of their deposits revealed in an offal pit excavation. The low lying terrace abuts another older surface and coverbeds overlying the older terrace indicate that its surface had not been inundated by lahars in at least the past 5,000 years.

7.7.2.3 *Site L*

Site L (see Figure 7.20 and Plate 7.13) is located at an important bridging point over the Whangaehu River, the upper Whangaehu Bridge and is approximately 55 km from Crater Lake. Here only two Onetapu members are correlated to both sides of the River, Ong and Onh. On the west bank of the River, members Ona, Onf, Onj and Onk are also exposed. Onetapu lahar deposits on both banks of the River have spilled over onto the older Tangatu surface.

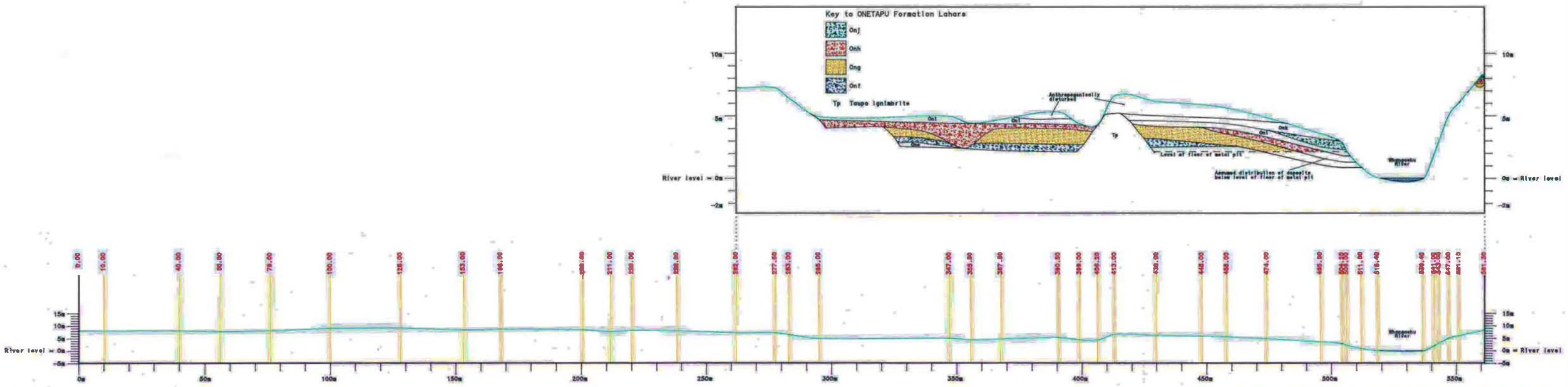

Figure 7.18 Surveyed cross-section of Onetapu Formation lahar deposits at Site E (see Figure 7.17).

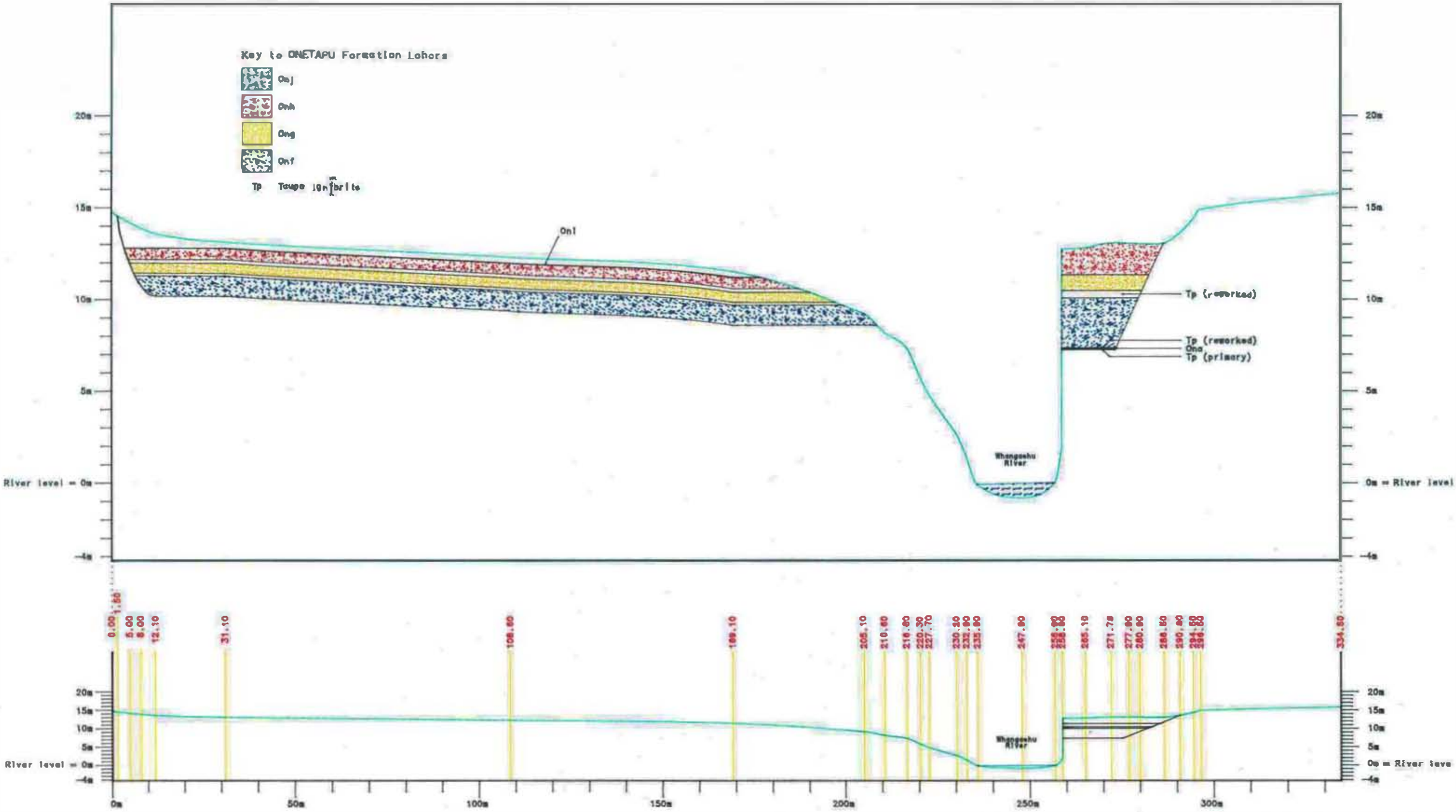

Figure 7.19 Surveyed cross-section of Onetapu Formation lahar deposits at Site H (see Figure 7.17).

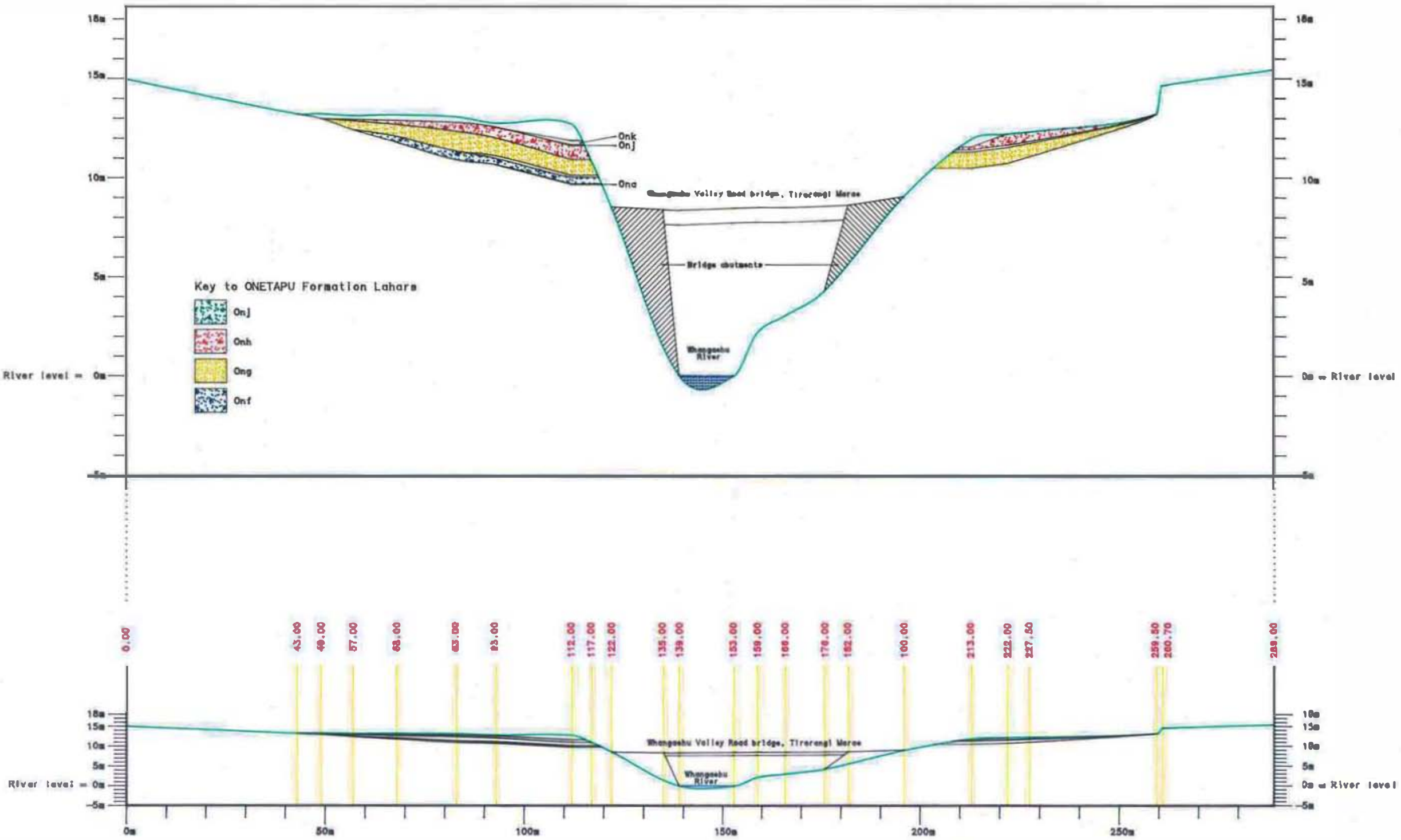

Figure 7.20 Surveyed cross-section of Onetapu Formation lahar deposits at Site L (see Figure 7.17).

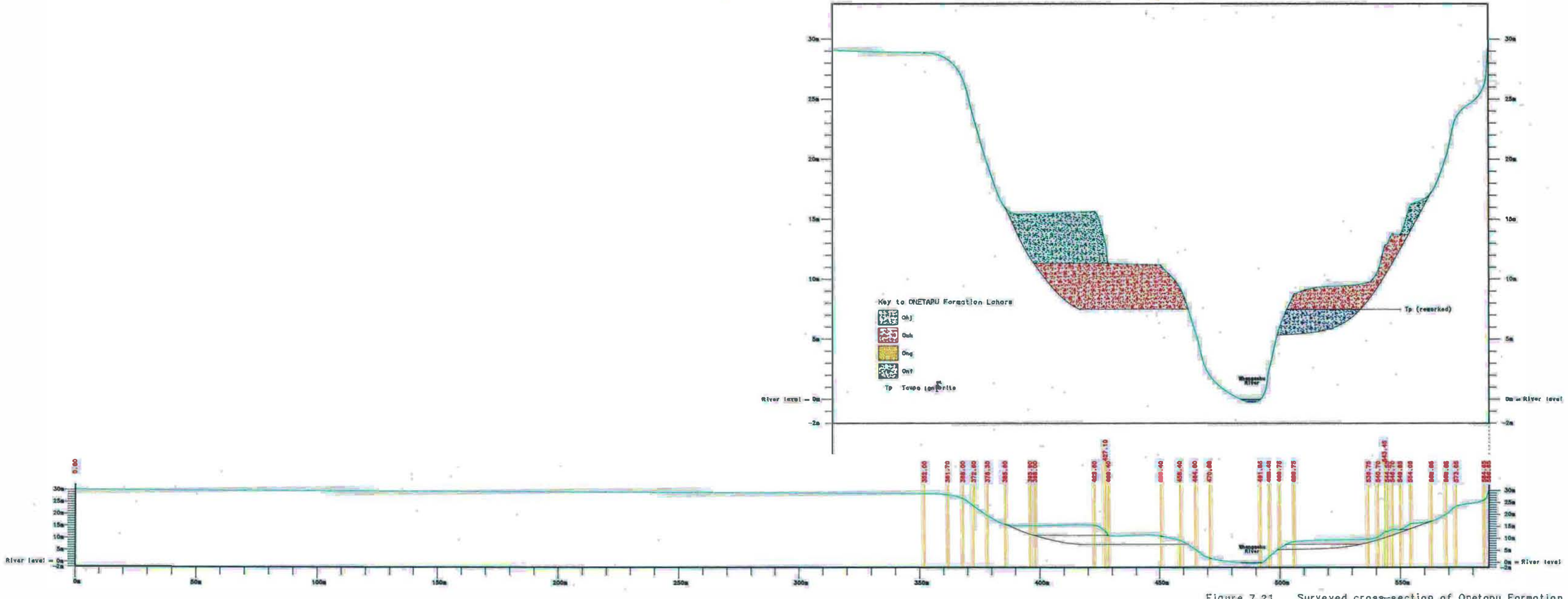

Figure 7.21 Surveyed cross-section of Onetapu Formation lahar deposits at Site S (see Figure 7.17).

7.7.2.4 *Site S*

Site S (see Figure 7.21, and Plate 1.3) marks the locality which was first investigated by Campbell (1973), when it was an actively quarried metal pit. This site is located approximately 137 km from Crater Lake. On the west bank of the River, Onetapu lahar deposits Onh and Onj form two low constructional terraces which abut an older higher surface comprising Tangatu Formation. On the east bank deposits abut bluffs cut into Tertiary mudstone. Member Onf was also observed at this locality, but only on the east bank of the river.

7.7.3 *RESULTS*

Calculated velocities for Onetapu lahars are presented in Figures 7.22- 23. In general the velocity of the prehistoric lahars falls with distance downstream and away from source, with the exception of Onh at Site S. Table 7.11 details the velocities measured from historic Onetapu lahars which occurred in the Whangaehu River in 1953 and 1975, and their decay in velocity downstream through the catchment is depicted in Figure 7.24. Localities where velocities were gauged or estimated are depicted in Figure 7.17.

Table 7.11 Gauged and estimated velocities (in m s^{-1}) for historic lahars in the Whangaehu River.

	Site 1	Site 2	Site 3	Site 4
	41 km	57 km	137 km	169 km
1953	4.9	ND	3.9	ND
1975	4.8	4.2	2.2	1.9

Comparing the values for historic lahars with those calculated for prehistoric lahars suggests that, at between approximately 40 and 50 km from source, lahars which emplaced Ong, Onh and Onj were travelling almost twice as fast as their historic counterparts. Prehistoric lahars at Site E were travelling between 5.7 and 9.1 m s^{-1}, and historic lahars between 4.8 and 4.9 m s^{-1}.

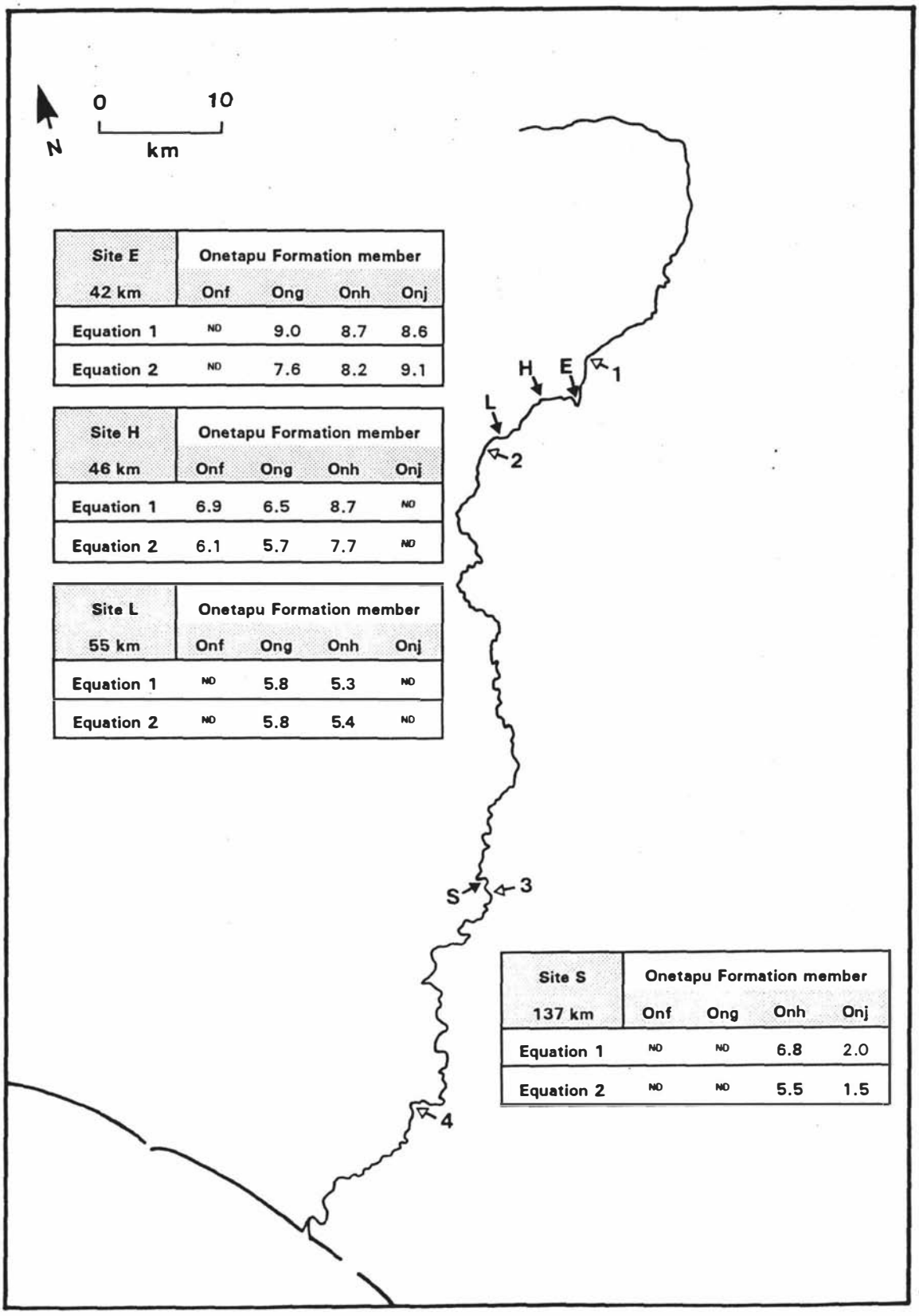

Site E 42 km	Onetapu Formation member			
	Onf	Ong	Onh	Onj
Equation 1	ND	9.0	8.7	8.6
Equation 2	ND	7.6	8.2	9.1

Site H 46 km	Onetapu Formation member			
	Onf	Ong	Onh	Onj
Equation 1	6.9	6.5	8.7	ND
Equation 2	6.1	5.7	7.7	ND

Site L 55 km	Onetapu Formation member			
	Onf	Ong	Onh	Onj
Equation 1	ND	5.8	5.3	ND
Equation 2	ND	5.8	5.4	ND

Site S 137 km	Onetapu Formation member			
	Onf	Ong	Onh	Onj
Equation 1	ND	ND	6.8	2.0
Equation 2	ND	ND	5.5	1.5

Figure 7.22 Calculated velocities (m s^{-1}) for prehistoric Onetapu lahars Onj, Onh, Ong and Onf at Sites E, H, L and S.

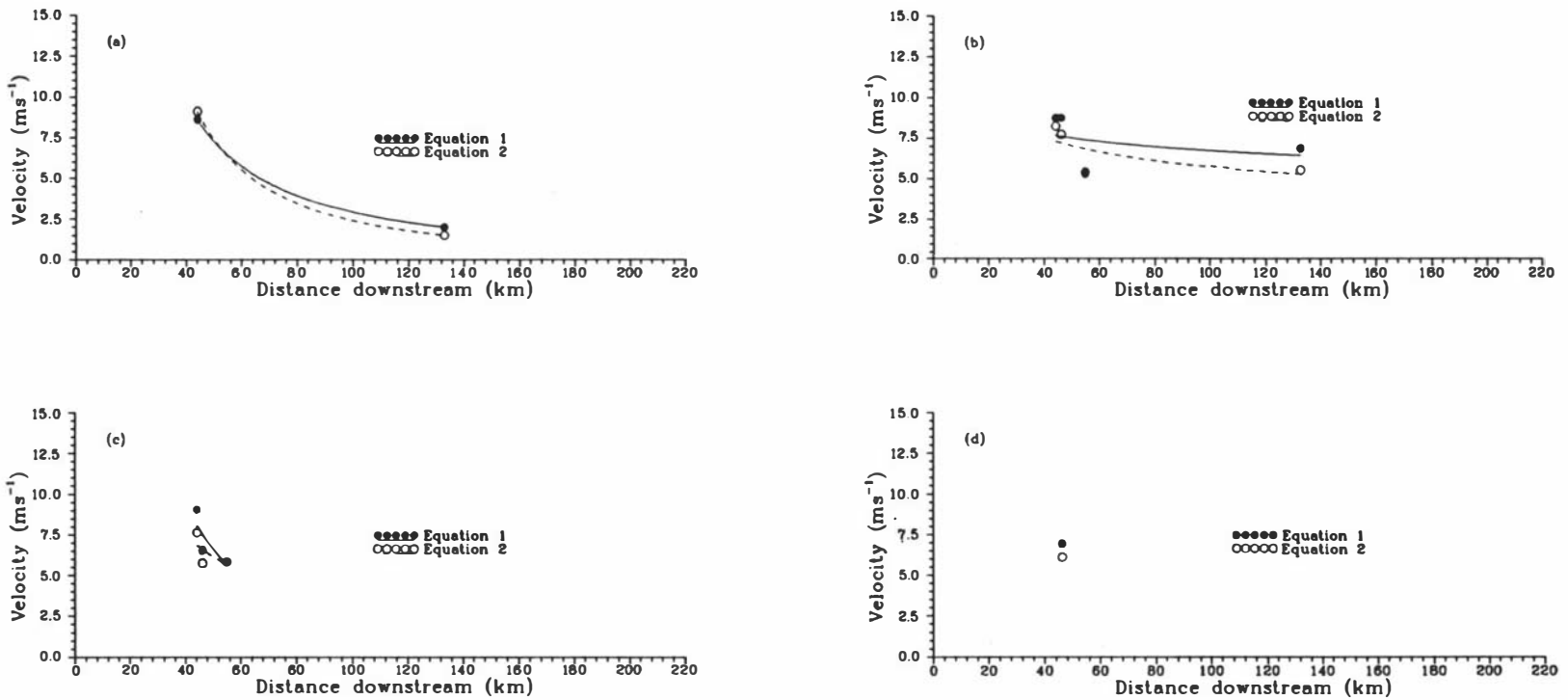

Figure 7.23 Downstream variation in calculated velocity (in $m^2 s^{-1}$) for Onetapu Formation members (a) Onj, (b) Onh, (c) Ong and (d) Onf.

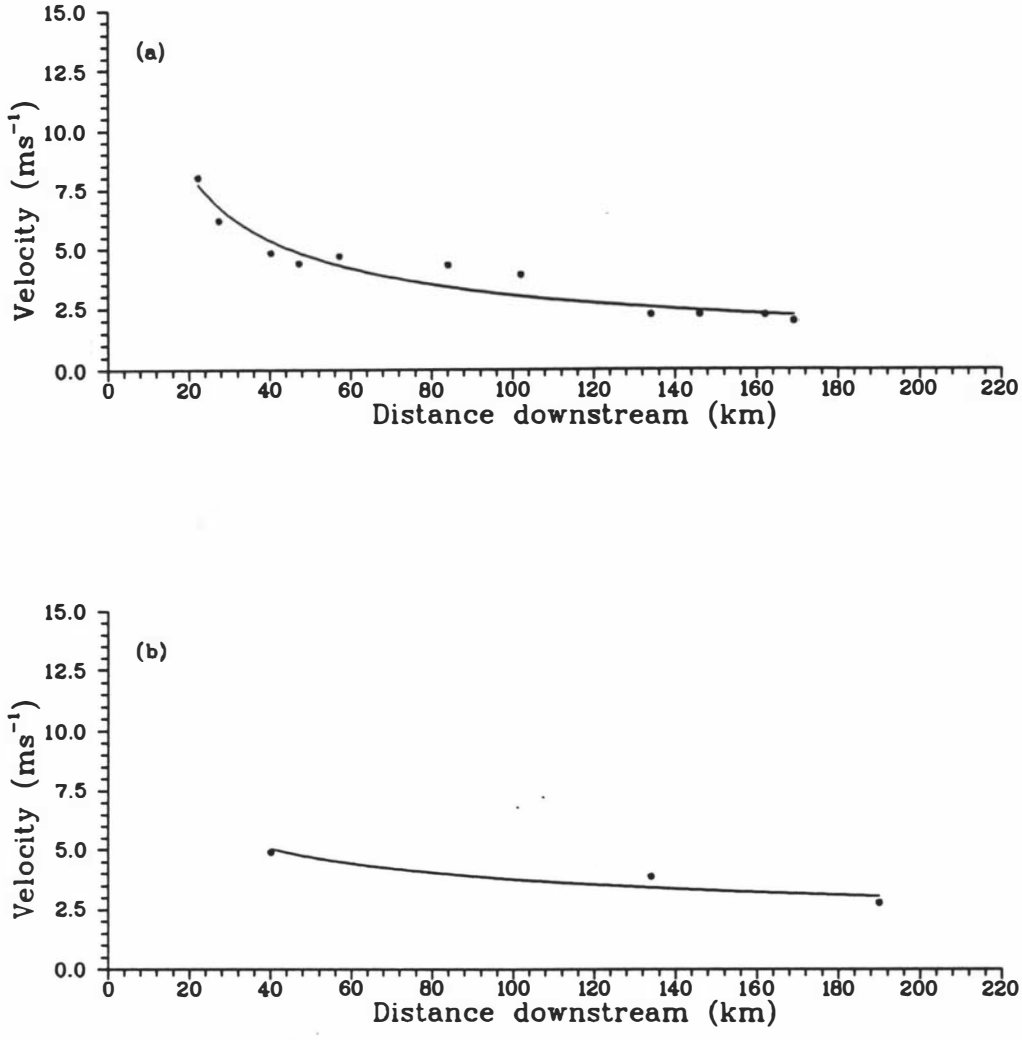

Figure 7.24 Downstream variations in velocity for historic (a) 1975 and (b) 1953 Onetapu lahars.

At 55 km from source, at Site L, prehistoric lahar velocity fell to between 5.3 and 5.8 m s^{-1}; at Site 2, 2 km further downstream the 1975 lahar was gauged to be flowing at 4.2 m s^{-1}. At 135 km from source, Site S, the velocities calculated for Onh was 6.8 and 5.5 m s^{-1}, and for Onj 2.0 and 1.5 m s^{-1}. The velocity estimated for the 1975 lahar at Site 3, 2 km downstream, was 1.9 m s^{-1}. The high velocity calculated for Onh, up to and over three times faster than Onj and 1975 lahars, may indicate that (1) this lahar had not lost velocity up to this point, or (2) that, at this locality, the calculated velocity has been overestimated. The implication of this latter explanation is that the measured difference in height for this deposit is too high, and degradation of deposits on the west bank of the River is the most likely explanation for the exaggerated **Δh**.

Minimum, intermediate, and maximum discharge rates calculated for prehistoric Onetapu lahars are presented in Figures 7.25-28, and are compared to discharges measured for 1953 and 1975 lahars (see Table 7.12 and Figure 7.29).

Table 7.12 Gauged and estimated discharges (in $m^3 s^{-1}$) for historic lahars in the Whangaehu River

	Site 1	Site 2	Site 3	Site 4
	41 km	57 km	137 km	169 km
1953	620	ND	ND	ND
1975	566	310	ND	121

The calculated minimum discharge rates are generally between 0.2 and 3 times those of historic lahars (not including Onh at Site S which, by virtue of the very high calculated velocity, has a calculated discharge 12 or 13 times that of the 1975 lahar). Intermediate discharge rates are between 0.6 and 12 times those of historic lahars, and maximum discharge rates are between 3 and 20 times higher. The trend for historic lahars was a systematic reduction in peak discharge rate and velocity with distance downstream. Discharge rate in prehistoric lahars is dependant on two variables, (1) their calculated velocity, and (2) the cross-sectional area of the deposits. In the former, with one exception, the trend is for a reduction in velocity downstream. Therefore the expected trend for prehistoric lahars would be a corresponding reduction in discharge downstream through the catchment. In general this relationship was NOT observed in prehistoric lahars. In Figure 7.27-28 downstream variations in minimum, intermediate, and maximum discharges, calculated using both velocity calculations, are plotted. At Site E both the minimum and intermediate discharges for Onj are below that of the 1953 and 1975 lahars at Site 1, but neither of these spilled over onto either of the surfaces (west or east bank) upon which Onj is found. Therefore, at this locality, it would be unreasonable to assume that the minimum or intermediate discharges calculated, approximate the actual peak discharge of the lahar.

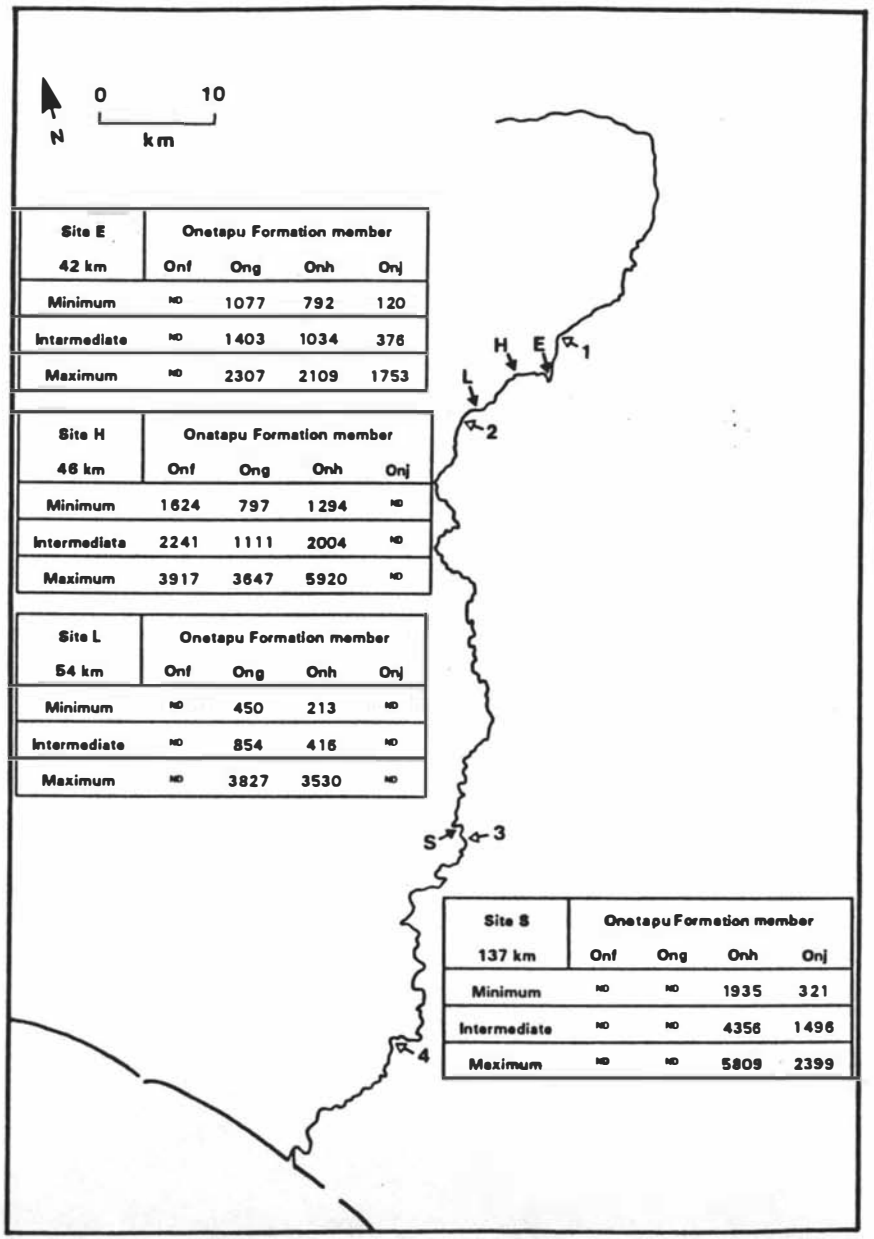

Site E 42 km	Onetapu Formation member			
	Onf	Ong	Onh	Onj
Minimum	ND	1077	792	120
Intermediate	ND	1403	1034	376
Maximum	ND	2307	2109	1753

Site H 46 km	Onetapu Formation member			
	Onf	Ong	Onh	Onj
Minimum	1624	797	1294	ND
Intermediate	2241	1111	2004	ND
Maximum	3917	3647	5920	ND

Site L 54 km	Onetapu Formation member			
	Onf	Ong	Onh	Onj
Minimum	ND	450	213	ND
Intermediate	ND	854	416	ND
Maximum	ND	3827	3530	ND

Site S 137 km	Onetapu Formation member			
	Onf	Ong	Onh	Onj
Minimum	ND	ND	1935	321
Intermediate	ND	ND	4356	1496
Maximum	ND	ND	5809	2399

Figure 7.25 Calculated discharge (in $m^3 s^{-1}$) for prehistoric Onetapu lahars members Onj, Onh, Ong and Onf. Discharge calculated using Equation 1

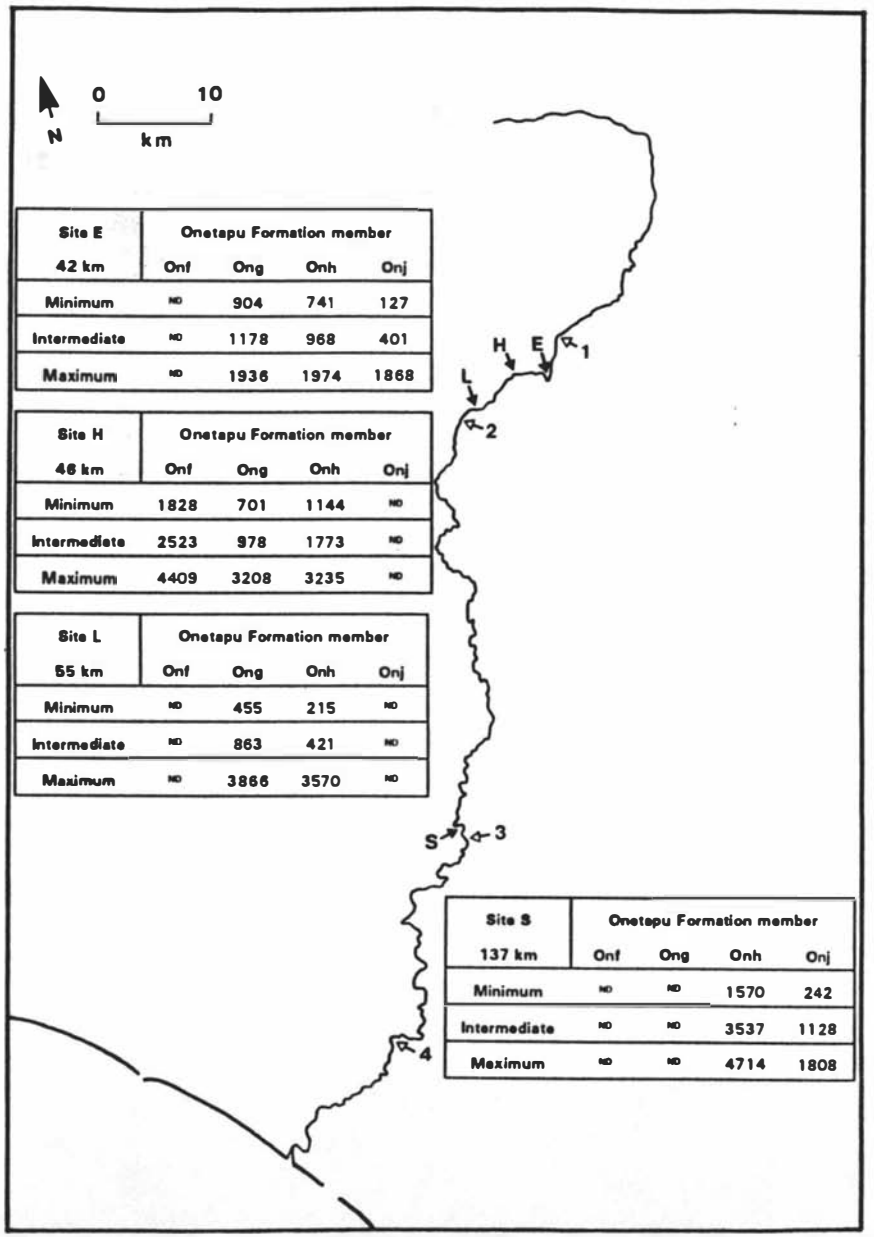

Site E 42 km	Onetapu Formation member			
	Onf	Ong	Onh	Onj
Minimum	ND	904	741	127
Intermediate	ND	1178	968	401
Maximum	ND	1936	1974	1868

Site H 46 km	Onetapu Formation member			
	Onf	Ong	Onh	Onj
Minimum	1828	701	1144	ND
Intermediate	2523	978	1773	ND
Maximum	4409	3208	3235	ND

Site L 55 km	Onetapu Formation member			
	Onf	Ong	Onh	Onj
Minimum	ND	455	215	ND
Intermediate	ND	863	421	ND
Maximum	ND	3866	3570	ND

Site S 137 km	Onetapu Formation member			
	Onf	Ong	Onh	Onj
Minimum	ND	ND	1570	242
Intermediate	ND	ND	3537	1128
Maximum	ND	ND	4714	1808

Figure 7.26 Calculated discharge (in $m^3 s^{-1}$) for prehistoric Onetapu lahars members Onj, Onh, Ong and Onf. Discharge calculated using Equation 2.

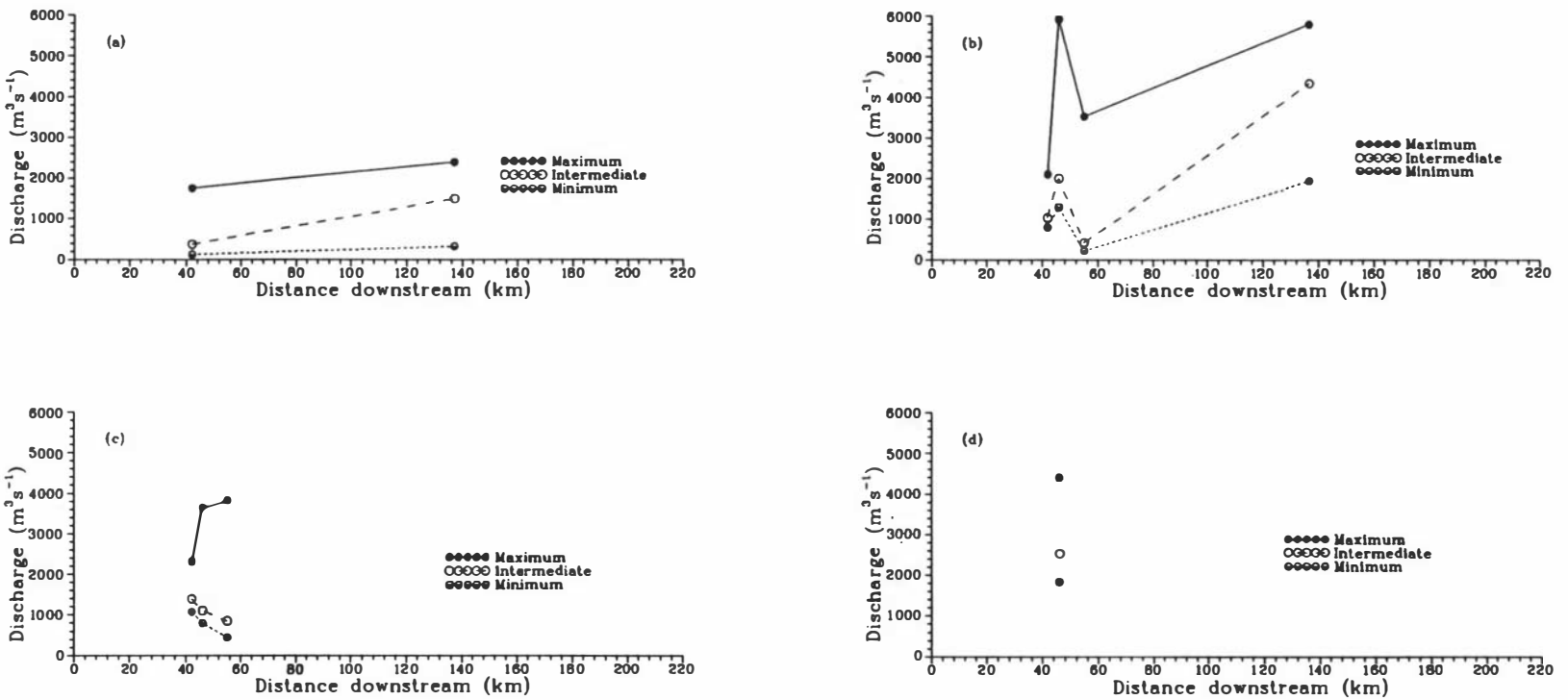

Figure 7.27 Downstream variations in calculated maximum, intermediate and minimum discharge for Onetapu members (a) Onj, (b) Onh, (c) Ong and (d) Onf. Discharge calculated using equation 7.2.

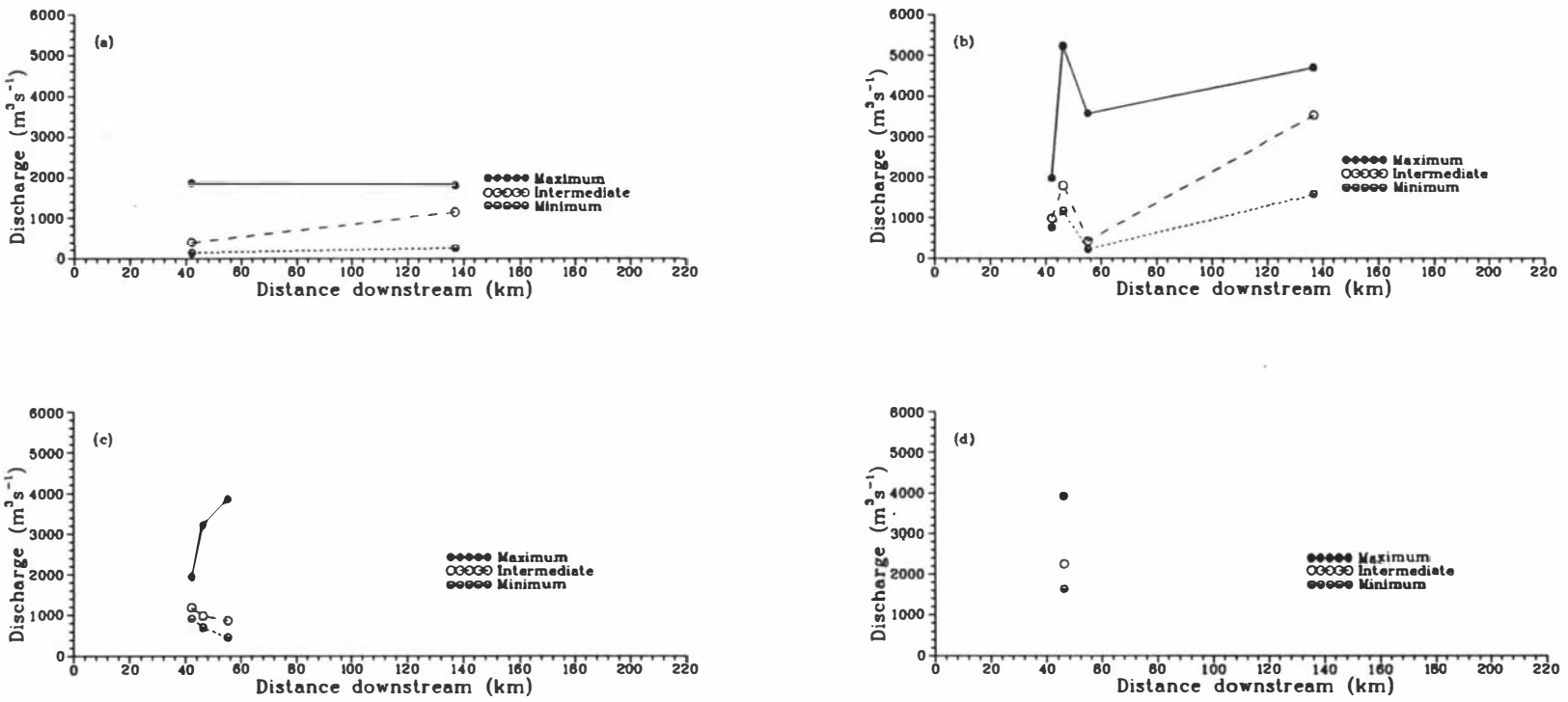

Figure 7.28 Downstream variations in calculated maximum, intermediate and minimum discharge for Onetapu members (a) Onj, (b) Onh, (c) Ong and (d) Onf. Discharge calculated using equation 7.1.

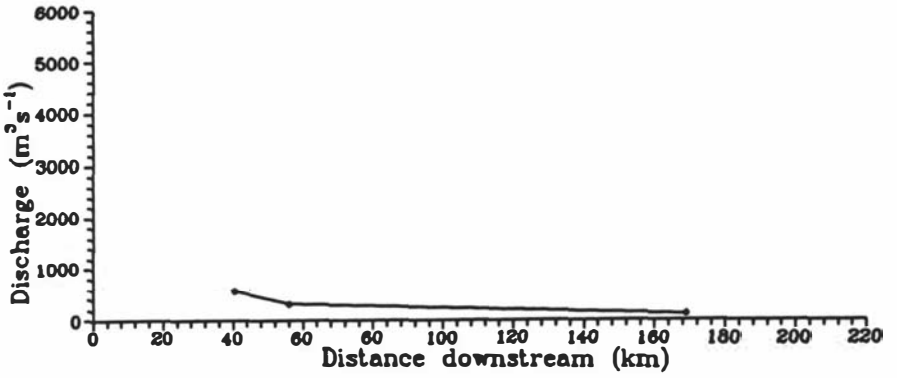

Figure 7.29 Downstream variation in discharge for the historic 1975 Onetapu lahar.

At Site H the maximum discharge for Onf, Ong, and Onh is much higher than their minimum and intermediate discharges. This may indicate that the maximum cross-sectional area measured is an overestimate of the actual distribution of the lahar. Maximum discharge at this locality for Ong is nearly twice, and for Onh nearly three times, as high as at Site E, which lends support to the argument that these values are overestimates. Minimum and intermediate values are similar for all members at Site H and here are considered to be more representative of the actual lahar discharge. At Site L the maximum discharge for Ong and Onh is again much higher than minimum and intermediate discharges, and the maximum disharges at Site E, and again is probably an overestimate.

At Site S there is considerable variation between minimum discharge for Onh and Onj. At this locality these discharges are between two and three times that of the 1975 lahar at the closest location where discharge for historic lahars was estimated, Site 4, which is 32 km further downstream. The maximum discharge is, however, up to 20 times higher for Onj, and 50 times for Onh. One process which would account for this increase in volume is "bulking up", through erosion into and incorporation of unconsolidated material in the bed and banks of the channel down which the lahar flowed. It is here considered that, at such a long distance from source (*i.e.* 137 km) and in a low grade section of the River this process cannot be invoked to account for the higher calculated discharge rates. Therefore in this lower region the minimum discharge rates are considered to be most representative of the actual discharge.

7.7.4 *DISCUSSION*

It is apparent that, in this study, there are problems associated with estimating discharge rate from calculated velocity of prehistoric lahars. These problems are likely to become exaggerated in older deposits when determining accurately the true cross-sectional area of the deposits, which have been buried or eroded, is more difficult.

However, it is unlikely that these methods would accurately model absolute velocity or discharge of lahars. Their application is of more value in quantifying events of different magnitudes. Therefore, for the purposes of this study, it seems likely that large prehistoric Onetapu lahars were at least twice, and may have been up to twenty times, as large as their historic counterparts.

7.8 PROPOSED MECHANISM OF EMPLACEMENT FOR ONETAPU FORMATION LAHARS

Deposits that comprise the Onetapu Formation occupy an interval of time marked by change on the volcanic edifice. The development of Crater Lake about 2,000 years ago (Donoghue, 1988, 1991) appears to have had a significant effect on the nature of laharic activity in the Whangaehu River. This section details the proposed mechanisms of emplacement for Onetapu Formation deposits, and pays particular attention to the impact that Crater Lake has had in this process. The existing semi-permanent resevoir of water on the summit region of Mount Ruapehu has increased the likelihood for lahar initiation. This has increased the risk from lahars because of the possibility of large lahars occurring in inter-eruptive periods.

In history two major lahar initiation processes have been reported, (1) lahars caused as a result of volcanic eruptions through the Crater Lake, and (2) lahars caused by catastrophic release of Crater Lake waters. Historic deposits are restricted, thin, and fine-grained, compared to their prehistoric counterparts. The lahars that resulted from these events were small compared with prehistoric Onetapu Formation lahars. Hence it has been difficult to compare the sedimentology of ensuing deposits with those from

prehistoric events in order to determine analogous triggering processes. There had to be, however, some process-oriented factor to account for the distinctive prehistoric Onetapu lahar deposits observed.

7.8.1 *ONETAPU FORMATION INFORMAL MEMBERS Ona, Onb AND Onc*

Onetapu Formation informal member Ona is thin, but widely distributed. It is here interpreted as a debris flow deposit. The muddy matrix and presence of hydrothermally altered clasts are characteristics also observed in the Mangaio Formation (Donoghue, 1991), which Ona overlies. Ona is here interpreted to represent deposits from a collapse from the same source rocks as the Mangaio Formation. Members Onb and Onc are similar in nature to Ona and probably represent later pulses from this same source.

7.8.2 *ONETAPU FORMATION INFORMAL MEMBER One AND Onf*

Members One and Onf are interpreted to have been emplaced by debris flow processes. Both lahar deposits have a high content of gravelly alluvium. Onf is one of the largest Onetapu lahars, and it is unlikely that a high rainfall event would supply enough water to trigger a lahar of the magnitude represented by the deposits in Onf. Examples of very large debris flows, the Osceola, Paradise, Round Pass and Electron mudflows, as sourced from Mount Rainier Volcano, U.S.A, are described (Crandell and Waldron, 1956; and Crandell 1963a, 1963b; Crandell, 1971). These were all considered to have been emplaced as a result of a collapse of hydrothermally altered sector of the Mount Rainier volcanic edifice. This interpretation was based on miner logical investigation of the mud component of the debris flows deposits and geomorphological interpretation of the volcanic edifice. The minerology indicated that the typically muddy matrix of all the debris flows contained minerals associated with hydrothermal alteration of rock. "Missing" portions of the volcano were interpreted to be the source area for the hydrothermally altered zones from which collapses may have occurred. The largest

debris flows associated with the 1980 Mount St. Helens eruption resulted from the catastrophic drainage of temporarily dammed lake water (Scott, 1988a, 1888b). The deposits from these lahars are observed to contain a high amount of gravelly alluvium. Scott (1988a) assigns a similar origin to gravelly Holocene debris flow deposits preserved in the geologic record at Mount St. Helens. These two mechanisms, (1) collapse of a hydrothermally altered sector of the volcano, and (2) catastrophic drainage of lake water, can be cited as possible triggers for the lahars which emplaced Onf. However neither Purves (1990) nor Donoghue (1991) present any evidence which would support a collapse of the Mount Ruapehu volcanic edifice at the time Onf was emplaced (*c.* 850 years B.P.). The muddy matrix, typical of both Onf and One, is similar to muddy Crater Lake sediments observed by this author, and is believed to have been sourced in these silts and clays. One and Onf are here considered to have been emplaced by lahars resulting from catastrophic drainage of Crater Lake waters on a vastly greater scale than that which triggered the 1953 lahar. Mineralogical investigations comparing the matrix of One and Onf with Crater Lake muds might confirm this hypothesis.

7.8.3 *ONETAPU FORMATION INFORMAL MEMBERS Ong1-3*

The pumiceous nature of the clasts in deposits of members Ong1, Ong2, and Ong3 indicates that the lahars incorporated quantities of pyroclastic material, either at the time of eruption or in post-eruptive intervals. At Section G2 and J1 Ong is overlain by a thin lens of andesite pumice which may represent reworking of one of the coarser members of the Tufa Trig Formation tephras. These tephras are dominantly fine-grained, and the coarse-grained pumice observed in Ong members is more likely to be remobilized Bullot Formation tephras. Members Ong1-3 are indistinguishable, and are here assumed to have a similar origin as eruption- and/or heavy rain-triggered lahars.

7.8.4 *ONETAPU FORMATION INFORMAL MEMBER Onh*

Member Onh represents deposits from probably the largest Onetapu lahar. Deposits from Onh are similar to those emplaced by historic lahars having a sandy rather than muddy matrix. Onh appears to have closely followed Ong3 in time. If these deposits represent eruption-triggered lahars then there may not have been time for large amounts of fine mud-sized material to have accumulated in Crater Lake before these lahars were triggered. The sheer scale of deposits which make up member Onh suggests a lake-breakout mechanism triggered the lahar which emplaced them. Onh is distibuted widely over the Whangaehu Fan and Rangipo Desert hence lending support to a Crater Lake origin for the fluid phase of the lahar.

7.8.5 *ONETAPU FORMATION INFORMAL MEMBER Onj*

Onj is characterised by the presence of abundant grey glassy clasts, which become increasingly vesicular with distance downstream. The monolithic nature of these clasts implies that they had a common origin, and are here interpreted to represent the products of a magmatic/phreatomagmatic eruption from Crater Lake. Onj represents deposits from one of the largest Onetapu Formation lahars. The absence of large quantities of gravelly alluvium in these deposits suggests that this lahar was of a different nature to either Onh or Onf. However the source of water for a lahar of the size of Onj can only have been sourced in a temporary lake, and most likely in Crater Lake. Thus the lahar is inferred to have resulted from an eruption through Crater Lake accompanied by catastrophic drainage of Lake water.

7.8.6 *ONETAPU INFORMAL MEMBERS Ond, Oni, and Onk-Ono*

The pumiceous nature of smaller Onetapu lahars Ond, Oni, Onk and Onl is here interpreted to indicate that they were emplaced by mobilization of pyroclastic material by high rainfall either during eruptions or in post-eruptive and inter-eruptive intervals.

Onetapu lahar Onm is believed to have resulted from the breakout of water from a temporary dam on the Rangipo in 1861 (refer forward to Chapter 8, section 8.2.1), and Onn a breakout of Crater Lake water in 1953. Ono was emplaced by the lahars which occurred in 1975 and was triggered by a phreatic eruption through Crater Lake. These, and other historic lahars are discussed in the following chapter.

CHAPTER 8

HISTORIC LAHARS

8.1 INTRODUCTION

Historic records of lahars in New Zealand do not extend further back than the middle of the last century. Since that time numerous eye-witness accounts of strange "flood" events (lahars) in the Whangaehu River have been reported. Certainly the most tragic and publicized event was the 24 December 1953 Tangiwai disaster. 151 people lost their lives when a lahar destroyed the rail bridge at Tangiwai where it crossed the Whangaehu River, as a north bound train traversed it. The train was unable to stop and the locomotive and five carriages were swept into the torrent. This flood occurred in fine weather and there had been no report of a volcanic eruption; the event was unexpected. However prior to this date there had been a number of reports of unusual flood events in the Whangaehu River.

This chapter will investigate the evidence of laharic activity in the Whangaehu River from the earliest recorded lahar in February 1861, to the most recent events. Since 1954, following the Tangiwai disaster, the Whangaehu River has been closely monitored allowing for a more accurate and comprehensive assessment of laharic activity. The investigation of historic records and scientific reports has, in this study, established that there have been nineteen historic lahars in the Whangaehu River.

8.2 THE HISTORICAL RECORD

Although rising on the east flank of Mount Ruapehu the Whangaehu River eventually drains south to the west coast of the North Island southeast of Wanganui. Immediately south of Mount Ruapehu, Tangiwai (see Plate 8.1) has long been an important bridging point and a number of accounts of unusual activity have been reported at this location. The middle reaches of the river are remote and, other than eye-witness accounts, details

of lahars in this region are few. Near to the coast at Whangaehu, State Highway 3 between Palmerston North and Wanganui crosses the Whangaehu River. Smaller bridges upstream (Kauangaroa Bridge and Wyley's Bridge) have provided useful gauging points for measured discharges of lahars. Prior to the Tangiwai disaster there was little quantitative data on the size of lahars and the connection between lahars and the Crater Lake on the summit of Mount Ruapehu was little understood, although it was known that the lake fed into the headwaters of the Whangaehu River.

and 8.2 (see pages 208 and 209)
Tables 8.1 provide a summary of the occurrence, triggering mechanisms, estimated and gauged discharges and impacts of historic lahars. This information has been drawn from a variety of publications. Early records are short on factual data, but give an impression of the scale of events. Information on the lowering of Crater Lake level, the height of the lahar and estimated peak discharges at bridging points can be used to compare with more recent events with known discharges.

8.2.1 *THE EARLIEST HISTORIC LAHAR IN THE WHANGAEHU RIVER*

On 14 February 1861 the Reverend Richard Taylor reported in his journal that there had been an unusual flood in the Whangaehu River on the previous day, which had brought down large quantities of snow and ice and sulphurous smelling silt and sand and destroyed a newly built bridge at Whangaehu (Taylor, 1861). A later journal reports that the flanks of Mount Ruapehu bore evidence of there having been an ice and rock avalanche and it was hypothesised that this avalanche dammed the river causing a temporary lake to build up (Crawford, 1870). When the barrier gave way the ensuing flood bulked up to form a lahar which travelled over 150 km to the coast, where the frontal "flood wave" was reported to be 4 m high (New Zealand Spectator and Cook's Strait Guardian, 1861). An eye-witness account described the lahar as "***...a floating mass of frozen snow and ice, mixed with timber and earth, fourteen feet in the perpendicular, and eight or ten chains in length, the entire width of the river, coming down in advance of a pent up torrent of water!***". A later account supplied by Mr Henry Sergeant describes his observation of the lahar in the vicinity of Wyley's Bridge, 32 km upstream: "***In the mid-summer of 1860-61...I was standing on the bank*** [of the Whangaehu River]***...when I suddenly saw coming***

around a corner in the distance a huge wave of water and tumbling logs. They filled the whole trough of the stream...As it passed us it appeared to be covered with what we first thought to be pumice but the intense cold which soon made us shiver and turn blue caused us to discover that... [this] *was no less than frozen snow. Mixed with this was a mass of logs and debris. Very soon a bridge passed us stuck in the roots of a giant tree and a few minutes later about a dozen canoes came down*" (Campion *et al.*, 1988). This must be the largest lahar ever reported in the Whangaehu River in historic times. In comparison the flood wave from the lahar of 24 December 1953 had dampened to < 1 m by the time it reached Whangaehu early in the afternoon on Christmas Day. Furthermore the total discharge of the most recent large lahar in 1975 was gauged as 1.8×10^6 m^3 with a rise in water level of only 1 m at Kauangaroa in the lower reaches of the catchment (Paterson, 1976) which represents little more than a moderate fresh in the River (Wells and Fowles, 1980).

For the 13 February 1861 lahar a number of calculations have been applied to observations made at Whangaehu, 194 km from Mount Ruapehu. By calculating the cross-sectional area of the river channel which lay beneath the maximum height of the lahar (*c.* 4 m) as reported in the Wanganui Chronicle and multiplying this by the velocity at which the lahar was assumed to be travelling an estimate of discharge rate for the 1861 lahar can be determined. The cross-sectional area of the lahar was 220 m^2. At Kauangaroa, 25 km upstream, mean velocity is approximately 1.39 m s^{-1} in the river under "normal" flow conditions and mean discharge rate is approximately 42.9 m^3 s^{-1} (Wells and Fowles, 1980). In 1975 the mean velocity of the lahar past this point was 1.94 m s^{-1} (Paterson, 1976), and peak discharge measured at 120 m^3 s^{-1} (Wells and Fowles, 1980). Using these values a maximum and minimum discharge rate for the 1861 lahar can be calculated. Assuming that the lahar was travelling in the order of 1.39 m s^{-1} (normal flow conditions) the discharge rate would have been in the order of 300 m^3 s^{-1}; if it was flowing as fast as the 1975 lahar, 1.94 m s^{-1}, the discharge rate would be would have been in the order of 420 m^3 s^{-1}. Based on these calculations the discharge of the 1861 lahar at Whangaehu was in the order of 3 times that of the two largest lahars (1953 and 1975) recorded since. The discharge rate at Tangiwai may have been in the order of 2,000 m^3 s^{-1}, and the total volume of the lahar in the order of 6×10^6 m^3.

8.3 LAHARS IN THE INTERVAL 1861 TO 1953

From the information available to the author there have been 4 lahar events of sufficient magnitude to be recorded between 1861 and the Tangiwai Disaster of 1953. The information on these events is, however, sketchy.

Hill (1892), in an address to the Hawke's Bay Philosophical Institute, quotes from a telegram which reported a volcanic eruption from Mount Ruapehu on 1 May 1889. Hill states that "***...the Whangaehu was in high flood, and rose 3ft. or 4ft. in the short space of a few minutes***"[1]. At this time there was still uncertainty as to whether the headwaters of the Whangaehu River were fed from the Crater Lake or not (Skey, 1869; Dunnage, 1886; Cussen, 1887; Allen, 1894; Hill, 1895, 1896).

In 1895 Walter Dunnage, in presenting an account of one of his ascents of Mount Ruapehu in April of that year, discussed the effects of an eruption which took place on 10 March 1895. He describes how the volcano "***...threw up a column of steam at least 1,000ft. above the crater...This lasted several days, the volume of steam rapidly diminishing...the whole crateral lake (about 10 chains by 12 chains) was a cauldron of boiling water***" and adds that "***the phenomena displayed by the Whangaehu River during the increased action on Ruapehu seems to confirm my supposition...that it issues from the crater***". He estimated that the lake level had fallen 2 to 3 m from the last time he was on the summit a year ago. If Crater Lake water had been ejected during the eruption which took place one month before his climb, then this fall in lake level is in the same order of magnitude as the loss associated with the eruption on 22 June 1969 which also generated lahars. The total volume for the 1969 lahar at Karioi Gauging Station on the Whangaehu River was 6.7×10^4 m^3. Thus the flood (lahar) reported in the Whangaehu River on 1895 may have been of similar size. Cowan (1927) quotes from an account written by Mr J. Martin, an Auckland photographer, who witnessed the eruption who described "***...a geyser eruption upon a scale of unparalled magnificence***". In this same quotation is a statement made by Mr Ross,

---

[1] *If the rise in River level of c. 1 m was reported at Tangiwai then this lahar (and the 3 February 1925 lahar) in the order of $^1/_6$ the volume of the 1953 lahar, where the rise in level at Tangiwai was 6 m, and $^1/_5$ the volume of the 1975 lahar, where the rise was c. 5m, i.e. between 2.6 and 3.6 $\times 10^5$ m^3. Hence the total volume of both these lahars is estimated to be c. 3 $\times 10^5$ m^3.*

proprietor of the then Terraces Hotel, Taupo, who witnessed the eruption and advised that "*The contents of the* [Crater] *lake were discharged...in rapid streams pouring down the mountain side and flooding the Whangaehu River*". This statement provides the strongest evidence for there having been lahars in the Whangaehu River at the time of the March 1895 eruption.

Although there are reports of volcanic eruptions from Mount Ruapehu during the subsequent 30 years the next report of a lahar comes in 1925. Two lahars were reported, the first on 23 January followed two weeks later by the second on 3 February. There were no reports of volcanic activity at this time. Both lahars were mentioned in submissions to the Tangiwai Railway Disaster Board of Inquiry. On 23 January the Acting District Engineer for the Railways Department reported that "*...yesterday* [22 January 1925] *a heavy swell came down the Whangaehu River, the river rising about 9ft. and going down through the night to almost normal this morning...I am unable to account for the heavy rise in the river as there has been no rain in the district for the past fortnight*". Although no theory was forwarded for the cause of this lahar it seems likely that release of Crater Lake waters was the trigger, considering there was no report of a volcanic eruption and, as stated, the weather conditions had been fine for at least two weeks prior to the event (Stilwell *et al.*, 1954). The discharge at the Tangiwai rail bridge for this lahar was estimated to be 405 $m^3 s^{-1}$ (Stilwell *et al.*, 1954). The peak discharge for the 1953 lahar which caused the Tangiwai disaster was estimated to be 810 $m^3 s^{-1}$, and the total discharge 1.65×10^6 m^3, a factor of 2,346 times the peak discharge. In the 1975 lahar peak discharge was 566 $m^3 s^{-1}$, and total discharge 1.8×10^6 m^3, 3180 times the peak discharge. By multiplying the estimated peak discharge in 1925 of 405 $m^3 s^{-1}$ by these two factors a value for the total discharge can be estimated. The values calculated are 9.5×10^5 m^3 using the multiplying factor for the 1953 lahar, and 1.3×10^6 m^3 using the factor for the 1975 lahar. Thus it can be assumed the total volume for the January 1925 lahar was probably in the order of one million cubic metres (1×10^6 m^3).

Some insight on the probable cause of this lahar resulted from field investigations reported after the lahar on 3 February. The Evening Post on March 3 covered an interesting account of the "*...strange phenomena in the Whangaehu River and the lake*

on Mount Ruapehu". This detailed the experiences of a climbing party, forwarded by Mr E. A. Merchant, which travelled up to the volcano on 3 February 1925. On their way up to the mountain they had crossed the road bridge at Tangiwai and, according to their report "*...before the bridge was reached, we encountered a strong smell of sulphur and after crossing over it noticed that the road had been recently flooded over...The river was quite normal but highly discoloured and reeking of...the usual "Rotorua" odours. the discolouration was not the usual flood one, and was extaordinary, being of an inky nature*". On 9 February the party ascended Mount Ruapehu and observed that there were no signs of thermal activity, but were "*perturbed*" when a huge fall of ice into the Crater Lake disturbed the peace of the climb. Mr Merchant conveyed that "*The lake appeared to be quite normal...*[but] *There was one point that was noticed and that was a slight indication of tidal marks on the beach*". Mr Merchant theorized that the icefalls temporarily dammed the outlet of the Crater Lake and that the water level rises "*...until its warm water melts the ice barrier, and then the accumulated water rushes through the cavern and floods the Whangaehu*". The newspaper article continued, reporting the occurrence of such a flood (lahar) about three weeks previously (*i.e.* early February 1925) which removed the decking of a farm bridge approximately 7 km below Tangiwai. The date for this event and the experience at Tangiwai by Mr Merchant and his companions closely match, and this author believes they represent the same event. An estimated volume for this lahar of 3×10^5 m^3 has been calculated by comparing the rise in River level at Tangiwai (at least *c.* 1 m?) with the rise associated with lahars in 1953 and 1975 (see footnote 1, this chapter).

Although there were reports of volcanic eruptions in the interval between 1925 and 1953 (Risberg, 1937; Reed, 1945, Oliver, 1945; Beck, 1951; Cotton, 1945; Allen 1949; various newspaper reports) no unusual activity was reported in the Whangaehu River. In 1945 volcanic activity temporarily displaced the Crater Lake waters during a volcanic dome building phase. When this activity waned the water began to accumulate once more and thengradually rose to its pre-1953 Tangiwai Disaster level.

8.4 THE TANGIWAI DISASTER

On December 25 1953 New Zealanders woke to hear the tragic news that a freak flood (lahar) had destroyed the Whangaehu River bridge at Tangiwai and that the Wellington-Auckland Express, filled with 267 Christmas travellers, had been swept into the torrent. 151 people lost their lives as a result of this disaster which holds a place as one of the worst accidents in the recent history of New Zealand. The events that took place on Christmas Eve 1953 are well documented (Stilwell *et al.*, 1954; Haydon *et al.*, 1954; O'Shea, 1954; Stewart, 1972).

The accident at Tangiwai rail bridge occurred at 10.22 p.m.. Mr Arthur Cyril Ellis, who received the George Medal for his bravery in helping rescue passengers following the accident, arrived at the bridge some minutes before the train and found that the road bridge was flooded. When he realized that the express train was approaching this bridging point he attempted to stop it by shining a torch at the oncoming locomotive and waving his arms for he was concerned that the railway bridge might also have been damaged. Evidence showed that the driver had applied the brakes and the fireman had turned off the fuel-supply tap, but with insufficient time to stop the train before it reached the bridge. Mr Ellis believed that the railway bridge was intact at this time, although he was only able to see the top part of the line. One account observed that the train had reached the northernmost span when it nose-dived into the river. Two piers, Pier No. 4 and No. 5, which supported the bridge in mid-channel were swept away. It is generally believed that Pier No. 4 was removed in the first stage of the lahar before the passage of the oncoming train (Stilwell *et al.*, 1954)[2]. As the train ran onto the unsupported track the bridge gave way and the locomotive and first five carriages plunged into the lahar. Damage to a third pier which rests on the north bank of the River was thought to have been caused by the locomotive crashing into it. The sixth carriage was left poised hanging on the sheared off rails of the bridge. It then toppled in, but a rescue attempt, lead in part by Mr Ellis, saved all lives but one from this carriage. The locomotive and first five carriages were wrecked in the accident (see Figure 8.1 and Plates 8.2 and 8.3).

---

[2]*In 1975 the lag time between the arrival of the lahar and peak discharge was 10 minutes (see later in text). Mr. Ellis arrived some minutes before the train and noticed the flooding; peak discharge may not have been achieved at this time and may have occurred coincident with the arrival of the train at the bridge.*

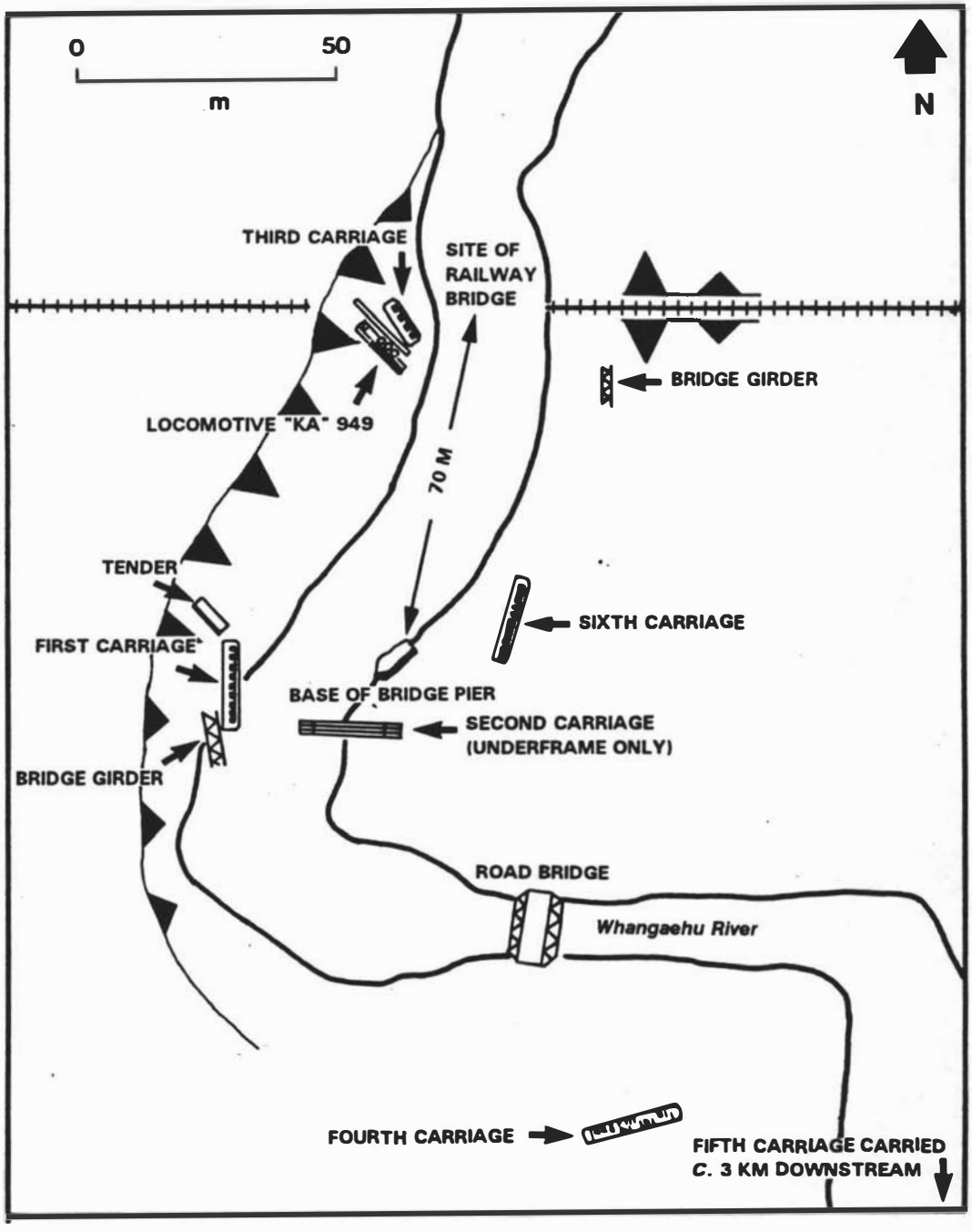

Figure 8.1 The scene at Tangiwai following the Christmas 1953 Disaster, adapted from Stewart (1972). Compare this sketch to the scene depicted in Plate 8.3.

The destruction of the locomotive and carriages was believed to have been caused by (1) the impact of the crash when the train plunged off the bridge, and (2) the destructive force of the lahar. The carriages were reduced to "***...tangled sheet steel and splintered woodwork with only the underframe remaining...***" (Stewart, 1972). One carriage was carried nearly three kilometres downstream; its chassis now rests on the west bank of the Whangaehu River on the edge of a metal pit at S21/287881 (Mr Strachan, *pers. comm.*). The eye-witness accounts of the disaster make for harrowing reading, and attest to the heroism of those involved in the immediate rescue attempts (Stewart, 1972). The bodies of those people who died were recovered from throughout the length of the Whangaehu River. Of the 151 people who died only 131 bodies were recovered and it is believed that the 20 missing were swept out to sea. A rope barrier was spread across the State Highway 3 Bridge near the coast in a vain endeavour to trap these bodies.

An official Board of Inquiry was appointed to inquire into and report on the following points with respect to the derailment of the train (Stilwell *et al.*, 1954):

"***(i)*** ***What was the cause of the accident?***

(ii) ***Whether at any material time or times any person in the service of the New Zealand Government failed to exercise reasonable care or to fulfil any duty or responsibility reasonably to be expected of him in relation to the circumstances leading to the accident.***

(iii) ***Generally, to inquire into and report upon such other matters arising out of the accident as may come to our notice in the course of our inquiries and which we consider should be investigated and upon any matter affecting the premises which we consider should be brought to your attention.***

(iv) ***What steps (if any) should be taken to prevent a similar accident?***"

8.4.1 *THE CAUSE OF THE 1953 LAHAR*

The cause of the lahar was not made clear until December 27 when a climbing party comprising J. P. Haydon, an engineer for the Ministry of Works, R. W. Harris an engineer for the Rangitikei Catchment Board and O. D. Bell an engineer for the Rangitikei County Council inspected the summit region. They reported evidence of there having been a major flood in the Whangaehu River below the Whangaehu Glacier, and described a hole approximately 15m wide in the ice wall on the south side of Crater Lake (see Plate 8.4). They estimated that the Lake level had fallen by about 8 m (Haydon *et al.*, 1954). James Healy, a Government Geologist, flew over the Crater Lake of Mount Ruapehu on December 28 and also observed this hole. Healy estimated the size of the hole to be 45 m wide by 33 m high, but added that the opening was much narrower inside. He climbed Mount Ruapehu on 29 December 1953, 8 January and 13 February 1954 in order to examine the head of the Whangaehu Glacier and the Crater Lake. During this time falling ice gradually blocked off the hole in the ice. Water continued to drain through the new ice cave until February when fallen ice all but blocked the entrance to the tunnel. Healy hypothesised that seepage of Crater Lake water through the glacier ice may have caused crevassing and increased erosion which lead to the collapse of the ice and ash barrier and subsequent catastrophic release of Lake waters (Stilwell *et al.*, 1954). This theory was supported by the fact that there was no evidence of any volcanic activity, and no high rainfall had been reported in the region on the night of the accident.

Haydon *et al.* (1954) reported that there were no signs of abnormally high discharge in the Wahianoa or Makahikatoa Streams, both of which drain Mount Ruapehu and are tributaries of the Whangaehu River. O'Shea (1954) expanded on Healy's theory, mentioned in the previous paragraph, stating that ***"...it seems likely that in the past blockage of the outlet tunnel has resulted in a rise in lake-level"***. Mount Ruapehu was very active between March and December 1945 (Oliver, 1945; Reed, 1945; Beck, 1951) and during this phase the glacier ice that surrounds Crater Lake receded. In the post-eruptive period the ice advanced again to its former position. O'Shea (1954) reports that the Lake's water level had been rising steadily following the 1945 eruptions and that by the end of 1953 the water was only held back by an ice wall. It was his belief that an ice tunnel was forming in this cliff, and that at some critical stage the barrier gave way resulting in the catastrophic release of 1.6×10^6 m^3 of Crater Lake water (Harris, 1954; O'Shea, 1954).

8.4.2 *THE NATURE OF THE 1953 LAHAR*

The 1953 lahar was initiated by the catastrophic release of Crater Lake water. By the time it reached Tangiwai, 40.2 km distant, it had incorporated large amounts of debris from the flanks of the mountain and the channel of the Whangaehu River. Stilwell et al. (1954) reported that the channels in the Whangaehu Gorge, on the flanks of the volcano, appeared "***...as though they had recently been cleared of loose debris...the flood as it moved down must have cleaned out large quantities of loose ash and boulders collected in the valley over a period of years***". The lahar was first observed by Mr. D. M. Chapman who was driving his passenger bus along the Desert Road. The bus radiator had overboiled and Mr Chapman wanted to collect some water from the River. When he arrived at the River it resembled thick grey soup (Morris, 1981). The 26 December 1953 issue of the Dominion newspaper reported that the river brought down trees and boulders, and that the grinding of the boulders could be heard above the roar of the flood. The strength of the lahar was such that it was able to lift and carry the 125 ton middle pier (Pier No. 4) of the railway bridge 70 m downstream (Stilwell *et al.*, 1954). Large boulders, many over 1 m in diameter, which had been transported by the lahar were deposited upstream of the Tangiwai Bridge, but deposits below the bridge were dominantly sandy (Stilwell *et al.*, 1954). One of the first to arrive at the scene of the accident was a doctor who stated that the people who had been in the accident "***...glowed with green-black silt***" (Tangiwai Memorial Service, June 1989, *pers. comm.*). It was reported that the linings of peoples clothes were filled with silt and sand from the lahar, and that in many cases the clothes were stripped from their bodies. The bodies recovered bore no outward signs of damage which suggests that it was the weight of the silt-laden clothing rather than the sheer force of the lahar that removed the clothing. The lack of marks on the bodies further implies that they were buoyed along in the lahar, and that laminar debris flow, rather than more turbulent hyperconcentrated flow, rheological conditions prevailed.

A local resident of Whangaehu, a small community near to the coast, described the arrival of the lahar at the State Highway 3 bridge on the afternoon of 25 December saying that the River was still heavily charged with debris including carriage seats, pillows, parts of carriages, branches and suitcases. Two bodies were found on

Whangaehu Beach, and lots of dead eels were found on the banks of the River and in metal pits (Mr J. Thompson, Whangaehu Beach Road, *pers. comm.*). At the present day the river supports no fish life, and it is supposed that the lahar in 1953 swept up into tributary streams, flushing out the fish. In the vicinity of Tangiwai the lahar backed up the Waitangi Stream and another small stream which drains Lake Otamataraha about 2 km south of the bridge (Mr Hammond, Turakina Valley Road, *pers. comm.*).

The lahar occurred overnight and the accounts which describe it relate more to the great noise and sulphurous smell as it passed. With an estimated density of 1.6 Mg/m^3 the lahar falls within the rheological range of hyperconcentrated flow (Costa, 1988). However it was accepted at the time of the Official Inquiry that this value was probably an underestimate of the density of the flow (Stilwell *et al.*, 1954). Since the lahar was able to transport large boulders, railway carriages and a bridge pile it is possible that the lahar had a greater density than that estimated. When the frontal snout of the lahar approached Strachan's bridge it appeared like a great wall which lifted the farm bridge "***...like a box of matches***" (Mr Strachan, *pers. comm.*). Such steep walled fronts are a typical feature of debris flows.

The lahar destroyed two further bridges downstream of Strachan's bridge, the road bridge at Tirorangi Marae, and the road bridge at the Mangaehuehu confluence (which was not rebuilt). At Manuwera it was necessary for the roadmen to push logs, which had been transported here by the lahar, under the span of the bridge, which crossed the River at this locality, to prevent it being swept away (Mr J. Polson *pers. comm.*). Mr Polson was involved in the search for bodies following the disaster. He found 26 bodies.

By the time the lahar had reached the coast it had deposited the coarser load and eye-witnesses report that it appeared as a "***flash flood***" (Mr C. O'Leary, Whangaehu Beach Road, *pers. comm.*), albeit heavily charged with debris. At this location the lahar had probably fallen below the sediment concentration threshold for hyperconcentrated flow, and was behaving as a Newtonian fluid, but with a higher sediment concentration than normal. The deposits from the lahar were dominantly of silt and fine sand. This

implies that the sediment load was much better sorted, and overall more finely grained than higher in the catchment. These sedimentological observations indicate the lahar in the lower catchment was more representative of normal streamflow.

8.4.3 *ARRIVAL TIMES AND ESTIMATED VELOCITY FOR THE 1953 LAHAR*

The velocity at which the lahar was travelling has been estimated from arrival times at observation points along the river. The first account of any unusual activity was that of a resident in Waiouru who reported hearing an unusual roaring from about 8 p.m. onwards that night. The Chateau Tongariro seismic station recorded a local small amplitude tremor from 8- 9 p.m. on the night of 24 December. These events were probably related to the catastrophic draining of Crater Lake water through the enlarged ice cave. According to the Tangiwai Railway Disaster Report of the Board of Enquiry the lahar arrived at Tangiwai at 10.17 p.m.. Thus the lahar had taken approximately 137 minutes to travel the 40.2 km from Crater Lake and would have been travelling at a mean velocity of 4.9 m s^{-1}. The lahar swept into the Managamahu valley, *c.* 140 km downstream from Crater Lake, at about 6.00 a.m. the following morning (Campion *et al.*, 1988). The lahar had taken approximately 10 hours to flow this far, and would have been travelling at a mean velocity of 3.9 m s^{-1}. The mean velocity between Tangiwai and Managamahu valley, a distance of about 100 km would have been approximately 3.7 m s^{-1}. At approximately 3.30 p.m. on 25 December the lahar reached the bridging point of State Highway 3 bridge near the coast. Overall it had taken 19.5 hours flowing at a mean velocity of 2.8 m s^{-1} to travel 194 km from Crater Lake.

8.4.4 *ESTIMATED DISCHARGE FOR THE 1953 LAHAR*

Prior to 24 December 1953 the surface area of Crater Lake was estimated to be 72 acres [1.8×10^5 m^2], based on aerial photograph interpretation. Following the catastrophic release of lake water, photographs indicated that the area was reduced to

47.4 acres [1.2 × 10^5 m^3]. Inspection of the Crater Lake by James Healy on 29 December 1953 indicated that the lake level had fallen by 9 m, and that a huge ice cave 45 m by 30 m had opened adjacent to the normal outlet (Stilwell *et al.*, 1954). A report by a Senior Engineer of the Works Department suggests that the lake level fell approximately 6 m in 150 minutes, with the corresponding discharge falling from an initial maximum of 810 m^3 s^{-1} to 35 m^3 s^{-1} (Stilwell *et al.*, 1954).

The day after the disaster a site inspection was made by R. W. Harris, Chief Engineer of the Rangitikei Catchment Board, who marked the high flood levels along the channel in proximity to Tangiwai. On 29 December he coordinated a flood investigation survey along a straight stretch of the River channel upstream from Tangiwai (Harris, 1954). This involved surveying a number of cross-sections along the channel, carefully noting the high flood (lahar) level marks, and slope area measurements. From these he was able to estimate the velocity of the lahar at this site, and from the cross-sections calculate the discharge rate for the lahar. A mean value for three of five cross-sections measured was accepted as being the most reliable. An estimated discharge rate of 23,000 cusecs [620 m^3 s^{-1}] ±20 %, was submitted as part of Harris' evidence on the nature of the lahar to the Board of Inquiry. This agreed with the general opinion that the peak discharge rate for the lahar was in the order of 30,000 cusecs [810 m^3 s^{-1}]. Harris also determined a flood hydrograph for the lahar based on estimations of lahar depths at Tangiwai as the lahar subsided during the rest of that night. From this he was able to calculate that the total volume discharged at Tangiwai was approximately 6.1 × 10^7 cubic feet [1.65 × 10^6 m^3]. Harris added that the accuracy of the interpreted hydrograph relied on subjective evidence as to the heights reached by the lahar, and that it represents in all likelihood a conservative estimate of the total volume of the lahar.

8.4.5 *RECOMMENDATIONS OF THE BOARD OF INQUIRY FOLLOWING THE TANGIWAI DISASTER*

Information supplied to the Board of Inquiry took the form of eye-witness accounts and experts' opinions. These both served to draw attention to the nature of the hazard of lahars, and their causal mechanisms. Furthermore the Board concluded that no persons

were responsible for the accident, but that measures should be put into place to prevent a disaster of this nature happening again. It was agreed that in order to prevent another accident, some sort of warning system needed to be installed in the Whangaehu River above the Tangiwai railway bridge (Stilwell *et al.*, 1954). Finally, Mr R. Hardie Boys, who acted as Counsel assisting the Official Board of Inquiry, highlighted the concerns raised by a number of witnesses who felt the need for closer monitoring of the level of Crater Lake and the condition of its outlet (Stilwell *et al.*, 1954). This echoes a comment made in the closing paragraphs of an account describing the probable connection between Crater Lake activity and lahars in the Whangaehu River presented by Mr E. A. Merchant in the Evening Post on March 3 1925. Mr Merchant states that "***...It is quite evident that something abnormal is happening in the source of the Whangaehu and should be investigated, as the destruction of property is possible if the flooding becomes worse***". In 1954, Mr. Hardie Boys recommended that moneys from the Earthquake and Disaster Funds might be made available to increase research into the characteristics of thermal activity in the mountain.

Following the Tangiwai disaster the New Zealand Railways investigated commercially available flood warning devices, but found that none were suited to the peculiar problems inherent to gauging lahars in the Whangaehu River. The problems they faced were (1) the unpredictable nature of the conditions existing during a lahar, (2) the high solid content of the lahar, and (3) that the inaccessibility of the river precluded using standard measuring devices available at the time. However the acid nature of the water in the Crater Lake and the River suggested a solution which would take advantage of the electrical conductivity of the water. The New Zealand Engineering Department worked out a system for a warning device and New Zealand Railways was entrusted with the engineering design and manufacture. The system they developed responds to an increase in water depth at a gauging site located *c.* 27 km downstream of Crater Lake, and 12.9 km upstream of Tang iwai railway bridge. At this site a concrete pylon 6 m high was constructed. On the downstream side of this pylon pairs of electrodes have been placed at 0.33 m intervals. The pylon is divided into five level-detecting zones, which correspond to the level of risk posed by lahars of different magnitudes. A cable from the pylon sends a message via a relay housed in a shelter on the bank of the River, and then through an underground cable, over 10 km to the control station at

Waiouru railway station. An illuminated column in the display panel at Waiouru station responds to a rise in flood level at the gauging station. Sustained high level flooding (for longer than 30 seconds), or a rapid rise to a flood level (in under 30 seconds) triggers both this visual alarm and a coded tone signal which is transmitted to warn the Controller of Trains (Stevens, 1957).

8.5 LAHARS IN THE WHANGAEHU RIVER FOLLOWING THE TANGIWAI DISASTER

As a direct result of the Tangiwai disaster lahar activity in the Whangaehu River has been closely monitored. A detailed record of unusually large discharge events was maintained by the Rangitikei-Wanganui Catchment Board at a now non-operating automatic water level recorder at Karioi.

During the interval April 1968 to July 1971 nine lahars in the order of magnitude of 10^3 to 10^4 m^3 were recorded at this site (Paterson, 1976; Houghton *et al.*, 1987). On 26 April 1968 a lahar, triggered by an eruption through Crater Lake, with total discharge of 7.3×10^5 m^3 was recorded. This was ten times larger than the total discharge from a lahar in the Whangaehu River following an eruption on 22 June 1969. No damage was reported following the 1968 lahar. However, during the 1969 eruption lahars were directed down the northwest face of the Volcano destroying the Dome Shelter near the summit and damaging the Staircase Kiosk on Whakapapa Skifield.

Other lahars recorded during this period of monitoring were caused by episodes of eruptive activity during May and July 1971 (Houghton *et al.*, 1987)). It is possible that a lahar observed by Mr B. Holliday, now of Marton, who was involved in the Tongariro hydro-electric power scheme, occurred during this eruptive phase. Mr Holliday was about 1.2 km upstream from Tangiwai Bridge when he saw what he describes as "***A wall, or wave, of chocolate brown mud, foaming, the width of the channel***" (*pers. comm.*). He estimated that the wave was about 1 m high, and that it was travelling at approximately 27 km/hr (7.5 m s^{-1}). Mr Holliday was unsure of the date that he witnessed this event, but remembers that the weather was fine that day, and believes that it was in the spring or summer. He may have observed one of the lahars that occurred during May 1971.

8.5.1 *LAHARS ASSOCIATED WITH THE APRIL 24 1975 ERUPTION OF MOUNT RUAPEHU*

At 3.59 a.m. on April 24 1975 a large eruption from the Crater Lake on Mount Ruapehu was the direct cause of lahars in several of the rivers that drain the Volcano (Paterson, 1976; Nairn *et al.*, 1979). The beginning of the eruption sequence was recorded on the morning of 24 April by by a seismometer sited 150 km south-southwest of Mount Ruapehu which registered an increase in seismic activity at 3.15 a.m. (Nairn *et al.*, 1979). At Mount Ruapehu the first indication that there had been an eruption was when a communication cable to the Top of the Bruce was cut by a lahar, setting off the Chateau Tongariro fire alarm (Paterson, 1976). This occurred at about 4.30 that morning. A lahar in the Whangaehu River triggered the New Zealand Railways flood warning device 13 km upstream of Tangiwai at 4.59 a.m., and within a few minutes the lahar level had exceeded the gauge maximum of 5 m above normal river level (Paterson, 1976). A total gauged discharge into the Whangaehu River of 1.8×10^6 m^3 made this the largest lahar in this catchment since the Tangiwai disaster which occurred over 20 years previously.

The lahars were caused primarily by bulking up of floods which followed the ejection of an estimated 1.6×10^6 m^3 of Crater Lake water (Paterson, 1976). Nairn *et al.* (1979) compared the eruption to an underwater nuclear detonation, hypothesising that an explosion through the floor of the lake released steam and gas from the lake waters which generated a vertical explosion column. Interaction between the cool lake water and hot ejecta would serve to impart greater energy to the eruption column. Base surges caused by collapse of the eruption column (Nairn *et al.*, 1979) probably spread water, lake sediments, ash and blocks of lava over the summit region. The flood waters which caused the lahars may have been augmented by melting of snow and ice by hot ejecta.

Although there were no fatalities associated with this event the increased development of the Mount Ruapehu region has created more areas of potential risk. Skifields at three locations on the mountain, Whakapapa, Turoa and Tukino were well established and skiing installations were damaged. Scientific monitoring equipment on the flanks of the Volcano was also damaged or destroyed (Nairn *et al.*, 1979).

At the time the Tongariro Power Development hydro electric power scheme was under construction. 18 km upstream of Tangiwai the Mangaio Tunnel was being excavated and Wahianoa Aqueduct constructed alongside the main Whangaehu River channel. Eight construction workers were lucky not to lose their lives as both engineering structures became choked with laharic debris (Paterson, 1976). A simple flood warning device had been installed 1.5 km upstream of the construction site as a precaution against lahars, but it is not known whether this functioned effectively.

8.5.1.1 *Observations of the April 1975 lahar in the Whangaehu River*

At Tangiwai the lahar burst out of the confines of the river channel and flooded the low lying flats in the vicinity. When it arrived here it was travelling at an estimated velocity of 4.82 m s^{-1} and peak discharge was estimated to be 566 m^3 s^{-1} (Fowles *et al.*, 1975). If lahar initiation was coincident with the major eruption at the crater then it took 106 minutes to flow from Crater Lake to Tangiwai, travelling at a mean velocity of 6.38 m s^{-1} (Paterson, 1976). The discrepancy between estimated velocities of the 1953 and 1975 lahars at this site probably reflects inaccuracies in estimating both the time of initiation of both lahars, and of the time of arrival for the 1953 lahar. Photographs taken the next morning at Tangiwai show the lag deposit left by the lahar (see Plate 8.4). This consisted largely of coarse sand with cobbles and boulders together with a large amount of organic debris from the Karioi forest[3]. At the Karioi recording station which lies 57 km from Crater Lake a peak discharge of 310 m^3 s^{-1} was recorded for the lahar. The total volume discharged past this point was 1.8×10^6 m^3. Mean velocity past this site was approximately 4.17 m s^{-1}, and mean velocity through the 57 km from Crater Lake was 5.56 m s^{-1} (Paterson, 1976).

The lahar arrived at Colliers junction, approximately 84 km from Crater Lake, at about 10.00 a.m.. Evidence from a still photograph taken at this point indicate that the lahar peaked at about 6 m above normal river flow level (see Plate 8.5). The lahar had taken about 360 minutes to arrive here from Crater Lake and had covered this distance at a

[3] *Pine cones found within previously undated deposits are indicators of lahars which occurred following the planting of this area with exotic pine trees. Donoghue (1991) and Hodgson (see Chapter 8, section 7.4.12) have been able to assign lahar deposits to historical events by this method.*

mean velocity of 3.89 m s^{-1}. Mr A. Reesby and Mr D. Head first observed the lahar 7 km upstream at Otuma. Mr Head, now of Wanganui, estimated that the frontal lobe of the lahar was 8 m high. The two men raced in their car down to Colliers junction where there is a bridging point over the River, arriving half an hour after first observing the lahar. Mr Head is an amateur cinematographer and took his cine-camera with him to this locality. The height of the lahar above normal river level had fallen about 1.5 m from the height recorded in Mr Matthews' photograph and the snout of the lahar had already passed by this time but Mr Head captured the flow of turbulent muddy waters that followed in its wake. Copies of this film have been transferred onto video tape and are held by Dr. V. E. Neall in the Department of Soil Science, Massey University. The nature of the flow as observed in the film indicate that hyperconcentrated flow conditions were operating. The frontal snout may have been a fully developed debris flow. The lahar was observed to pick up and move boulders up to two metres in diameter, and boulders crashing against the bridge caused the people who had been observing the lahar from this vantage point to move.

Mr Matthews, a local farmer, who took the still photograph, collected a sample of the lahar as it passed. The sample is stored in a 750 ml bottle and approximately half of this volume was sediment comprising sand, silt and clay. In the laboratory sediment with a similar grain size distribution was extracted from a sample of Onetapu Formation member Ong. Comparable sediment and water volumes and weights for the original sample were determined using a bottle of similar size, and rheological parameters calculated. The sediment concentration in this sample is approximately 52 % (by weight) and 30 % (by volume) and bulk density 1.47 Mg/m^3. The values for sediment concentation and bulk density all fall within the range proposed by Costa (1988) to define the upper and lower rheological limits for hyperconcentrated flow.

The lahar arrived at Aranui station, 14 km further downstream, at 11.00 a.m.. This was one hour after arriving at Colliers Junction. It travelled this distance at a mean velocity of 3.89 m s^{-1}. Its mean velocity over the c.100 km from Crater Lake is estimated to be 3.95 m s^{-1}. Mr R. Collins, who farms the station, descibed its appearance as grey brown and soupy and full of rubbish, indicating that the lahar had incorporated loose material which lay on the banks and in the channel of the river. In

the upper and middle reaches of the river sections of the river bank were stripped bare of vegetation by the lahar. This stripped vegetation line continues to be visible today giving an indication of the height that the 1975 lahar reached.

The frontal wave arrived at Mangamahu 137 km from source at 2.30 p.m. travelling at a mean velocity of 2.22 m s^{-1}, having covered the distance from Crater Lake at a mean velocity of 2.96 m s^{-1}. It arrived at Wyley's Bridge, 162 km from source, at 4.45 p.m. travelling at a mean velocity of 2.2 m s^{-1}, and a mean velocity from source of 2.8 m s^{-1}. It arrived at Kauangaroa Bridge water level recorder, 169 km from Crater Lake, at 5.45 p.m. travelling at a mean velocity of 1.94 m s^{-1} and a mean velocity from Crater Lake of 2.7 m s^{-1}. All values for velocity and distance from Crater Lake are taken from Paterson (1976).

The time lag between the arrival of the frontal wave and the peak flow increased from 10 minutes at Tangiwai to 135 minutes at Kauangaroa. At Kauangaroa the lahar had dampened down significantly, with the river level rising only 1 m. Total discharge past Kauangaroa Bridge was 1.6×10^6 m^3 (Paterson, 1976).

8.5.1.2 *Recommendations following the 1975 lahar*

Paterson (1976) advised that, following increased infrastructure developments in the upper catchment of the Whangaehu River (namely the Moawhango Tunnel and Wahianoa Aqueduct) the lahar warning system installed by the New Zealand Railways Engineering Department was inadequate, and that a further flood warning device should be installed in the Whangaehu River headwaters. Following the 1975 lahar a further lahar warning system was erected at the lower end of the upper Whangaehu gorge.

8.5.2 *THE MOST RECENT LAHARS IN THE WHANGAEHU RIVER*

The two most recent lahars, which occurred on 2 November 1977 and 10 December 1988, both resulted from eruptions through Crater Lake. The total volume of the 1977 lahar was 1.3×10^5 m^3 (Houghton *et. al*, 1987), only 1 % of the total volume discharged in 1953 or 1975.

A period of relative quiescence on the volcano followed this 1977 eruption, which ended with the eruption in December 1988. This eruption was much smaller than either the 1975 or 1977 eruptions. Water, mud, and rocks were ejected to the north of the Crater Lake and where ash and water concentrated on the surface of the Whangaehu Glacier a small mudflow, a few metres wide and 500 m long, formed (Nairn *et al*, 1988, Bogie, 1989). The outlet area, south of Crater Lake, was washed by surges of Lake water up to 2 m above Lake level. The water from these surges ponded in an ice cave below the outlet, being unable to drain through the ice cave into the headwaters of the Whangaehu River. The depth of this temporary pond was estimated to be about 10 m (Nairn *et al.*, 1988).

In the summer of 1989/90 collapse of glacier ice below the Lake outlet again impounded drainage through to the Whangaehu River, forming a temporary lake which was seen as a potential flood (lahar) hazard. However this water drained away harmlessly. In October 1990 ponding was again occurring, and by January 1991 the volume of this latest temporary lake was estimated to be about $1\text{-}\ 1.5 \times 10^4$ m^3. The lake was being fed by both glacier melt water and Crater Lake water. It was estimated that up to 1.5×10^5 m^3 of water could be stored in this depression, this being about 10 % the volume of the 1953 lahar. Blockage of the outlet is believed to be caused by "freeze-up" and glacier flow during the winter, or accumulation of volcanic debris (Keys, 1991).

Table 8.1 Occurrence, triggering mechanisms, estimated and gauged discharges, and impacts of historic lahars in the Whangaehu River, February 1861 to June 1969; [E] marks estimated and [G] marks gauged velocity and discharge.

Date	Cause	Discharge ($m^3 s^{-1}$)	Crater Lake Level (m)	Whangaehu R. Level (m)	Velocity ($m s^{-1}$)	Impact	Total volume (m^3)
22 June 1969	*Eruption*	Total Q at Karioi: [G]67,000	- 2	Tangiwai: +0.3		*No damage in Whangaehu valley. [Dome Shelter and Staircase Kiosk on Whakapapa skifield destroyed]*	[E]6.7×10^4
26 April 1968	*Eruption*	Total Q at Karioi: [G]729,000	- 3.5				[E]7.3×10^5
24 July 1966							[E]1×10^3
24 December 1953	*Sudden collapse of ice and tephra barrier damming Crater Lake*	Peak Q at Tangiwai: [E]620 $\bar{m}$ Q at Tangiwai: [E]270 [Total Q at Tangiwai: [E]1,647,000]	- 6 initial 150 mins - 9 total [1.6×10^6 m^3]	Tangiwai: +6 Field's Track: +9 Colliers Bridge: +5 Whangaehu: +1	Tangiwai: 4.5	*Destroyed rail bridge at Tangiwai. Death toll 153; passengers on north bound train which was swept in o the lahar.* *Damage to road bridge at Tangiwai. Destroyed bridges at Strachen's, Ngamoiai, Toklahuru inlet, Otumu. Flooding at Manurewa*	[E]1.65×10^8
2 February 1926	*Eruption? Ice fall?*		Lowered	+1?		*Road flooded at Tangiwai; Removed decking of bridge at Strachen's.*	[E]3×10^5
23 January 1925	*Release of Crater Lake waters?*	[E]15,000 cusecs		Tangiwai: +3		*2- 3m of scour on upstream side of rail bridge at Tangiwai*	[E]1×10^6
10 March 1895	*Eruption*		- 2 to - 3	Abnormal flooding			[E]6.7×10^4
1 May 1889	*Eruption*			+1			[E]3×10^5
16 February 1861	*Ice and debris avalanche*			Whangaehu: +4		*Destroyed bridge at Whangaehu*	[E]6×10^6

Table 8.2 Occurrence, triggering mechanisms, estimated and gauged discharges, and impacts of historic lahars in the Whangaehu River, May 1971 to December 1988; ^{E} marks estimated and ^{G} marks gauged velocity and discharge

Date	Cause	Discharge ($m^3 s^{-1}$)	Crater Lake Level (m)	Whangaehu R. Level (m)	Velocity ($m s^{-1}$)	Impact	Total volume (m^3)
8 December 1988	*Eruption*						
2 November 1977	*Eruption*	Total Q: ^{G}130,000	- 0.2				^{G}1.3 × 10^{5}
24 April 1975	*Eruption*	Total Q at Karioi: ^{G}1,800,000 Peak Q at Tangiwai: ^{E}566 Peak Q at Karioi: ^{G}310 Peak Q at Keuangaroa: ^{G}121	- 8 (1.8 × 10^{9}m^{3})	Karioi: + 4 Otumu: + 9 Keuangaroa: + 1	Tangiwai: 4.82 Fern bridge: 4.33 Karioi: 4.12 Mangamahu: 2.22 Wyley's Bridge: 2.20 Keuangaroa: 1.94	*Wahianoa Aqueduct and Mangaio tunnel (Tongariro Power Development) flooded with debris. (Damage to ski installations and scientific equipment on Whakapapa skifield)*	^{G}1.8 × 10^{6}
4 July 1971	*Eruption*						^{G}1.9 × 10^{4}
3 July 1971	*Eruption*						^{G}5 × 10^{3}
21 May 1971	*Eruption*	Total Q at Karioi: ^{G}9,000					^{G}9 × 10^{3}
19 May 1971	*Eruption*	Total Q at Karioi: ^{G}18,000					^{G}1.8 × 10^{4}
16 May 1971	*Eruption*	Total Q at Karioi: ^{G}58,000	~ - 0.5				^{G}5.8 × 10^{4}
16 May 1971	*Eruption*	Total Q at Karioi: ^{G}72,000					^{G}7.2 × 10^{4}
8 May 1971	*Eruption*	Total Q at Karioi: ^{G}41,000					^{G}4.1 × 10^{4}

CHAPTER 9

THE LAHAR HAZARD IN THE WHANGAEHU RIVER

9.1 INTRODUCTION AND OBJECTIVES

The Whangaehu River flows through one of the more remote regions of the North Island of New Zealand and from the evidence presented in the preceding Chapters 4 to 8 it has been shown that the Whangaehu River has long been a route for lahars from Mount Ruapehu. The remoteness of the Whangaehu Valley, however, does not mean that the hazard from these lahars is any less than in more populated regions. Their potential risk in terms of dollars may not be as high but the relative isolation of the local population, particularly in the middle reaches of the River, deems it imperative that they are able to respond effectively to any potential crisis that a lahar may cause. For the people who live and work in the Valley and the Ministry of Civil Defence a comprehensive hazard assessment provides an invaluable tool to help them prepare for a lahar which could be larger than any that has been witnessed to date. Repetition of some of the events recorded in the geological history of the Valley could result in potential loss of life and property damage on a disastrous scale. The intention of this following section is, therefore, to assess the lahar hazard in the Whangaehu River. The primary objectives are (1) to determine the frequency of lahars of different magnitudes, (2) to identify zones of potential hazard from lahars, and (3) discuss the risk associated with lahar hazards in the River.

9.2 METHODS

Lahars are now recognised as one of the most hazardous phenomena occurring in volcanic environments (Crandell and Mullineaux, 1967; Neall 1976a, Crandell, 1980; Major and Newhall, 1989; Pierson, 1989; Pierson *et al.* 1992). In Chapter 3, section 3.1.1, Neall (1976a) was quoted as stating that "***A review of the causal mechanisms of lahars, flow behaviour and protective measures...is therefore appropriate to the***

understanding of this major geological hazard". By following the first two lines of inquiry mentioned a comprehensive record of lahar activity over the past *c.* 180,000 years has been resolved for the Whangaehu River. From the chronology established for the timing of lahar events their frequency can be determined, and mapping their distribution delineates those areas impacted by different lahar events. These two outcomes form the basis for lahar hazard assessment at many volcanic centres, principally in the Northwest U.S.A. (Crandell, 1971; Mullineaux and Crandell, 1962; Crandell and Mullineaux, 1975; Mullineaux *et al.*, 1976; Scott, 1989; Crandell, 1980; Hoblitt *et al.*, 1987; Pierson et al., 1992).

In this study three methods of assessing the lahar hazard in the Whangaehu Catchment have been used. These include (1) determining mean recurrence intervals between events of different scales, (2) determining the rate of accumulation of laharic debris in the catchment, and extrapolating any observed trends to predict probable future events, and (3) determining hazard zones based on the likelihood of inundation by lahars of different aged surfaces.

At present there is no effective way to predict when destructive lahars may occur; and in fact precursory seismic activity anticipated the 1975 Mount Ruapehu volcanic eruption and ensuing lahars by only 9 minutes. Therefore any interpretation of the results of this hazard assessment exercise must NOT assume that the predictions are absolute, and should recognize that they reflect what is known about the <u>past</u> behaviour of Mount Ruapehu Volcano, rather than its future activity.

9.2.1 *MAGNITUDE VERSUS FREQUENCY*

Latter (1985) stated that "***The frequency of eruptions, whether estimated on the basis of return period for a given size, or on the basis of annual frequency, is an essential parameter in calculating the risk for a given locality...***". Latter includes lahars as one of the major secondary destructive effects of eruptions. At Mount Ruapehu, and other overseas volcanoes, there is ample evidence for laharic activity in post- and inter-eruptive intervals; thus lahars are not always an eruption associated event. However

it is appropriate to apply the same methods employed in assessing the primary hazards of eruptions (including lava flows, pyroclastic flows, ignimbrites and airfall tephra) to lahars. The same problems are present with both hazard types - determining accurate volumes and ages for events. Crandell and Mullineaux (1967), in a paper examining the volcanic hazards at Mount Rainier, Washington, U.S.A., state that "***Assessment of the potential hazards of a volcanic environment is especially difficult, for prediction of the time and kind of volcanic activity is still an imperfect art...***". They emphasize that any predictions can only be based on the known past behaviour of the volcano and that only a truly comprehensive geological investigation could provide a reliable guide to the past behaviour. The problems associated with using the geological record for hazard assessment reliably are (1) dating, and (2) estimating the total original volume or discharge of the preserved events. The following section will detail how these issues were addressed with respect to lahar deposits in the Whangaehu catchment, and will present a comprehensive lahar magnitude versus frequency hazard assessment.

Lahar magnitude versus frequency relationships have been derived utilizing estimated volumes for lahar deposits (or groups of lahar deposits in their formational status). This information has been assessed over three different time intervals (1) including all lahar deposits from emplacement of the Whangaehu Formation to the present day, (2) including only Onetapu Formation lahar deposits, the stratigraphy of which is well established, and (3) including only historic lahars, for which there is a comprehensive record extending back to 1861 A.D. One major uncertainty in this assessment lies in determining the actual volume of material emplaced during each individual lahar, or group of lahars (here defined as formations). In all but the most recently gauged lahars a best estimate was used, and the following section will detail how this was calculated. The method used here follows closely that proposed by Latter (1985).

9.2.1.1 *Chronology and volume of late Quaternary lahars in the Whangaehu River*

The Whangaehu Formation

In Chapter 4 the Whangaehu Formation was described as a catastrophic debris flow resulting from a flank collapse from Mount Ruapehu, with associated post-collapse eruption-triggered lahars. The maximum and minimum ages for the Formation are *c.* 180,000 and 140,000 years ago, respectively (see Chapter 4, section 4.4.2.4). It was not possible in this study to date each individual lahar deposit recognized. Thus deposits in the Whangaehu Formation are treated as a single event, with a mean age of *c.* 160,000 years ago. The total volume of deposits that remain in the Formation is 7 $\times$ 10^8 m^3. However in this exercise a calculated projected volume of 1.2 $\times$ 10^9 m^3 (see Chapter 4, section 4.3.3) will be used.

The Mangatipona pumice sand and Apitian lahars

The Mangatipona pumice sand is observed at one locality and the total volume of this deposit, estimated to be $<$ 10 m^3, is here not considered to be significant when compared to volumes of the other lahar deposits recognised in this study, and the Mangatipona pumice is not included in this hazard exercise.

The distribution of Apitian lahars is also very limited, and the volume of their deposits correspondingly low. It was therefore very difficult to determine their original distribution, particularly in the upper and middle catchment, and consequently their probable original volume. A minimum estimate is provided by the volume of remaining deposits of *c.* 1.8 $\times$ 10^6 m^3. The maximum and minimum age for Apitian lahars are 32,000 and 25,500 years respectively (see Chapter 5, section 5.), and for this exercise they are assigned a mean age of 28,750 years ago.

Te Heuheu Formation

Te Heuheu Formation deposits form a thin veneer overlying Whangaehu Formation on the southern Mount Ruapehu ring plain in the upper catchment of the Whangaehu River. The volume of Te Heuheu deposits in this study, 2×10^6 m^3, is insignificant when compared to their volume, 6×10^9 m^3, estimated by Donoghue (1991). In the upper catchment studied by Donoghue (1991) on the southeast ring plain Te Heuheu Formation comprises the most voluminous lahar deposits described. Therefore the volume estimated by Donoghue is used in this exercise. Donoghue defined the upper age limit for the Formation as *c.* 14,700 years B.P., based on the overlying 14,700$\pm$110 years B.P. Rerewhakaaitu Tephra. This author considers that Te Heuheu Formation probably started to accumulate contemporaneously with the onset of the Ohakean stadial, *c.* 25,500 years B.P. A mean age for the Formation of 20,000 years B.P. is considered appropriate for this exercise.

Tangatu Formation

The Tangatu Formation is widely distributed throughout the upper and middle catchment of the River. The total volume of deposits on the Mount Ruapehu ring plain is 9.4×10^7 m^3. Combined with the estimated projected volume for deposits in this study of 1.28×10^8 m^3, a total volume of 2.22×10^8 m^3 has been calculated. The Tangatu Formation accumulated between emplacement of the Rerewhakaaitu Tephra at *c.* 14,700$\pm$110 years B.P., and the Motutere Tephra, *c.* 5,370$\pm$90 years B.P. These provide maximum and minimum ages for the Formation, and a mean age of 10,000 years B.P.

Manutahi and Mangaio Formations

The lower and upper age limits on the Manutahi Formation are 5,460 and 3,260 years B.P. respectively (Donoghue, 1991, and see Chapter 6, section 6.8) giving a mean age of 4,360 years B.P. This Formation is only occasionally observed in the area of this study, and no estimate of total volume was made. Therefore the volume of 5×10^7

m^3 calculated by Donoghue (1991) for this Formation on the Mount Ruapehu ring plain is used in this hazard assessment.

The Mangaio Formation is also very restricted in its distribution in the middle and lower reaches of the catchment. Lower and upper age brackets for this Formation are *c.* 4,940 and 3,360 years B.P. giving a mean age of 4,100 years B.P. The estimated volume of 2×10^4 m^3 for Formation deposits in this study was minor compared to the 3.4×10^7 m^3 preserved on the ring plain (Donoghue, 1991). This latter figure is used in this assessment.

Prehistoric Onetapu Formation lahars

Age constraints on all prehistoric members of the Onetapu Formation are well established (Refer to Chapter 7, section 7.4) and these are detailed in Table 9.1. Of more importance to this exercise was the problem of working out the actual volume of the lahar which emplaced each member. In an example from Mount St. Helens, Scott (1988b) estimated that the mappable remaining deposits of PC1, a Holocene lahar from Mount St. Helens, were about 3×10^7 m^3. By applying the principles of superelevation to determine velocity[1], and hence discharge, Scott calculated that the probable total volume of the lahar was in the order of 1×10^9 m^3, about 33 times the volume remaining. At Mount Ruapehu the total gauged volume of the 1975 lahar was 1.6×10^6 m^3. Purves (1990) estimates that deposits remaining from this lahar on the Mount Ruapehu ring plain were about 9×10^4 m^3, this about 5 % of the original lahar volume. In this study the total volume of remaining 1975 lahar deposits (Onetapu member Ono) was only 2.4×10^3 m^3. When combined with the volume estimated by Purves (1990) this is still only $^1/_{20}$ the volume of the original lahar. Therefore, in this study, a ratio of 1:20 was used to project the total volume of the lahar which emplaced each Onetapu member deposit. Projected total volumes are presented in Table 9.1.

[1]*This method was detailed in Chapter 7, section 7.7, where it was applied to Onetapu Formation lahar deposits.*

The total projected volume for Onetapu Formation lahars is 8.55×10^8 m^3. In this study, and that of Purves (1990), all deposits overlie and thus post-date the 1,850±10 years B.P. Taupo Ignimbrite. Therefore, in this exercise the lower age for the Formation is set at 1,860 years B.P., and the upper age limit the present day. For the lahar recurrence the mean age is calculated at 947 years B.P.

Table 9.1 The existing and projected volumes for Onetapu Formation informal members with age details.

Member identifier	Existing Volume (m^3)	Projected volume (m^3)	Age range in years B.P. or (calendar years)	Estimated age in years B.P. or (calendar years)
Ono	9.24×10^4	1.8×10^8	(< 1928)	(1975)
Onn	7.2×10^2	1.65×10^8	(< 1750)	(1953)
Onm	1.6×10^3	6×10^8	(1750 - 1950)	(1861)
Onl	6.6×10^2	1.32×10^4	505 - 335	400
Onk	3.6×10^3	6×10^4	505 - 335	400
Onj	8.4×10^6	1.68×10^8	477 - 395	450
Oni	3.4×10^6	9.6×10^7	615 - 337	550
Onh	1.8×10^7	3.6×10^8	615 - 337	600
Ong	3.5×10^6	7×10^7	930 - 700	700
Onf	3.2×10^6	6.4×10^7	930 - 700	850
One	1.8×10^6	3.6×10^7	930 - 700	900
Ond	2.7×10^3	5.4×10^4	1860 - 850	1200
Onc	1.8×10^3	3.6×10^4	1860 - 850	1650
Onb	6×10^2	1.2×10^4	1860 - 850	1750
Ona	3×10^6	6×10^7	1860 - 850	1800

Historic Lahars

Many of the recent lahars have been gauged, thus providing reliable absolute volumes (see Table 9.2). Where lahars were not gauged the discharges and total volumes were estimated using the methods detailed in Chapter 8.

9.2.2 *RECURRENCE INTERVALS FOR EVENTS OF MAGNITUDES 10^3 TO 10^9 M^3*

From Table 9.2 a recurrence interval (R.I.) of 140,000 years can be calculated for lahar events of the magnitude of those which emplaced the Whangaehu and Tangatu Formations (10^9 m^3). Reduced volumes of lahar events give correspondingly lower R.I.s. Events on the scale of the Mangaio Formation (10^7 m^3) for example can be expected to recur every *c.* 31,811 years. If the R.I. is calculated based on lahar accumulation following the Te Heuheu Formation, *i.e.* during the past *c.* 20,000 years the R.I. for events of size 10^7 m^3 of is 4,763±4,126 years.

Table 9.2 Recurrence intervals for lahar events in the time interval *c.* 160,000 to the present day.

Lahar event (age in years B.P)	Total volume (m^3)	Time interval between lahars (years)			
		≥ 10^6 m^3	≥ 10^7 m^3	≥ 10^8 m^3	≥ 10^9 m^3
Onetapu Formation (c. 947)	8.55 × 10^9	3,153	3,153	9,053	-
Mangaio Formation (c. 4,100)	3.4 × 10^7	260	260	-	-
Manutahi Formation (c. 4,360)	5 × 10^7	5,840	5,840	-	-
Tangatu Formation (c. 10,000)	2.76 × 10^9	10,000	10,000	10,000	-
Te Heuheu Formation (c. 20,000)	6 × 10^9	6,750	140,000	140,000	140,000
Apitian lahars (c. 28,750)	2 × 10^9	131,250	-	-	-
Whangaehu Formation (c. 160,000)	1.2 × 10^9	-	-	-	-
	Mean interval	26,509±51,436	31,811±60,585	53,018±75,330	140,000

A much more detailed record of lahar activity is established for recent Onetapu-aged lahars. Recurrence intervals for magnitudes 10^3 m^3 to 10^8 m^3 are presented in Table 9.3. Only one event was 10^8 m^3 in magnitude, with a calculated recurrence interval of 1,310 years. Of most interest is the R.I. for lahars with magnitudes 10^7 m^3 (5 to 25 times larger than either the 1953 or 1975 lahars), which is 208±292 years. The last lahar of this magnitude occurred *c.* 450 years ago (Onetapu member Onj) and another lahar of this magnitude could be expected in the next 50 years.

Table 9.3 Recurrence intervals for lahar events in the time interval *c.* 1,800 years B.P. to the present day.

Lahar event (age in years B.P.)	Total volume (m^3)	Time interval between lahars (years)					
		≥ 10^3 m^3	≥ 10^4 m^3	≥ 10^5 m^3	≥ 10^6 m^3	≥ 10^7 m^3	≥ 10^8 m^3
2 November 1977	1.3×10^5	2.53	2.53	-	-	-	-
24 April 1975	1.8×10^6	3.81	3.81	6.99	21.38	-	-
4 July 1971	1.9×10^4	0.00	0.12	-	-	-	-
3 July 1971	5×10^3	0.01	-	-	-	-	-
21 May 1971	9×10^3	0.00	-	-	-	-	-
19 May 1971	1.8×10^4	0.01	0.01	-	-	-	-
16 May 1971	5.8×10^4	0.00	0.00	-	-	-	-
16 May 1971	7.2×10^4	0.02	0.02	-	-	-	-
8 May 1871	4.1×10^4	1.88	1.88	-	-	-	-
22 June 1969	6.7×10^4	1.15	1.15	-	-	-	-
26 April 1968	7.3×10^5	1.77	14.34	14.34	-	-	-
24 July 1966	1×10^3	12.57	-	-	-	-	-
24 December 1953	1.65×10^6	28.69	28.89	28.89	28.92	-	-
3 February 1925	3×10^5	0.03	0.03	0.03	-	-	-
23 January 1925	1×10^6	29.87	29.87	35.73	35.73	-	-
10 March 1895	6.7×10^4	5.86	5.86	-	-	-	-
1 May 1889	3×10^5	28.20	28.20	28.20	28.20	-	-
16 February 1861	6×10^6	311.13	311.13	311.13	311.13	-	-
Oni (*c.* 400)	1.32×10^4	0	0	0	0	-	-
Onk (*c.* 400)	6×10^4	50	50	50	50	-	-
Onj (*c.* 450)	1.68×10^6	100	100	100	100	100	-
Oni (*c.* 550)	9.6×10^7	50	50	50	50	50	1310
Onh (*c.* 600)	3.6×10^6	100	100	100	100	100	-
Ong (*c.* 700)	7×10^7	150	150	150	150	150	-
Onf (*c.* 850)	6.4×10^7	50	50	50	50	50	-
One (*c.* 900)	3.6×10^7	300	300	810	810	810	-
Ond (*c.* 1,200)	5.4×10^4	350	350	-	-	-	-
Onc (*c.* 1,650)	3.6×10^4	100	100	-	-	-	-
Onb (*c.* 1,750)	1.2×10^4	50	50	-	-	-	-
Ona (*c.* 1,800)	6×10^7	-	-	-	-	-	-
	Mean interval	60 ± 98	66 ± 102	115 ± 208	133 ± 218	208 ± 282	1310

A record for lahars of the magnitude 10^3 m^3 to 10^6 m^3 is provided by the historic record, here augmented by volume estimates for pre-1953 lahars calculated in this study (see Chapter 8). Significantly the R.I. for lahars of the magnitude of the 1953 and 1975 lahars (10^6 m^3) is 29 ± 6 years (see Table 9.4), and a further lahar of this magnitude could be expected in the next 17 years, *i.e.* before 2010 A.D. The R.I. for the smallest lahars recorded is one lahar in every *c.* 7 years.

Table 9.4 Recurrence intervals for lahar events in the time interval 1861 calendar years to the present day.

Lahar event	Total volume (m^3)	Time interval between lahars (years)			
		≥ 10^3 m^3	≥ 10^4 m^3	≥ 10^5 m^3	≥ 10^6 m^3
2 November 1977	1.3×10^5	2.63	2.63	-	-
24 April 1975	1.8×10^6	3.81	3.81	6.99	21.38
4 July 1971	1.9×10^4	0.00	0.12	-	-
3 July 1971	5×10^3	0.01	-	-	-
21 May 1971	9×10^3	0.00	-	-	-
19 May 1971	1.8×10^4	0.01	0.01	-	-
16 May 1971	5.8×10^4	0.00	0.00	-	-
16 May 1971	7.2×10^4	0.02	0.02	-	-
8 May 1971	4.1×10^4	1.88	1.88	-	-
22 June 1969	6.7×10^4	1.15	1.15	-	-
16 April 1968	7.3×10^5	1.77	14.34	14.34	-
24 July 1966	1×10^3	12.57	-	-	-
24 December 1953	1.65×10^6	28.89	28.89	28.89	28.92
3 February 1926	3×10^5	0.03	0.03	0.03	-
23 January 1926	1×10^6	29.87	29.87	35.73	35.73
10 March 1895	6.7×10^4	5.86	5.86	-	-
1 May 1889	3×10^5	28.20	28.20	28.20	28.20
16 February 1861	6×10^6	-	-	-	-
	Mean interval	7 ± 11	9 ± 12	19 ± 14	29 ± 6

9.2.3 *ACCUMULATION RATES FOR LAHARS IN THE WHANGAEHU RIVER*

Accumulation rates for lahars in the Whangaehu River, here expressed as the number of years required for 1 km^3 of lahar material to amass, have been calculated over three different time scales (1) between *c.* 160,000 years and the present day, (2) between *c.* 1,800 years B.P. and the present day, and (3) between 1861 A.D. and the present day (see Figures 9.1 to 9.3). The total cumulative projected volume of lahar events is plotted against the mean age for each successive lahar event. Linear regression lines are fitted to these graphs based on observed trends in accumulation rate.

For the interval of time *c.* 160,000 years ago to the present day accumulation rates of 1 km^3 every 42,435 (minimium) and 23,191 (maximum) years have been calculated. Between *c.* 1,800 years B.P. and the present day accumulation rates have accelerated dramatically to 1 km^3 in 1,700 (minimum) and 589 (maximum) years. This provides further evidence for the inception of Crater Lake at *c.* 1,850 years B.P., resulting in a greater incidence of lahars in the Whangaehu Catchment. During historic time, however, the accumulation falls to approximately 1 km^3 every 18,523 years, which compares to the maximum accumulation rate determined over the past *c.* 160,000 years.

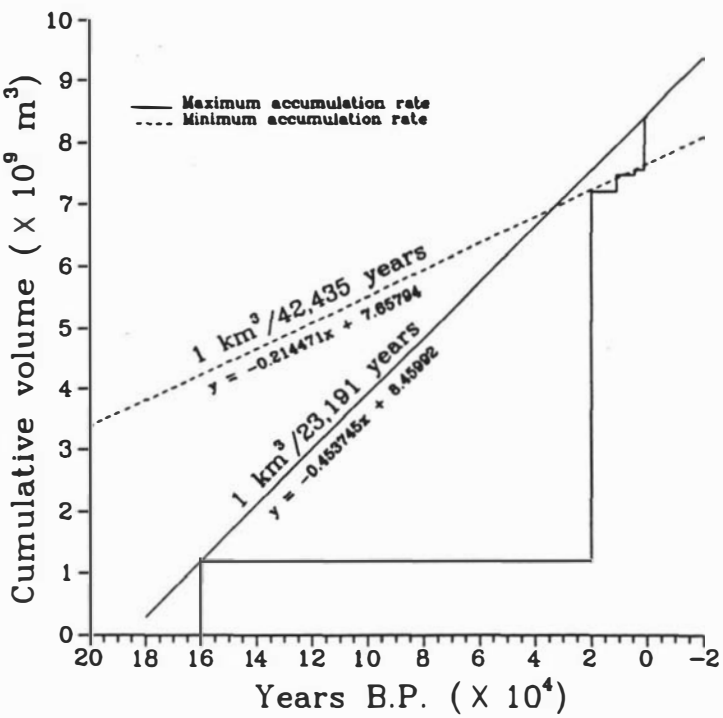

Figure 9.1 Lahar accumulation rate from *c.* 160,000 years ago to the present day

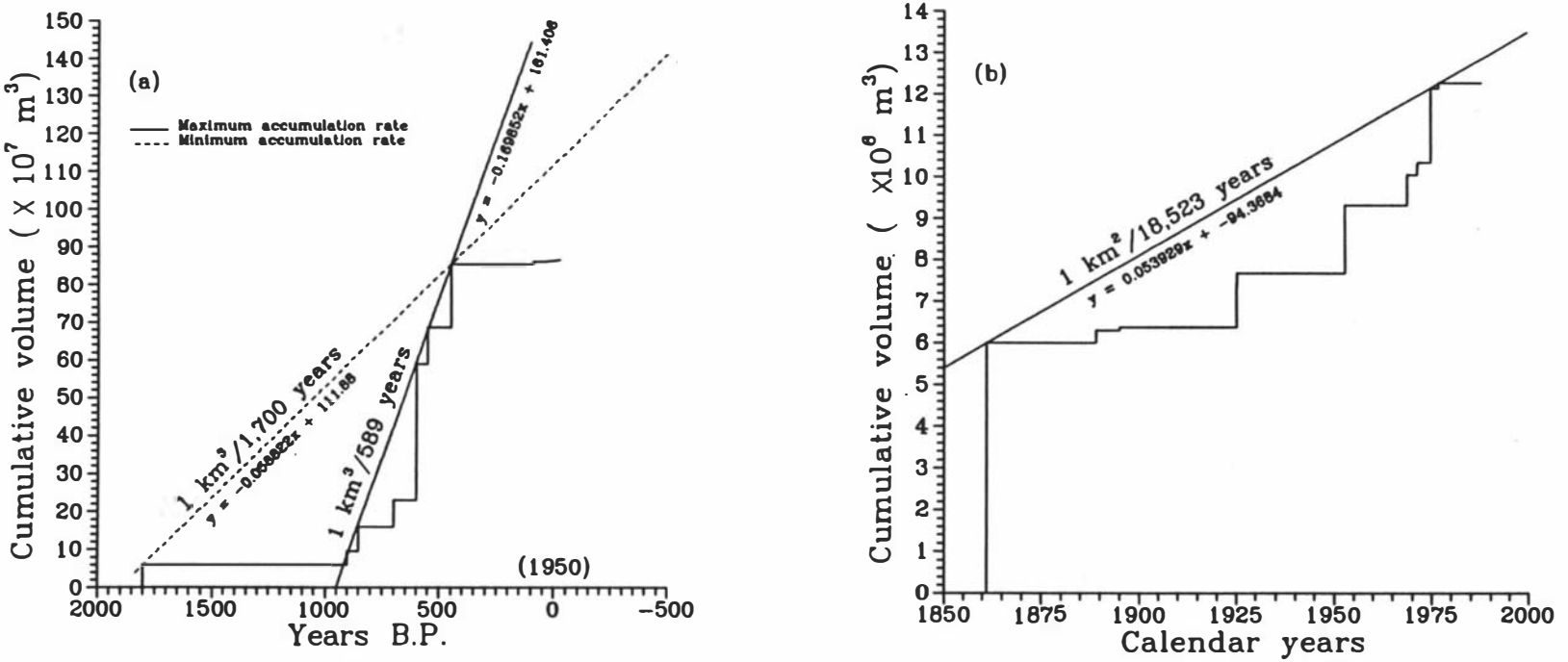

Figure 9.2 Cumulative volume for (a) prehistoric and historic combined, and (b) historic Onetapu Formation lahars.

9.2.4 *LAHAR HAZARD ZONES*

Lahar hazard zones for surfaces in the Whangaehu Catchment have been recognised on the following criteria. Age constraints are well established for the most recent events, defined in this study as the Onetapu Formation. However within older Tangatu and Whangaehu Formations specific timing of individual events is not possible. Where surfaces are multiple, *i.e.* if a surface consisted of Whangaehu Formation overlain by Tangatu and Onetapu Formations, the hazard assessment was determined on the distribution of the more recent deposits recorded on the surface, *i.e.* the R.I. for Onetapu lahars. Mapped late Quaternary river terraces, which are likely to have formed partly from downstream floods associated with lahars in the upper and middle catchment of the River, are also included in these hazard zones.

Eight different zones of lahar hazard have been delineated by this method, ranging from zones which are likely to be inundated once in every 10 years, to zones where this has occurred once in the past 160,000 years (see Maps 7 & 8).

The highest hazard zone essentially delineates the channel of the Whangaehu River. The most recent lahar which flowed down this channel occurred 16 years ago, despite the R.I. for lahars in the River being at a higher frequency, *i.e.* 1 lahar about every 7 years. A likelihood of inundation by a lahar once in every 10 years is considered appropriate for this hazard zone 1.

The last lahar which was sufficiently large to cause structural damage occurred in 1975, and had a total volume of 1.8×10^6 m^3. There have been four lahars of a similar magnitude in historic times, three of which (1861, 1953 and 1975) have left deposits in the catchment. These are included in lahar hazard zone 2 where there is a likelihood of being inundated by lahars once every 30 years.

The R.I. for Onetapu lahars of the magnitude 10^7 m^3 is 1 lahar every *c.* 200 years; this defines the likelihood of inundation for surfaces in lahar hazard zone 3. With increasing distance downstream, and laterally away from the channel, the total number of Onetapu lahars in any stratigraphic sequence decreases, and consequently so does the potential for lahar inundation.

Hazard zone 4 delineates the extent of the largest Onetapu lahars, and in this zone the likelihood of inundation is once in every 500 years.

The mapped extent of Tangatu Formation constitutes lahar hazard zone 5. In this study individual events within the Formation were not dated, and in this exercise hazard zone 5 delineates a surface upon which lahars began accumulating *c.* 14,700 years B.P., but have not been inundated since *c.* 5,370 years B.P. Included in this zone are all Holocene-aged river terraces.

The extent of Te Heuheu Formation (where not overlain by younger lahar deposits) delineates hazard zone 6. Lahars accumulated on this surface between 25,500 and 14,700 years ago. Included in this zone are Ohakean-aged river terraces.

Lahar hazard zone 7 combines the mapped extent of the next oldest group of lahar deposits, the Apitian lahars, which accumulated on this surface between 32,000 and 25,500 years ago, and Ratan-aged river terraces, upon which Apitian lahar deposits lie. The Mangatipona pumice sand, *c.* 37,000 years B.P. in age is also included in this hazard zone.

No older lahar deposits were mapped between the Mangatipona pumice sand and the Whangaehu Formation (which comprises the oldest lahar deposits mapped in the Whangaehu River Catchment). The Whangaehu Formation is associated with a single major collapse of the southern flank of Mount Ruapehu, and a subsequent series of lahar events shortly afterwards, probably associated with catastrophic Plinian eruptive activity. The mean age of the Whangaehu Formation is 160,000 years. Here the mapped extent of the Formation delineates hazard zone 8, which has only been inundated once in the past *c.* 160,000 to 40,000 years. Included in this zone are all surfaces younger than the Whangaehu Formation, but older than those surfaces mapped in hazard zone 7.

9.2.5 DISCUSSION

The zones of greatest hazard are located on the valley floor of the Whangaehu River. In this zone the likelihood of inundation is about 1 lahar in every 10 years, and the whole length of the channel of the River from Crater Lake to the coast below Whangaehu is likely to be impacted. In the past small frequently occurring lahars have had serious consequences on aquatic life (Fowles *et al.*, 1975; Welles and Fowles, 1980), and these must be seen as a severe risk for any industrial or agricultural use of the River waters. With increasing distance downstream and laterally away from the main flow channel (the Whangaehu River) likelihood of inundation is reduced. However, these zones are likely to be impacted by lahars with greater magnitudes than those which are confined to the channel of the River. The destructiveness of these larger lahars would be much greater, and would impact much more extensive areas. Therefore, although the risk from these lahars is less, *i.e.* they occur less frequently, their effects would be much greater. The risk from lahars will be discussed in the following section.

Probable triggers for lahars in the River include (1) flank collapse of part of the volcano, (2) Plinian and sub-Plinian eruptions, (3) catastrophic drainage of Crater Lake, and (4) phreatomagmatic eruptions through Crater Lake. Examples of the deposits from the first mechanism are Whangaehu and Mangaio Formations. The distribution of the former delineates the lowest hazard zone due to there not having been a similar single event of this large (10^9 m^3) magnitude in the past 140,000 years; however if a repeat event did happen the repercussions would be devastating, with lahars conceivably engulfing the entire catchment of the Whangaehu River. Similarly the hazard from lahars triggered by Plinian eruptions would impact the entire width of the present River valley plain. This is evidenced in the distribution of pumiceous Tangatu Formation lahar deposits. These form thick aggradational suites of deposits up to and exceeding 30 m in depth in the upper and middle catchment of the River. In the lower reaches of the River the impacts from lahars triggered by large scale eruptions in both the short and long term would principally be flooding, and bridging points over the River would be at risk.

The recent record (< 1,850 years B.P.) of lahars in the Whangaehu River is dominated by frequently occurring lahars triggered by catastrophic drainage of Crater Lake waters in both syn-eruptive and inter-eruptive intervals. Close to the channel of the Whangaehu River these pose a very high hazard, inundating these areas once in every 30 to 500 years, $10^6 m^3$ - $10^8 m^3$, respectively.

9.3 THE RISK FROM LAHARS IN THE WHANGAEHU RIVER

The risk associated with a natural hazard combines the physical characteristics and frequency of the hazard, or event, with the value and vulnerability of human resources perceived to be under threat. These resources include buildings, bridges, roads and railways, defined here as infrastructure. Recreational, industrial and agricultural landuses are also defined as resources. The distribution of these resources within the Whangaehu River Valley was detailed in Chapter 1. The immediate consequences of lahars in populated zones are likely to include (1) loss of life, (2) destruction of property and (3) overwhelming of agricultural land. The social and economic repercussions of these consequences may be severe. The socio-economic repercussions may be long lasting; one year after the initial catastrophic 1991 eruption at Mount Pinatubo, which was followed by destructive lahars which became the principal volcanic hazard, *c.* 70,000 people remain in emergency evacuation areas (PHI VOLCS, 1992). Lahars occur not only at the time of an eruption, but may also occur in inter-eruptive intervals in the years following eruptions (Waldron, 1966; Rodolfo *et al.*, 1989; Arguden and Rodolfo, 1990; Rodolfo, 1991; Pierson *et al.*, 1992). The unpredictability of these events deems them particularly hazardous (Pierson, 1989).

9.3.1 *THE WHANGAEHU VALLEY*

The area mapped in this field study is delineated in the north at Tangiwai. This locality marks an important bridging point over the Whangaehu River for State Highway 49 and the North Island Main Trunk Line. In 1925 and 1953 the road bridge at this locality was damaged, and in 1953 the rail bridge destroyed, by lahars. Stratigraphical

evidence shows that the east bridge abutment is built on a *c.* 400 year old lahar surface which was also inundated by lahars in 1953 and 1975. This must be considered as one of the highest risk areas in the Valley. On the west bank of the River the railway bridge abuts a *c.* 10,000 year B.P. lahar surface on which the Karioi Pulp Mill is situated. Although the Mill lies in proximity to the Whangaehu River it is not considered to be a high risk zone due to the older age of this surface.

The main communication artery in the Whangaehu Valley is the Whangaehu Valley Road, which is routed alongside the channel of the Whangaehu River. This road first bridges the Whangaehu River in the north at Tirorangi Marae. This bridge was removed by the 1953 lahar, and stratigraphic evidence indicates that the surface on which the bridge abuts on both sides of the River was engulfed by lahars as recently as *c.* 400 years B.P. These lahars may have been up to 20 times larger than the 1953 lahar. This bridging point is considered to be a high risk area for 2 reasons, (1) there are no other bridging points which cross the River between this locality and Colliers junction, *c.* 30 km downstream. If the bridge was destroyed by a lahar, gaining access by road to the population isolated on the east bank of the River would only be possible by a circuitous route via Raetihi and State Highway 4; (2) a farm bridge located *c.* 8 km upstream which provides access to a station on the east bank of the River was destroyed in 1925, 1953 and 1975. In 1953 access to the station was only possible via a track cut into the River bank, beginning at Tirorangi Marae and following the east bank of the River north to the station. This track is now inaccessible. If both the farm bridge and the bridge at the Marae were destroyed access to this station would be very difficult.

A bridge located at the confluence of the Mangaehuehu stream and the Whangaehu River was damaged by the 1953 lahar and now no longer exists. This locality is also considered to be a high risk zone; it marks an area where dwelling houses have been built close to River level, and where *c.* 600 year B.P. lahars have backed up the Mangaehuehu Stream. Below this point the Whangaehu River is entrenched below the cliffs of the lower Whangaehu gorge. Both the Whangaehu Valley Road, and buildings belonging to the small local community are here located on the high *c.* 30 m above River level Whangaehu Formation terrace, and the risk from lahars is not considered to be high. However, there is evidence that Apitian and Tangatu lahars, *c.* 28,750 and 10,000 years B.P. respectively, flowed across this surface, signifying that this is a moderate risk zone.

There are no reports of the road bridge at Colliers junction being damaged by historic lahars. However a *c.* 600 year B.P. lahar deposit on the surface which this bridge abuts indicates that if an event of this magnitude occurred again it would be likely to cause great damage. The bridge provides access to State Highway 4, a route preferred by most of the local population when travelling to and from Wanganui in the south. If both bridges at Colliers junction and Tirorangi Marae were destroyed gaining access to and from the east bank of the River would be difficult.

Between Colliers junction and Mangamahu there are 6 bridging points over the River, all providing access to property and dwelling houses on the west bank of the River. These bridges mostly abut a *c.* 450 B.P. lahar surface. If these bridges were destroyed, and a bridge at Manawaimai (S21/173667) which abuts a *c.* 1,850 year old surface, the local population on the west bank of the River would effectively be isolated.

The village of Mangamahu is largely constructed on Tangatu and Holocene-aged (both *c.* 10,000 years B.P., see Plate 1.3) surfaces. The risk from lahars is not so high in these areas. However access to dwelling houses, agricultural and horticultural land on the west bank of the River is via a bridge abutting a *c.* 450 year old lahar surface. The Whangaehu Valley Road has been cut through these deposits on the east side of this bridging point. At risk here is the bridge and the people living on the west bank of the River.

Below Mangamahu the valley floor of the River widens and is characterised by suites of constructional terraces comprising Onetapu and Tangatu Formation lahar deposits. The youngest lahar to have spilled out onto the lower Onetapu surface is *c.* 450 years B.P. The lower Onetapu and upper Tangatu lahar surfaces mapped here are used primarily for grazing and cropping. The potential loss of productive farm land in this area, if inundated by a lahar (which is likely to happen once in every 500 years on the lower terrace), renders this a high risk zone.

The highest lahar hazard zone below Wyley's Bridge is inundation by one lahar every ten years, restricted to the channel of the River. Otherwise lahar surfaces in this lower region have not been impacted by lahars in the past 10,000 years. In the lower reaches

of the catchment the risk from lahars is lower; and in fact the risk from normal river floods is likely to be much higher. However it must be remembered that the 1861 lahar was of sufficient magnitude (estimated to be 6×10^6 m^3) in this distal locality to sweep away the road bridge at Whangaehu. Both State Highway 3 and the Marton New Plymouth Railway cross the River in this vicinity, and these bridging points must be considered highly vulnerable zones.

Finally, the lahar risks discussed so far are related to their impact on the existing infrastructure in the Whangaehu Valley. However, a further application of the lahar hazard assessment presented here involves assessing the lahar risk for prospective future infrastructure developments.

Recently a proposal to locate a hydro electric power scheme on the Whangaehu River solicited an immediate inquiry into the lahar hazard in the River. The scheme involves an upper section drawing water from the Mangaehuehu tributary, away from the path of recent lahars. However, the proposed Karioi Power Station in the upper section, below the Mangaehuehu confluence, and the entire lower section involving a tunnel and the Whangaehu Power House, are all in the direct route along which 19 lahars have flowed in the past 130 years. It is here considered that the risk from lahars on this scheme would be extremely high, and this author recommends that the scheme should not proceed.

CHAPTER 10

CONCLUSIONS

10.1 SYNOPSIS

This study was designed to reconstruct the lahar history in the Whangaehu River downstream of Tangiwai and to study the origins and modes of emplacement of lahars in the catchment. Three main methods of investigation were employed to achieve these objectives. These included:

1. Detailed field mapping and description of lahar deposits currently exposed in the River valley.

2. Dating of these deposits using coverbed stratigraphy and/or radiocarbon dating of organic material found beneath, within or above the deposits.

3. Compiling a record of the sedimentology of each deposit, the likely triggering mechanisms of the initiating lahar, and the mode of emplacement of each lahar deposit.

From the information gathered in this study a stratigraphic record has been established for all Whangaehu River lahars during the past *c.* 180,000 years. Episodes of laharic activity are recognised by the distinctive lithology and similar age of their deposits. Newly defined Whangaehu Formation, and formerly defined Te Heuheu, Tangatu, Manutahi, Mangaio and Onetapu Formations are described and interpreted in this study. Two new informally named deposits - the Mangatipona pumice sand and Apitian lahars - are also recognized. Each of these suites of deposits corresponds to a period of lahar aggradation in the Whangaehu River.

The earliest historic lahar is reported on February 16, 1861, and this study has established that 18 subsequent lahars have occurred in the Whangaehu River.

The intention of this chapter is to conclude the findings of this study by reconstructing the lahar history of the Whangaehu River. Finally, suggestions for future avenues of research are proposed.

10.2 LATE QUATERNARY LAHARS IN THE WHANGAEHU RIVER: A RECONSTRUCTION

The occurrence, volumes, ages, and probable causes of Whangaehu River lahars are detailed in Table 10.1, this forming the basis of the discussion which follows.

The oldest lahar deposits recognized in this study are included in the newly defined Whangaehu Formation. The Formation comprises Mount Ruapehu-sourced upper Pleistocene gravel- and sand-dominated diamictites which extend from the southern sector of the Mount Ruapehu ring plain for over 160 km to the coastal plains near the mouth of the Whangaehu River.

Lithofacies identified within the Formation include (1) bouldery, (2) pebbly, and (3) sandy diamictites. Bouldery diamictites, commonly up to 30 m thick, dominate Formation deposits in localities close to the volcano. These are considered to have been emplaced by a single catastrophic debris flow resulting from the collapse of the south flank of the volcano. The absence of megaclasts precludes this deposit being that of a debris avalanche, although diagnostic lithofacies may be buried beneath younger diamictites closer to the volcano. Pebbly and sandy diamictites comprise veneer and distal deposits and are interpreted to represent smaller debris flows and hyperconcentrated flows emplaced after the initial catastrophic event. The presence of pumice lapilli and blocks, and volcanic bombs in the upper beds implies that the collapse was followed by Plinian eruptive activity at the volcano.

Near to the coast the Formation is confined within a valley cut in the Ngarino marine terrace. This valley was cut subsequent to 180,000 years ago, providing a maximum age for the Formation. A minimum age is provided by overlying loess and tephra coverbeds which indicate the Formation was deposited prior to accumulation of Marton

loess, *c.* 140,000 years ago. The total preserved volume of deposits in the Whangaehu Formation is 0.7 km^3, although the projected original volume of material emplaced is estimated to have been at least 1.2 km^3.

Bouldery diamictites are also recognized in the Hautapu Valley (the Hautapu Valley Agglomerate) and the Mangawhero Valley. Coverbeds overlying both suites of deposits indicate that they were both emplaced prior to the Last Interglacial, *c.* 120,000 years ago. They are here both considered to be correlatives of the Whangaehu Formation.

For the next 123,000 years following emplacement of the Whangaehu Formation this study found no evidence that lahars had flowed down the Whangaehu River, although upper Pleistocene-aged lahar deposits recognized on the western ring plain demonstrate that Mount Ruapehu was probably active during this time interval.

The next youngest lahar deposit recognized in the Valley is the Mangatipona pumice sand. This deposit is recognized at only one locality, and comprises clast-supported pumice sands and granules, and is here considered to have been emplaced by a hyperconcentrated flow. The clasts within the deposit are dominantly dacitic, and the emplacing lahar is likely to have originated as a pyroclastic flow from Mount Ruapehu which transformed to a lahar as it was assimilated into the existing river water draining the Volcano. Charcoal found within the deposit was dated at *c.* 37,000 years B.P.

Pebbly diamictons overlying Ratan gravels, thus post-dating the Ratan stadial, and overlain by Ohakean loess, thus predating the Ohakean stadial, are here informally named the Apitian lahars. These diamictons are pumiceous and here are interpreted to have been emplaced by hyperconcentrated flows, resulting from lahars triggered by eruptive activity at Mount Ruapehu. Lower and upper ages for these lahar deposits are *c.* 30,000 and 25,500 years B.P., and thus they are considered to have accumulated entirely within the Apitian interstadial.

The Te Heuheu Formation comprises Mount Ruapehu-sourced gravelly andesitic diamictons and diamictites which form the major constructional surfaces of the southeastern Mount Ruapehu ring plain. The Formation is not widely distributed in the

middle and lower Whangaehu River catchment. The wider distribution of Te Heuheu Formation on the southeast ring plain and in the Hautapu River Catchment implies that, at this time, the Hautapu River drained the southeast flank of Mount Ruapehu and that the majority of Te Heu heu Formation lahars flowed down this River's valley. This route was effectively cut off by faulting along the Whangaehu escarpment, *c.* 14,700 years ago, uplifting land to the east and beheading the headwaters of the Hautapu River.

Bouldery deposits dominate exposures of Te Heuheu Formation diamictites on the southeast ring plain, with finer-grained pebbly deposits observed in exposures on the southern edge of the ring plain. The Formation is considered to have been emplaced by debris flows triggered by both eruptions and sector collapses at Mount Ruapehu. In this study the Formation is considered to have been emplaced entirely within the last (Ohakean) stadial, with lahar propagation augmented by ablation of the more extensive glaciers on the Volcano at this time.

The Tangatu Formation comprises Mount Ruapehu-sourced andesitic and dacitic diamictons, which extend from the southeast ring plain to the lower catchment of the Whangaehu River. Lithofacies identified within this Formation include (1) gravelly and (2) sandy diamictons. Clast-supported deposits, up to 20 m thick, dominate Formation deposits in the upper and middle Catchment of the River, here considered to have been emplaced mainly by hyperconcentrated flows. Tangatu Formation deposits are commonly pumiceous and are stratigraphically associated with Bullot Formation tephras. Both these lines of evidence support the contention that the Tangatu Formation accumulated as a result of mobilization of Bullot Formation tephras by high rainfall events.

Lower and upper age limits for the Tangatu Formation are 14,700 and 5,370 years B.P. respectively. The total preserved volume of material emplaced by Tangatu Formation lahars is estimated to be 2.16×10^8 m^3.

Neither of the two next youngest lahar deposits Manutahi nor Mangaio Formations are widely recognized in this study. The virtual absence of deposits correlated to Manutahi Formation is here interpreted to indicate that only small lahars (with one exception - the

Mangaio Formation) occurred between *c.* 5,370 and 1,850 years B.P. when these deposits were emplaced. The total volume of Manutahi Formation deposits is estimated to be 5×10^7 m^3.

The Mangaio Formation is identified by its distinctive yellow-brown clayey matrix. Mangaio Formation was emplaced by an eastward collapse of a hydrothermally altered sector of Mount Ruapehu *c.* 4,600 years ago. In outcrops of the Formation below Tangiwai, clasts are dominantly Mount Ruapehu-sourced lithic andesite, with a few soft altered clasts. These clasts are commonly rounded and are considered to represent downstream fluvial reworking of the Mangaio Formation, and not deposition from the initial sector collapse. The total volume of preserved Mangaio Formation deposits is estimated to be 3.4×10^7 m^3.

The youngest lahar deposits in the Whangaehu Valley, collectively mapped as the Onetapu Formation, comprise Mount Ruapehu-sourced andesitic diamictons which post-date the *c.* 1,850 years B.P. Taupo Ignimbrite. The Formation includes deposits from historic lahars.

Lithofacies within the Formation include (1) bouldery, (2) pebbly and (3) sandy diamictons. Bouldery diamictons, up to 2.4 m thick, are considered to have been emplaced by highly competent debris flows. These deposits are only found in the upper Catchment of the River. Pebbly and sandy diamictons are observed throughout the upper and middle catchment of the River and are interpreted to have been emplaced by lower competence debris flows and hyperconcentrated flows.

Lithologies within the Onetapu Formation are varied. Five main lithological groups were identified. These are (1) gravelly deposits with lithic clasts and a distinctive yellow-grey muddy matrix, (2) gravelly deposits with lithic clasts which are commonly subrounded to rounded, (3) gravelly deposits, with lithic clasts which are commonly rounded, but with a sandy matrix, (4) gravelly deposits containing abundant grey glassy lithic clasts and a distinctive muddy matrix, and (5) sandy pumiceous deposits. These distinguishing characteristics have formed the basis for establishing a stratigraphy for 17 informal members identified within the Formation, each member corresponding to

an individual lahar event.

Recognition of individual members in sequential exposures allows identification further downstream of flow transformations within each lahar as it travelled from source. A transformation from debris flow to hyperconcentrated flow lithofacies is observed in two members, Onh and Onj. Particle size distribution parameters calculated for lahar deposits at selected sites show an overall trend for a reduction in maximum, modal and mean clasts size, and an improvement in sorting with distance downstream. Variations in maximum and modal clast sizes over short distances reflect differences between the thick, highly competent central portion of the debris flows, and their thinner, less competent lateral margins. Improvements in sorting correspond to different lithofacies and can be used (in combination with lithofacies descriptions) to distinguish between debris flows and hyperconcentrated flows.

Velocities and discharges are calculated for selected Onetapu members based on surveyed topographic and stratigraphic cross-sections at four localities in the upper and middle catchment of the River. These show that large prehistoric Onetapu lahars were at least twice, and on occasions were up to twenty times as large as their historic counterparts.

Of the 17 members identified, 7 were sandy and pumiceous. These are considered to have been emplaced either by lahars resulting (1) directly from eruptions at Mount Ruapehu at this time or (2) from the continued remobilization of Bullot Formation tephras. Tephras erupted from Mount Ruapehu during the period of emplacement of Onetapu Formation are named the Tufa Trig Formation. This Formation comprises tephras which are dominantly fine-grained lithic ashes, with few pumice lapilli recorded. It seems more likely that the coarse pumice observed in Onetapu Formation lahars is sourced from the older Bullot Formation tephras mantling the middle flanks of the Volcano, supporting explanation (2), above.

Four members contain common rounded gravels, One, Onf, Onh and Onj (although in member Onj this alluvial content was deposited entirely on the Whangaehu Fan). These are considered to have been emplaced by lahars resulting from catastrophic drainage of

Crater Lake. This lake is considered to have evolved *c.* 2,000 years ago. Large floods resulting from the lake-breakouts eroded into and incorporated fluvial gravels from the bed of the Whangaehu River. Such floods may or may not have been associated with an eruption through Crater Lake.

Outcrops of Member Onj below Tangiwai are characterised by their high content of grey glassy clasts. In the lower catchment these are dominantly scoriaceous. The monolithic nature of these clasts, which are supported in a distinctive grey muddy matrix, indicates that Onj probably originated as an eruption through Crater Lake, triggering catastrophic drainage of Lake water, with an ensuing lahar.

The three remaining members are correlated to historic Onetapu lahars.

There have been 19 lahars in historic times, four of which had total discharges with magnitudes of $\geq 10^6$ m^3. The principal triggering mechanisms for these lahars were probably volcanic eruptions (15 lahars). Four historic lahars resulted from inter-eruptive catastrophic drainage of Crater Lake waters, as exemplified by the 1953 Tangiwai Disaster. However all historic lahars (excluding the 1861 event) were associated with release of Crater Lake water, either due to (1) ice falling into and displacing the Lake water, (2) collapse of the ice and tephra barrier which dams the Lake, or (3) violent ejection of Lake water during eruptions. The presence of Crater Lake in the active vent on Mount Ruapehu has undoubtedly greatly increased the hazard from lahars in the Whangaehu River.

The total volume of preserved Onetapu Formation deposits is estimated to be 4.28×10^7 m^3, and an estimated projected volume of the lahars which emplaced them is 8.55×10^8 m^3.

10.2 SEDIMENTOLOGY OF LAHAR DEPOSITS

The principal lithofacies groups recognized within the formations described in this study are (1) bouldery, (2) pebbly and (3) sandy diamictons and diamictites.

Bouldery lithofacies are interpreted to have been emplaced by highly competent, highly energetic debris flows, and, in this study, are recognised in the Whangaehu and Onetapu Formations. In the Whangaehu Formation, bouldery lithofacies are considered to have been emplaced by a single catastrophic debris flow. In the Onetapu Formation, bouldery lithofacies are not common, and deposits are confined to higher gradient areas of the Mount Ruapehu ring plain. These deposits are interpreted to have been emplaced by lahars that resulted from catastrophic drainage of Crater Lake water. From these lines of evidence it is apparent that the triggering mechanisms which are likely to result in very coarse-grained rapidly flowing lahars are sector collapses and catastrophic lake-breakouts.

Pebbly lithofacies are interpreted to have been emplaced by low competence debris flows and hyperconcentrated flows. In this study these flow types are recognised in all the formations described and are generally considered to have been initiated by eruptions at Mount Ruapehu. There are 3 possible explanations for the finer grain size of these lahars compared to the bouldery deposits described above. These are (1) that large amounts of rapidly flowing water were not available for lahar propagation, (2) the lahars were only able to transport finer-grained material or (3) only finer-grained material was available for transport. The first explanation seems unlikely, because pebbly deposits are commonly observed in Onetapu Formation members which are likely to have been triggered by catastrophic releases of Crater Lake water. However, there is support for the second explanation. This study examined deposits on the edge of the Mount Ruapehu ring plain, and in distal areas within the valley of the Whangaehu River. Plots of maximum and modal clast size in Onetapu Formation debris flow deposits show clearly a reduction in competence with increasing distance downstream as the lahars progressed into the lower gradient reaches of the River's channel. Implicit in the third explanation is that only pebbles and smaller clast-sizes were available for transport. The material transported by lahars has two sources (1) primary eruptives which are directly assimilated into lahars, and (2) pre-existing debris on the flanks of the volcano and in the banks and channel along the lahar flowpath. In proximal areas lahars are recognised to be highly erosive, and indeed may "bulk"

Table 10.1 Occurrence, age, volume and probable cause of lahar events in the Whangaehu River.

Lahar event	Volume	Age (years B.P.)	Triggering event, and mode of emplacement
Onetapu Formation	4.28×10^7 m^3	1,850-present day	*Lahars resulting from catastrophic drainage of Crater Lake in eruptive and inter-eruptive intervals.*
			(Inception of Crater Lake at c. 2,000 years B.P.)
Mangaio Formation	3.4×10^7 m^3	4,940-3,400	*Flank collapse from the southeast flank of Mount Ruapehu, with lahars resulting from the transformation of the collapse event to a debris flow.*
Manutahi Formation	5×10^7 m^3	5,460-3,400	*Lahars resulting from remobilization of Bullot Formation tephra deposits by high rainfall events.*
Tangatu Formation	2.22×10^8 m^3	14,700-5,370	*Sub-Plinian eruptions at Mount Ruapehu, with lahars resulting from high rainfall events. The earlier Tangatu lahars may have resulted from interaction of volcaniclastics with ablating valley glaciers during the transition from glacial to post-glacial conditions.*
Te Heuheu Formation	6×10^9 m^3	25,500-14,700	*Sector collapses and sub-Plinian eruptions at Mount Ruapehu, with lahars resulting from erupted material interacting with more extensive valley glaciers of the last (Ohakean) stadial.*
Apitian lahars	1.8×10^8 m^3	30,000-25,500	*Eruptions at Mount Ruapehu, with lahars triggered by high rainfall events.*
Mangatipona pumice sand	-	37,030 ± 730	*Transformation of a Mount Ruapehu-sourced pyroclastic flow into a lahar by incorporation into existing streamflow.*
			(Between c. 160,000 and 37,000 years ago no lahar deposits recognized in the Whangaehu Valley)
Whangaehu Formation	7×10^8 m^3	180,000-140,000	*Flank collapse from southern sector of the Mount Ruapehu volcanic cone, followed by large scale Plinian eruptive activity. Lahars resulting from transformation of the initial collapse event to a debris flow phase, and from erupted material interacting with the existing drainage, and/or floods caused by high rainfall events.*

considerably by eroding into and incorporating channel and bank alluvium as they flow downstream. Gravelly Onetapu Formation deposits which contain large amounts of ripped-up rounded gravelly alluvium are interpreted to have been emplaced by lahars triggered by catastrophic release of Crater Lake water. However neither rip-up clasts nor outsize clasts are commonly observed in pebbly lithofacies of the Tangatu or Whangaehu Formations. The deposits are comprised principally of common pumice and scoriaceous lithic clasts. It is difficult to prove whether coarser or denser material was available for transport, but the absence of such clasts in these deposits implies that it is unlikely they were, and that even if they had been, the lahars were neither erosive enough nor competent enough to entrain them and transport them. It seems likely from this evidence that the lahars which emplaced pebbly lithofacies in these Formations were not emplaced by catastrophic events (*e.g.* sector collapses, or lake-breakouts) but were emplaced by lahars resulting from the assimilation of erupted material into existing rivers and streams, or mobilization of newly erupted or pre-existing debris by floods resulting from high rainfall events. Thickly stacked sequences of the deposits from these lahars indicate that a continued supply of material for lahar propagation was maintained, probably from continuing eruptions at source.

Sandy lithofacies are interpreted to have been emplaced by low competence hyperconcentrated flow. Evidence of hyperconcentrated flows is commonly observed in sandy lahar deposits examined in this study. The sand is dominantly pumiceous, this implying a genetic association between the initiation of low competence lahars during eruptions. This may reflect the nature of the material available for transport, *i.e.* frequently occurring smaller watery lahars which were readily initiated under conditions of normal drainage, with a continuous supply of relatively easily transported pumiceous material. In this manner hyperconcentrated flows seem able to transport large amounts of sediment away from the volcano, as evidenced in the thick sequences of hyperconcentrated flow deposits observed in this study, especially in the Tangatu Formation.

Hyperconcentrated flow deposits become increasingly abundant in distal lithofacies of all Formations described. This may reflect (1) a reduction in competence of the lahars in lower gradient distal areas leading to a transition from debris flow to hyperconcentrated flow, or (2) that hyperconcentrated flows were able to flow further than the coarser pebbly and bouldery debris flows. The transition within individual flows from debris flow to hyperconcentrated flow could not be directly established for

older Whangaehu and Tangatu Formations. In the Onetapu Formation, however, a progressive downstream change from matrix-supported bouldery and pebbly lithofacies to clast-supported sandy lithofacies, and improvements in sorting values from very poorly to poorly sorted deposits, provide both lithological and sedimentological evidence for this flow transition in two members (Onh and Onj). This supports the first explanation, that hyperconcentrated flow occurs through dilution of the debris flow phase of a lahar. Other Onetapu Formation members were hyperconcentrated throughout their flow history (*e.g.* Ongl-3). Hyperconcentrated flow facies were observed at distances of > 170 km from source in both the Whangaehu and Tangatu Formations, demonstrating that even although these flow types are considered to be low competence they are able to support and transport clasts, albeit dominantly pumice and scoriaceous lithic clasts, over great distances from the volcano, and to transport large volumes of volcaniclastic material away from the volcano.

10.3 THE TEMPORAL PATTERN OF LAHAR ACCUMULATION IN THE WHANGAEHU RIVER AND PREDICTED FUTURE ACTIVITY

For the interval of time between 160,000 years ago to the present day accumulation rates for lahars in the Whangaehu River range from 1 km^3 every 23,191 (maximum) to 42,435 (minimum) years. According to this pattern of accumulation a predicted *c.* 4.3×10^6 m^3 (maximum) or 2.4×10^6 m^3 (minimum) of laharic material could be emplaced in the next 100 years, the maximum value being equivalent to between two and three events on a similar scale to the 1953 and 1975 lahars. However, the pattern of lahar cumulative volumes has accelerated in the past *c.* 2,000 years to 1 km^3 in every 589 years (maximum), or 1 km^3 in every 1,700 years (minimum). According to this pattern an estimated 1.7×10^8 m^3 (maximum) to 5.9×10^7 m^3 (minimum) volume of lahars could be anticipated over the next 100 years, this representing 170 (minimum) to 59 (minimum) lahars of the 10^6 m^3 magnitude. The total volume of historic lahars is estimated to be 1×10^7 m^3, which is $^1/_6$ the minimum value for lahar cumulative volumes predicted by the record of the past 2,000 years. It is now *c.* 450 years since the last lahar of 10^7 m^3 (Onj). Hence, in the past 450 years, lahar accumulation appears to have slowed down. The recurrence interval for lahars of 10^7 m^3 is 208 ± 292 years, and another event could be expected in the next 100 years.

10.4 ENVOI

The information gathered in this study shows that the Whangaehu River has for a long time been subjected to the impacts of lahars, ranging from large magnitude events of 10^8 - 10^9 m^3, to much smaller lahars with magnitudes of 10^3 m^3. It is possible, through close examination of the lahar deposits, to distinguish between lahar events with different triggering mechanisms. These mechanisms include flank collapses, volcanic eruptions and catastrophic drainage of Crater Lake.

The deposits from flank collapses commonly form thick bouldery deposits, exemplified by coarse-grained diamictites recognized in both the Whangaehu and Te Heuheu Formations. Although events of the magnitude of the Whangaehu and Te Heuheu lahars have not occurred frequently, any recurrence would have disastrous impacts, encompassing the whole of the Whangaehu Valley.

The initial sector collapse which emplaced the bouldery marginal lithofacies of the Whangaehu Formation was followed by eruptions at Mount Ruapehu, and ensuing eruption-triggered lahars. Deposits of these lahars are pebbly and pumiceous. However, the best examples of eruption-triggered lahars are observed in the Tangatu Formation which is dominated by thick aggradational sequences of pumice-rich pebbly and sandy deposits. Lake breakout lahars, which are considered to have occurred frequently in the past *c.* 2,000 years, may display characteristics of both flank collapse-triggered lahars (*e.g* deposits which contain coarse-grained clasts) and eruption-triggered lahars (*e.g* deposits which contain pumiceous clasts). In proximity to the volcano lake-breakout lahars were highly erosive and were able to rip-up gravelly alluvium from the river channel. However they also incorporated loose debris, *i.e.* previously erupted tephra, lying on the flanks and ring plain of Mount Ruapehu.

In the past 2,000 years the lahar accumulation rate has greatly accelerated as a result of the development of Crater Lake, and the introduction of a new triggering mechanism for lahars. These lahars occur frequently, without warning, and thus present a very high risk to lives and property in the Whangaehu Valley.

10.5 FUTURE WORK

1. Establishing a more detailed chronology, and consequently total volumes (and projected volumes) for individual lahar events within Tangatu, Te Heuheu and Whangaehu Formations would greatly improve the hazard assessment for lahars in the Valley. One immediate improvement would be the reduction in standard deviation for calculated lahar recurrence intervals. This author did not find any datable material in the Tangatu and Te Heuheu Formations, both of which lie within the range for radiocarbon dating. The free draining, aerobic conditions common to lahar deposits in the catchment do not favour preservation of organic material, and the casts of branches and twigs were commonly observed in Tangatu Formation. Therefore, although radiocarbon dating of the youngest Onetapu Formation lahar deposits successfully established a detailed chronology for these events, some other technique is required for older deposits, *e,g.* Argon/Argon dating of primary mineral phases of pumice clasts.

2. At present the association between Bullot tephras and Tangatu lahars is well established on stratigraphical evidence. However, determining a direct link between these eruptions and lahar initiation in both the Te Heuheu and Tangatu Formations would provide further evidence of the secondary impacts of eruptions at Mount Ruapehu and at great distances from the Volcano. The possible genetic relationship between the Bullot tephras and both Te Heuheu and Tangatu lahars could be established through mineralogical fingerprinting of primary mineral phases and glass in pumice clasts within both the tephra and lahar deposits.

3. During field mapping in this study in the Whangaehu River Valley landslides were commonly recognized (see Maps 2-6) throughout the whole catchment. In the north of the middle catchment landslides occur where the underlying Whangaehu Formation and underlying siltstone have been deeply incised by the Whangaehu River. These features were estimated to be late Pleistocene in age, and possibly post-date the Kawakawa Tephra. Small lakes have ponded behind slump blocks, and marshes developed where the River was forced to change its

course when dammed by landslide material. In the middle and lower catchment landsliding has occurred in both Tertiary and Quaternary siltstones and sandstones. At present the Whangaehu Valley Road is often rendered impassable by slips. In 1961 a landslide blocked the Whangaehu River at Taonui, *c.* 30 km upstream of Mangamahu. This small landslide occurred at the toe of a much larger landslide. In the coastal reach of the catchment landslides occur in Quaternary sandstones and siltstones and Whangaehu Formation diamictites. In one example, at the north end of Ruatangata Road a landslide blocked the channel of the Whangaehu River, which was then redirected further west. The earlier channel is now a marsh. South of the junction of Kauangaroa and Budge Road a landslide in Whangaehu Formation diamictites resulted in two small lakes ponding behind slump blocks. Coring of lake sediments at both the sites discussed here might provide means of dating these events. Determining their triggering mechanisms would complete a landslide hazard assessment for the Valley. The risk from landslides should be considered in any plans for hydro electric power schemes in the Whangaehu Valley.

REFERENCES

Allen, G. F. 1894. Willis' Guide Book of New Routes for Tourists. Willis, Wanganui, 200pp.

Allen, G. F. 1949. Activity at Nguaruhoe, April-May, 1948. *New Zealand Journal of Science and Technology*, Vol. B30, p. 187-193.

Alloway, B. V. 1989. Late Quaternary coverbed stratigraphy and tephrochronology of Northeastern and Central Taranaki, New Zealand. Unpublished Ph.D Dissertation, Massey University, New Zealand.

Alloway, B. V., Stewart, R. B., Neall, V. E. and Vucetich, C. G. 1992. Climate of the last glaciation in New Zealand, based on aerosolic quartz influx in an andesitic terrain. *Quaternary Research*, Vol. 38, p. 170-179.

Alloway, B. V., Neall, V. E. and Vucetich, C. G. 1987. *Localised volcanic loess deposits in North Taranaki, North Island, New Zealand.* In Eden, D.N. and Furkert, R.J. eds, Loess: Its distribution, geology and soils, Proceedings of an International Symposium on loess, New Zealand 14-21 February, 1987, Balkema, Rotterdam.

Apmann, R. P. 1973. Estimating discharge from superelevation in bends. *Journal of the Hydraulics Division, Proceedings of the American Society of Civil Engineers*, Vol. 99, No. HY1, p. 65-79.

Arguden, A. T. and Rodolfo, K. S. 1990. Sedimentologic and dynamic differences between hot and cold laharic debris flows of Mayon Volcano, Philippines. *Geological Society of America Bulletin*, Vol. 102, p. 865-876.

Bagnold, R. A. 1955. Some flume experiments on large grains but little denser than the transporting fluid, and their implications. *Institute of Civil Engineers*, Proceedings Paper No. 6041, p. 184.

Beck, A. C. 1951. Volcanic Activity at Mount Ruapehu from August to December, 1945. *New Zealand Journal of Science and Technology*, Vol. B31, No. 5, p. 1-13.

Berryman, K. A. 1992. Stratigraphic age of Rotoehu Ash and Pleistocene climate interpretation based on marine terrace chronology, Mahia Peninsula, North Island, New Zealand. *New Zealand Journal of Geology and Geophysics*, Vol. 35, p. 1-7.

Beu, A. G. 1969. Index macrofossils and New Zealand Pliocene and lower Pleistocene time-stratigraphy. *New Zealand Journal of Geology and Geophysics*, Vol. 12, No. 4, p. 643-658

Beu, A. G. and Edwards, A. R. 1984. New Zealand Pleistocene and late Pliocene glacio-eustatic cycles. *Palaeogeography, Palaeoclimatology, Palaeoecology*, Vol. 46, p. 119-142.

Beverage, J. P. and Culbertson, J. K. 1964. Hyperconcentrations of suspended sediment: *Journal of the Hydraulics Division, Proceedings of the American Society of Civil Engineers*, Vol. 90, No. HY6, p. 117-128.

Bogie, D. 1989. Volcano Watch. *"Tongariro" The Journal of Tongariro National Park*, No.34, summer 1988-89, p. 22-25

Borius, S. and Salazar, O. 1973. The 1971 and 1973 eruptions of Volcan Fuego, Guatemala and some socio-economic considerations for the volcanologist. *Bulletin Volcanologique*, Vol. 37, No. 3, p. 394-400.

Bowles, F. A. 1975. Palaeoclimatic significance of quartz/illite variations in cores from the Eastern Equatorial North atlantic. *Quaternary Research*, Vol. 5, p. 225-235.

Bussell, M. R. 1992. Late Pleistocene palynology of terrestrial cover beds at the type section of the Rapanui Terrace, Wanganui. *Journal of the Royal Society of New Zealand*, Vol. 22, No. 2, p. 77-90.

Bussell, M. R. and Pillans, B. 1992. Vegetational and climatic history during oxygen isotope stage 9, Wnaganui district, New Zealand, and correlation of the Fordell Ash. *Journal of the Royal Society of New Zealand*, Vol. 22, No. 1, p. 41-60.

Campbell, I. B. 1977. Soils of part Wanganui County, North Island, New Zealand. *New Zealand Soil Bureau Bulletin* 40, 99pp.

Campbell, I. B. 1973. Recent Aggradation in Whangaehu Valley, Central North Island, New Zealand. *New Zealand Journal of Geology and Geophysics*, Vol. 16, No. 3, p. 643-649.

Cole, J. W. and Nairn, I. A. 1975. *Part XXII New Zealand*, in Active volcanoes of the world including solfatara fields. International Association of Volcanology and Chemistry of the Earths Interior, Naples, 156pp.

Cole, J. W., Graham, I. J., Hackett, W. R. and Houghton, B. F. 1986. Volcanology and Petrology of the Quaternary Composite Volcanoes of Tongariro Volcanic Centre, Taupo Volcanic Zone. *Royal Society of New Zealand Bulletin* 23, p. 224-250,

Costa, J. E. 1988. Rheologic, geomorphic, and sedimentologic differentiation of water floods, hyperconcentrated flows and debris flows. In, Baker, V.R.; Kochel, R.C. and Patton, P.C. *eds.*, Flood Geomorphology. New York: John Wiley and Sons, p. 113-122.

~~Cotton, C. A. 1945. Ruapehu in 1945. *New Zealand Science Review*, Vol. 3, p. 3-4.~~

Cotton, C. A. 1946. The 1945 eruption of Ruapehu. *Geographical Journal*, Vol. 107, p. 140-143.

Cowan, J. 1927. The Tongariro National Park, New Zealand. Tongariro National Park Board, Wellington, 156pp.

Cowie, J. D. 1964. Aokautere Ash in the Manawatu District, New Zealand. *New Zealand Journal of Geology and Geophysics*, Vol. 2, p. 569-577.

Crandell, D. R. 1963a. Paradise Debris flow at Mount Rainier, Washington. *United States Geological Survey Professional Paper* 475-B, p. .

Crandell, D. R. 1971. Postglacial Lahars from Mount Rainier Volcano, Washington. *United States Geological Survey Professional Paper* 677, 73pp.

Crandell, D. R. 1980. Recent Eruptive history of Mount Hood, Oregon, and Potential Hazards from Future Eruptions. *United States Geological Survey Bulletin* 1492, 48pp.

Crandell, D. R. 1988. Gigantic debris avalanche of Pleistocene age from Ancestral Mount Shasta Volcano, California, and debris avalanche hazard zonation. *United States Geological Survey Bulletin* 1861, 32pp.

Crandell, D. R. and Waldron, H. H. 1956. A Recent volcanic Mudflow of Exceptional Dimensions from Mount Rainier, Washington. *American Journal of Science*, Vol. 254, p. 349-362.

Crandell, D. R. and Fahnstock, R. K. 1965. Rockfalls and Avalanches from Little Tahoma Peak on Mount Rainier, Washington. *United States Geological Survey Bulletin* 1221-A, 30pp.

Crandell, D. R. and Mullineaux. 1967. Volcanic Hazards at Mount Rainier, Washington. *United States Geological Survey Bulletin* 1238, 26pp.

Crandell, D. R. and Mullineaux, D. R. 1975. Technique and Rationale of volcanic hazards appraisals in the Cascades Range, Northwestern United States. *Enviromental Geology*, Vol. 1, p. 23-32.

Crandell, D. R., Miller, C. D., Glicken, H. X., Christiansen, R. L. and Newhall, C. G. 1984. Catastrophic debris avalanche from ancestral Mount Shasta volcano, Califonia. *Geology*, Vol. 12, p. 143-146.

Crawford, J. C. 1870. On the Geology of the Province of Wellington. *Transactions of the New Zealand Institute*, Vol. 2, p. 342-360.

~~Cummans, J. 1980. Mudflows resulting from the May 18, 1980, eruption of Mount St. Helens, Washington. *United States Geological Survey Circular* 850-B, p. 479-486.~~

Cussen, L. 1887. Thermal activity in the Ruapehu Crater. *Transactions of the New Zealand Institute*, Vol. 19, p. 374-380.

Donoghue, S.L. 1988. Holocene geology of the Upper Whangaehu River, Mount Ruapehu. *Geological Society of New Zealand Miscellaneous Publication* 41a, p. 61.

Donoghue, S. L. 1991. Late Quaternary volcanic stratigraphy of the Southeastern sector of the Mount Ruapehu ring plain, New Zealand. Unpublished Ph.D Dissertation, Massey University.

~~Donoghue, S. L., Hodgson, K. A., Neall, V. E., and Palmer, A. S. 1991. Volcanic hazards - Southeastern ring plain of Ruapehu Volcano. *Geological Society of New Zealand Miscellaneous Publication* 59B.~~

Dunnage, W. H. 1895. An ascent of Mount Ruapehu. *Appendix to the Journal of the New Zealand House of Representatives*, Vol. C-1, p. 70.

Dunnage, W. H. 1886. Notes on the Crater Lake of Ruapehu. *Appendices of the Journal of the House of Representatives of New Zealand*, Vol. 1A, p. 16.

Escher, B. G. 1922. On the "lahar" (mudflow) of the Valley of Ten Thousand Smokes (Alaska). *Proceedings of the Royal Academy of Amsterdam*, Vol. 24, p. 282-293.

Emiliani, C. 1955. Pleistocene temperatures. *Journal of Geology*, Vol. 63, p. 538-578.

Enos, P. 1977. Flow regimes in debris flow. *Sedimentology*, Vol. 24, p. 133-142.

~~Fisher, R. V. 1971. Features of coarse-grained, high-concentration fluids and their deposits. *Journal of Sedimentary Petrology*, Vol. 41, No. 4, p. 916-927.~~

Fleming, C. A. 1953. The Geology of Wanganui Subdivision. *New Zealand Geological Survey Bulletin* n.s. 52. 362pp.

Fowles, C. R., Barnett, H.I . and Malone, M. J. 1975. Eruptions of Crater Lake, Mount Ruapehu, April 1975. Report to Rangitikei-Wanganui Catchment Board, 12pp.

Francis, P. W., Gardeweg, M., Ramirez, C. F., Rothery, D .A. 1985. Catastrophic debris avalanche deposit of Socompa Volcano, northern Chile. *Geology*, Vol. 13, p. 600-603.

Froggatt, P. C. 1981. Motutere Tephra Formation and redefinition of Hinemaiaia Tephra Formation, Taupo Volcanic Centre, New Zealand. *New Zealand Journal of Geology and Geophysics*, Vol. 24, p. 99-105.

Froggatt, P. C. and Lowe, D. J. 1990. A review of late Quaternary silicic and some other tephra formations from New Zealand: their stratigraphy, nomenclature, distribution, volume and age. *New Zealand Journal of Geology and Geophysics*, Vol. 33, p. 89-109.

Gorshkov, G. S. and Dubik, Y. M. 1970. Gigantic directed blast at Shiveluch Volcano (Kamchatka). *Bulletin Volcanologique*, Vol. 34, No. 1, p. 261- 288.

Gorshkov, G. S. 1959. Gigantic eruption of the Volcano Bezymianny. *Bulletin Volcanologique*, Vol. 20, p. 77-109.

Grange, L. I. 1931. Conical hills on Egmont and Ruapehu volcanoes. *New Zealand Journal of Science and Technology*, Vol. 12, p. 376-384.

Gregg, D. R. 1960. The Geology of Tongariro Subdivision. *New Zealand Geological Survey Bulletin* n.s. 40.

Grindley, G. W. 1960. Sheet 8 Taupo 1:250,000 Geological Map of New Zealand. New Zealand Geological Survey.

Hackett, W. R. 1985. Geology and Petrology of Ruapehu Volcano and related vents. Unpublished PhD thesis, Victoria University of Wellington, New Zealand.

Hackett, W. R. and Houghton, B. F. 1989. A facies model for a Quaternary andesite composite volcano: Ruapehu, New Zealand. *Bulletin of Volcanology*, Vol. 52, p. 51-68.

Hampton, M. A. 1979. Buoyancy in debris flows. *Journal of Sedimentary Petrology*, Vol. 49, No. 3, p. 753-758.

Harris, R. W. 1954. Report on flood - Whangaehu River. Rangitikei Catchment Board, 6pp.

Harrison, S. and Fritz, W. J. 1982. Depositional features of March 1982 Mount St. Helens sediment flows. *Nature*, Vol. 299, p. 720-722.

Hay, R. F. 1967. 1:250,000 Geological map of New Zealand Sheet 7 Taranaki. New Zealand Geological Survey.

Haydon, J. P., Harris, R. W. and Bell, O. D. 1953. Preliminary Report on the Whangaehu River flood of the 24th. December 1953. Rangitikei/Wanganui District Council, 3pp.

Healy, J, Lloyd, E. F., Rishworth, D., Wood, C. D., Glover, R. B. and Dibble, R. R. 1978. The eruption of Ruapehu, New Zealand, on 22 June 1969. *New Zealand Department of Scientific and Industrial Research Bulletin* 224, 88pp.

Hill, H. 1895. Ruapehu- a retrospect and prospect. *New Zealand Alpine Journal*, Vol. 2, p. 76-82.

Hill, H. 1896. Ruapehu and the Volcanic Zone in 1895. *Transactions of the New Zealand Institute*, Vol. 37, p. 445-464.

Hoblitt, R. P., Miller, C. D. and Scott, W. E. 1987. Volcanic hazards with regard to siting nuclear-power plants in the Pacific Northwest. *United States Geological Survey Open-File Report* 87-297, 196pp.

Houghton, B. F, Latter, J. H. and Hackett, W. R. 1987. Volcanic hazard assessment for Ruapehu composite volcano, Taupo Volcanic Zone, New Zealand. *Bulletin of Volcanology*, Vol. 49, p. 737-751.

Imbrie, J., Hays, J. D., Martinson, D. G., McIntyre, A., Mix, A. C., Morley, J. J., Pisias, N. G., Prell, W. L. and Shackleton, N. J. 1984. The orbital theory of Pleistocene climate: support from a revised chronolgy of the marine $\delta\ ^{18}O$ record. In, A. L. Berger *et al. eds.*, Milankovitch and climate, Part 1, p. 269-305. D. Reidel Publishing Company.

Janda, R. J., Scott, K. M., Nolan, K. M. and Martinson, H. A. 1981. Lahar movement, effects, and deposits, in Lipman, P. W. and Mullineaux, D. R., eds., The 1980 eruptions of Mount St. Helens, Washington. *United States Geological Survey Professional Paper* 1250, p. 461-478.

Johnson, A. M. 1970. Physical processes in geology. San Francisco, Freeman, Cooper and Co., 577pp

Johnson, P. R. and Beavers, A. H. 1959. A mineralogical classification of some loess-derived soils in Illinois. *Soil Science Proceedings*, p. 143-146.

Keys, H. 1991. Glacier ice collapse. *"Tongariro" The Journal of Tongariro National Park*, No. 39, summer 1990/91, p. 14-15.

Kohn, B. P., Pillans, B and McGlone, M. S. 1992. Zircon fission track age for middle Pleistocene Rangitawa Tephra, New Zealand: Stratigraphic and palaeoclimatic significance. *Palaeogeography, Palaeoclimatology, Palaeoecology*, Vol. 95, p. 73-94.

Latter, J. H. 1985. Frequency of eruptions at New Zealand volcanoes. *Bulletin of the New Zealand National society for Earthquake Engineering*, Vol. 18, No. 1, p. 55-110.

Lensen, G. J. 1959. Sheet 10 Wanganui 1:250,000 Geological Map of New Zealand Sheet. New Zealand Geological Survey.

Lowe, D. R. 1975. Water escape structures in coarse-grained sediments. *Sedimentology*, Vol. 22, 157-204.

1974.

Lowe, D. R. and LoPiccolo, R. D. The characteristics and origins of dish and pillar structures: *Journal of Sedimentary Petrology*, Vol.44, No. 2, p. 484-501.

Lowe, D. R., Williams, S. N., Leigh, H., Connor, C. B. and Gemmell, J. B. 1986. Lahars initiated by the 13 November 1985 eruption of Nevado del Ruiz, Colombia. *Nature*, Vol. 324, p. 51-53.

M^{c}Arthur, J. L. and Shepherd, M. J. 1990. Late Quaternary glaciation of Mount Ruapehu, North Island, New Zealand. *Journal of the Royal Society of New Zealand*, Vol. 20, No. 3, p 287-296.

Major, J. J. and Newhall, C. G. 1989. Snow and ice perturbation during historical volcanic eruptions and the formation of lahars and floods. *Bulletin of Volcanology*, Vol. 52, p. 1-27.

Marden, M. and Neall, V. E. 1990. Dated Ohakean terraces offset by the Wellington Fault, near Woodville, New Zealand. *New Zealand Journal of Geology and Geophysics*, Vol. 33, p. 449-453.

Middleton, G. V. 1970. Experimental studies related to problems of flysch sedimentation. In, Lagoie, J. *ed.* Flysch Sedimentology in North America. *Geological Association of Canada Special Paper 7*, p. 253-272.

Milne, J. D. G. 1973a. Upper Quaternary geology of the Rangitikei drainage basin, North Island, New Zealand. Unpublished Ph.D thesis, Victoria University, New Zealand.

Milne, J. D. G. 1973b. Maps and sections of river terraces in the Rangitikei Basin, North Island, New Zealand. *New Zealand Soil Survey Report*, 4

Milne, J. D. G. and Smalley, I. J. 1979. Loess deposits in the southern part of the North Island of New Zealand: an outline stratigraphy. *Acta Geologica Academiae Scientiarum Hungaricae*, Vol. 22 No. 1-4, p. 197-204.

Mitchell, B. D., Smith, B. F. L. and de Endredy, A. S. 1971. The effect of buffered sodium dithionite solution and ultrasonic agitation on soil clays. *Israel Journal of Chemistry*, Vol. 9, p. 45-52.

Morris, B. 1981. Tangiwai tragedy that stunned a nation. In *Darkest Days*, Auckland, Wilson and Horburn, Ltd.

Mullineaux, D. R. and Crandell, D. R. 1962. Recent lahars from Mount St. Helens, Washington. *Geological Society of America Bulletin*, Vol.73, p. 855-870.

Mullineaux, D. R., Miller, C. D. and Harlow, D. 1976. Reconnaissance study of volcanic hazards from Cotopaxi Volcano, Ecuador. *United States Geological Survey Project Report (IR)EC-5*, 20pp.

Nairn, I. A., Wood, C. P. and Hewson, C. A. Y. 1979. Phreatic eruptions of Ruapehu: April 1975. *New Zealand Journal of Geology and Geophysics*, Vol. 22, No. 2, p. 155-173.

Nairn, I. A. 1971. Rotoehu Ash and the Rotoiti Breccia Formation, Taupo Volcanic Zone, New Zealand. *New Zealand Journal of Geology and Geophysics*, Vol. 15, No. 2, p. 251-261.

Nairn, I. A., Scott, B.J. and Otway, P. M. 1988. Ruapehu Crater Lake Inspection and Eruption Investigations: December 9 1988. *New Zealand Geological Survey Immediate Report*, 7pp.

Naylor, M. A. 1980. The origin of inverse grading in muddy debris flow deposits - A review. *Journal of Sedimentray Petrology*, Vol. 50, No. 4, p. 1111-1116.

Neall, V. E. 1976a. Lahars as major geological hazards. *Bulletin of the International Association of Engineering Geology*, No. 14, p. 233-240.

Neall, V. E. 1976b. Lahars - Global occurrence and annotated bibliograpy. Publication of the Geology Department, Victoria University of Wellington, New Zealand. No.5, 18pp.

Nemec, W. and Steel, R. J. 1984. Alluvial and coastal conglomerates: their significant features and some comments on gravelly mass-flow deposits. In, Koster, E.H. and Steel, R.J. *eds*, Sedimentology of Gravels and Conglomerates. *Canadian Society of Petroleum Geologists Memoir* 10, p. 1-31.

O'Shea, B. E. 1954. Ruapehu and the Tangiwai Disaster. *New Zealand Journal of Science and Technology*, Vol. B36, p. 174-189.

Oliver, R. L. 1945. Further activity of Mount Ruapehu, New Zealand, May-July, 1945. *New Zealand Journal of Science and Technology*, Vol. B27, p. 24-32.

Otway, P. M., Scott, B. J. and Nairn I. A. 1991. Summary of Crater Lake Inspections 1988-91. *New Zealand Volcanological Record*.

Palmer, B. A. 1991. Holocene lahar deposits in the Whakapapa catchment, Northwestern ring plain, Ruapehu Volcano (North Island, New Zealand). *New Zealand Journal of Geology and Geophysics*, Vol. 34, p. 177-190.

Palmer, B. A. and Neall, V. E. 1989. The Murimotu Formation - 9,500 year old deposits of a debris avalanche and associated lahars, Mount Ruapehu, North Island, New Zealand. *New Zealand Journal of Geology and Geophysics*, Vol. 32, p. 477-486.

Palmer, B. A. and Walton, A. W. 1990. Accumulation of volcaniclastic aprons in the Mount Dutton Formation (Oligocene-Miocene), Marysville volcanic field, Utah. *Geological Society of America Bulletin*, Vol. 102, p. 734-748.

Palmer, B. A., Alloway, B. V. and Neall, V. E. 1991. Volcanic-debris-avalanche deposits in New Zealand - lithofacies organization in unconfined, wet-avalanche flows. In R. V. Fisher and G. A. Smith *eds*, Sedimentation in Volcanic Settings, *Society for Sedimentary Geology (SEPM) Special Publication* No. 45., p. 89-98.

Palmer, B. A., Purves, A. M. and Donoghue, S. L. (1993) Controls on accumulation of a volcaniclastic fan, Ruapehu composite volcano, New Zealand. *Bulletin of Volcanology*, Vol. 55, p. 176-189.

~~Park, J. 1887. Narrative of an ascent of Ruapehu. *Transactions of the New Zealand Institute*, Vol. 19, p. 327-331.~~

Park, J. 1910a. On the glacial till in Hautapu Valley, Rangitikei, Wellington. *Transactions of the New Zealand Institute*, Vol. 42, p. 575-580.

Park, J. 1910b. The great Ice Age of New Zealand. *Transactions of the New Zealand Institute*, Vol. 42, p. 589-612.

Park, J. 1926. Morainic mounds on the Waimarino Plain near Ruapehu. *Transactions of the New Zealand Institute*, Vol. 56, p. 382-383.

Paterson, B. R. 1976. The effects of the lahars from the 1975 April Mount Ruapehu eruption and the threat of future eruptions on Tongariro Power Development. *New Zealand Geological Survey Unpublished Geology Report* EG 230.

Phillippe, M. M. and White, J. L. 1950. Quantitative estimation of minerals in the fine sand and silt fractions of soild with the geiger counter X-Ray spectrometer. *Soil Science Society proceedings*, p. 138-142.

PHI VOLCS (Philippine Institute of Volcanology and Seismology). 1992a. Pinatubo: Lava dome extruded into caldera lake; small steam-and-ash ejections;lahars and secondary explosions. *Bulletin of the Global Volcanism Network*, Vol. 17, No. 6, p.7-8.

PHI VOLCS (Philippine Institute of Volcanology and Seismology). 1992b. Pinatubo: Lava dome growth; pyroclastic flow deposits spawn destructive lahars and secondary explosions. *Bulletin of the Global Volcanism Network*, Vol. 17, No. 9, p. 8-10.

PHI VOLCS (Philippine Institute of Volcanology and Seismology). 1993a. Mayon: Eruption continues; pyroclastic flows; lava extrusion. *Bulletin of the Global Volcanism Network*, Vol. 18, No. 2, p. 9-10.

PHI VOLCS (Philippine Institute of Volcanology and Seismology). 1993b. Mayon: Stombolian eruption; activity wanes. *Bulletin of the Global Volcanism Network*, Vol. 18, No. 3, p. 4-5.

Pierson, T. C. 1980. Erosion and deposition by debris flows at Mount Thomas, North Canterbury, New Zealand. *Earth Surface Processes Landforms*, Vol. 5, p. 227-247.

Pierson, T. C. 1981. Dominant particle support mechanisms in debris flows at Mt. Thomas, New Zealand, an implications for flow mobility. *Sedimentology*, Vol. 28, p. 48-60.

Pierson, T. C. 1985. Initiation and flow behaviour of the 1980 Pine Creek and Muddy River lahars, Mount St. Helens, Washington. *Geological Society of America Bulletin*, Vol. 96, p. 1056-1069.

Pierson, T. C. 1986. Flow behaviour of channelised debris flows, Mount St. Helens, Washington. In Abrahams, A.D *ed.*, Hillslope Processes, p. 269-296. Boston, Allen and Unwin.

Pierson, T. C. 1989. Hazardous hydrologic consequences of volcanic eruptions and goals for mitigative action: An overview. In Starosolszky, O. and Melder, O. M. *eds*, *Hydrology of disasters, Proceedings of the Technical Conference in Geneva organized by the World Meteorological Organization, November 1988*, p. 220-225. James and James, London.

Pierson, T. C. and Scott, K. M. 1985. Downstream dilution of a lahar: Transition from debris flow to hyperconcentrated streamflow. *Water Resources Research*, Vol. 21, No. 10, p. 1511-1524

Pierson, T. C. and Costa, J. E. 1987. A rheologic classification of subaeriel sediment-waterflows. *Geological Society of America Reviews in Engineering Geology*, Vol. VII, p. 1-12

Pierson, T. C., Janda, R. J., Thouret, J. and Borrero, C. A. 1990. Perturbation and melting of snow and ice by the 13 November 1985 eruption of Nevado del Ruiz, Colombia, and consequent mobilization, flow and deposition of lahars. *Journal of Volcanology and Geothermal Research*, Vol. 41, p. 17-66.

Pierson, T. C., Janda, R. J., Umbal, J. A. and Daag, A. S. 1992. Immediate and long term hazards fom lahars and excess sedimentation in rivers draining Mt. Pinatubo, Philippines. Vancouver, Washington: *United States Geological Survey Water Resources Investigations Report* 92-4039, p. 182-203.

Pillans, B. J. 1988. Loess Chronology in Wanganui Basin, New Zealand. In Eden and Furkert *eds*, *Loess*, p. 175-191. Balkema, Rotterdam.

Pillans, B. J. 1990. Late Quaternary marine terraces South Taranaki-Wanganui. *New Zealand Geological Survey Miscellaneous Series*, Map 18.

Pillans, B. J. 1991. New Zealand Quaternary stratigraphy: an overview. *Quaternary Science Reviews*, Vol. 10, p. 405-418.

Purves, A. M. 1990. Landscape ecology of the Rangipo Desert. Unpublished Masters thesis, Department of Soil Science, Massey University, New Zealand.

Risberg, C. 1937. Eruption of Mount Ruapehu. *Journal of the New Zealand House of Representatives*, Vol. C-10, p. 5.

Rodolfo, K. S., Arguden, A. T., Solidum, R. U. and Umbal, J. V. 1989. Anatomy and behaviour of a post-eruptive rain lahar triggered by a typhoon on Mayon Volcano, Philippines: *Bulletin of the International Association of Engineering Geology*, Vol. 40, p. 55-66.

Rodolfo, K. S. 1989. Origin and early evolution of lahar channel at Mabinit, Mayon Volcano, Philippines. *Geological Society of America Bulletin*, Vol. 101, p. 414-426.

Scott, K. M. 1988a. Origins, behaviour, and sedimentology of lahars and lahar-runout flows in the Toputle-Cowlitz River system. *United States Geological Survey Professional Paper* 1447-A, 74pp.

Scott, K. M. 1988b. Origins, behaviour, and sedimentology of prehistoric catastrophic lahars at Mount St. Helens, Washington. *Geological Society of America Special Paper* 229, p. 23-35.

Scott, K. M. 1989. Magnitude and frequency of lahars and lahar-runout flows in the Toutle-Cowlitz River system. *United states Geological Survey Professional Paper* 1447-B, 33pp.

Scrivenor, J. B. 1929. The mudstreams "Lahars" of Gunong Keloet in Java. *Geological Magazine*, Vol. 66, p. 433-434.

Shackleton, N. J. and Opdyke, N. D. 1973. Oxygen and palaeomagnetic stratigraphy of equatorial Pacific Core V28-238: oxygen isotope temperature and ice volumes on a 10-5 and 10-6 year scale. *Quaternary Research*, Vol. 3, p. 39-55.

Sharp, R. P. and Nobles, L. H. 1953. Mudflow of 1941 at Wrightwood, Southern California. *Bulletin of the Geological Society of America*, Vol. 64, p. 547-560.

Shultz, A. W. 1984. Subaeriel debris-flow deposition in the upper Paleozic Cutler Formation, Western Colorado. *Journal of Sedimentary Petrology*, Vol. 54, No. 3, p. 759-772.

Siebert, L. 1984. Large volcanic debris avalanches: Characteristics of source areas, deposits, and associated eruptions. *Journal of Volcanology and Geothermal Research*, Vol 22, p. 163-197.

Skey, W. 1869. On the water from the Whangaehu River, Onetapu, Auckland. *Transactions of the New Zealand Institute*, Vol. 1, p. 28.

Smith, G. A. 1986. Coarse-grained nonmarine volcaniclastic sediment: terminology and process. *Geological Society of America Bulletin*, Vol. 97, p. 1-10.

Smith, G. A. 1987. The influence of explosive volcanism on fluvial sedimentation: the Deschutes Formation (Neogene) in Central Oregon. *Journal of Sedimentary Petrology*, p. 613-629.

Smith, G. A. and Fritz, W. J. 1989. Volcanic influences on terrestrial sedimentation. *Geology*, Vol. 17, p. 375-376.

Smith, G. A. and Lowe, D. R. 1991. Lahars: Volcano-hydrologic events and deposition in the debris flow-hyperconcentrated flow continuum. In, R. V. Fisher and G. A. Smith *eds.*, Sedimentation in Volcanic Settings, *Society for Sedimentary Geology (SEPM) Special Publication* No. 45., p. 59-70.

Stevens, J. R. H. 1957. Flood warning system for the New Zealand Railways. *Electrical Times*, London.

Stewart, G. 1972. Christmas disaster that stunned New Zealand. Tangiwai Disaster and 30 other railway accidents in New Zealand. Printed by Wilson and Horton, Ltd. Auckland.

Stewart, R. B., Neall, V. E. and Syers, J. K. 1986a. Accumulation of aerosolic quartz in an andept chronosequence, North Island, New Zealand. *Geoderma*, Vol. 37, p. 331-340.

Stewart, R. B., Neall, V. E. and Syers, J. K. 1986b. Origin of quartz in selected soils and sediments, North Island, New Zealand. *New Zealand Journal of Geology and Geophysics*, Vol. 29, p. 147-152.

Stewart, R. B., Neall, V. E., Pollock, J. A. and Syers, J. K. 1977. Parent material stratigraphy of an Egmont loam profile, Taranaki, New Zealand. *Australian Journal Soil Research*, Vol. 15, p. 177-190.

Stilwell, W. F., Hopkins, H. J. and Appleton, W. 1954. Tangiwai railway disaster. Report of the Board of Inquiry. Government Printer, Wellington, 31pp.

Suggate, R. P. 1990. Late Pliocene and Quaternary glaciations of New Zealand. *Quaternary Science Reviews*, Vol. 9, p. 175-197.

Tadahide, U. and Glicken, H. 1986. Internal structural variations in a debris-avalanche deposit from ancestral Mount Shasta, California, USA. *Bulletin of Volcanology*, Vol. 48, p. 189-194.

Taylor, R. Journal of Rev. Richard Taylor, 1833-73. Typescript in AlexanderTurnbull Library, Wellington.

Till, R. and Spears, D. A. 1969. The determination of quartz in sedimentary rocks using an x-ray diffraction method. *Clays and Clay Minerals*, Vol. 17, p. 323-327.

Topping, W. W. 1973. Tephrostratigraphy and chronology of late Quaternary eruptives from the Tongariro Volcanic Centre, New Zealand. *New Zealand Journal of Geology and Geophysics*, Vol. 16, No. 3, p. 397-424.

Topping, W. W. and Kohn, B. P. 1973. Rhyolitic tephra marker beds in the Tongariro area, North Island, New Zealand. *New Zealand Journal of Geology and Geophysics*, Vol. 16, p. 375-395.

Topping, W. W. 1974. Some aspects of of Quaternary history of Tongariro Volcanic Centre. Unpublished PhD thesis, University of Victoria, Wellington, New Zealand.

Trostel, L. J. and Wynne, D. J. 1940. Determination of quartz (free silica) in refactory clays. *Journal of the American Ceramic Society*, vol. 23, no. 1, p. 18-22.

Ulate, C. A. and Corrales, M. F. 1966. Mud floods related to the Irazu Volcano eruptions. *Journal of the Hydraulics Division, Proceedings of the American Society of Civil engineers*, Vol. 92, No. HY6, p. 117-129.

Vallance, J. W. 1986. Late Quaternary volcanic stratigraphy on the Southwestern flank of Mount Adams volcano, Washington. Unpublished Masters Thesis, University of Colorado, U.S.A.

Van Bemmelen, R. W. 1949. The Geology of Indonesia, Vol. 1A. General geology of Indonesia and adjacent archipeligoes. *Special edition of the Bureau of Mines in Indonesia*. Goverment Printing Office, The Hague, Netherlands.

Vucetich C. G. and Pullar W. A. 1973. Holocene tephra formations erupted in the Taupo area and interbedded tephras from other volcanic sources. *New Zealand Journal of Geology amd Geophysics*, Vol. 16, p. 754-780.

Waitt, R. B., Jr., Pierson, T. C., MacLeod, N. S., Janda, R. J, Voight, B. amd Holcomb, R. T. 1983. Eruption-triggered avalanche. flood, and lahar at Mount St. Helens: Effects of winter snowpack. *Science*, Vol. 221, p. 5596-5614.

Waldron, D. H. 1966. Debris flow and erosion control problems caused by the ash eruptions of Irazu Volcano, Costa Rica. *United States Geological Survey Bulletin* No. 1241-I, 377pp.

Walton, A. W. and Palmer, B. A. 1988. Lahar facies of the Mount Dutton Formation (Oligocene-Miocene) in the Marysvale Volcanic Field, Southwestern Utah. *Geological Society of America Bulletin*, Vol. 100, p. 1078-1091.

Welles, P. C. and Fowles, C. R. 1980. Water Resources of the Whangaehu River. Report to the Rangitikei-Wanganui Catchment Board, 175pp.

Wilson, C. N. J., Switsur, V. R. and Ward, A. P. 1988. A new ^{14}C age for the Oruanui (Wairakei) eruption, New Zealand. *Geological Magazine*, Vol. 125, p. 297-300.

Wilson, C. N. J., Houghton, B. F., Lanphere, M. A. and Weaver, S. D. 1992. A new radiometric age estimate for the Rotoehu Ash from Mayor Island volcano, New Zealand. *New Zealand Journal of Geology and Geophysics*, Vol. 35, p. 371-374.

Youd, T. L. 1973. Liquefaction, flow and associated ground failure. *United States Geological Survey Circular* 688, 12pp.

Rodolfo, K. S. and Arguden, A. T. 1991. Rain-lahar generation and sediment-delivery systems at Mayon Volcano. In R. V. Fisher and G. A. Smith *eds*, Sedimentation in volcanic settings. *Society for Sedimentary Geology (SEPM) Special Publication* No. 45, p. 71-88.

Takahashi, T. 1982. Debris flow. *Annual Review of Fluid Mechanics*, Vol. 13, p. 57-77.

Te Punga, M. T. 1953. The Geology of the Rangitikei Valley. *New Zealand Geological Survey Memoir*, No. 8, 46pp.

Voight, B., Glicken, H., Janda, R. J. and Douglas, P. M. 1981. Catastrophic rockslide avalanche of May 18. In P. W. Lipman and D. R. Mullineaux *eds*, The 1980 Eruptions of Mount St. Helens, Washington. *United States Geological survey Professional Paper*, No. 1250, p. 347-378.

Wallace, R. C., Stewart, R. B. and Neall, V. E. 1985. Volcanic glass laboratory test and procedure to prepare thin sections of the sand fraction of soils. *Massey University Department of Soil Science Occasional Report*, No. 7, 7pp.